Glucose-sensing in the hypothalamic arcuate nucleus: electrophysiological and mathematical studies

Ratchada Pattaranit

A thesis written in partial fulfilment of the criteria set for the degree of Doctor of Philosophy

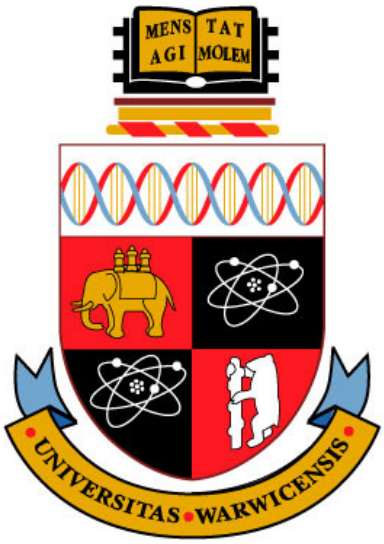

THE UNIVERSITY OF WARWICK

MOAC Doctoral Training Centre, University of Warwick

December 2009

Table of Contents

List of Figures

List of Tables

Publications

Papers:

Pattaranit R. & van den Berg H.A. (2008). Mathematical models of energy homeostasis. *Journal of the Royal Society, Interface/ the Royal Society* **5**: 1119-1135.

Pattaranit R., van den Berg H.A. & Spanswick D. (2008). The development of insulin resistance in Type 2 diabetes: insights from knockout studies. *Science Progress* **91**: 285-316.

Acknowledgements

I would like to express my sincere gratitude to both of my supervisors, Professor David Spanswick and Dr. Hugo van den Berg for giving me the opportunity to undertake this project and for their support and invaluable guidance given throughout my PhD. Without their encouragement, great supervision, useful suggestions and advice, constructive comments and patience, this thesis would not have been accomplished. I am indebted to them for introducing me to the world of new research area for me. I am deeply thankful to Professor David Spanswick for his belief in me who had no experience in patch-clamp technique before I came to do this project, which indeed is a great encouragement for me. I am grateful to Dr. Hugo van den Berg for his enthusiasm, mathematical comments and some language advice throughout my project.

I would express my special thanks to Dr. Marco van den Top for his assistance with experiments and biological background, useful suggestions, selfless advice, excellent supports and invaluable expertise that he has shared with me.

I would like to thank Professor Alison Rodger, the Director of Molecular Organisation and Assembly in Cells (MOAC), for giving me an invaluable opportunity to continue my study in MSc and PhD, for her encouragements, trust and kindness. Without her I would not come this far.

I am very grateful to the Royal Thai Government for the full financial support.

I would like to thank all the people with whom I have had the pleasure of working in the lab with over the course of my PhD, in particular, Dawn Collins, David Lyons, Jasmeet Virdee, Louise Saker, Andrew Whyment, Paul Giles, Ross Jeggo, Petra Mai, Stuart Greenhill and Tony Rush for their moral support, friendship and many good moments that we have shared. I am also very grateful to all people in MOAC especially 2004 intake cohort for their encouragement, friendship and moral supports.

My sincere thanks go to my good friends who have made my life in UK lively, warmth, enjoyable and complete, in particular, Kannika Thampanishvong, Amornrat Aungwerojwit, Jittiwut Suwatthikul, Pattarawit Polpinit, Paradee Tungtang, Issavara Sirirungruang, Wila-sini Wongkaew, Moncharai Kulvanich, Pornpinun & Sanha Hemvanich, Warithorn Samana, Antony Harfield, Atipat Boonmoh, Sakkapop Panyanukul, Paneeya Nitiwanakun, Nattavudh Powdthavee, Nateecha Ratanadilok Na

Bhuket, Lankani Sikurajapathy, Lahari de Alwis, Irene Boonwikrom, Antony Holmes, Gemma Warren, Yi Wah Chan, Anin Meksuksai, Prim Plansangkate, Apichart Limpichaipanit and Kraijakr Thiratayakinant for their wonderful friendship, moral supports, proofreading and happy and sad moments that we have shared

Very special thanks go to the special person, Ponglit Viriyapong, for his love, caring and tireless moral support.

Finally, my deepest gratitude goes to my beloved parents, Jakkrit Pattaranit and Sopida Pattaranit, and brother, Worrawit Pattaranit, for their unconditional love, invaluable advice and endless support and encouragement. Without them this project would never have been completed.

Declaration

I hereby declare that this thesis has been composed solely by myself and that it has not been accepted in any previous application for a degree. All work has been done by myself, with the exception of some electrophysiology in chapter 4 which was carried out in collaboration with Dr. Marco van den Top; Figure 1.1 which was adapted from Dr. Hugo van den Berg; and the review of mathematical models of energy homeostasis in Chapter 2 was carried out in collaboration with Dr. Hugo van den Berg. All the sources used have been specifically acknowledged by means of a reference.

Ratchada Pattaranit

Summary

1. Energy homeostasis requires the co-ordination of several metabolic fluxes at the systemic level among various peripheral organs and the central nervous system. A breakdown of these metabolic fluxes can lead to hyperglycaemia. An explicit representation of this complex dynamical system can aid the interpretation of diagnostic tests and help formulate therapeutic interventions. Hence, mathematical models could constitute a valuable clinical tool in the management of hyperglycaemia associated with diabetes. However, a very large range of such models is available, making a judicious choice difficult. To better inform this choice, the most important models published to date are presented in a uniform format, discussing similarities and differences in terms of the decisions faced by modellers. We review models for glucostasis, based on the glucose-insulin feedback control loop, and consider extensions to long-term energy balance, dislipidæmia and obesity.

2. Whole-cell patch-clamp recording techniques were used in isolated hypothalamic brain slice preparations to investigate and compare the electrophysiological properties of arcuate nucleus (ARC) neurones from fed and fasted rats, including a fed control group housed as fasted animals. Subthreshold active conductances were differentially expressed in ARC neurones including: anomalous inward rectification (I_{an}), A-like transient outward rectification (I_A), time and voltage-dependent inward rectification (I_h) and T-type calcium-like conductance. Significant differences in active and passive subthreshold membrane properties of ARC neurones were observed between the three groups, including: changes in magnitude of I_A and I_h, action potential duration, membrane time-constant (tau), neuronal input resistance and spontaneous activity. Furthermore, both housing and fasting conditions affected electrophysiological properties of rat ARC neurones, suggesting both stress and fasting can modify electrophysiological properties of ARC neurones.

3. The effects of intracellular adenosine triphosphate (ATP) on neuronal excitability of ARC neurones were investigated and compared between fed and fasted rats. This was performed by manipulating extracellular glucose levels from 2.0 to 0.0 mM whilst intracellular ATP was manipulated by changing the levels in the patch pipette solution (0.0, 1.0, 2.0, 5.0 and 10.0 mM). The level of ATP required to maintain resting membrane potential and glucose-sensing capability of ARC neurones was determined. Data from this study suggests 1.0 mM and 5.0 mM ATP for fasted and fed rats, respectively, were appropriate levels for maintaining electrophysiological and glucose-sensing integrity of these neurones. Hence levels of or sensitivity to ATP appears subject to modulation depending on the energy status of organism.

4. Glucose-sensing neurones and associated underlying mechanisms in ARC neurones in both fed and fasted states were studied. Extracellular glucose levels (2.0 – 0.2 – 0.5 – 1.0 – 2.0 – 5.0 mM) were manipulated with appropriate intracellular ATP levels determined as outlined above. Three types of glucose-sensing neurone were identified: glucose-excited (GE) neurones, glucose-inhibited (GI) neurones and glucose-rapidly adapting (GRP) neurones. The proportions of these three groups of neurones varied between fed and 24-hour fasted rats. Changing energy status, fasting, also appeared to affect the sensitivity of

glucose-sensing neurones, i.e. the threshold levels of glucose they detect. GE neurones operated through ATP-sensitive potassium (K_{ATP}) channel-dependent mechanisms in fed and fasted rats and through a chloride-dependent mechanism in fed rats. GI neurones detect changes in glucose levels through chloride and/or non-selective cation conductance-dependent mechanisms. Finally a potential mechanism of GRA neurones may be through transient opening of chloride conductances. Further work is required to confirm the ionic mechanisms of these glucose-sensing neurones.

5. Analysis of responses observed in ARC glucose-sensing neurones was also examined using a mathematical approach. An empirical sigmoid response function was assumed to describe the time course of the transition in neuronal activity and the integral of this function was fitted to cumulative action potential numbers to characterise the response dynamics. Four parameters were estimated for each transition, employing the least-squares criterion; the activity prior to and at the end of each change in extracellular glucose concentration, the half sigmoid time before the neuronal activity changes following a step change in extracellular glucose and the duration of the transition. Statistical tests revealed a statistically detectable difference in response delay of GE neurones following step changes in glucose levels between fed and 24-hour fasted rats. In addition, in fed rats, statistical test revealed that GE neurones required a significantly shorter delay time in changing their activity but longer change-over times than GI neurones. In 24-hour fasted rats, only the difference in activity of neurones at the start and at the end of glucose application was found to be statistically significant difference between GE and GI neurones. Further work is required to confirm these data.

Abbreviations

5-HT	5-Hydroxytryptamine
AcCoA	Acetyl-CoA carboxylase
aCSF	Artificial cerebrospinal fluid
ACTH	Adrenocorticotropic hormone
ADP	Adenosine diphosphate
AGRP	Agouti-related peptide
AHP	Afterhyperpolarisation
AMP	Adenosine monophosphate
AMPA	α-amino-3-hydroxy-5-methyl-4-isoxazole proprionic acid
AMPK	AMP-activated protein kinase
ANS	Autonomic nervous system
ARC	Arcuate nucleus
ATP	Adenosine triphosphate
BBB	Blood-brain-barrier
BMI	Body mass index
cAMP	Cyclic adenosine-mono-phosphate
CART	Cocaine- and Amphetamine- regulated transcript
CCK	Cholecystokinin
CFTR	Cystic fibrosis transmembrane conductance regulator
CNS	Central nervous system
CO_2	Carbondioxide
CRF	Corticotrophin releasing factor
CRH	Corticotrophin-releasing hormone
CSF	Cerebrospinal fluid
db/db	Leptin receptor deficiency
DMH	Dorsomedial hypothalamic nucleus
DMSO	Dimethylsulphoxide
EGTA	Ethylene glycol-bis(aminoethylether) N,N,N’,N’-tetraacetic acid
EPSPs	Excitatory postsynaptic potentials
Fruc6P	Fructose 6-phosphate
GABA	Gamma Aminobutyric Acid

GALP	Galanin-like peptide
GE	Glucose-excited
GH	Growth hormone
GHRH	Growth hormone-releasing hormone neurones
GHSR	Growth hormone secretagogue receptor
GI	Glucose-inhibited
GK	Glucokinase
GLP-1	Glucagons-like peptide 1
GLUT	Glucose transporter
GR	Glucose-responsive
GRA	Glucose-rapidly adapting
GS	Glucose-sensitive
HEPES	N-(2-hydroxyethyl)piperazine-N'-(2-ethanesulfonic acid)
HGE	High-glucose-excited
HGI	High-glucose-inhibited
I_A	A-like outward rectifier
I_{an}	Anomalous inward rectifier
ICV	Intracerebroventricularly
IGF-1	Insulin-like growth factor 1
I_h	Hyperpolarisation-activated non-selective cation channel
ILG-1	Insulin-like growth 1
IPSPs	Inhibitory postsynaptic potentials
IR	Insulin receptor
IRS	Insulin receptor substrate
IVC	Individually ventilated cage
JAK	Janus kinase
K_{ATP} channels	ATP-sensitive potassium channels
KCO	Potassium channel opener
KIR	Inward rectifying potassium channel
LH	Lateral hypothalamus
MAPK	Mitogen-activated protein kinase
MCH	Melanin concentrating hormone
MC-R	Melanocortin receptor
ME	Median eminence

MIRKO	Muscle-specific insulin receptor knockout
mRNA	Messenger ribonucleic acid
α-MSH	α- melanocyte stimulating hormone
mTOR	Mammalian target of rapamycin
Na-ATP	ATP disodium salt
NBQX	6-nitro-7-sulphamoylbenzo(*f*)-quinoxaline-2,3-dione
NE	Norepinephrine
NEFAs	Non-esterified fatty acids
NGS	Non glucose-sensing
NIRKO	Neuron-specific insulin receptor knockout
NMDA	N-methyl-D-aspartate
NPY	Neuropeptide Y
NTS	Nucleus of the tractus solitarius
ob/ob	Leptin deficiency
Ob-R	Long-form leptin receptor
OXR	Orexin receptor
PFA	Perifornical area of hypothalamus
PI3K	Phosphoinositide 3-kinase
POMC	Pro-opiomelanocortin
PYY	Peptide YY
PVN	Paraventricular nucleus of the hypothalamus
SCN	Suprachiasmatic nucleus
SEM	Standard error of the mean
SNS	Sympathetic nervous system
SPNs	Sympathetic preganglionic neurones
STAT	Signal Transducers and Activator of Transcription
SUR1	Sulfonylurea receptor 1
SUR2	Sulfonylurea receptor 2
TAG	Triacylglyceride
TASK	Tandem-pore acid sensitive potassium channel
Tau	Membrane time constant
Thy	Thyroid gland
TRH	Thyrotrophin-releasing hormone neurones

TSH	Thyrotrophs
TTX	Tetrodotoxin
T3	Triiodothyronine
T4	Thyroxine
UDP-GlcNac	UDP-*N*-acetylglucosamine
VMH	Ventromedial hypothalamus
VMN	Ventromedial nucleus of the hypothalamus
WHO	World Health Organisation

Chapter 1

General introduction

An animal maintains bodyweight via an intricate balance between energy intake (food consumption) and expenditure. Moreover, body adipose stores are maintained within narrow limits by a regulatory system that matches energy intake to expenditure. Maintaining energy homeostasis is a complex process consisting of multiple interacting homeostatic and behavioural signalling pathways. These pathways include glucose and lipid homeostasis, short-term satiety, macronutrient pathways, hypothalamic and autonomic central effector pathways and the hypothalamic-pituitary-adrenal axis. Sustaining and co-ordinating body homeostasis thus relies in large part on the autonomic nervous system.

1.1 The autonomic nervous system

The autonomic nervous system (ANS) is a part of the central nervous system (CNS) which controls the visceral functions of the body. The ANS plays a key role in maintaining homeostasis and controls the body's internal environment, as well as adapting body physiology to environmental changes. The ANS innervates almost all tissues and organs within the body, except skeletal muscle, to maintain homeostasis. The ANS is mainly an efferent system that transmits impulses from the CNS to the peripheral organ systems. Its effects include the control of heart rate, body temperature, blood pressure, force of contraction, digestion, respiration and relaxation of smooth muscle in many organs. It can be divided into three divisions: the parasympathetic nervous system (PNS), the sympathetic nervous system (SNS) and the enteric nervous system (ENS). The ENS consists of a network of nerve fibres that controls gastrointestinal motility and secretions and innervates the gastrointestinal tract, pancreas and gall bladder. Here we focus on the PNS and the SNS and their complementary roles in maintaining homeostasis.

Both the PNS and the SNS consist of preganglionic neurones originating in the CNS that make synaptic connections with postganglionic neurones in the periphery, which then innervate the effector organs. The neurotransmitter acetylcholine is released by preganglionic neurones of both systems at the pre-post ganglionic synapse. The two systems differ as regards the location of the preganglionic neurones in the CNS and also with respect to the neurotransmitter that is released from the postganglionic neurones. Parasympathetic preganglionic neurones are located in nuclei throughout the brainstem and in the sacral spinal cord,

whereas the sympathetic preganglionic neurones originate in the thoracic and lumbar regions of the spinal cord (Loewy, 1990). The neurotransmitters released from postganglionic neurones in the two systems are also different: parasympathetic postganglionic neurones release acetylcholine, whereas noradrenaline is released from sympathetic postganglionic neurones. An exception to this rule is the sympathetic innervation of the sweat glands, which uses acetylcholine as a transmitter.

Broadly speaking, the SNS promotes a "fight or flight" response that requires energy mobilization and inhibition of digestion, whereas the PNS promotes digestion and a slowing of visceral function, known as the "rest and digest" response. It stands to reason that homeostasis is achieved as a balance of the two systems, which in this respect act synergistically.

Both the PNS and the SNS receive afferent signals from the periphery and the CNS. Many of these signals are integrated in a region called the hypothalamus. The hypothalamus may be regarded as a group of "head autonomic ganglia" that act as the integrator that is necessary to regulate and coordinate basic life functions, including the maintenance of energy homeostasis.

1.2 Energy homeostasis

Energy homeostasis is a complex process whereby energy intake and energy expenditure are balanced over extended periods of time. Disruption of this system leads to several disorders, including diabetes and obesity (see Section 1.9.1). An understanding of energy homeostasis is essential to overcoming these disorders, which are fast becoming a global problem. The central nervous system (CNS) plays a major role in regulating energy homeostasis by receiving and integrating information originating from the periphery, processing this information and formulating an appropriate physiological response. The CNS receives inputs from the periphery which signals energy status through humoral and neuronal signalling pathways informing the CNS of the whole-body metabolic status, either to the brainstem or hypothalamus, which are reciprocally connected (see Figure 1.1). Hormones involved in the pathways relaying information regarding energy status from the periphery to CNS include insulin from pancreas, leptin from fat, and ghrelin and Peptide YY_{3-36} (PYY_{3-36}) from the gut.

Key brain areas first associated with sensing and responding to changes in energy balance were shown to be located in the hypothalamus by means of experiments in which lesions were made in the lateral hypothalamic (LH) area and the ventromedial nucleus (VMN) of hypothalamus. The lesions of the LH increased energy expenditure and weight loss and induced hypophagia. Hence, the LH was considered to be the 'feeding' centre. Conversely, lesions of the VMN caused hyperphagia, decreased energy expenditure, and weight gain (Hetherington & Ranson, 1940; Anand & Brobeck, 1951). Thus the VMN was considered to be the 'satiety' centre.

As both humoral and neuronal signalling pathways were found to convey information on the body's energy status to the brain, an understanding of the nature of these signals became essential. Two main hypotheses were formulated: the first one, proposed by Mayer in 1953, was the 'glucostat hypothesis' according to which glucose is a key regulator in energy homeostasis. Mayer assumed that small changes in plasma glucose levels trigger meal initiation and termination (Mayer, 1953; Mayer, 1955). However, this hypothesis did not take into account information regarding energy expenditure and body-weight control. Another hypothesis, proposed by Kennedy in 1953, suggested that food intake is linked to the amount of energy that is stored in the body in the form of fat. This 'lipostat hypothesis' proposed that humoral signals are generated in proportion to the amount of stored energy (fat mass) and that the brain uses these signals to modulate food intake and energy expenditure, allowing a better long-term control of overall energy balance and body weight (Kennedy, 1953). The Kennedy model was subsequently extended in many studies relating to CNS control of energy balance (Kaiyala *et al.*, 1995; Schwartz *et al.*, 1999). Insulin and leptin, which are hormones whose levels are proportional to the fat mass in the body (Bagdade *et al.*, 1967; Considine *et al.*, 1996), play an important role in controlling body weight. These two hormones engage and regulate two principal pathways within the CNS. These are the *anabolic* and *catabolic* pathways, which work in parallel and in an opposing way resembling the synergistic relationship between the PNS and SNS in many respects. The anabolic pathway stimulates food intake and suppresses energy expenditure whereas the catabolic pathway inhibits food intake and increases energy expenditure, in order to maintain body weight around a certain set point. For general reviews on the central control of energy

homeostasis, see Schwartz *et al*. (1999), McMinn *et al*. (2000), Schwartz *et al*. (2000), and Gao & Horvath (2007).

A combination of the glucostat hypothesis and the lipostat hypothesis would suggest that there is an integration of short-term signals, many originating within the CNS, and adiposity-related long-term signals, from the periphery. A number of neuropeptides released from hypothalamic nuclei, including those released from glucose-sensing neurones, as proposed by the glucostat model, have a role in controlling short-term signals, whereas adiposity-related levels of plasma insulin and leptin have a role in controlling the long-term signals (Schwartz *et al.*, 1999; Schwartz *et al.*, 2000).

1.3 The hypothalamus

The hypothalamus is a small cone-shaped structure within the brain, located below the thalamus in the basal region of the diencephalon, adjacent to the third ventricle. It is the control centre involved in the mediation of autonomic, endocrine and behavioural functions. It plays a pivotal role in the homeostasis of many physiological systems including hunger, salt and water balance, body temperature, thirst, sexual and emotional behaviours, reproduction, the control of circadian and endocrine function, and energy balance. Many studies have reported that within the hypothalamus there are several nuclei that have specific functional roles. For example, the LH is responsible for controlling sleep and arousal, the suprachiasmatic nucleus (SCN) controls circadian rhythms and the VMH is involved in neuroendocrine control.

The present study is focussed on the role of the hypothalamus in controlling energy balance and body weight. Energy homeostasis is controlled by a number of nuclei including the arcuate nucleus (ARC), the LH, the VMH, the paraventricular nucleus (PVN) and the dorsal medial hypothalamus (DMH). Involvement of these nuclei was first brought to light by lesion-based studies, as mentioned in Section 1.2. More recently, among the nuclei regulating energy homeostasis within the hypothalamus, the ARC has received the most attention.

1.4 The arcuate nucleus (ARC)

The arcuate nucleus (ARC) is an elongated collection of neuronal cell bodies occupying an arc-like region located in the mediobasal hypothalamus, adjacent to the third ventricle, immediately above the median eminence (ME; Chronwall, 1985), and proximal to a compromised blood-brain-barrier (BBB; Broadwell *et al*., 1983; Fry *et al*., 2007). The close proximity of the ARC to the ME is believed to allow circulating factors (such as the hormones insulin, leptin, ghrelin) and nutrients (such as glucose) to access the ARC more readily than other areas. Hence, the ARC is able to sense and respond to factors relating to energy balance. Insulin and leptin bind to the insulin receptor and the long-form leptin receptor (Ob-R), respectively. These receptors are expressed at high levels on the cellular membrane of ARC neurones. Engagement of these receptors modulates the neurones' electrical activity, which suggests that these cells play a key role in conveying information concerning the body's energy status from the periphery to the brain (Marks *et al.*, 1990; Mercer *et al.*, 1996; Spanswick *et al.*, 1997; Elmquist *et al.*, 1998; Spanswick *et al.*, 2000; Cowley *et al.*, 2001). Ghrelin released from the stomach activates its receptor, the growth hormone secretagogue receptor (GHS-R) which is expressed at high levels within the ARC, to increase appetite. Glucose may also signal at the level of the ARC, as proposed by the Mayer hypothesis, where some neurones have been reported to sense a change in extracellular glucose levels (Ashford *et al.*, 1990a; Spanswick *et al.*, 1997; Ibrahim *et al.*, 2003; van den Top *et al.*, 2007). Glucose may gain access to the ARC by diffusion across the ependyma from the cerebrospinal fluid (CSF) in the third ventricle (Elmquist *et al.*, 1998). Figure 1.1 presents an overview of these hormones, peptides and nutrients as well as neuronal pathways involved in the control of energy acquisition and expenditure.

The ARC not only receives inputs from the periphery but also from other hypothalamic nuclei involved in controlling energy homeostasis, including the LH, PVN, SCN, DMH and VMH (Saper *et al.*, 1979; Chronwall, 1985; Cone *et al.*, 2001; Williams *et al.*, 2001). It therefore appears that the ARC is a major integrative centre within the hypothalamus; see Figure 1.2. These hypothalamic afferents to the ARC employ a range of neuropeptides and neurotransmitters such as orexin (in the LH), and cocaine and amphetamine-related transcript (in the PVN and the LH; Chronwall, 1985; Horvath *et al*., 1997; Broberger, 1999).

Efferent targets of the ARC reside in several brain areas, including the PVN, SCN, LH, DMH, ME, brainstem and nucleus tractus solitarius (NTS; see Figure 1.2 and Wiegand & Price, 1980; Chronwall, 1985; Sim & Joseph, 1991; Baker & Herkenham, 1995). These efferent outputs activate second-order neurones involved in the maintenance of energy homeostasis. Moreover, a number of brain areas, such as the PVN, LH, SCN and DMH, have both afferents to the ARC and efferents from the ARC, indicative of multiple reciprocal connections between these areas.

Neurones within the ARC contain several neuropeptides involved in feeding, including neuropeptide Y (NPY), agouti-related peptide (AgRP), pro-opiomelanocortin (POMC), cocaine and amphetamine-related transcript (CART), neuromedin U, galanin, dopamine, prolactin and α-MSH (Chronwall, 1985; Hahn *et al.*, 1998; Howard *et al.*, 2000; Reyes *et al.*, 2001). Two of these subsets of neurones in the ARC are major components of the anabolic and catabolic pathways and operate in an opposing way. Around 90% of NPY neurones co-express agouti-related protein (AgRP) (Broberger *et al.*, 1998b). These NPY/AgRP neurones are inhibited by leptin and insulin but activated by ghrelin. They drive the anabolic pathway, increasing food intake and decreasing energy expenditure. Inasmuch as NPY/AgRP neurones lead to increased food intake, they are said to be *orexigenic*. By contrast, POMC/CART neurones lead to a decrease in food intake and are therefore said to be *anorexigenic*. The POMC precursor peptide is cleaved into melanocyte-stimulating hormones (α-, β-, γ-MSH), adrenocorticotropic hormone (ACTH) and β-endorphin (Cone, 2005). Among these hormones, α- and β-MSH act on melanocortin receptor subtype 3 and 4 (MC3/4R) receptors (Adan *et al.*, 1994), which are present at high levels in the ARC, LH, DMH and PVN (Mountjoy *et al.*, 1994), to suppress food intake and increase energy expenditure. These two neuronal populations, NPY/AgRP and POMC/CART, are to a large extent located anatomically adjacent within the ARC, NPY/AgRP neurones having their origins in the ventromedial part (Chronwall, 1985; Allen *et al.*, 1986) and POMC/CART neurones located more laterally (Bloom *et al.*, 1978). In sum, these two groups of neurones in the ARC are of paramount importance in the control of feeding and energy balance and the ARC may be regarded as the fundamental centre for the maintenance of energy homeostasis.

1.5 Orexigenic and anorexigenic neuropeptides

Several of the neuropeptides that play key roles in the control of appetite will now be discussed in more detail.

1.5.1 Orexigenic neuropeptides

Orexigenic neuropeptides act to increase food intake. Examples of these neuropeptides are NPY, AgRP and orexin, each of which will now be discussed in turn.

1.5.1.1 NPY (neuropeptide Y)

NPY is an orexigenic neuropeptide, discovered in the hypothalamus in 1982 (Tatemoto *et al.*, 1982). It is a 36-amino acid peptide which is expressed throughout the mammalian brain with the highest levels found in the PVN and the ARC (Adrian *et al.*, 1983; Chronwall, 1985). NPY has been shown to be involved in a host of regulatory actions ranging from the control of blood pressure to circadian rhythms (Albers & Ferris, 1984) and body temperature (Billington *et al.*, 1991). NPY-containing neurones act to decrease energy expenditure and increase food intake (Kalra *et al.*, 1991a). A direct injection of NPY into either cerebral ventricles, PVN or perifornical LH and VMH stimulates robust feeding responses in a dose-dependent manner, leading to hyperphagia and obesity (Stanley *et al.*, 1986; Stanley *et al.*, 1993; Zarjevski *et al.*, 1993). The starvation state is characterized by an increase in both NPY and NPY mRNA (Sanacora *et al.*, 1990; White *et al.*, 1990; Kalra *et al.*, 1991a; Schwartz *et al.*, 1993; Sahu, 1998). In model obese animals, the levels of NPY gene expression and NPY are increased (Kalra *et al.*, 1991b; Wilding *et al.*, 1993; Dryden *et al.*, 1995; Stephens *et al.*, 1995). Increases in food intake following NPY injection can be blocked by NPY antagonists (Beck, 2006). Overall, these studies point to a role of NPY in producing a shift to a state of positive energy balance.

Six NPY receptors have been identified. Only five of them have been found in the rat brain: these are the NPY-Y_1, -Y_2, -Y_3, -Y_4 and -Y_5 receptors, whereas NPY-Y_6 has been characterised in the mouse (Gerald *et al.*, 1996; Balasubramaniam, 1997). These six NPY receptors are G-protein coupled receptors. Cloning studies have

reported that NPY can act on the NPY-Y_1, -Y_2, -Y_4 and -Y_5 receptors and all have been reported to be present in the hypothalamus, with high levels in the ARC (Larhammar *et al.*, 1992; Grundemar *et al.*, 1993; Bard *et al.*, 1995; Gerald *et al.*, 1995; Gerald *et al.*, 1996). With regard to the NPY-Y_3 receptor, a pharmacological study has suggested its location to be mainly the brainstem nucleus of the solitary tract (NTS; Grundemar *et al.*, 1991). Of all of these receptors, only three receptors located in the hypothalamus have been reported to be involved in feeding; these are NPY-Y_1, -Y_2 and -Y_5 (Gerald *et al.*, 1996). Within the ARC, NPY-Y_1 receptors are located on many POMC neurones and only at the postsynaptic membrane, whereas NPY-Y_2 receptors are found on NPY neurones which they inhibit when activated, and may act as a presynaptic autoreceptors (Broberger *et al.*, 1997) to regulate neurotransmission (Rhim *et al.*, 1997). The NPY-Y_5 receptor has also been found in the ARC and the activation of this receptor depresses ARC synaptic transmission (Rhim *et al.*, 1997).

1.5.1.2 AgRP

AgRP is an orexigenic peptide that is co-expressed with NPY but not with POMC in the ARC (Hahn *et al.*, 1998). It is an endogenous antagonist for the MC-3 and MC-4 receptors and expressed at a high level within the hypothalamus (Broberger *et al.*, 1998a; Hahn *et al.*, 1998). The administration of AgRP leads to an increase in food intake and body weight (Ollmann *et al.*, 1997). Further evidence shows that overexpression of AgRP leads to obesity, supporting the conclusion that AgRP is an MC-4 receptor antagonist (Ollmann *et al.*, 1997). Ablation of AgRP neurones results in acute reduction of feeding, showing that these neurones are critical for energy homeostasis (Gropp *et al.*, 2005). Taken together, these studies indicate that AgRP plays a role in controlling body weight.

1.5.1.3 Orexin

Orexins were named for the Greek •ρεξις meaning lust or appetite. They occur in two forms: orexin-A and orexin-B (also known as hypocretin 1 and 2) (Sakurai *et al.*, 1998). They are abundantly expressed in the LH (Kojima *et al.*, 1999) and bind to two G-protein coupled receptors, orexin receptor-1 (OX_1R) and orexin

receptor-2 (OX_2R; Sakurai *et al*., 1998). Orexin neurones are found in clusters only in the LH, the dorsal hypothalamic area and the perifornical hypothalamus (de Lecea *et al.*, 1998; Sakurai *et al.*, 1998) and nowhere else in the CNS (Bernardis & Bellinger, 1996; Bing *et al.*, 1996).

Orexin-A and orexin-B share a 46.0% amino acid sequence identity and are derived from the 130 amino acid precursor protein and prepro-orexin. Both OX_1R and OX_2R mRNA have been shown to be expressed in many areas throughout the brain, especially within the hypothalamus where OX_1R is most abundantly expressed in the VMH and OX_2R is expressed at a high level in the PVN (Trivedi *et al.*, 1998). Administration of orexin promotes feeding, leading to an increase in orexin mRNA levels (Sakurai *et al.*, 1998; Dube *et al.*, 1999). Approximately 50% of orexin neurones express the leptin receptor (Sakurai *et al.*, 1998) and around 30% are regulated by the plasma glucose concentration, as is indicated by their response to insulin-induced hypoglycemia (Moriguchi *et al.*, 1999). In the fasted state, prepro-orexin mRNA is up-regulated. Taken together, these studies implicate the orexins as key regulators of the energy balance. In addition, disruptions or dysfunction of orexin signalling induces narcolepsy, indicating an important role of orexin in maintaining an appropriate arousal state and regulation of the sleep/wake cycle (Chemelli *et al.*, 1999; Lin *et al.*, 1999).

1.5.1.4 Melanin-concentrating hormone (MCH)

Melanin-concentrating hormone (MCH; Moran, 2006) is a cyclic orexigenic hypothalamic peptide which plays a central role in the control of feeding behaviours and regulating stress, and which is highly expressed in the LH and the zona incerta, a region which lies adjacent to the LH (Bittencourt *et al.*, 1992). Two receptors for MCH have been characterised, namely MCH-1 and MCH-2, both which are G-protein-coupled receptors. Administration of MCH to the brain increases food intake and weight gain (Qu *et al.*, 1996). Moreover, mRNA levels of MCH are increased during fasting (Ludwig *et al.*, 1998). Mice lacking MCH are lean and hypophagic, whereas overexpression of MCH induces obesity and hyperleptinemia (Shimada *et al.*, 1998). Although MCH and orexin neurones originate in the LH, they project directly to POMC and NPY neurones in the ARC (Broberger *et al.*, 1998a; Elias *et al.*, 1998b). MCH increases NPY and AgRP release, while decreasing

α-MSH and CART release from hypothalamic explants (Abbott *et al.*, 2003). Within the LH, there are reciprocal connections between MCH, orexin and other nearby neurones (Guan *et al.*, 2002).

1.5.2 Anorexigenic neuropeptides

Anorexigenic neuropeptides are those peptides that can induce a decrease in food intake. Examples include POMC, CART, Corticotropin-releasing hormone (CRH) and Cholecystokinin (CCK), all of which are described below.

1.5.2.1 POMC

POMC is the precursor of a family of melanocortin peptides including α-melanocyte stimulating hormone (α-MSH) and adrenocorticotrophic hormone (ACTH), both of which have been characterised as main regulators of energy balance. Within the brain, POMC is expressed exclusively in hypothalamus and NTS in the brainstem (Jacobowitz & O'Donohue, 1978; Watson & Akil, 1979). POMC binds to five G-protein coupled melanocortin receptors (MC1-R to MC5-R). However, only two melanocortin receptors, MC3-R and MC4-R, are expressed within the hypothalamus and are involved in controlling energy homeostasis. Many studies have shown that POMC plays a key role in feeding. Ablation of POMC induces obesity (Xu *et al.*, 2005), whereas the administration of an α-MSH analogue reduces food intake (Fan *et al.*, 1997), indicating that α-MSH acts to limit food intake and body mass. This is further supported by data from MC4-R knockout mice which produce a syndrome of obesity (Huszar *et al.*, 1997). Injection of MC4-R agonists causes anorexia and selective MC4-R antagonists induces sustained hyperphagia and obesity (Fan *et al.*, 1997; Schioth *et al.*, 1999). Furthermore, a disruption of the MC4-R gene is a key factor associated with the form of dominantly inherited morbid obesity that is most commonly found in humans (Vaisse *et al.*, 1998; Yeo *et al.*, 1998; Ho & MacKenzie, 1999; Mergen *et al.*, 2001; Farooqi *et al.*, 2003; Valli-Jaakola *et al.*, 2004; Farooqi & O'Rahilly, 2006).

Thirty percent of POMC neurones have been shown to carry the long isoform of the leptin receptor, with mRNA for this receptor expressed at high levels in the ARC, indicating that POMC neurones are direct targets of leptin in the hypothalamus

(Cheung *et al.*, 1997). Block of MC4-Rs has been shown to suppress the ability of leptin to decrease food intake and body weight (Seeley *et al.*, 1997). In the starvation state (when the leptin levels are reduced) or in the ob/ob mouse (which lacks the leptin receptor), POMC mRNA levels have been shown to be decreased, associated with a state of positive energy balance (Mizuno *et al.*, 1998; Cone, 1999). This state is reversed following leptin treatment (Schwartz *et al.*, 1997). Electrophysiological data have shown that POMC neurones are activated by leptin through activation of non-selective cation channels via a phosphoinositide 3-kinases (PI3K)-dependent downstream pathway (Cowley *et al.*, 2001; Hill *et al.*, 2008; Rother *et al.*, 2008). However, insulin inhibits POMC neurones, also through a PI3K-dependent pathway (Hill *et al.*, 2008).

1.5.2.2 CART

Cocaine- and amphetamine-regulated transcript (CART) was first identified and added to the long list of neuropeptides expressed and produced in hypothalamic neurones in 1995 (Douglass *et al.*, 1995). It is found to be expressed at high levels within the hypothalamus (Douglass *et al.*, 1995), its mRNA being the third most abundantly expressed neuropeptide in the hypothalamus (Gautvik *et al.*, 1996). CART is widely expressed throughout the rat brain and it has been shown to be co-localised with numerous neuropeptides in the hypothalamus, such as MCH in the LH, as well as oxytocin and vasopressin in the PVN (Vrang *et al.*, 1999). Within the ARC, 95% of CART-expressing neurones have been shown to be co-localised with POMC, whereas CART is not co-localised with NPY (Elias *et al.*, 1998a; Vrang *et al.*, 1999). Inasmuch as CART is expressed widely in the brain, it has been suggested to be involved in several physiological processes such as feeding, stress, pain and reproduction. However, the specific role of this peptide remains unclear, not least because its receptor and target of action remain unidentified.

1.5.2.3 CRH

Corticotropin-releasing hormone (CRH), originally named corticotrophin-releasing-factor, is a 41-amino acid peptide derived from a 191-amino acid preprohormone. It is a polypeptide hormone and neurotransmitter involved in the

stress response. CRH is expressed by neurones mainly in the hypothalamus within the PVN region; it is also produced in some peripheral tissues such as T lymphocytes and highly expressed in the human placenta (Robinson *et al.*, 1988). It plays an important role in regulating the activity of the hypothalamic-pituitary-adrenal axis (Neary *et al.*, 2004), food intake, and the stress response. Central injection of CRH inhibits food intake and decreases body weight and energy expenditure (Arase *et al.*, 1988; Rothwell, 1990; Vettor *et al.*, 2002). Administration of CRH antagonists promotes expression of NPY, suggesting a role for CRH in inhibiting orexigenic NPY neurones (Hanson & Dallman, 1995; Arora & Anubhuti, 2006). Leptin infusion has been shown to stimulate CRH secretion and CRH mRNA expression in the PVN (Huang *et al.*, 1998). Further evidence supporting a role of leptin in stimulating the secretion of CRH is the finding that treatment by leptin after CRH antagonist administration leads to markedly decreased cumulative food intake and body weight (Masaki *et al.*, 2003). Hence, CRH is another key factor in the control energy homeostasis.

1.5.2.4 CCK

Cholecystokinin (CCK), originally named cholecystokinin-pancreozymin, is a brain-gut peptide. It was first found in 1928 as a hormone in the gastrointestinal tract (Ivy & Oldberg, 1928) and was much later shown to be expressed in the CNS (Hokfelt *et al.*, 1985; Szewczyk & Laudeman, 2003). It is widely expressed throughout the CNS and has been shown to play a role in many physiological processes, especially the reduction of food intake by eliciting a feeling of satiety (Gibbs *et al.*, 1973; Degen *et al.*, 2001). The response to CCK is mediated by two specific G-protein-coupled receptors, namely CCK1R and CCK2R (Wank *et al.*, 1992), where CCK1R is mainly expressed peripherally and CCK2R is abundantly found in the brain (Moran *et al.*, 1986). A role of CCK in feeding has been shown to be dependent on agonist-induced activation of peripheral CCK1 receptors, which is a potential target for pharmacological treatment of obesity (Szewczyk & Laudeman, 2003).

1.6 Hormonal and nutrient signalling related to energy homeostasis

The CNS receives inputs from the periphery, humoral as well as neuronal, that carry information concerning the body's energy status, subsequently integrates this information and ultimately formulates an appropriate output to maintain energy homeostasis. A host of hormones communicate the energy-status from the periphery to the CNS; these include insulin, leptin, ghrelin, Peptide YY_{3-36} (PYY_{3-36}), adipocytokines and glucagon-like peptide 1 (GLP-1).

1.6.1 Leptin

Leptin (from the Greek *λεπτος* meaning thin) is the protein encoded by the obese (*ob*) gene, produced by adipocytes in proportion to the body fat stores (Considine *et al*., 1996). It regulates both short-term and long-term responses driving energy homeostasis. As a short-term regulator, leptin modulates meal size depending on energy status. Leptin administration, either by injection or chronic infusion, to obese or wild-type animals leads to a dose-dependent reduction in body weight and a decrease in food intake (Campfield *et al*., 1995; Halaas *et al*., 1995; Pelleymounter *et al*., 1995; Stephens *et al*., 1995; Halaas *et al*., 1997). Additionally, leptin is thought to increase energy expenditure leading to a greater weight loss than accounted for by reduced food intake alone (Levin *et al*., 1996; Scarpace *et al*., 1997). Both ob/ob (leptin deficiency) and db/db (leptin receptor deficiency) mice evince an obese phenotype (Lee *et al.*, 1996). Plasma leptin concentrations are increased in most obese humans and animal models of obesity. However, leptin administration to these animals is without significant effect indicating a state of "leptin resistance" in these obese animals (Considine *et al*., 1996; Heymsfield *et al*., 1999).

With a low level of plasma leptin and therefore diminished leptin signalling to the hypothalamus during weight loss, the anabolic pathways are activated (increasing food intake and reducing energy expenditure) and the catabolic pathways are suppressed: these concerted effects involve an increase in NPY/AgRP release and concomitant limitation of POMC/CART activity, resulting in increased meal size and reduced energy expenditure (Schwartz *et al*., 2000). On the other hand, higher leptin levels with stronger leptin signalling to the CNS lead to a reduction of food intake and an increase in energy expenditure (Friedman & Halaas, 1998; Schwartz *et al.*, 2000). Leptin binds to its receptors, of which there are at least six splice variants.

Within the hypothalamus, leptin exclusively binds to the long form of the receptor (Ob-Rb; Tartaglia *et al*., 1995; Lee *et al*., 1996). Ob-Rb is normally expressed in several areas in the hypothalamus, including the ARC, PVN, VMH, DMH and LH (Fei *et al.*, 1997; Hakansson *et al.*, 1998; Jequier, 2002). The binding of leptin to its receptor has been shown to induce activation of the JAK/STAT and PI3K pathways (Bjorbaek *et al.*, 1997; Niswender *et al.*, 2001; Bates & Myers, 2004). Furthermore, leptin also activates mTOR activity in the hypothalamus, although it reduces the activity of hypothalamic AMPK, causing a reduction in food intake (Minokoshi *et al*., 2004; Cota *et al*., 2006).

Leptin has been found to modulate synaptic transmission in the ARC (Glaum *et al*., 1996) and to modulate hypothalamic neurones by activation of K_{ATP} channels through a PI3K-dependent signalling mechanism (Spanswick *et al.*, 1997; Mirshamsi *et al.*, 2004). Recently it has been shown that leptin depolarises POMC neurones through activation of non-selective cation channels, a response that also appears to be dependent upon a PI3K-dependent downstream signalling pathway (Hill *et al.*, 2008; Rother *et al.*, 2008). Furthermore, leptin has been shown to exert differential effects on rat VMN *vs.* ARC neurones within the physiological range of brain glucose concentrations and acts on both glucose-sensing and non-glucose-sensing VMN neurones in a glucose-independent fashion (Irani *et al.*, 2008). Irani *et al*. confirmed earlier findings by Spanswick *et al*. indicating that the inhibitory effects of leptin are mediated through the activation of K_{ATP} channels and PI3K (Spanswick *et al.*, 1997) and are independent of the mitogen-activated protein kinases (MAPK) pathway (Irani *et al.*, 2008). In sum, leptin has been shown to be a factor in regulating food intake and energy balance. Moreover, failure of leptin-mediated signalling is a key factor contributing to obesity in animals and humans.

1.6.2 Insulin

Insulin (from the Latin *insula*, meaning islet) was first proposed to be a long-term regulator of food intake, energy balance, and body adiposity by Woods and colleagues (Porte & Woods, 1981). It is a peptide hormone which is synthesized, secreted and stored by the β-cells of the pancreatic islets. It plays an important role in the regulation of carbohydrate, lipid and protein metabolism. The secretion of insulin is exquisitely sensitive to small changes in the plasma glucose concentration.

In addition, insulin also has a role in maintaining glucose levels in the physiological range of 80-100 mg/dL. Three major targets for insulin action are muscle, adipose tissue and the liver (see Figure 1.3). Insulin acts as an adiposity signal, much like leptin, as its secretion is proportional to the amount of body fat stored. Insulin receptors are expressed widely throughout many brain regions including the ARC, VMN, and PVN in the hypothalamus (Baskin *et al.*, 1988; Marks *et al.*, 1990; Pardini *et al.*, 2006). Within the ARC, the NPY and melanocortin systems are believed to be important for the effects of insulin on food intake and body weight, because insulin receptors in the ARC are known to be co-localised with α-MSH and NPY. Insulin is not produced and secreted in the CNS but it is transported to the CNS within a period of hours after the plasma insulin concentration increases, supporting the proposal that it is a long-term regulator of body adiposity (Schwartz *et al.*, 1991). Administration of insulin intracerebroventricularly (ICV) suppresses food intake and body weight (Brief & Davis, 1984; Foster *et al.*, 1991). Furthermore, Air *et al*. showed that ICV administration of insulin induces a dose-dependent reduction of food intake and body weight in normal rats and increases POMC mRNA expression (Air *et al.*, 2002).

The role of insulin receptors in the brain remains unclear, because neurones metabolise glucose in an insulin-independent manner. Therefore, mice with neuron-specific insulin receptor knockout (NIRKO) were generated by Bruning *et al*. (2000) in order to investigate the physiological role of insulin signalling in CNS. NIRKO mice exhibit a marked increase in food intake and have larger adipose stores. Moreover, NIRKO mice exhibit mild insulin resistance, hypertriglyceridemia and hyperinsulinemia. Despite elevated leptin levels, obesity still occurs in these mice, suggesting a resistance to leptin action associated with insulin resistance. This evidence points to crosstalk between insulin and leptin in the regulation of body weight (Bruning *et al.*, 2000). Insulin has been shown to be able to regulate electrical properties of ARC neurones through activation of ATP-sensitive K^+ (K_{ATP}) channels and via a PI3K-dependent signalling pathway (Spanswick *et al.*, 2000; Hill *et al.*, 2008; Rother *et al.*, 2008). Taken together, the studies strongly suggest that both insulin and insulin receptors in the brain, especially in the ARC, play a pivotal role in food intake and glucose homeostasis.

1.6.3 Ghrelin

Ghrelin (from Proto-Indo-European *ghre* meaning to grow) is a peptide hormone of 28 amino acids, secreted from the endocrine cells of the stomach. It acts on a G-protein-coupled receptor, namely the growth hormone (GH) secretagogue receptor (GHSR; Sun *et al*., 2004), which has two subtypes, GHSR 1a and GHSR 1b (Smith *et al.*, 2004). Ghrelin has been demonstrated to play a pivotal role in GH release from the pituitary gland (Kojima *et al.*, 1999), the control of ACTH secretion, glucose and lipid metabolism, and reproduction (van der Lely *et al.*, 2004). It has also been shown to play a key role in feeding: in states of positive energy balance, ghrelin secretion is down-regulated whereas it is up-regulated in states of negative energy balance such as in the starvation state (Ariyasu *et al.*, 2001). This is further supported by data showing a dose-dependent increase in food intake and body weight and a decrease in energy expenditure during ghrelin administration in rodents, leading to hyperphagia and obesity (Tschop *et al.*, 2000; Wren *et al.*, 2001b). Prolonged administration of ghrelin to rodents induces an increase in fat mass and body weight and a reduction in lipid oxidation (Tschop *et al.*, 2000). The intravenous infusion of ghrelin in humans induces hunger and causes short-term stimulation of food intake (Wren *et al.*, 2001a). Antagonism of ghrelin signalling leads to a decrease in body weight and suppression of food intake (Asakawa *et al.*, 2003).

Ghrelin acts in the ARC to activate GHSR-expressing NPY/AgRP neurones, (Willesen *et al.*, 1999) and ghrelin inhibits POMC/CART neurones in the ARC (Cowley *et al.*, 2003; van den Top *et al.*, 2004), opposing the action of leptin. Ghrelin has also been found to promote the expression of NPY and AgRP mRNA in both *ad libitum* fed and fasted rats (Kamegai *et al*., 2000; Kamegai *et al*., 2001; Nakazato *et al*., 2001; Seoane *et al*., 2003). The level of ghrelin in the circulation goes up before a meal and rapidly falls after a meal (Tschop *et al.*, 2000). The plasma ghrelin level is also elevated in *anorexia nervosa* patients (Tolle *et al.*, 2003), whereas it is suppressed in obese humans (English *et al.*, 2002), evidence that supports a role of ghrelin in regulating energy balance. Interestingly, elevated circulating ghrelin levels have been shown to be associated with Prader-Willi syndrome, a rare inherited form of human obesity (DelParigi *et al.*, 2002), suggesting an involvement of high levels of ghrelin in inducing obesity. Such patients might benefit from lowering ghrelin levels in the circulation or blocking the effects of ghrelin in the CNS.

There is further evidence showing a co-localisation of leptin and ghrelin receptors in the NPY neurones within the hypothalamus (Mondal *et al.*, 2005). This suggests leptin and ghrelin work to oppose each other in their action on the same neurones (Zigman *et al.*, 2006).

1.6.4 PYY

Peptide YY (PYY) is a 36-amino acid peptide gut hormone, synthesised and secreted from enteroendocrine cells called L-cells. PYY has two main endogenous forms, namely PYY_{1-36} and PYY_{3-36}, the latter being abundantly found in the circulation (Grandt *et al.*, 1994; Batterham *et al.*, 2006; Korner *et al.*, 2006). PYY belongs to the family of peptides that includes pancreatic polypeptide (PP) and NPY, and its effects are mediated through five Y-receptors (Y_1, Y_2, Y_4, Y_5 and Y_6; Cabrele & Beck-Sickinger, 2000). PYY_{1-36} binds to all Y-receptors, whereas PYY_{3-36} shows high affinity for Y_2 receptor but lower affinity for Y_1 and Y_5 receptor (Larhammar, 1996). The level of PYY in the circulation is proportional to the energy content of the meal (Lin & Chey, 2003). Thus it is low in the fasting state, increases following the ingestion of food, reaches a peak at 1-2 hours after a meal and then remains elevated for several hours (Adrian *et al.*, 1985). Intraperitoneal injection of PYY_{3-36} in rodents causes a dose-dependent reduction in food intake, whereas peripheral administration of PYY_{3-36} in normal-weight humans results in a reduction of food intake which lasts up to 24 hours (Batterham *et al.*, 2002; Challis *et al.*, 2003) and an increase in energy expenditure (Sloth *et al.*, 2007). Injection of PYY_{3-36} into the ARC, where the Y_2-receptor is exclusively expressed, results in inhibition of feeding (Batterham *et al.*, 2002). In addition, mice lacking PYY have been shown to be hyperphagic and obese (Batterham *et al.*, 2006). PYY_{3-36} depolarises and increases the firing frequency of POMC neurones in the ARC (Batterham *et al.*, 2002). The postprandial peak PYY concentration negatively correlates with changes in body weight over 6 months and is a significant determinant of changes in waist circumference over time, indicating an involvement of PYY in the long-term regulation of body weight (Guo *et al.*, 2006). Taken together, these studies indicate that PYY plays a key role in the regulation of energy homeostasis; not surprisingly, the PYY system is currently a major therapeutic target for the treatment of obesity.

1.6.5 Adipocytokines

Adipocytokines or adipokines are cytokines that are secreted from adipose tissue. Adipose tissue is now considered an endocrine organ in its own right, producing adipocytokines that are involved in energy homeostasis, glucose regulation, immunity, lipid metabolism and the regulation of the neuroendocrine system. Two major adipocytokines, which are abundant in the circulation, are leptin and adiponectin. These two adipocytokines fulfill opposing functions as regards the regulation of food intake. Leptin is secreted primarily from adipocytes in proportion to the fat stores. Elevated plasma leptin levels communicate to the CNS the repletion of body energy stores, which acts as a signal to reduce food intake and increase energy expenditure (Friedman & Halaas, 1998). This is further supported by the work of Minokoshi *et al*., showing that leptin suppresses food intake by decreasing hypothalamic AMP-activated protein kinase (AMPK) activity (Minokoshi *et al.*, 2004). Low levels of plasma leptin are associated with a fasted state and lead to elevated food intake, reduced energy expenditure and modulation of neuroendocrine function to conserve energy stores (Ahima *et al.*, 1996; Rosenbaum *et al.*, 2005). In diametric contrast to leptin, adiponectin acts as a starvation signal: its levels increase in response to fasting and decrease in obesity (Kadowaki & Yamauchi, 2005). Decreases in the level of adiponectin lead to insulin resistance and glucose intolerance, associating with type 2 diabetes (Kadowaki *et al.*, 2008). Apart from this, adiponectin has been shown to exert central effects on energy homeostasis. Adiponectin signals through two seven-transmembrane domain-containing proteins, namely adipoR1 and adipoR2, which induce AMPK phosphorylation and activity, and which are expressed widely, including within the hypothalamus (Kadowaki & Yamauchi, 2005; Kubota *et al.*, 2007). This is further supported by data from Qi *et al*. who reported that intravenous adiponectin administration leads to increased levels of this adipocytokine in cerebrospinal fluid, whereas central administration of adiponectin increases energy expenditure and decreases body weight, plasma glucose and serum lipid levels, thus strongly suggesting a role for adiponectin in regulating food intake (Qi *et al.*, 2004).

1.6.6 GLP-1

Glucagon-like peptide 1 (GLP-1) is another gut hormone working in a similar way to PYY. It is derived from the post-translational processing of preproglucagon gene in the L-cells in the distal intestinal tract and released into the circulation after a meal (Hoyt *et al.*, 1996). GLP-1 has been shown to enhance glucose-induced insulin secretion, reduce glucagon secretion and inhibit gastric emptying (Nauck *et al.*, 1997); hence it has been put forward as a potential treatment for diabetic patients. GLP-1 high-affinity binding sites are mostly found in hypothalamus and brainstem (Merchenthaler *et al.*, 1999). There is also evidence that both peripheral and central GLP administration influences the neurones in the ARC, PVN, and NTS (Larsen *et al.*, 1997). At the level of the PVN, GLP-1 has been shown to reduce NPY-induced feeding (Turton *et al.*, 1996; Furuse *et al.*, 1997) and to induce a reduction in food intake following microinjection of GLP-1 into the PVN, suggesting a role of GLP-1 the suppression of food intake or by increasing satiety.

Several neuropeptides and hormones within the hypothalamus, both orexigenic and anorexigenic, including other signalling factors involved in controlling energy homeostasis, have been discussed in this section and the preceding section. Still, not all of them can be discussed here in detail. A comprehensive list of these neuropeptides and hormones is instead presented in Table 1.1.

Table 1.1 Neuropeptides and hormones involved in regulating energy homeostasis

Orexigenic (stimulatory)	Anorexigenic (inhibitory)
Neuropeptide Y (NPY)	Adiponectin
Agouti-related protein (AgRP)	Cholecystokinin (CCK)
Melanin concentrating hormone	Corticotropin-releasing hormone (CRH)
Hypocretins/orexins	Thyrotropin-releasing hormone (TRH)
Ghrelin	Glucagon-like peptide 1 (GLP-1)
Galanin	Pro-opiomelanocortin (POMC)
Growth hormone-releasing hormone (GHRH)	Cocaine- and Amphetamine- regulated transcript (CART)
Gamma Aminobutyric Acid (GABA)	Galanin-like peptide (GALP)
Uncoupling proteins	Insulin
Dynorphin	Leptin
Beacon	Peptide YY_{3-36} (PYY_{3-36})
B-Endorphin	Neuromedin U
	α- Melanocyte stimulating hormone (α-MSH)
	Somatostatin
	Oxytocin
	Amylin
	Serotonin
	Bombesin
	Oxyntomodulin
	Urocortin
	Motilin

1.7 Glucose homeostasis at a whole body level

Glucose (from the Greek *γλυκύς* meaning sugar or sweet) is a monosaccharide nutrient that is vital for all living animals and which serves a fundamental energy source of most mammalian cells. In particular, it is a major fuel for muscle and brain tissue. The liver is an important organ within the body involved in the control of glucose homeostasis, storing excess glucose as glycogen which can be mobilised in times of need. Most of the glucose released from the liver is produced by two processes, glycogenolysis (glycogen breakdown) and gluconeogenesis (the synthesis of new glucose from three-carbon fragments). The latter process plays a major role in the immediate post-absorptive state, whereas the first is important in the fasted state.

Plasma glucose concentrations are maintained within a narrow range. Normal plasma glucose levels (*euglycaemia*) are considered to be in the range 80-100 mg/dL. Plasma glucose concentrations below or above these levels are considered to represent states of *hypoglycaemia* and *hyperglycaemia*, respectively. Insulin and glucagon play a key role in maintaining the plasma glucose level. Insulin is secreted from β-cells and glucagon is secreted from α-cells, both cell types being located in the Langerhans islets scattered throughout the pancreas. Figure 1.4 explains diagrammatically how these two hormones regulate plasma glucose levels.

When the plasma glucose concentration is low, glucagon is released from the pancreatic α-cells, which acts on liver cells; these liver cells then release glucose into the plasma, thus increasing the plasma glucose level. On the other hand, when the plasma glucose level is high, insulin is secreted from β-cells and inhibits hepatic glucose production and induces excess glucose uptake by the liver and other cells, leading to a reduction in the plasma glucose concentration.

Glucose is metabolised by many tissues within the body including muscle, adipose tissue, and the CNS. In the resting state, the brain uses approximately 65% of the available glucose (Tuch *et al.*, 2000). Glucose enters brain cells through a family of specialised transporter proteins called glucose transporters (GLUTs) which are facilitative (passive) transporters. To date, thirteen members of this family of glucose transporters have been identified (Joost & Thorens, 2001) four of which, namely GLUT1, GLUT2, GLUT3 and GLUT4, play a major role in regulating glucose levels. GLUT1 is widely expressed in most tissues within the body and is involved in non-insulin-mediated glucose uptake, including the CNS and the BBB. GLUT2 is

expressed in the islet β-cells, liver, intestine and kidney, and in association with glucokinase forms the β-cells' glucose sensors. GLUT3 is expressed mostly in neurones and together with GLUT1 is involved in non-insulin-mediated uptake of glucose into the brain. GLUT4 is distributed in adipose tissue (both brown and white), heart and muscle. It is responsible for insulin-stimulated glucose uptake in these tissues. The "classic" hypoglycaemic action of insulin is illustrated in Figure 1.5. For an extensive review of GLUTs, see Joost & Thorens (2001).

Most neurones use glucose as fuel to support metabolic activity and the energy demands. However, a specific group of neurones also use glucose as a *signalling molecule* in order to directly regulate their electrical activity. This group of neurones are referred to as "glucose-sensing neurones" which form the main focus of this thesis. The details of these specialised glucose-sensing neurones are discussed in the next section.

1.8 Glucose homeostasis in the brain

The question of how the brain can sense the plasma glucose level in order to regulate energy balance was first addressed by Mayer, who formulated the "glucostat hypothesis" in 1953. He postulated that glucose was sensed by glucoreceptors in the brain and that an increase or decrease in glucose levels regulates meal termination and initiation, respectively. Glucose regulation is sufficiently important in the brain that it sports putative "glucose sensors" located on neurones in several key areas scattered throughout the brain, including the hypothalamus (Ashford *et al.*, 1990a; Shiraishi, 1991; Spanswick *et al.*, 1997; Song *et al.*, 2001), NTS (Mizuno & Oomura, 1984), hippocampus (Zawar & Neumcke, 2000) and the hindbrain (Ritter *et al.*, 1998; Ritter *et al.*, 2000; Balfour *et al.*, 2006). However, there is also evidence from many studies that only 10-40% of the neurones within the brain actually alter their firing frequency in response to variations in extracellular glucose concentrations (Nakano *et al.*, 1986; Ashford *et al.*, 1990a; Song *et al.*, 2001). These are called "glucose-sensing neurones."

Glucose-sensing neurones were first discovered by Anand and Oomura in 1964. They found neurones in the LH and VMH that alter their firing properties in response to changes in glucose levels (Anand *et al.*, 1964; Oomura *et al.*, 1964). Subsequently, such neurones were also found within the ARC and other areas of the

hypothalamus (Ashford *et al.*, 1990a; Spanswick *et al.*, 1997). The physiological range of glucose concentrations at the level of the ARC, to which ARC glucose-sensing neurones are thought to be exposed, has been suggested to range from 0.1 mM to 5.0 mM (Wang *et al.*, 2004), whereas the glucose-sensing neurones in VMN are thought to be exposed to much lower levels, below 2.5 mM (Song & Routh, 2006). The putative explanation for these findings that the BBB may be compromised in the vicinity of the ARC, potentially exposing ARC neurones to higher levels of glucose than any other areas within hypothalamus (Peruzzo *et al.*, 2000). However, no direct measurement of glucose levels have to date been performed *in vivo* in and around the ARC, as a result of which this issue remains the subject of considerable debate.

Within physiological ranges of extracellular glucose concentrations, there are two main types of glucose-sensing neurones; ***glucose-excited*** (GE) neurones, also called glucose-responsive (GR) neurones, which increase their firing frequency in response to an increased glucose level, and ***glucose-inhibited*** (GI) neurones, also called glucose-sensitive (GS) neurones, which decrease their firing frequency in response to an increased glucose level (Levin *et al.*, 1999). Both GE and GI neurones are exclusively expressed within hypothalamic nuclei and the brainstem, regions involved in regulating food intake. GE neurones alter their electrical excitability by sensing changes in extracellular glucose through modulation of activity of K_{ATP} channels (Ashford *et al.*, 1990a, 1990b; Rowe *et al.*, 1996; Spanswick *et al.*, 1997; Lee *et al.*, 1999; Spanswick *et al.*, 2000; Miki *et al.*, 2001; Zhang *et al.*, 2004); increasing levels of glucose acting to inhibit K_{ATP} channels, increasing electrical excitability in a dose-dependent manner (Song *et al.*, 2001; Wang *et al.*, 2004; Song & Routh, 2005). This mechanism of glucose sensing in GE neurones is analogous to the glucose-stimulated insulin secretion in pancreatic β-cells (for further details of β-cells glucose-sensing see Ashcroft & Gribble, 1999 and Schuit *et al*., 2001).

Although there is some evidence suggesting that glucose-induced inhibition of GI neurones is mediated by an opening of chloride channels, the mechanism underlying glucose-induced changes in electrical excitability of GI neurones remains the subject of debate (Song *et al.*, 2001; Routh, 2002; Fioramonti *et al.*, 2007). Another mechanism, also proposed by Oomura *et al*. (1974), is that an inhibition of GI neurones by glucose is mediated by the Na^+/K^+ ATPase pump in which glucose stimulates the Na^+/K^+ ATPase pump, which drives electrogenic exchange ($3Na^+$ per

$2K^+$; Oomura *et al*., 1974). Recently, glucose-inhibited orexin neurones in the LH were revealed to signal through the involvement of tandem-pore domain potassium channels (TASK; Burdakov *et al*., 2006) although these findings have subsequently come under severe criticism and scrutiny (Burdakov & Gonzalez, 2009).

At glucose levels above 5.0 mM, Fioramonti and colleages found two further types of glucose-sensing neurones within the ARC, namely high-glucose-excited (HGE) neurones and high-glucose-inhibited (HGI) neurones (Fioramonti *et al.*, 2004; Penicaud *et al.*, 2006). High-glucose excitation was found to be mediated through a K_{ATP}-independent manner and is thought to involve activation of a non-selective cation channel. However, to date the mechanism of HGI neurones that respond to shifts to higher glucose levels has remained unexplored, due to the small number of HGI neurones existing in the ARC.

Glucose-sensing neurones within the ARC include NPY-containing neurones that were shown to be GI neurones (Muroya *et al.*, 1999). However, whether or not POMC neurones are GE neurones remains unclear, not least due to the conflicting and contradictory data reported from three separate studies on this issue (Ibrahim *et al*., 2003; Wang *et al*., 2004; Fioramonti *et al*., 2007). In glucoprivic states, which are characterized by a lack of utilisable glucose, there is an increase in the expression of hypothalamic neuropeptides including NPY and AgRP (Andrew & Ritter, 2003; Li & Ritter, 2004), leading to hypoglycaemia-induced food intake (Fraley & Ritter, 2003; Sindelar *et al.*, 2004). For a review of glucose-sensing neurones, see Levin *et al*. (2004); Levin (2006); Marty *et al*. (2007); Routh *et al*. (2007).

On the balance of the currently available evidence, it seems very likely that glucose-sensing neurones play a pivotal role in controlling energy balance by linking neuronal activity with nutrient availability through function-specific pathways in the CNS, although a clearer appreciation and understanding of the functional organisation and interactions between the component parts of the glucose-sensing circuitry is still needed. Furthermore, it may safely be surmised that glucose-sensing neurones are relevant to many disorders where energy balance is subject to change or disruption, especially in relation to obesity and diabetes; such disorders form the subject of the next section.

1.9 Disorders of energy homeostasis and scope for pharmacological treatments

Due to the complexity in the CNS pathways that control food intake and the huge number of signalling molecules involved in maintaining energy homeostasis, any number of disruptions within these pathways can lead to a variety of disorders, such as obesity and diabetes.

1.9.1 Obesity

Obesity is a medical condition in which there is excessive body fat accumulation that presents a risk to health with an accompanying reduction in life expectancy (Haslam & James, 2005). It is fast becoming a worldwide problem with major repercussions on health and economy. Data from the world health organisation (WHO) show that globally, in 2005, there were approximately 1.6 billion overweight adults and more than 400 million obese adults. WHO also predicts that by 2015 approximately 2.3 billion adults will be overweight, whereas at least 700 million will be obese. The standard way to clarify whether or not a person is obese is by calculating the body mass index (BMI):

$$BMI = \frac{weight\ (kg)}{(height\ (m))^2}\ .$$

If this is equal to or greater than 25 kgm^{-2}, the person is classified as *overweight*, whereas if it is equal to or greater than 30 kgm^{-2}, the person is classified as *obese*. It must be admitted that this index has grave limitations; e.g. individuals who are more than averagely muscular might mistakenly be classified as overweight or obese.

Obesity results from an imbalance between energy intake (by ingestion) and energy expenditure (by basal metabolic rate, diet-induced thermogenesis and exercise) where excess energy is stored in the form of fat. The causes are complex and include the modern lifestyle, characterised by an increase in the consumption of high-caloric food and a trend towards reduced physical activity, as well as genetic factors, alcohol, and medical conditions including impaired neuronal circuits and hormonal signalling. Obesity is a major risk factor for many chronic diseases, such as type 2 diabetes, stroke, heart disease and some cancers. Although the past six decades have seen a huge effort to increase our understanding of the physiology and pathophysiology of energy homeostasis and to find a potential target or drug for obesity treatment, based on a vast number of studies trying to unravel the neural

circuits and new signalling pathways involved in the regulation of food intake and energy expenditure, the current reality is that the homeostatic systems controlling energy balance remain elusively complex. A greater understanding of the physiology and systems controlling energy balance, at all levels ranging from the molecular to the whole-body physiology, remains essential.

The standard approach to tackle obesity is a well-balanced diet together with regular exercise. However, this regime may not work for all obese people. In such cases, pharmaceutical intervention is considered as an option. Anti-obesity drugs have been developed for over a century. Some drugs that were approved for use and entered the market subsequently had to be withdrawn due to severe side effects. Currently, there are two anti-obesity drugs which are approved on the market for long-term treatment of obesity, namely orlistat and sibutramine. Another drug known as rimonabant that reduces body weight and improves metabolic comorbidities is also used in some obese people who are less vulnerable to the adverse effects, whereas it is withdrawn from patients who experience unpleasant side effects including symptoms of depression, sleep disorders, agitation and anxiety (Van Gaal *et al.*, 2005; Rubio *et al.*, 2007).

Orlistat is a gastric and pancreatic lipase inhibitor which reduces dietary triglyceride hydrolysis resulting in an inhibition of total calorie intake (Rubio *et al.*, 2007). However, there are some common side effects including diarrhoea, headache, leaking of oil from the rectum, flatulence with discharge and fatty stools (Davidson *et al.*, 1999; Rubio *et al.*, 2007; Adan *et al.*, 2008). Sibutramine is a 5-HT (5-hydroxytryptamine or serotonin) and noradrenaline reuptake inhibitor which induces satiety, making the subject feel full for longer and inhibiting food intake (Luque & Rey, 2002). However, this drug also has side effects which include tachycardia, hypertension, constipation, dry mouth and sleeping problems (James *et al.*, 2000).

Notwithstanding these developments, it seems unlikely that a single drug will prove to be effective for the treatment of all forms of obesity, which is caused by the disruption of multiple complex interacting systems. Hence, new targets for anti-obesity drugs are avidly sought. A number of studies have concentrated on the neurotransmitters and neuropeptides involved in the neural circuits which affect energy homeostasis. Among these, melanocortin receptor agonists are presently in the early phases of anti-obesity drug development (Nargund *et al.*, 2006).

In addition, the histamine system is also a good potential target for obesity treatment since there is evidence that histamine H_1 receptor antagonists increase food intake and body weight (Mercer *et al.*, 1994; Tokita *et al.*, 2006). Furthermore, drugs that mimic the action of CCK, GLP-1, oxyntomodulin, PYY_{3-36} and amylin which increase satiety, and antagonists of ghrelin receptors (GHSR) which decrease feelings of being hungry, could be a potential drug target for obesity treatment (Moran, 2006; Zanella & Ribeiro Filho, 2009). For a review of anti-obesity drugs, see Rubio *et al*. (2007); Adan *et al*. (2008); Zanella & Ribeiro Filho (2009).

1.9.2 Insulin resistance and type 2 diabetes

One of the major risk factors of obesity is type 2 diabetes, the incidence of which is now increasing dramatically worldwide. Globally, the total number of diabetics for all age groups is projected to increase from 171 million in 2000 to 366 million in 2030 (Wild *et al.*, 2004). There are two types of diabetes mellitus, both characterised by hyperglycaemia. Type 1 or ‘‘insulin-dependent’’ diabetes mostly occurs early in life and is caused by insulin deficiency due to damage to the β-cells in the pancreatic islets of Langerhans. Type 2 or ‘‘insulin-independent’’ diabetes is more common and occurs mostly in obese people and those over the age of forty. The main cause of this type of diabetes is insulin resistance, a condition in which normal amounts of insulin are inadequate to elicit a normal response to insulin in adipose, muscle and liver cells, resulting in hyperglycaemia.

Whereas type 1 diabetic patients can be treated mainly by insulin injection, there is an urgent need for a greater understanding of the pathogenesis of type 2 diabetes and the development of better treatments. An essential prerequisite is to understand how insulin signalling is normally regulated. Type 2 diabetes is thought to develop when a primary defect arises in any one component of the glucose homeostatic system, making greater demands on the system, leading to a cascade of secondary ‘‘knock-on’’ defects. The role of any of these primary defects can now be studied in isolation, following the advent of tissue-specific gene knockout techniques that allow such focal defects to be mimicked by using Cre-loxP system in mice, for example, muscle-specific insulin receptor knockout (MIRKO) including neurone-specific insulin receptor knockout (NIRKO). Numerous knockout-mouse studies addressing the key issues associated with type 2 diabetes and insulin

resistance have been reported; a summary of the phenotypes of whole-body knockout mice, both monogenic and polygenic, for the insulin receptor and genes related to insulin signalling including tissue-specific insulin receptor knockout mice, has been reviewed in Kahn (2003) and Pattaranit *et al*. (2008).

The concept of tissue-specific insulin signalling defects could explain the diverse aetiology of insulin resistance syndrome in humans. We might come to classify patients with this syndrome as ‘‘skeletal muscle resistors,’’ ‘‘liver resistors,’’ ‘‘adipose resistors,’’ and so on, each requiring a specific treatment strategy tailored to the site of resistance. This approach may prove to be substantially more effective than present treatments. For instance, one therapeutic agent that has been used to remedy hepatic insulin resistance is metformin, an oral antidiabetic agent that decreases glucose production by the liver and lowers plasma glucose levels (Tiikkainen *et al.*, 2004). For further reviews of the development of insulin resistance in type 2 diabetes, see Kahn (2003) and Pattaranit *et al*. (2008).

1.10 Aims of the present thesis

Obesity and diabetes present a mounting global problem. Hence, a greater understanding of the mechanisms that underlie the control of energy homeostasis is fundamental to our understanding of the development and manifestation of conditions associated with compromised states of energy balance and for the development of future strategies for therapeutic intervention. The main aims of the present study were: to investigate the mechanisms and neural circuits by which physiological and pathophysiological levels of glucose are detected at the level of the ARC of the hypothalamus and to undertake a mathematical modelling approach to understanding energy homeostasis at a whole body level, based on the glucose-insulin feedback control loop including the extensions to long-term energy balance relating to central nervous system.

The specific objectives of the current project were:

1. To study the mathematical models of energy homeostasis at the whole-body level based on the glucose-insulin relationship which was further extended by other hormones from the periphery and the CNS (Chapter 2)

2. To investigate the effects of a negative state of energy balance, “fasted”, on the electrophysiological properties of ARC neurones (Chapter 4)
3. To investigate the role of intracellular ATP concentration on ARC glucose-sensing neurones in different states of energy balance (fed *ad libitum* and fasted; Chapter 5)
4. To investigate the glucose-sensitivity of ARC neurones in rats fed *ad libitum* and fasted (24 hours; Chapter 6)
5. To characterise the dynamical response of ARC neurones to changes in extracellular glucose concentration (Chapter 7)

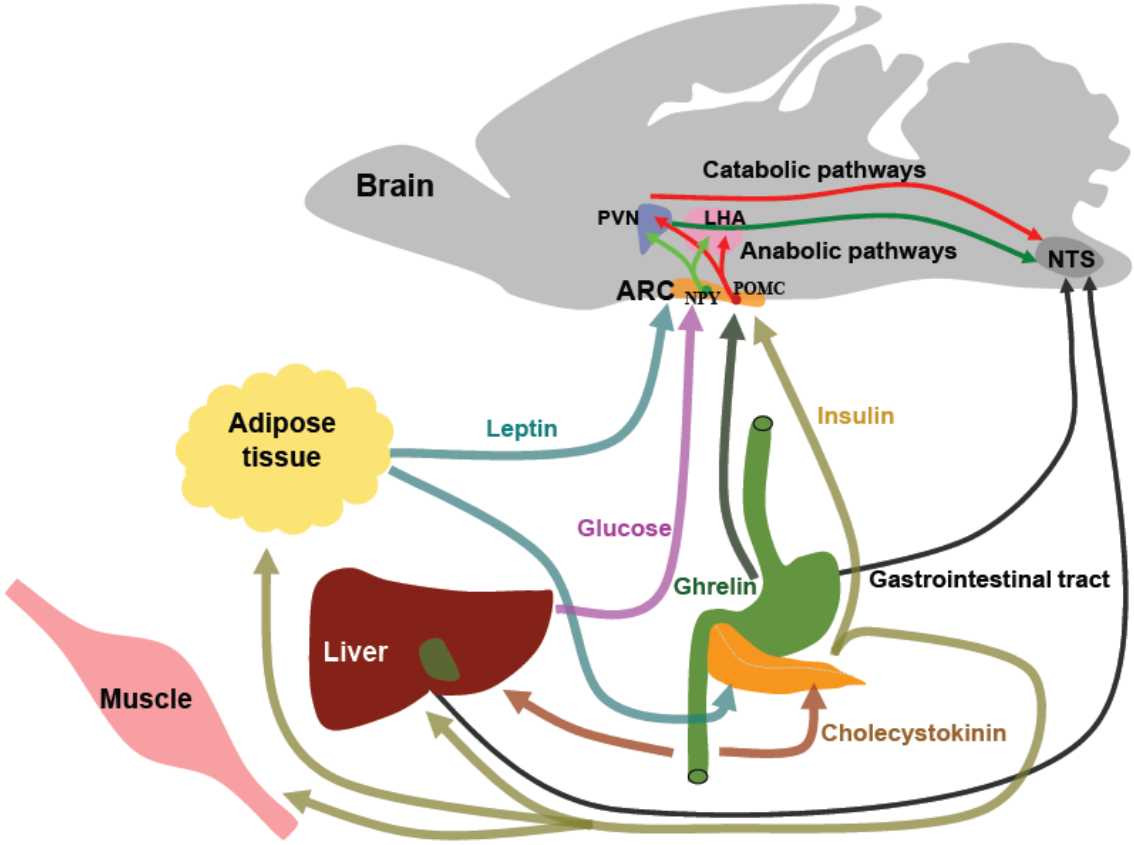

Figure 1.1: The central control of energy homeostasis

Pathways by which peripheral signals such as leptin released from adipose tissue, insulin released from pancreas, glucose from the liver and some peptides such as ghrelin and cholecystokinin, which are released from the gastrointestinal tract, all send information concerning of energy status of the whole body to the brain, particularly at the hypothalamus, and interact with central autonomic circuits to modulate meal size. The nucleus of the tractus solitarius (NTS) receives some inputs from peripheral vagal and sympathetic afferents and integrates this input with descending inputs from hypothalamus. The hypothalamus and brainstem are also reciprocally connected to regulate changes in feeding and control energy homeostasis. Peripheral hormones differentially activate either the anabolic pathway (neuropeptide Y (NPY) neurones) or the catabolic pathway (pro-opiomelanocortin (POMC) neurones) that originate within the arcuate nucleus (ARC). Both NPY (green) and POMC (red) neurones are first-order neurones which project to the paraventricular nucleus (PVN) and the lateral hypothalamus area (LHA) where the second-order neurones involved in energy homeostasis are located. These second-order neurones then synapse with neurones that generate satiety signals. Furthermore, both NTS and hypothalamus receive inputs from the brainstem, giving a negative feedback loop within the body to modulate the regular meal size, leading to controlling of energy homeostasis.

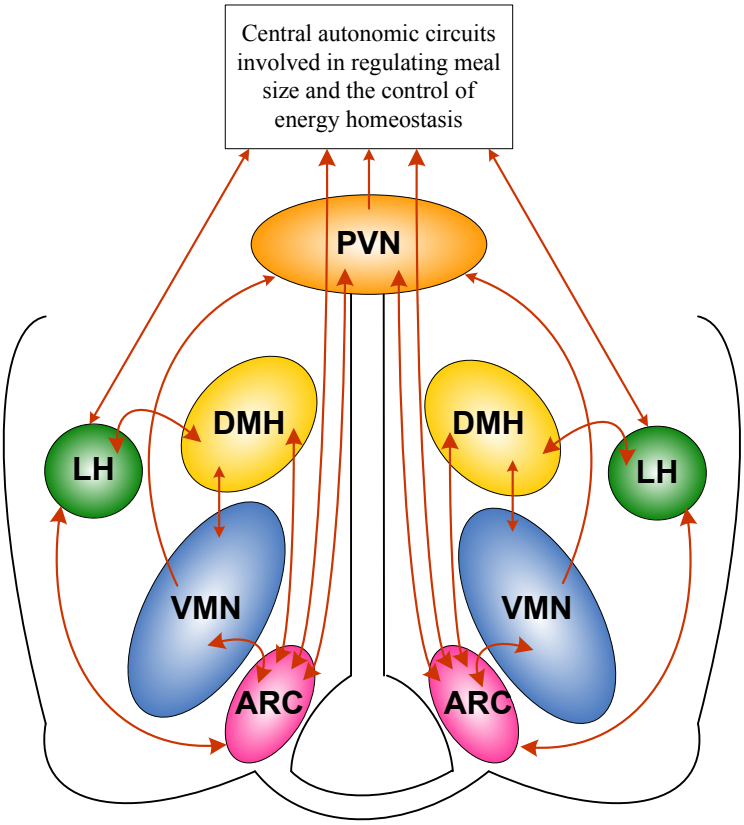

Figure 1.2: Overview of hypothalamic nuclei involved in energy homeostasis

Schematic drawing of the hypothalamus showing the location of the nuclei involved in feeding and energy homeostasis. These include the arcuate nucleus (ARC), ventromedial nucleus (VMN), lateral hypothalamus (LH), the dorsomedial hypothalamic nucleus (DMH) and paraventricular nucleus (PVN) where there are connections to the central autonomic circuits relating to energy homeostasis. There are reciprocal connections, as shown as arrows, between many of the nuclei that enable these nuclei to generate a coordinated response to maintain energy homeostasis.

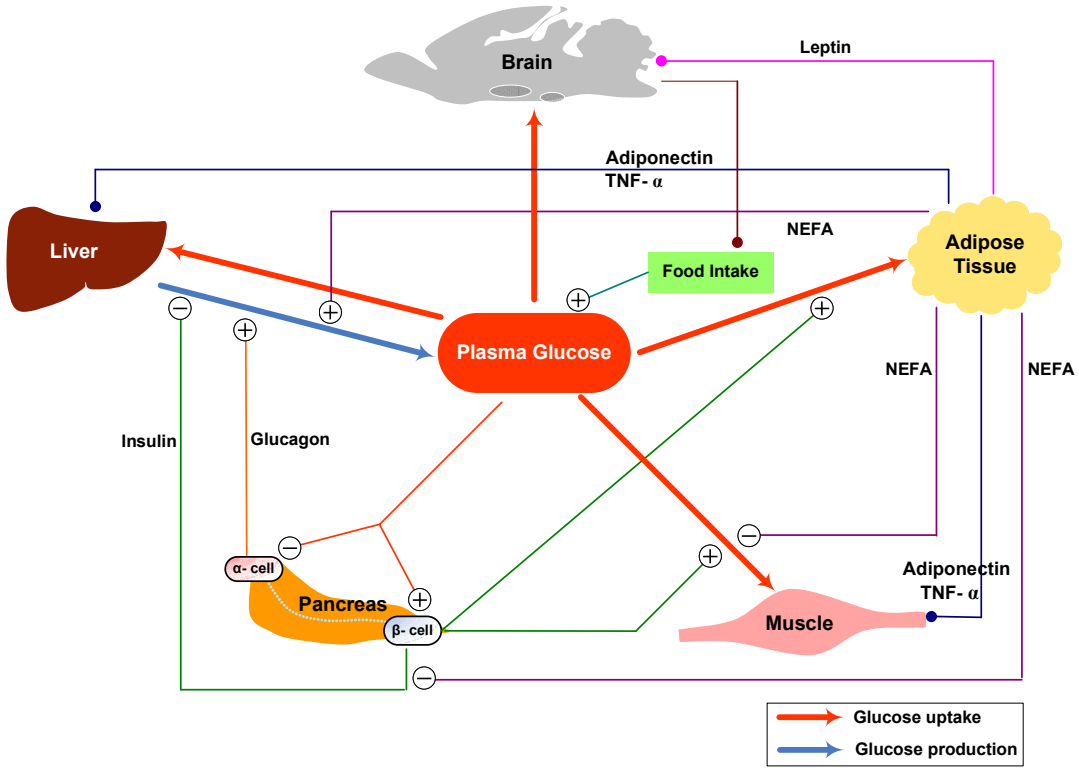

Figure 1.3: **Cross-talk between tissues to regulate glucose homeostasis**

Thick arrows represent the fluxes (metabolic conversions). Thin arrows show regulatory interactions: positive as plus signs, negative as minus signs and modulatory as disks. NEFA: non-esterified fatty acids; TNF-α: tumour necrosis factor α.

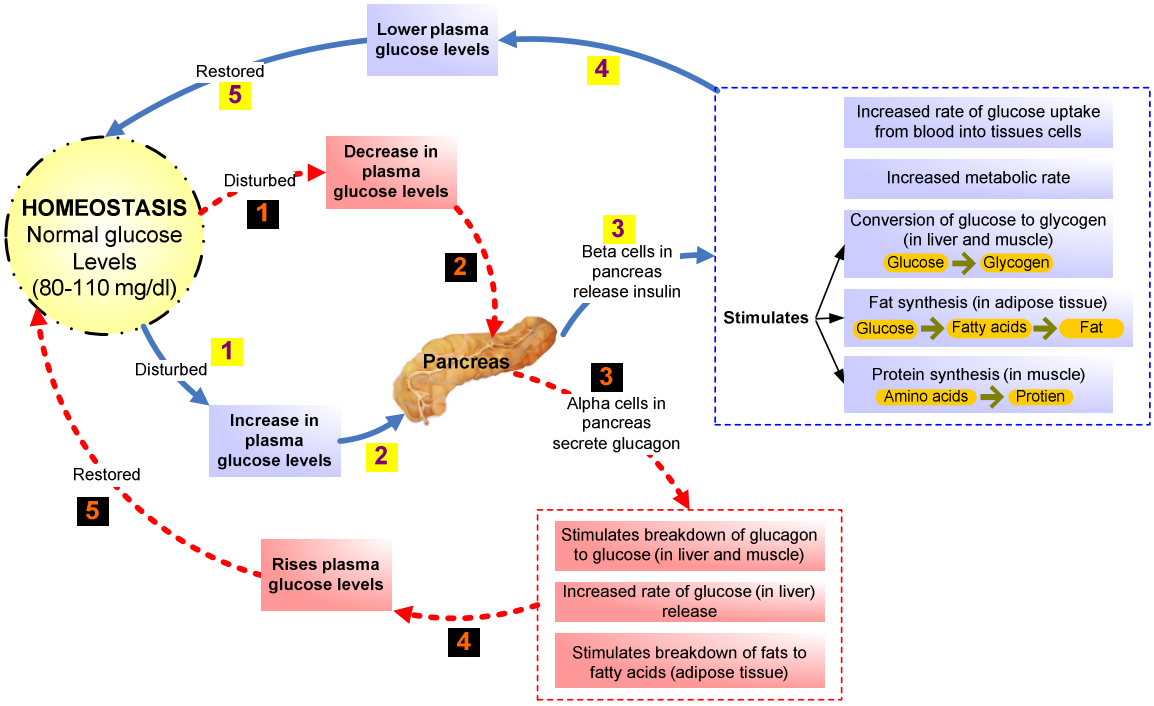

Figure 1.4: **Physiological glucose-insulin regulatory system**

The red dashed line shows the case where plasma glucose is decreased and the blue line shows the case where plasma glucose is increased. The numbers in both cycles represent the order of each process.

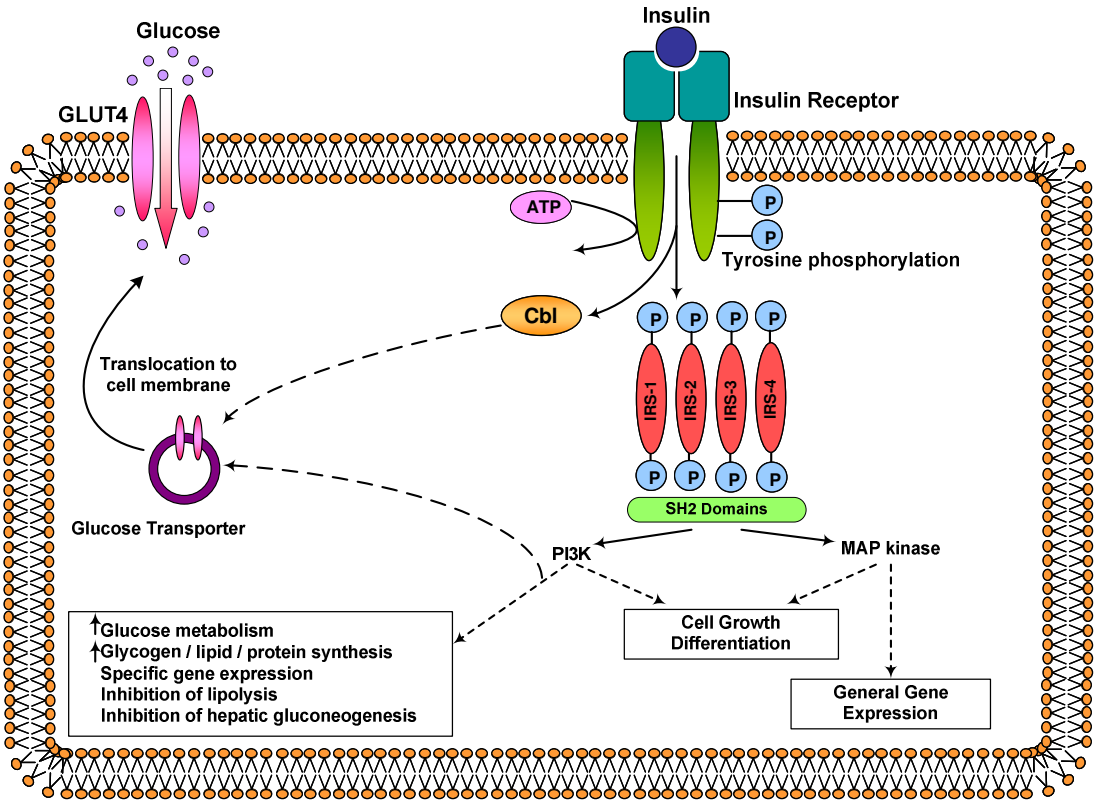

Figure 1.5: **Schematic overview of insulin signalling pathways leading to glucose transport**

Insulin binds to its receptor, resulting in phosphorylation of the receptor and intracellular substrates such as the insulin receptor substrates (IRSs) molecules and protein Cbl. When the tyrosine residues are phosphorylated, these substrates serve as docking proteins between the insulin receptor and a complex network of intracellular signalling molecules containing Src homology 2 (SH2) domains. These interactions lead to a diverse range of insulin signalling pathways, involving the activation of phosphoinositide 3-kinase (PI3K), mitogen-activated protein (MAP) kinase and other proteins which mediates most metabolic actions of insulin, including stimulation of GLUT4 (glucose transporter 4, an insulin-dependent transporter) and metabolism.

Chapter 2

Mathematical models in energy homeostasis

Diabetes and obesity present a mounting global challenge. Clinicians are increasingly turning to mechanism-based mathematical models for a quantitative definition of physiological defects such as insulin resistance, glucose intolerance and elevated obesity set points, and for predictions of the likely outcomes of therapeutic interventions. However, a very large range of such models is available, making a judicious choice difficult. To better inform this choice, the most important models published to date in a uniform format, discussing similarities and differences in terms of the decisions faced by modellers were presented. We review models for glucostasis, based on the glucose-insulin feedback control loop, and consider extensions to long-term energy balance, dislipidæmia and obesity.

2.1 Introduction

Energy homeostasis requires the co-ordination of several metabolic fluxes. In broad outline, these fluxes comprise (i) the use of nutrients as metabolic fuels; (ii) the disposition into storage of any nutrient supply surplus to immediate demands; and (iii) the mobilisation of nutrients from these stores when required (e.g. Frayn, 2003). Among the hormonal factors regulating these fluxes, insulin occupies a central position due to its wide-ranging effects on blood glucose levels, cell growth and appetite, as well as internal energy stores (Brook & Marshall, 2001). The latter effect is predominantly anabolic: insulin stimulates glycogenesis, the accumulation of triglycerides in adipose tissue, and amino acid uptake into muscle, while it inhibits gluconeogenesis, lipolysis and (in muscle) proteolysis (Brook & Marshall, 2001). One could regard the insulin control loop as the fundamental "first-order" endocrine control, with other factors (thyroxine, cortisol, glucagon, GH, ILG-1, adipokines, catecholamines) providing a "second-order" adjustment to the precise physiological circumstances (Schwartz *et al.*, 1987; Raju & Cryer, 2005).

The co-ordination of metabolic fluxes at the systemic level requires an interplay between various organs and tissues which each make different contributions to the overall energy balance. Break-down of this coordination leads to abnormalities in energy stores and the blood levels of glucose, lipids, ketone bodies and electrolytes (e.g. Salway, 2004). This web of mutually exacerbating abnormalities may stress the insulin control loop until its ability to compensate for the deviations is finally overcome. Consequently, hyperglycæmia is a common end

point, whether or not the initial defect occurred in insulin production, secretion or sensitivity. The resulting syndrome of diabetes mellitus is associated with a variety of long-term complications, many of which are thought to arise from hyperglycæmia via protein glycation and oxidative stress (Brownlee, 2001; Fajans *et al.*, 2001).

The clinical management of hyperglycæmia (and attendant abnormalities in blood lipids and lipid stores) requires a thorough understanding of the interactions between the liver, pancreas, fat stores and blood nutrient levels. An explicit representation of this complex dynamical system can aid the interpretation of diagnostic tests and help formulate therapeutic interventions. To this end, a large range of various mathematical models have been proposed in the literature. The purpose of this chapter is to bring together these mathematical models and present them, for ease of comparison, in a uniform format. Thus, we present the various models in a standardised notation (summarised in Table 2.1) and a uniform graphical format (viz. dynamical charts). We emphasise connections between the models in term of different choices the modeller has to make, and we discuss these choices with reference to the underlying physiology.

We stress the central ideas behind the models and the key insights that can be gained from them, as well as the relationships between models and on their physiological grounding. The present chapter thus complements previous reviews that explicitly list systems of equations for the models available in the literature (for such reviews see van Reil, 2004; Boutayeb & Chetouani, 2006; Makroglou, 2006). We hope that the survey will prove useful to modellers as well as to endocrinologists and clinicians who wish to apply mathematical models in their research and require a general orientation.

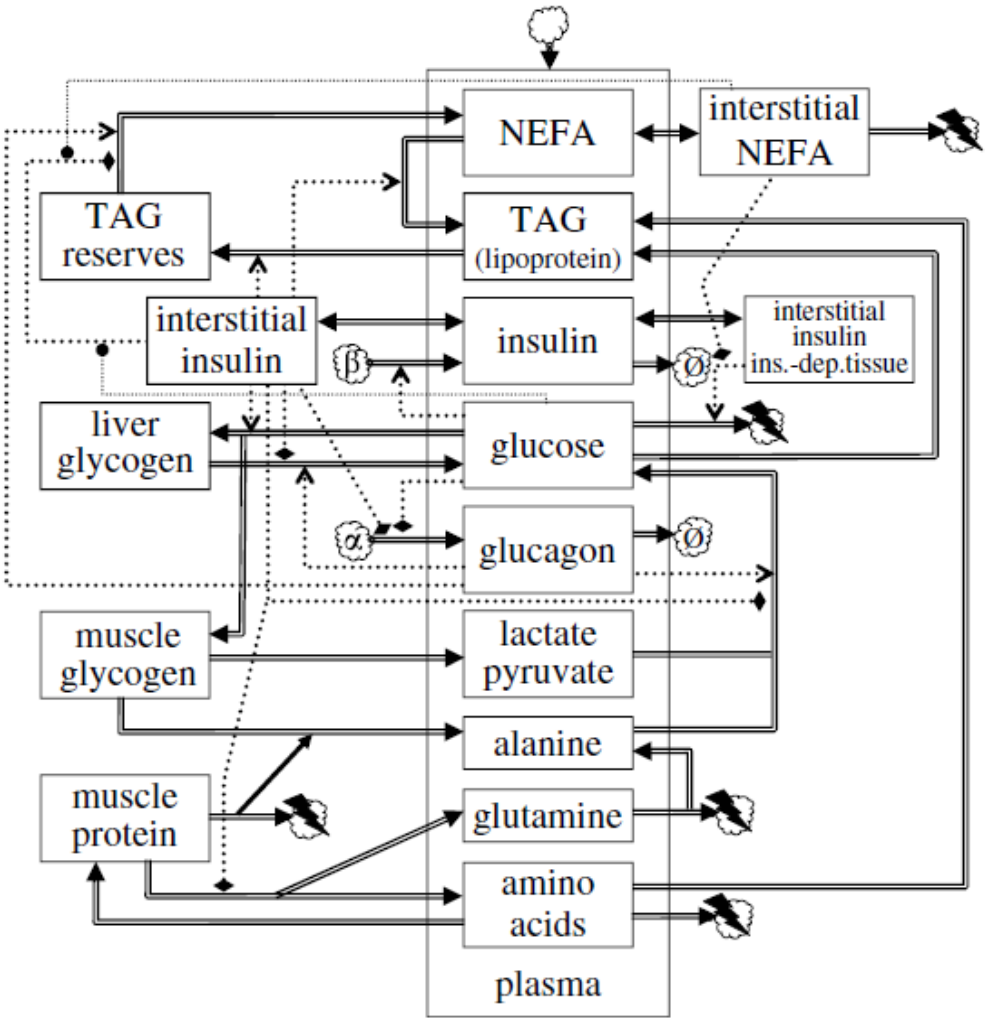

Figure 2.1: Dynamics chart of energy homeostasis

State variables are shown as rectangular boxes: those in the enclosure marked 'plasma' represent blood plasma concentrations. Boxes on the left-hand side represent internal stores. Fluxes are represented as double arrows. Endocrine interactions are shown as dotted arrows: positive as normal arrowheads, negative as flattened diamonds, modulatory as circles. Sources or sinks are represented as clouds. The top cloud represents an influx from the diet or clinical administration of substances. The cloud marked 'α' represents pancreatic α-cells and the cloud marked 'β' represents pancreatic β-cells; clouds marked 'ϕ' correspond to degradation and those with a lightning flash correspond to the usage as metabolic fuel. TAG: triacylglycerides; NEFA, non-esterified fatty acids; ins.-dep. tissue, insulin-dependent tissue. Further details are explained in the discussion of individual models.

2.2 Overview of energy homeostasis models

The main physiological and endocrine interactions underlying energy homeostasis in humans are depicted schematically in Figure 2.1. This chart shows how the various models proposed in the literature fit together (generally in dynamics charts, state variables are shown as boxes, rates or fluxes as double arrows going into or out of these state variable boxes, and flows of information (i.e. regulatory dependencies) are shown as dotted arrows, while sources or sinks are shown as clouds). Plasma glucose and plasma insulin are at the heart of all these models, and therefore the survey will start with 'glucocentric' models that focus on these two factors. More elaborate models include the non-esterified fatty acid (NEFA) pool, as well as internal stores (glycogen for carbohydrate, adipose tissue for lipids, protein for amino acids); moreover, dynamically more refined models differentiate between interstitial pools and the general blood compartment as well as time delays for certain physiological response components. These elements will be discussed in more detail below.

Mathematically, the models typically assume the form of a system of (generally non-linear) ordinary differential equations; thus, each state variable (box) in Figure 2.1 corresponds to a first-order ordinary differential equation. Section 2.3.2 below discusses extensions to delay-differential equations and integro-differential equations.

2.3 Models of glycæmic regulation

Insulin and glucose are at the heart of the dynamics chart (Figure 2.1) and form the fundamental glycæmic homeostatic feedback loop. Only two state variables are needed for a model limited to this fundamental loop, and more advanced models can be viewed as variations of this simple two-state model.

2.3.1 Basic glucostasis

At the heart of glucostasis lies the basic glycæmic feedback loop represented in Figure 2.2. The simplest mathematical model of this loop deals only with the plasma levels of insulin and of glucose (Bolie, 1961). The following ODEs are basic balance equations:

$$\frac{d}{dt} I^{[p]} = \Phi_I(G^{[p]}) - \lambda_I I^{[p]} \tag{2.1}$$

$$\frac{d}{dt} G^{[p]} = \Phi_G(I^{[p]}, G^{[p]}, t) - \Psi_G(I^{[p]}, G^{[p]}) \tag{2.2}$$

where $I^{[p]}$ is the plasma level of insulin and $G^{[p]}$ denotes the plasma level of glucose. Insulin is secreted by the pancreatic β-cells at a rate Φ_I, treated as a function of $G^{[p]}$ alone. Insulin is cleared from the plasma with a physiological half-life equal to $\ln\{2\}/\lambda_I$, where λ_I is the insulin clearance rate constant. More generally, it is reasonable to suppose that Φ_I also depends on $I^{[p]}$; Kulkarni *et al.* (1999) show that in β-cell insulin receptor knockout mice, first-phase insulin secretion in response to glucose is ablated. It is known that β-cells express an insulin receptor, although regulation of β-cell proliferation may be the primary function (Okada *et al.*, 2007). A case could also be made for an explicit dependence on t of the term Φ_I , to account for the parasympathetic influence on β-cells.

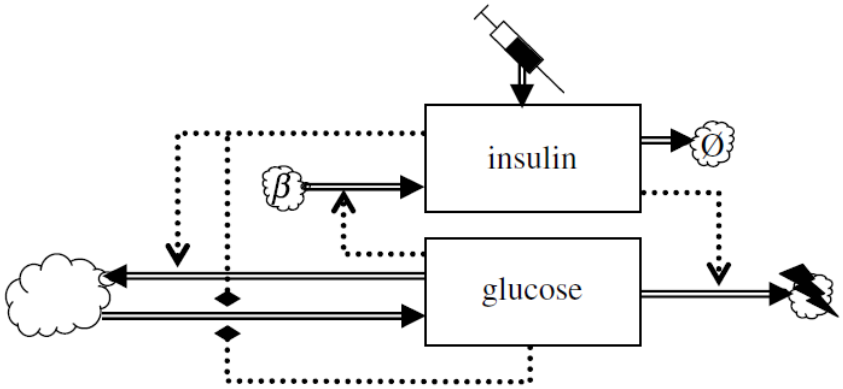

Figure2.2: Two-component glycæmic feedback model

The syringe represents administration of insulin. The large cloud represents the combined glucose sources and sinks.

The gastro-intestinal tract is the main exogenous source of glucose. Endogenous sources are glycogen mobilisation and hepatic gluconeogenesis from muscle protein or muscle glycogen via pyruvate or lactate (Frayn, 2003). The basic model lumps all these processes together into a single term Φ_G, whose explicit dependence on time t accommodates the dependence on the exogenous input

regime. Glucose transport into the tissues is represented by Ψ_G. This is also a lumped term, combining (i) insulin-independent transport, which depends only on $G^{[p]}$, (ii) insulin-dependent transport which depends on $I^{[p]}$ as well as $G^{[p]}$ (Frayn, 2003), and, (iii) renal excretion of glucose; this flux is important in hyperglycæmia (Watkins, 2003).

The mode of action of this negative feedback mechanism is intuitively clear (cf. Figure 2.2): increased $G^{[p]}$ promotes insulin secretion, and insulin in turn promotes the clearance of glucose from the plasma, stimulating both the formation of glycogen storage and utilisation of glucose as a metabolic fuel in the insulin-dependent tissues (Brook & Marshall, 2001). In the simple two-state model, these are sources and sinks outside the scope of the model, whereas more comprehensive models treat the internal stores as explicit state variables. The dynamics of the basic model is illustrated in Figure 2.3.

2.3.1.1 Analysis of the basic model: quantification of insulin sensitivity

Clinical management of diabetes is aimed at a restoration of $G^{[p]}$ to normal values, or at least prevent excursions beyond the range of concentrations found in healthy subjects (Watkins, 2003). This is reasonable in view of the fact that diabetic complications (such as vascular disease, neuropathy, retinopathy, nephropathy) are thought to result from hyperglycæmia via a small number of common pathways (Watkins, 2003).

Suppose that the exogenous glucose input is held constant, so that the glucose gain term loses its explicit time dependence: $\Phi_G(I^{[p]}, G^{[p]}, t) \equiv \overline{\Phi}_G(I^{[p]}, G^{[p]})$. The plasma glucose equilibrium value $\overline{G}^{[p]}$ is defined implicitly by:

$$\overline{\Phi}_G\left(\frac{\Phi_I(\overline{G}^{[p]})}{\lambda_I}, \overline{G}^{[p]}\right) = \Psi_G\left(\frac{\Phi_I(\overline{G}^{[p]})}{\lambda_I}, \overline{G}^{[p]}\right) \qquad (2.3)$$

(from equations (2.1) and (2.2)). This equation may have zero, one, or more solutions $\overline{G}^{[p]}$ and the precise functional form of the flux terms determines whether any of these is an attractor of the system's dynamics. On the basis of the

physio-endocrinological interpretation of the flux terms it is reasonable to assume that $\overline{\Phi}_I$ is monotone increasing in $G^{[p]}$, while Φ_G is monotone decreasing in both its arguments and Ψ_G is monotone increasing in both its arguments. Under these assumptions it can be shown that if equation (2.3) has a solution $\overline{G}^{[p]}$, it is unique and locally a stable attractor. The extent of the hyperglycæmic excursion (e.g. the "area under curve" or AUC which is the time-integral of $G(t)^{[p]} - G(t)_{\infty}^{[p]}$ following a glucose challenge, where $G(t)_{\infty}^{[p]}$ denotes the normoglycæmic value) depends on the slowest mode of the system (the fast mode is essentially λ_I): a faster slow mode implies a smaller excursion. The slow mode corresponds to *insulin sensitivity* of the system, given by the following formula:

$$\frac{\partial \Phi_I}{\partial G^{[p]}}\left(\frac{\partial \Psi_G}{\partial I^{[p]}} - \frac{\partial \Phi_G}{\partial I^{[p]}}\right)$$

(to be evaluated at the equilibrium point). A diminished ability of the pancreatic cells to respond to a glucose challenge may be due to a reduced β-cell mass, or reduced responsiveness of individual β-cells, or both (Watkins, 2003). This diminished pancreatic responsiveness corresponds to a reduction of the term $\partial \Phi_I / \partial G^{[p]}$. A major factor in the ætiology of diabetes is *insulin resistance* (Watkins, 2003), a reduced effectiveness of insulin on some of insulin's target tissues due to a reduced sensitivity to insulin. In the model, insulin resistance is reflected by a reduction of the second term, which will normally be dominated by $\partial \Psi_G / \partial I^{[p]}$. Further details on the use of these ideas in the analysis of glucose tolerance tests can be found in the papers by (Toffolo *et al.*, 1980; Steil *et al.*, 1993; Saad *et al.*, 1994; Prigeon *et al.*, 1996).

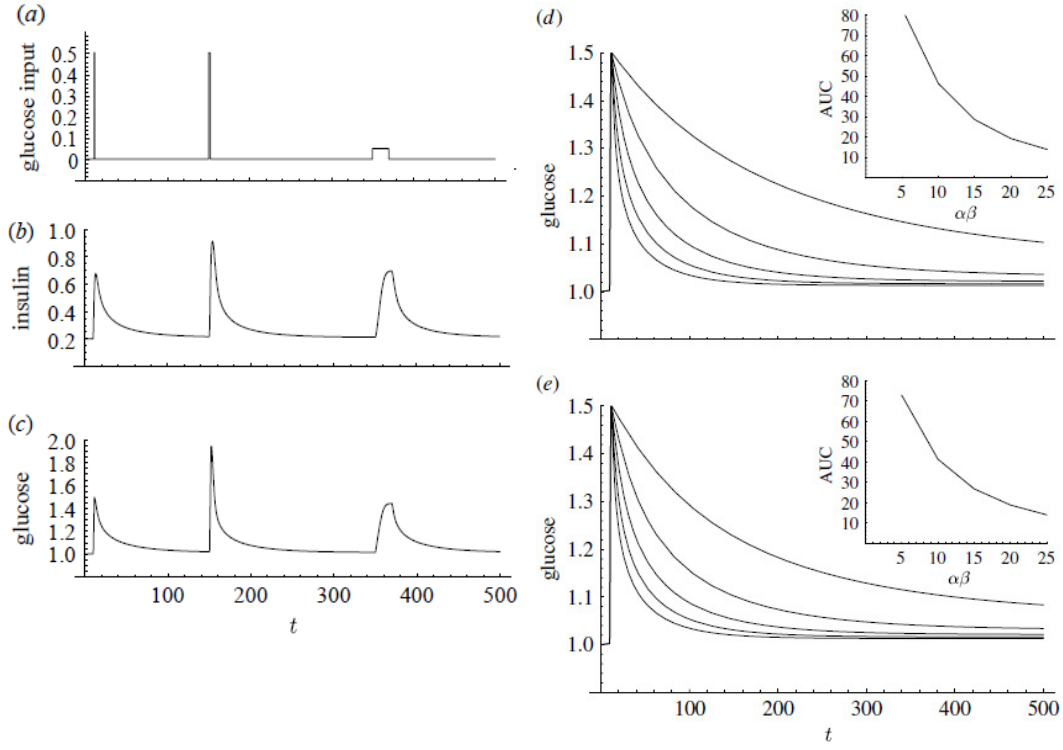

Figure 2.3: **Dynamics of a two-component glycæmic feedback model**

Model equations (in dimensionless units) are $\dot{x} = (1 + 4\exp\{\alpha(1 - y(t))\}^{-1} - x(t)$ (insulin) and $\dot{y} = \phi(t) - (1 + 200\exp\{\beta(0.2 - x(t))\})^{-1}(1 + \frac{\varepsilon}{y(t)})^{-1}$ (glucose). Parameter values are $\alpha = \beta = 5$, $\varepsilon = 0.05$. (a-c) Simulated time courses for a given scaled glucose input function $\phi(t)$ ((a) glucose input flux, (b) scaled plasma insulin concentration, (c) scaled plasma glucose concentration). (d) Glucose plasma response curves to a fixed glucose input pulse at various values of β-cell sensitivity (α); the slower return corresponds to diminished pancreatic glucose sensitivity. The sensitivity coefficient for this system is $\alpha\beta$. The area under curve (AUC), which is a measure for the extent of the glucose excursion, is shown as a function of $\alpha\beta$ in the inset. (e) Glucose plasma response curves to a fixed glucose input pulse at various values of insulin sensitivity (β); the slower return corresponds to insulin insensitivity. AUC is shown as a function of $\alpha\beta$ in the inset.

2.3.1.2 Functional specification of the flux terms

The system, equations (2.1, 2.2), leaves the flux terms unspecified. Simple obvious choices include linear models of the form

$$\Phi(X) = \Phi_0 + \alpha_X X \tag{2.4}$$

where Φ is some flux dependent on a factor X and Φ_0 and α_X are (possibly negative) parameters, and Hill-type expressions:

$$\Phi(X) = \Phi_X \frac{X^{m_X}}{K_X^{m_X} + X^{m_X}} \tag{2.5}$$

where Φ_X, K_X, and m_X are positive parameters; K_X is the value of X such that $\Phi(X) = \Phi_{\max}/2$ and m_X governs how steeply the function rises about this midpoint. Fluxes that depend on multiple factors (X,Y) are often taken to be bilinear terms $\propto XY$. Inhibitory interactions are often modelled in this way, with the risk that the flux spuriously changes sign somewhere during the simulated process. A more prudent choice for an inhibitory interaction is multiplied Hill terms, e.g.:

$$\Phi(X,Y) = \Phi_X \frac{X^{m_X}}{K_X^{m_X} + X^{m_X}} \times \frac{K_{YX}^{m_{YX}}}{K_{YX}^{m_{YX}} + Y^{m_{YX}}} \tag{2.6}$$

where Y represents the concentration of a factor that inhibits the flux, characterised by location and steepness parameters K_{YX} and m_{YX}.

The justification for such specifications is limited. It is hoped that they are qualitatively correct and it is tacitly hoped or assumed that the details will not affect the outcome appreciably. This may be reasonable in view of the uncertainties that accrue on a more mechanistic approach, which splits the lumped terms into numerous terms representing processes in various different tissues. Even if each term could be modeled accurately, accurate parameter estimation may be difficult. This provides some rationale for the cruder, simpler approach. Another difficulty is that the molecular transport machinery is embedded in cellular regulation. To indicate the problems encountered we consider the example of insulin-dependent glucose transport.

Insulin-dependent glucose transport

A simple model for insulin-dependent glucose uptake is the bilinear model $\propto I^{[p]}G^{[p]}$. If we take into account all relevant sub-cellular processes, such as intracellular insulin signalling, glycolytic pools of hexoses and trioses and their regulation, we end up with a dynamical system with > ~100 state variables. For example, Sedaghat *et al*. (1992) formulate a model with 20 state variables for the insulin/GLUT4 part of the system alone (GLUT means glucose transporter, GLUT4 being the insulin-responsive variant; see Silverman, 1991). The purposes at hand dictate which of these approaches is most suitable. For instance, in the analysis of a glucose tolerance test, it suffices to know that GLUT4 translocation to the cell membrane in the presence of insulin happens quasi-exponentially with a relaxation time of about 5 minutes; this reduces the 20 state variables in the Sedaghat model to just one. On the other hand, when one is interested in how a drug affects this relaxation time, the 20-dimensional model is appropriate.

The influence of intracellular metabolites can be appreciated by considering the following simple, but mechanistically reasonable expression for glucose transport into a cell:

$$\psi^{[GLUT]} = \vartheta n_{GLUT} \frac{K_d (G^{[p]} - G^{[i]})}{(G^{[p]} + K + K_d)(G^{[i]} + K + K_d) - K_d^2} \qquad (2.7)$$

(see (Keener & Sneyd, 1998), for a derivation). Here ϑ, K, and K_d are positive parameters and n_{GLUT} is the number of GLUT molecules translocated to the cellular membrane, and $G^{[i]}$ is the intracellular concentration of glucose. Let $\phi_P(G^{[i]}, \omega)$ denote the rate at which glucose is converted into glucose-6-phosphate (the first metabolic conversion which immediately follows uptake). Here the vector ω collects the intracellular factors that affect this rate. If ω is fixed, $G^{[i]}$ is found by solving $\psi^{[GLUT]} = \phi_P$; this flux can then be computed from n_{GLUT} and $G^{[P]}$. However, the situation is more complicated since any changes in $G^{[i]}$ generally lead to compensatory changes downstream in glycolysis and ATP generation. This means that ω will change as well, and this must be taken into account to determine the shape of the response curve which describes $\psi^{[GLUT]}$ as a function of $G^{[P]}$.

A detailed analysis shows that the asymptotic maximum of this curve is determined by metabolic demand rather than n_{GLUT} and that the midpoint of this curve is an increasing function of the ratio between metabolic demand and n_{GLUT}. If we approximate the actual response curve by a Hill-type function, we have that the 'midpoint' parameter K_X is (i) an increasing function of metabolic demand, and (ii) inversely proportional to n_{GLUT}. For tissues that express GLUT1, which is not insulin-responsive, n_{GLUT1} does not depend on $I^{[P]}$ and the midpoint parameter can be expected to rise linearly with the demand flux. By contrast, in tissues that express GLUT4, n_{GLUT4} depends on $I^{[P]}$ and the dependence on the midpoint parameter on demand becomes more complicated, being insensitive at low demand and very sensitive at high demand. These different responses necessitate a decomposition of Ψ_G into several terms, corresponding to the fluxes borne by tissues expressing different glucose transporters.

An important consequence of the role of intracellular regulation in this model is that it explains why the effectiveness of insulin is reduced under hyperglæmia or hyperlipidæmia. According to the model, insulin levels do not affect the maximum flux, but only act to reduce the midpoint parameter. This allows effective regulation of insulin-dependent glucose uptake as long as plasma glucose levels remain sufficiently low. The critical level where effective control starts to fail is lower when metabolic demand for glucose is lower, for instance when β-oxidation of fatty acids provides a substantial flux of AcCoA.

2.3.2 Glycæmic loop models with time delays in cellular responses

Cellular responses are not instantaneous and thus introduce delays into the system. Pancreatic β-cells and liver cells introduce such delays in their responses to, respectively, glucose and insulin; see Figure 2.4. These delays can introduce dynamical instability, that is, oscillations in the $I^{[P]}, G^{[P]}$ dynamics.

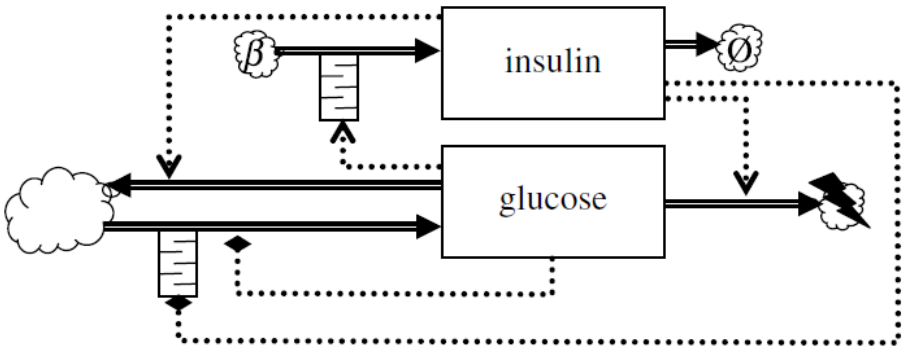

Figure 2.4: Two-component glycæmic feedback model extended with time delays, indicated by queue symbols, in the pancreatic β-cell response to glucose and in the hepatic response to insulin.

2.3.2.1 'Hard' delay models

Pancreatic β-cells introduce a time delay as the insulin secretion rate takes some time to adapt to the plasma glucose levels. From a modelling perspective, one option is to represent this delay explicitly:

$$\Phi_I(G^{[P]}(t)) \rightarrow \Phi_I(G^{[P]}(t-\tau_{I,d})) \tag{2.8}$$

where $\tau_{I,d}$ is the response delay incurred by the pancreatic β-cells as they respond to changes in the plasma glucose levels. A 'hard' delay $\tau_{I,d}$ in the pancreatic β-cell response was investigated by (Bennette, 2004; Li, 2007).

A generalisation of the delay replacement (equationn (2.8)) is as follows:

$$\Phi_I(G^{[P]}(t)) \rightarrow \Phi_I(\tilde{G}^{[P]}(t)) \tag{2.9}$$

where $\tilde{G}^{[P]}(t)$ is a new auxiliary variable, defined by:

$$\tilde{G}^{[P]}(t) = \int_{-\infty}^{0} G^{[P]}(t+s)\ \omega(s)ds$$

where ω is a convolution kernel function. The 'hard' delay, equation (2.8), is retrieved by taking the kernel $\omega(s)$ to be the Dirac delta function $\delta(\tau_{I,d}+s)$.

2.3.2.2 'Soft' delay models

Many delay models proposed in the literature use the gamma kernel:

$$\omega(s) = \frac{(-s)^{n-1} \exp\{+ns/\tau_{I,d}\}}{(\tau_{I,d}/n)^n \Gamma(n)}. \tag{2.11}$$

The advantage of this kernel is that it can be implemented by extending the dynamics with a finite number of state variables. Thus, n auxiliary state variables are defined, with the following dynamics:

$$\frac{d}{dt} x_1(t) = \frac{n}{\tau_{I,d}} (G^{[p]}(t) - x_1(t)) \tag{2.12}$$

$$\frac{d}{dt} x_i(t) = \frac{n}{\tau_{I,d}} (x_{i-1} - x_i) \quad for \;\; i = 2,...,n \tag{2.13}$$

and $x_n(t)$ is used instead of $I^{[p]}(t - \tau_{G,d})$. For $n \to \infty$, the Gamma kernel approaches the 'hard' Dirac kernel. The effects of delays can often be effectively be mimicked with a relatively low n. At least for small n, the mathematical analysis of such a 'soft' delay approximation can be easier to deal with than the corresponding 'hard' delay formulation, for instance in local stability analysis.

There is also a delayed response in hepatic glucose production from glycogenolysis. Tolić *et al*. (2000) consider a 'soft' hepatic time delay (n = 3) $\tau_{G,d}$ for $G^{[p]}$ as input to Φ_G:

$$\Phi_G(I^{[p]}(t), G^{[p]}(t), t) \to \Phi_G(I^{[p]}(t), G^{[p]}(t - \tau_{G,d}), t) \tag{2.14}$$

whereas Engelborghs *et al*. (2001) investigated the hard delay case. More complex models incorporate both the pancreatic delay and the hepatic delay. These have been studied by Li *et al*. (2001) and Li *et al*. (2006). Explicit time delays constitute a fairly phenomenological approach to cellular response lags. Li *et al*. (2006) point out that a physiologically realistic model would have to describe the kinetics of intracellular pools (e.g. the hexose phosphate pool and the triose phosphate pool) as well as the activation/inactivation kinetics of key enzymes such as glucokinase, glucose 6-phosphatase, and phosphofructokinase. In as much as a physiologically realistic model would add a finite (and preferably modest) number of additional state

variables, it would introduce a 'soft' rather than a 'hard' delay. One could thus argue that an $n = 3$ 'soft' delay is a more reasonable ersatz for a physiologically realistic model than an explicit delay.

Other delay kernels

De Gaetano and Arino (2000) considered a 2-ODE minimal model extended to a DDE model with a generalised delay on β-cell insulin secretion. For the glucose kinetics they assume the Roy specification, equation (2.22), with $\alpha = 0$, whereas for the insulin secretion rate they adopt the specification

$$\Phi_I(\tilde{G}^{[p]}(t)) \to \eta \tilde{G}^{[p]}(t) \tag{2.15}$$

(with positive parameter η). Finally, they assume the following *uniform kernel*:

$$\omega(s) = \begin{cases} \dfrac{1}{\tau_{I,d}} & for\ -\tau_{I,d} < s < 0 \\ 0 & otherwise \end{cases}. \tag{2.16}$$

On these assumptions, De Gaetano and Arino (2000) showed that the dynamics admits no more than one equilibrium with both $I^{[p]}$ and $G^{[p]}$ positive. Mukhopadhyay and his coworker showed that this result obtains for this model in the more general case where ω is a probability density function whose mean exists; the Dirac kernel, the gamma kernel and the uniform kernel all belong to this class (Mukhopadhyay, 2004). Li *et al*. (2006) studied the same model, but replacing specification equations (2.22) and (2.15) by more general functions.

2.3.3 Extended models for glucostasis

The simple two-state variable model is based on the implicit assumption that other dynamic degrees of freedom relax more quickly than those included in the simple model. However, this assumption is not warranted in general. Modellers have thus turned to models with additional state variables, as illustrated in Figure 2.5.

2.3.3.1 Endocrine dynamics

The model (equations (2.2) and (2.1)) lumps exogenous and endogenous glucose inputs into a single term Φ_G. The endogenous processes (glycogenolysis and gluconeogenesis) are controlled by insulin and various other endocrine factors, the most important of which is glucagon. Making this regulatory loop implicit, the positive flux term is replaced by an exogenous and an endogenous term:

$$\Phi_G(I^{[p]}, G^{[p]}, t) \xrightarrow{\text{replace in equation (2.2)}} \Phi_G^{[exo]}(t) + \Phi_G^{[endo]}(I^{[p]}, A^{[p]}) \quad (2.17)$$

where $A^{[p]}$ is the glucagon concentration in the blood plasma (the term $\Phi_G^{[endo]}$ still lumps together glycogenolysis and gluconeogenesis). The exogenous input is a *forcing function*: it depends on t, reflecting the fact that the time course of glucose supply is controlled by external factors. The term $\Phi_G^{[endo]}$ can be calculated as the rate at which glucose is absorbed from the diet or supplied by infusion, divided by the volume of the glucose distribution space (e.g. Roy and Parker, 2006). To close the system, an ODE for $A^{[p]}$ must be supplied, e.g.,

$$\frac{d}{dt}A^{[p]} = \Phi_A(I^{[p]}, G^{[p]}) - \lambda_A A^{[p]} \quad (2.18)$$

where $\ln\{2\}/\lambda_A$ is the physiological half-life of glucagon and $\Phi_A(I^{[p]}, G^{[p]})$ is the production function dependent on $G^{[p]}$ and $I^{[p]}$. The dependence on $G^{[p]}$ is included because glucagon is secreted in response to low glucose levels (Brook & Marshall, 2001) whereas the dependence on $I^{[p]}$ accommodates the inhibitory effect of insulin on glucagon secretion (Greenstein & Wood, 2006). A quasi-steady state approximation for A is $\Phi_A(G^{[p]})/\lambda_A$, which provides a justification for the dependence of Φ_G on $G^{[p]}$ in the two-state variable model described previously. If the desired time resolution is no finer than $1/\lambda_A$ the original formulation can be retained.

(a)

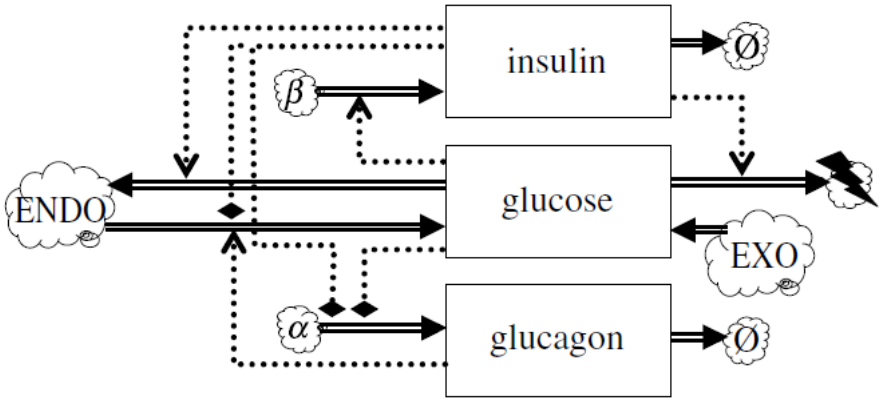

(b)

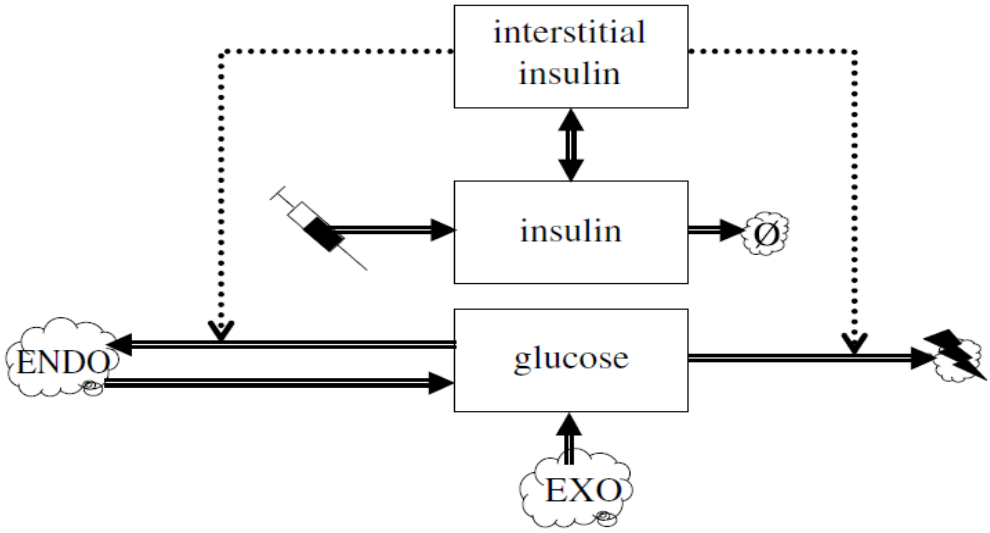

Figure 2.5: Glycæmic feedback models with additional state variables. (a) model extended with plasma glucagon. (b) the standard minimal model, the two-component model extended with an additional interstitial insulin compartment. Clouds marked 'EXO' represents exogenous sources of glucose, clouds marked 'ENDO' endogenous sources.

2.3.3.2 Interstitial space: tissue compartments

The physiological response to insulin may appear to lag behind the response expected on the basis of the insulin plasma level $I^{[p]}$. Part of this lag can be explained from the distribution kinetics of insulin. To account for this, one may add one or more tissue compartments to the model, also known as *remote compartments* (Roy & Parker, 2006). For each compartment, an additional ODE must be supplied to describe $I_\ell^{[is]}$ the *interstitial fluid concentration* of insulin in the ℓth tissue compartment:

$$\frac{d}{dt} I_{\ell}^{[is]} = \kappa_{I,\ell} (I^{[p]} - I_{\ell}^{[is]}). \tag{2.19}$$

This equation models a passive exchange process with transport parameter $\kappa_{I,\ell}$ (e.g. Sturis *et al.*, 1991; Tolic *et al.*, 2000). To balance these exchange fluxes, equation (2.1) must be modified, as follows:

$$\frac{d}{dt} I^{[p]} = \Phi_I(G^{[p]}) - \lambda_I I^{[p]} - \sum_{\ell} \kappa_{I,\ell} (I^{[p]} - I_{\ell}^{[is]}) \tag{2.20}$$

where the sum is taken over all additional tissue compartments accounted for in the model. Glucose kinetics (equation (2.2)) must also be adapted to reflect the fact that the endogenous fluxes respond to the interstitial insulin concentration rather than the plasma level. Thus, equation (2.2) becomes:

$$\frac{d}{dt} G^{[p]} = \Phi_G^{[exo]}(t) + \Phi_{G,0}^{[endo]}(I_0^{[is]}, G_p) - \sum_{\ell} \Psi_{G,\ell}(I_{\ell}^{[is]}, G_p) \tag{2.21}$$

Here, $\ell = 0$ denotes the hepatic tissue compartment, where endogenous glucose generation from glycogenolysis and gluconeogenesis are realised (muscle glycogenesis yields three-carbon intermediates which are converted to glucose in the liver). The index ℓ is included in the utilisation terms to reflect the possible variation in insulin sensitivity among tissue compartments. A model with three interstitial compartments (following the central plasma compartment) for glucose and two for insulin is analysed in detail in the excellent paper by Silber *et al.*, 2007. Their model illustrates another use for interstitial insulin compartments: *viz.* to simulate the slow-release effect from a bolus injection (bolus injections are represented mathematically as a Dirac inputs; such an input at time $t = 0$ can equivalently by implemented by a non-zero initial condition).

When the transport coefficient is assumed to be equal for all compartments ($\kappa_{I,\ell} \equiv \kappa \forall \ell$), the interstitial insulin concentrations will likewise converge to a common value. Discounting the initial transient, a single state variable $I^{[is]}$ then suffices. The resulting model, Figure 2.5 (b), is a three-ODE model known as the s*tandard minimal model*, first proposed by Bergman *et al.*, 1981. Roy and Parker (2006) propose simple functional specifications for the glucose fluxes:

$$\left.\begin{array}{ll} & \Phi_G^{[endo]}(I^{[is]}) \to \Phi_0 - \alpha I^{[is]} \\ and & \\ & \Psi_G(I^{[is]}, G^{[p]}) \to (\beta + \gamma I^{[is]}) G^{[p]} \end{array}\right\} \qquad (2.22)$$

where Φ_0 is a baseline glucose release rate from the liver, the coefficient α expresses the inhibitory effect of insulin on gluconeogenesis (Gibney, 2003; Salway, 2004); β corresponds to insulin-independent glucose utilisation and γ accounts for insulin-dependent glucose utilisation. In a diabetic subject with $I^{[p]} \equiv 0$, the plasma glucose concentration then relaxes toward the value Φ_0 / β, which is the subject's baseline glycæmia.

Of course, additional interstitial state variables can be introduced for other soluble factors (e.g. the model described in section 2.4.1 accounts for interstitial fatty acids). Simpler models omit such compartments. The justification is analogous to the above argument for glucagon dynamics: thus, for any substance X, if $\kappa_{X,\ell}$ is sufficiently large, the tissue compartment lag will not be appreciable and $X^{[is]}$ (where X is any substance) can be replaced by $X^{[p]}$.

A generalised interstitial/plasma exchange model favoured by some authors (e.g. Roy and Parker, 2006) is as follows:

$$\frac{d}{dt} I_\ell^{[is]} = \kappa_{I,\ell}^{out} (I^{[is]} - I_{baseline,\ell}^{[is]})_+ - \kappa_{I,\ell}^{in} (I^{[p]} - I_{baseline,\ell}^{[p]})_+ \qquad (2.23)$$

where $(x)_+ = x$ if $x > 0$ and $(x)_+ = 0$ if $x \le 0$. This model has transport coefficients $\kappa_{I,\ell}^{in}$ and $\kappa_{I,\ell}^{out}$ which may have different values, for transport into and out of the interstitial compartments. The baseline parameters are positive constants which ensure that transport does not take place when the concentration in the donor compartment is below the baseline.

2.4 Integrated models of carbohydrate, fat, and protein metabolism

A key aspect of energy homeostasis is the coordinated use of various metabolic fuels. The glycæmic feedback loop is central to this coordination, since insulin also serves as a regulator of the use of lipids and protein as metabolic fuels (Figure 2.1; for the sake of conciseness, various endocrine factors which modulate insulin's action are omitted). The links with utilisation of fatty acids as a metabolic fuel is particularly important, and has been the focus of attention in integrated models, while the link with protein metabolism has received less attention.

2.4.1 Integrated lipid/glucose models

The glucose-fatty acid cycle is central to the interactions between carbohydrate and lipid metabolism (Randle *et al.*, 1963). Through its effects on the metabolic control of the glycolytic pathway, the oxidation of fatty acids reduces the uptake and oxidation of glucose, with the consequence that glucose utilisation is reduced compared with that expected at given concentrations of insulin and glucose in the plasma; this manifests itself as insulin resistance (as discussed in sections 2.3.1.1 and 2.3.1.2). The glucose load following a meal will activate insulin secretion, which stops the release of fatty acids from the adipose stores and promotes the disposition of plasma NEFAs toward these stores via low-density lipoproteins, while glucose and insulin drop to baseline levels between meals, promoting lipolysis and utilisation of NEFAs (Frayn *et al.*, 1993; Frayn, 2003).

2.4.1.1 Fatty acid utilisation

The key characteristics of the glucose cycle have been incorporated in the model proposed by Roy and Parker (2006). This model is based on the standard minimal model (see section 2.3.3) modified to have two interstitial compartments for insulin and an additional interstitial compartment for NEFAs which communicates with a plasma NEFA compartment, a new state variable $F^{[p]}$ (see the dynamics chart, Figure 2.6). One of the interstitial insulin state variables drives glucose disposition (marked "ins.-dep" in Figure 2.6) whereas the other drives disposition of NEFAs in adipose storage (a sink/source in this model). There are no endogenous sources of insulin, so insulin gains are due to external inputs (there is an additional

production term which causes insulin degradation to change sign at a "baseline value"). The model includes the standard dietary gain terms for plasma glucose and plasma NEFA. Fluxes that depend on a hormone concentration and a substrate are modelled as bilinear terms (e.g., $\propto I^{[is]}G^{[p]}$).

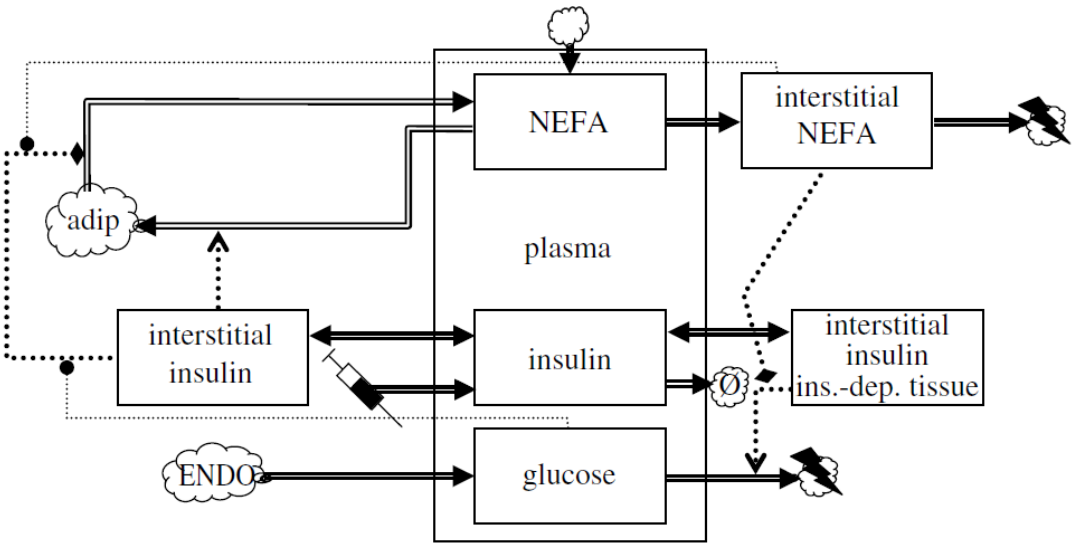

Figure 2.6: The standard minimal model extended with the glucose-fatty acid cycle. NEFA, non-esterified fatty acids; ins.-dep. tissue, insulin-dependent tissue; adip, adipocyte.

Noteworthy elements in the model are two modulatory interactions. First, Roy and Parker (2006) have included the inhibitory effect of plasma NEFA on glucose disposition, as a bilinear gain term $\propto G^{[p]}F^{[]p]}$, (again they include an additional gain term which causes a spurious sign change at baseline values). The model thus accommodates a form of insulin resistance. In addition, plasma glucose ($G^{[p]}$) and plasma NEFA ($F^{[p]}$) modulate lipolysis (NEFA mobilisation from adipose stores); this term is of the form $\propto F^{[p]}G^{[p]}\exp\{-G^{[p]}/G_0\}$ (with G_0 a positive parameter) and represents modulatory interactions which are experimentally observed (Knight & Iliffe, 1973). Roy and Parker (2006) obtain good model fits to experimental data, which include (i) decay of plasma NEFA under euglycæmic hyperinsulinæmic clamp; (ii) glucose disposition under intralipid infusion; and (iii) decay of $I^{[p]}$ and $G^{[p]}$ in response to an intravenous glucose tolerance test.

2.4.1.2 The glucose cycle with internal store dynamics

A model similar to the Roy & Parker model was proposed by Maas and Smith (2006); a dynamics chart is shown in Figure 2.7. The model differs from the previous model in that it explicitly represents internal reserves (glycogen and triacylglyceride [TAG] stores) as state variables. Both insulin and glucagon are represented as state variables. There are no interstitial compartments. The model contains an additional state variable which evolves on a slow time scale. Slow dynamics will be discussed below in section 2.5.2.1.

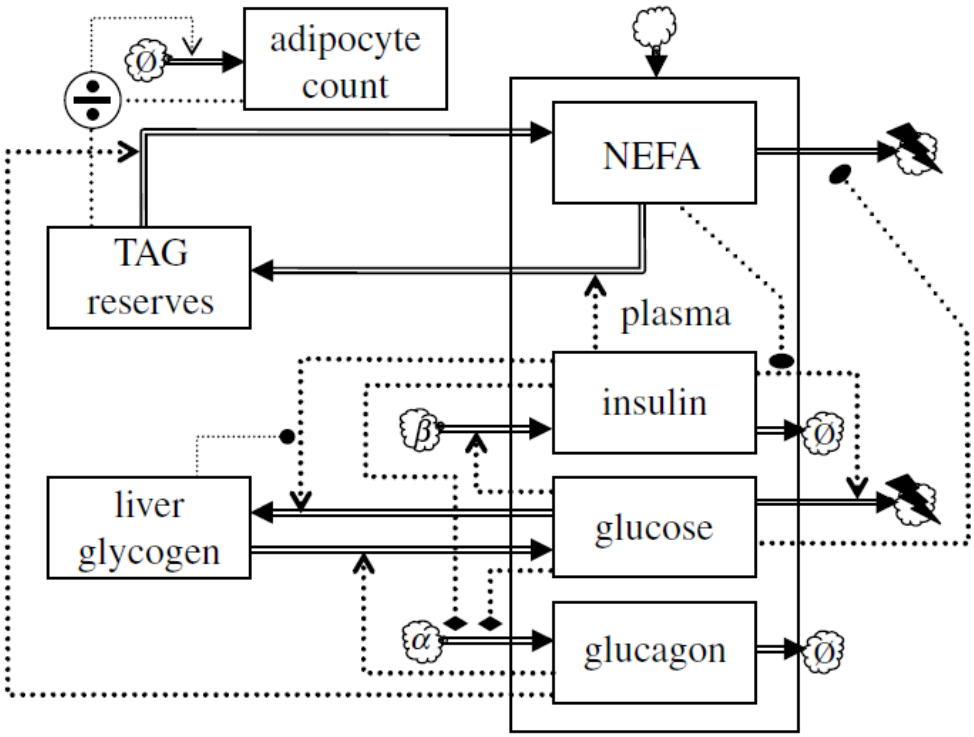

Figure 2.7: Glycæmic feedback model extended with fatty acid utilisation and a slow feedback loop based on adipocyte proliferation. The quotient symbol indicates computation of the ratio of the inputs.

Noteworthy features of this model are the inclusion of the inhibitory effect of insulin on glucagons secretion (modelled as a bilinear term $\propto I^{[p]}G^{[p]}$); and the division of energy utilisation into a component that is obligatory glucose-fuelled and a component which can use either glucose or NEFAs. In the latter component, the ratio of glucose utilisation over NEFA utilisation is assumed to be proportional to the corresponding ratio of plasma levels, $G^{[p]} : F^{[p]}$. The model also includes glycogen auto-regulation, which is a physiological phenomenon where the rate of glycogen

accumulation diminishes as the glycogen store size approaches a maximum capacity (Laurent *et al.*, 2000). Maas and Smith (2006) represent this by making the corresponding term proportional to the difference between the current glycogen store size and the maximum value.

2.4.2 The need to integrate 'glucocentric' models with protein metabolism

Muscle protein represents a considerable energy store. Under conditions of prolonged starvation or disuse atrophy, this store is mobilised and the amino acids derived from muscle proteolysis either serve as metabolic fuel, or are converted into glucose or fat (Karl *et al.*, 1976; Salway, 2004). Protein breakdown is connected to the glycæmic feedback loop since insulin is involved in the regulation of proteolysis (see Figure 2.1). Proteolysis is inhibited by insulin and promoted by cortisol and triiodothyronine (Karl *et al.*, 1976; Fereday *et al.*, 1998). Moreover, alanine is a substrate for gluconeogenesis. In view of these important links, it is perhaps surprising that protein metabolism is virtually ignored by the foregoing "glucocentric" models. However, this can be justified. To explain this, we first need to discuss the interface between carbohydrate and protein metabolism.

Amino acids can serve as metabolic fuel: muscle breaks down branched-chain amino acids, the liver covers half its energy requirements from amino acids and glutamine is an important metabolic fuel for mucosal intestinal cells (Frayn, 2003). However, use of protein for oxidation is a limited portion of total energy requirements in a well-fed subject. Second, while alanine certainly serves to carry nitrogen to the liver (which is cleared as urea), the carbon in alanine may derive primarily from pyruvate generated by glycolysis of muscle glycogen and glucose taken up by the muscle (Garber *et al.*, 1976a, 1976b; Karl *et al.*, 1976). Alanine is thus just a tricarbon shuttle in a pathway from muscle glycogen reserves to plasma glucose via gluconeogenesis in the liver. The justification of models of the type considered in section 2.3 is that these effectively subsume the alanine pathway, together with other gluconeogenic precursors, in the overall flux of glucose derived from a "lumped" source which accounts for hepatic as well as extra-hepatic glycogen reserves.

Nevertheless, representation of the glucogenic precursor pathways would be appropriate in more detailed models which explicitly represent muscle and liver glycogen stores as separate state variables. Besides the alanine cycle, such models would also account for the *Cori cycle* in which muscle releases the gluconeogenic precursors lactate and pyruvate (Salway, 2004). It has become clearer in recent years that these stores follow different dynamics and that extra-hepatic glycogen serves an important role as a post-prandial buffer of the carbohydrate load ingested with the meal (Taylor *et al.*, 1993; Taylor *et al.*, 1996; Meyer *et al.*, 2002). In fact, Woerle *et al*. (2003) found that almost a third of glycogen formation following a meal may be via the indirect pathway, via a gluconeogenic precursor such as alanine, pyruvate or lactate, some of which is temporarily stored as extra-hepatic glycogen. Models which treat liver and muscle glycogen stores as important separate components are appropriate for the analysis of these recent studies. Moreover, such models seem certain to be relevant to disorders of energy homeostasis, since the dynamic buffer function of muscle glycogen is impaired in type 2 diabetes (Carey *et al.*, 2003). Moreover, extra-hepatic glycogen stores play a role in the response to a positive energy balance (see below, section 2.5.2.2).

2.4.3 Glucoplastic versus ketoplastic carbon reserves

Glycogen reserves and muscle protein together constitute reserves of moderately to highly oxidised carbon, in contrast to lipid reserves, which store carbon almost exclusively in a more reduced form. This distinction is not only important from the point of view of energetic density per unit weight (Frayn, 2003), but also because mammals cannot synthesise glucose (or any other metabolite derived from the Krebs cycle intermediates succinyl-coA through to oxaloacetate) from fatty acids; while carbon atoms will readily pass through β-oxidation and the Krebs cycle, there can be no net gain since 2 carbon atoms are lost as CO_2 for every 2 atoms derived from fatty acids (Salway, 2004). The distinction between the two kinds of carbon is physiologically important since the ketoplastic carbon atoms of lipid reserves cannot be turned back into glucoplastic carbon atoms, whereas the latter can still be converted into ketoplastic carbon (the glycerol carbons of lipid reserves remain glucoplastic, of course; moreover, since one anabolic pathway branches off between the CO_2-evolving steps, there are amino acids such as

glutamine that must be reckoned as $\frac{1}{5}$th ketoplastic, and thus protein is in fact a mixed store of glucoplastic and ketoplastic carbon; similarly, citrate and isocitrate are $\frac{1}{3}$rd ketoplastic). Consequently, ketoplastic reserves are less versatile as anabolic precursors (i.e. building blocks for growth): most of the carbon in the lipid reserves will have to be used as fuel—lipid reserves are "deferred catabolism." On the other hand, carbon stored as glycogen can to some extent be "deferred growth," built-up in times of shortage of high-quality nutrition (minerals, nitrogen). Deferred growth is not only relevant to juveniles, but also to adults: while adults no longer grow, the females do supply building blocks to growing offspring. In sum, the rate at the whole-body level of conversion of glucoplastic to ketoplastic carbon represents a key life-history trade-off; if this rate does not, over prolonged periods of time, matches the rate at which carbon is oxidised to CO_2, obesity ensues.

2.5 Long-term dynamics

The models considered thus far were concerned with the physiological time scale at which the system absorbs acute glucose challenges. This is the minutes-to-hours time scale which is relevant for the response to short-term starvation between meals and for nutrient disposition following a meal. However, the processes underlying the development of obesity, diabetes (and their interplay in insulin resistance syndrome, or metabolic syndrome) take place on a longer (days-to-years) time scale. We here discuss various modeling approaches to this longer time scale.

2.5.1 Diabetic ætiology

Diabetes can develop as a primary dysfunction of glucostasis or secondarily when the demands placed on the glycæmic control system over-stress its capabilities. We discuss two modelling approaches to the long-term compensatory mechanisms.

2.5.1.1 Regulation of the pancreatic β-cell mass

The basic glycæmic feedback loop has what engineers call finite gain: the loop does not effectuate perfect regulation of plasma glucose levels. From equation (2.17) we have

$$\overline{\Phi}_G(I^{[p]}, G^{[p]}) \equiv \overline{\Phi}_G^{[exo]} + \Phi_G^{[endo]}(I^{[p]}, A^{[p]}),$$

where $\overline{\Phi}_G^{[exo]}$ is the fixed external glucose load. Thus the function $\overline{\Phi}_G$ is different for different glucose loads, and so is the glucose equilibrium point, via equation (2.3). However, a slow-acting second feedback mechanism operates, which ensures (at least under physiological conditions) that the long-term average plasma glucose is regulated to a value which does not depend on the average load. The mode of action is essentially what a control engineer would call integrating control (cf. Milhorn, 1966). This slow mechanism is based on the dynamics of the pancreatic β-cell mass:

$$\frac{d}{dt} M_\beta = M_\beta(\mu_\beta(G^{[p]}) - \lambda_\beta) \tag{2.24}$$

where M_β is the β-cell mass; $\mu_\beta(\cdot)$ is the β-cell proliferation function which relates the rate of β-cell proliferation to the plasma glucose level; glucose is known to potentiate the effect of IGF-1 which stimulates β-cell proliferation (Hugl *et al.*, 1998); and λ_β is the β-cell death rate. The specific pancreatic β-cell growth rate μ_β not only depends in plasma glucose, but has recently been shown to depend critically on insulin as well (Okada *et al.*, 2007). Thus a more realistic model would make μ_β also dependent on $I^{[p]}$.

To connect β-cell mass dynamics to the glycæmic loop model, the following replacement is made:

$$\Phi_I(G^{[p]}) \xrightarrow{\text{replace in equation (2.1)}} M_\beta \phi_I(G^{[p]}) \tag{2.25}$$

where ϕ_I is the insulin secretion rate per pancreatic β-cell. The resulting three-state variable model is depicted in Figure 2.8. Like Φ_I, the cell-specific function ϕ_I is assumed to be monotone increasing. With the assumptions as stated in section 3.3.1, $\overline{G}^{[p]}$ becomes a monotone decreasing function of M_β. This function can be substituted into equation (2.24) to obtain a scalar ODE for the slow time scale.

Let us assume, in the first instance, that $\mu(\cdot)$ is monotone increasing (i.e. glucose promotes β-cell proliferation). It is then easy to see that, on the slow time scale, $\frac{d}{dt}\ln M_\beta$ is a monotone decreasing function of M_β with a single zero corresponding to a stable global attractor. Thus, $\overline{G^{[p]}}$ will tend to the long-term equilibrium value $\mu_\beta^{-1}(\lambda_\beta)$ regardless of the glucose load (of course, variations in the glucose load will determine the extent of variations of $G^{[p]}$ around this value). This effect is typical of integrating control.

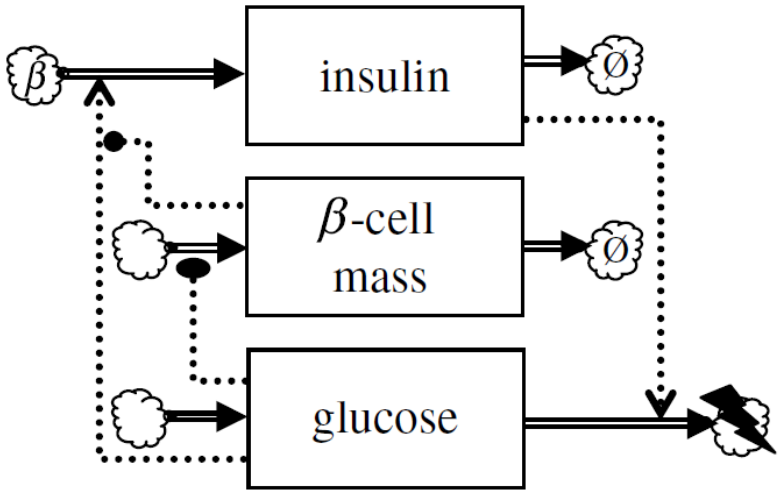

Figure 2.8: Glycæmic feedback model extended with slow feedback loop based on β-cell mass proliferation.

Catastrophic failure of the long-term loop

Topp *et al*. (2000) speculate that glucose tends to inhibit β-cell proliferation at high concentrations. Thus μ_β becomes a hump-shaped function, which first increases, then decreases (without becoming negative). As a result, M_β now has two equilibrium points, the lower of which is unstable. Consequently, sustained hyperglycæmia can induce net β-cell loss, which promotes further hyperglycæmia. The result is a catastrophic feed-forward loop. Thus, as normal hyperglycæmia episodes become more frequent or longer, β-cell mass dynamics may be pushed past this catastrophic point: Topp *et al*. (2000) analyse this transition in detail and discuss the mechanism as a possible route to diabetes. This analysis raises the

possibility of β-cell mass involution leading to non-autoimmune, fulminant type 1 diabetes mellitus; interestingly, precisely such a syndrome has been recently described by Imagawa *et al*., 2000.

2.5.1.2 Evaluating therapeutic regimes

De Winter and his coworkers in 2006 (De Winter, 2006) took a different approach to the long-term dynamics of diabetic ætiology. To describe the deterioration of β-cell function and insulin sensitivity they introduce two functions, denoted $B(t)$ and $S(t)$, corresponding to remaining population of fully-functional β-cells and insulin sensitivity, respectively. The long-term dynamics of plasma glucose is described by the following integro-differential equation:

$$\frac{d}{dt}\left\langle G^{[p]}\right\rangle(t) = \frac{\varphi_S(t)S(t)\exp\{\mu_I t\}}{\int_{-\infty}^{t}(\varphi_B(\tau)B(\tau)\left\langle G^{[p]}\right\rangle(\tau) - G^{[p],\Diamond})\exp\{\mu_I\tau\}d\tau} - \mu_G\left\langle G^{[p]}\right\rangle(t) \quad (2.26)$$

where angled brackets indicate long-term averages; μ_G and μ_I are rate constants, $G^{[p],\Diamond}$ denotes the optimal plasma glucose concentration, and $\varphi_B(t)$ and $\varphi_S(t)$ are two forcing functions describing the effect of therapeutic intervention. To assess the success of the therapeutic regime $\{\varphi_B(t),\varphi_S(t)\}$ an output function is required; for this De Winter *et al*. 2006 used

$$H(t) \propto \exp\{-\mu_H t\}\int_{-\infty}^{t}\left\langle G^{[p]}\right\rangle(\tau)\exp\{\mu_H\tau\}d\tau \quad (2.27)$$

where H represents damage (glycosylated hemoglobin) and μ_H is the hemoglobin turn-over constant. The usefulness of this approach hinges on the choice of two empirical functions ($B(t)$ and $S(t)$) that represent the progressive loss of functionality; De Winter *et al*., 2006 took these to be logistic sigmoid curves. A conceptual difficulty with this approach is that the therapeutic intervention may have an effect on the disease progression, i.e. on the functions $B(t)$ and $S(t)$

(since therapy affects $\left\langle I^{[p]} \right\rangle$ and $\left\langle G^{[p]} \right\rangle$ which may changes the stress on β-cells and insulin sensitivity). In De Winter *et al.*'s formulation, these functions are autonomous. This dynamic feedback can taken into account by augmenting the system with ODEs for B and S.

2.5.2 Adiposity dynamics in positive energy balance

When energy intake exceeds energy expenditure for a prolonged period (even by only a few percent), accumulation of stored energy will occur. Excess carbohydrate and amino acids are largely converted into lipids (although net lipogenesis is likely to play a major role only if the ingested diet is unusually rich in carbohydrates; Aarsland *et al.*, 1997; Frayn, 2003). Thus, a food intake which supports a positive energy balance over the long term results in the laying down of fat reserves. When the ability of adipocytes to absorb this supply is taxed to capacity, elevated plasma fatty acids levels may result. Since NEFA utilization is regulated in a simple donor-control fashion by the availability of plasma NEFA (Izzekutz, 1967), glucose utilisation will be reduced and sustained elevated levels of plasma glucose and insulin will result. Moreover, sustained insulinæmia which extends beyond the normal post-prandial peak could contribute to insulin receptor down-regulation (Okabayashi *et al.*, 1989), further reducing insulin sensitivity. The key step in this route to diabetes via dislipidæmia is the stress on the assimilatory capacity of the adipocytes.

2.5.2.1 Adipocyte proliferation

Maas and Smith (2006) model the rate at which plasma NEFA is absorbed into adipose reserves as a bilinear term $\rho_{Adip} n_{Adip} I^{[p]} F^{[p]}$ where n_{Adip} is the number of adipocytes in the body. Thus, the model simulates the elevated lipidæmia and hyperinsulinæmia when the adipocyte count n_{Adip} is low in comparison with the energy excess in the dietary intake. Adipocyte resistance to the action of insulin is represented here by the quantity $1/\rho_{Adip}$; this parameter may be under hormonal control, since adipocytes secrete resistin which reduces the efficacy of glucose transport into adipocytes (Faust *et al.*, 1978; Steppan *et al.*, 2001) and may likewise

affect insulin-stimulated NEFA uptake.

Adipocyte proliferation, i.e., an increase of n_{Adip}, can compensate for the elevated $I^{[p]}$ and $F^{[p]}$. Maas and Smith (2006) model this by taking n_{Adip} to be a state variable with slow dynamics ("adipocyte count" in Figure 2.7). Maas and Smith (2006) model the rate of proliferation phenomenologically, letting $(d/dt)n_{Adip}$ depend on the mean adipocyte lipid content via a very steep Hill function. If Q_{TAG} denotes the total TAG content of adipocytes, the mean adipocyte lipid content is equal to Q_{TAG}/n_{Adip} (this is represented by the quotient symbol in Figure 2.7). This model is physiologically plausible: individual adipocytes greater than a certain size (and hence lipid content) are not observed, suggesting that adipocytes which have reached their maximum girth emit a signal which stimulates the proliferation and/or differentiation of preadipocytes. This is the *critical fat cell size hypothesis* (Hausman *et al.*, 2001). In addition to a peripheral paracrine mechanism, central modulation via a neuroendocrine axis may also play a role (Steppan *et al.*, 2001). The effect of the steep Hill function is to keep the ratio Q_{TAG}/n_{Adip} close to the upper size limit of adipocytes as long as positive energy balance persists.

In mathematical terms, it can be shown that the Maas and Smith (2006) model implies that TAG reserves over the long term exhibit a sigmoid (not a first-order) relaxation toward an asymptotic value that is proportional to $\sqrt{\left\langle I^{[p]}F^{[p]}\right\rangle / \left\langle A^{[p]}\right\rangle}$, where the quantities in angle brackets $\langle\cdot\rangle$ indicate long-term averages and Q_{TAG}/n_{Adip} is assumed to be kept constant (or very nearly so) by the steep 'adipostat' function. When glucagon levels are low, as they are likely to be under conditions of positive energy balance and insulinæmia, TAG reserves grow without bound as approximately $\sqrt{t}$ as long as $\left\langle I^{[p]}F^{[p]}\right\rangle$ is kept at a fixed value. However, the increase in Q_{TAG} over the long term is already mathematically determined. The slow dynamics of Q_{TAG} is fixed by the average positive energy balance in the long term which is imposed as a forcing function in this model. This mathematical determination is very interesting in physiological terms, since it means that $\left\langle I^{[p]}F^{[p]}\right\rangle$ is effectively governed by the imposed energy imbalance. To the biologist, this may seem counter-intuitive since the effect seems to turn

causality on its head. This paradox is resolved by the interplay between the fast and slow time scales.

The positive correlation between adiposity ΔQ_{TAG} and $\left\langle I^{[p]} F^{[p]} \right\rangle$ is an interesting model property; since ΔQ_{TAG} must in the long term reflect the imposed dietary excess, the quantity $\left\langle I^{[p]} F^{[p]} \right\rangle$ must be greater than normal during adiposity gains. In other words, hyperinsulinæmia or hyperlipidæmia are a necessary concomitant of adiposity gains in this model. Moreover, they combine multiplicatively; $\left\langle I^{[p]} F^{[p]} \right\rangle$ is essentially an overlap integral. In normal subjects, $F^{[p]}$ quickly falls as soon as $I^{[p]}$ rises (Frayn *et al.*, 1993). Thus, since the overlap is normally quite small, it may be increased appreciably by shifts in the timing of NEFA clearance even when mean levels do not change by much.

The Maas & Smith model explains why weight gains occur so readily after a diet. If adiposity before the diet is Q_{TAG}^{pre} and after the diet Q_{TAG}^{post}, then the rate of fatty acid disposition into storage will be $\frac{Q_{TAG}^{pre}}{Q_{TAG}^{post}}$ times elevated, *ceteris paribus*, when compared with normal subjects who have always been at adiposity Q_{TAG}^{post}, because the number of adipocytes in the post-diet subjects is elevated by that factor, due simply to the pre-diet adaptation of n_{Adip} to Q_{TAG}^{pre} via the steep Hill function, combined with the model assumption that adipocytes do not die. This elevated lipogenesis predisposes to renewed adiposity gains, especially if the subjects eat more to compensate for this enhanced flux into storage. These predictions are more likely to be relevant in middle-aged and older subjects, as a result of a second term that Maas and Smith (2006) include in the dynamics of Q, besides the steep "adipostat" Hill function. This second term is proportional to the body growth rate (which they impose as a forcing function). As a result, the effects noted here are masked in young adult life since the adolescent increase in n_{Adip} tends to keep the ratio $\frac{Q_{TAG}}{n_{Adip}}$ low.

2.5.2.2 Adaptive response to positive energy balance

In the Maas & Smith model, the energy imbalance is imposed from without, and the response is an adaptive increase of n_{Adip}, which allows the adipose tissues to absorb the energy surplus. However, it is now well established that signals emanating from adipocytes (adipokines) play a central role (Kennedy, 1953; Benoit *et al.*, 2004). A positive imbalance between intake and expenditure can be redressed by reducing the intake, increasing the expenditure, or both. Food intake, basal metabolic rate and thermogenesis are centrally coordinated in the hypothalamus; Figure 2.9 depicts major signalling pathways. The main sensory input center is the arcuate nucleus (ARC), which contains neurones that are sensitive to the plasma levels of insulin, glucose, ghrelin and the adipokine leptin. These neurones modulate food intake as well as the thyroid hormone axis (Chen, 1993; Spanswick *et al.*, 1997; Kim *et al.*, 2000; Spanswick *et al.*, 2000; Barsh & Schwartz, 2002; Nowak *et al.*, 2002; Dobbins *et al.*, 2003; van den Top *et al.*, 2004).

The hypothalamus also regulates muscle glycogen synthesis through the autonomous nervous system (ANS; Perrin *et al.*, 2004). As noted above, extra-hepatic glycogen stores can serve as buffers which temporarily absorb the energy excess (in particular, its carbohydrate component) while preadipocyte proliferation takes place. Leptin stimulation (via the ANS) of glucose transport into extra-hepatic stores may also be involved (Kamohara *et al.*, 1997; Haque *et al.*, 1999; Shiuchi *et al.*, 2001). In hyperleptinæmic rats, adipose TAG reserves all but disappear, in contrast to pair-fed controls, while energy intake and body weight were the same in these controls (Chen, 1993), suggesting that energy expenditure must have been nearly equal in the two groups (intracerebroventricular infusion of leptin results in increased expenditure, but the effect is much stronger after 3 days than after 14 days; Halaas *et al.*, 1997). Energy reserves at the end of the experiment must therefore have been comparable despite the marked difference in adiposity, pointing to the involvement of glycogen stores—particularly extra-hepatic stores, given that liver weight did not change in similar experiments on mice (Levin *et al.*, 1996).

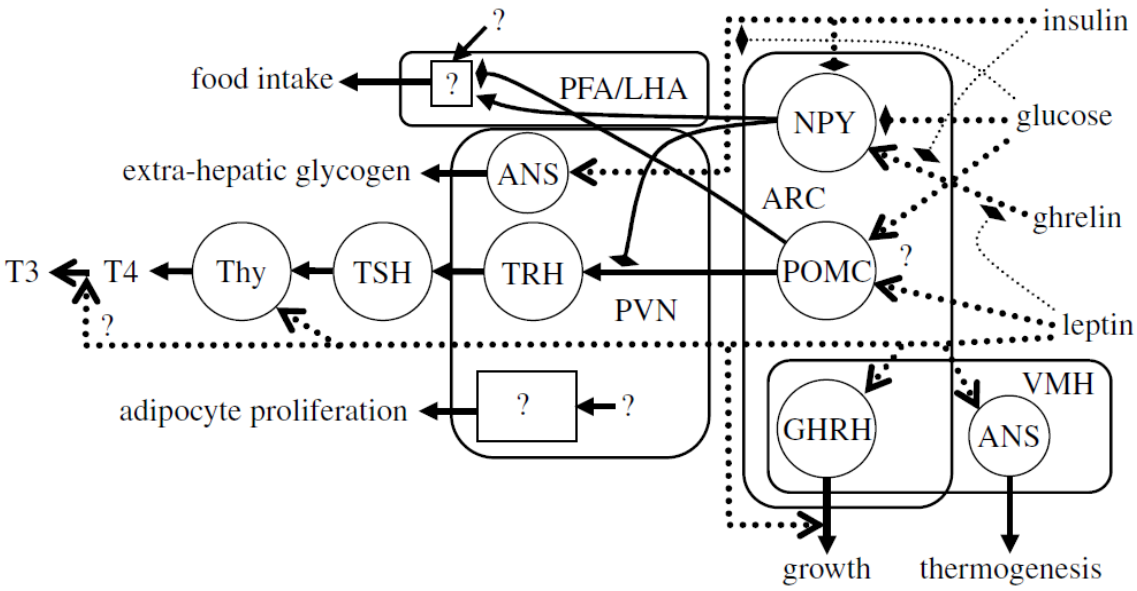

Figure 2.9: Schematic of the neuroendocrine control loop. ARC, arcuate nucleus; VMH, ventromedial hypothalamus; PFA/LHA, perifornical area & lateral hypothalamus; PVN, periventricular nucleus; NPY, neuropeptide Y/agouti-related peptide neurones; POMC, pro-opiomelanocortin neurons; GHRH, growth hormone releasing hormone neurones; TRH, thyrotrophin releasing hormone neurones; TSH, thyrotrophs; Thy, thyroid gland; T3, triiodothyronine; T4, thyroxine; ANS, autonomous nervous system neurons. Question marks indicate unknown interactions or components.

To account for these centrally co-ordinated compensatory changes in energy intake and expenditure, the Maas & Smith can be extended as shown in Figure 2.10. The plasma leptin level is included as a state variable and treated as the main adiposity signal driving the central response (Benoit *et al.*, 2004). The central nervous system (CNS) modulates food intake and energy expenditure. The long-term behaviour of this modified Maas & Smith model depends on the mathematical specification of the secretion term in the leptin kinetics, as well as on the specification of the input/output behaviour of the CNS. It is worthwhile to discuss this question of formulating an appropriate model in some depth, since it is connected with several very topical issues in obesity research.

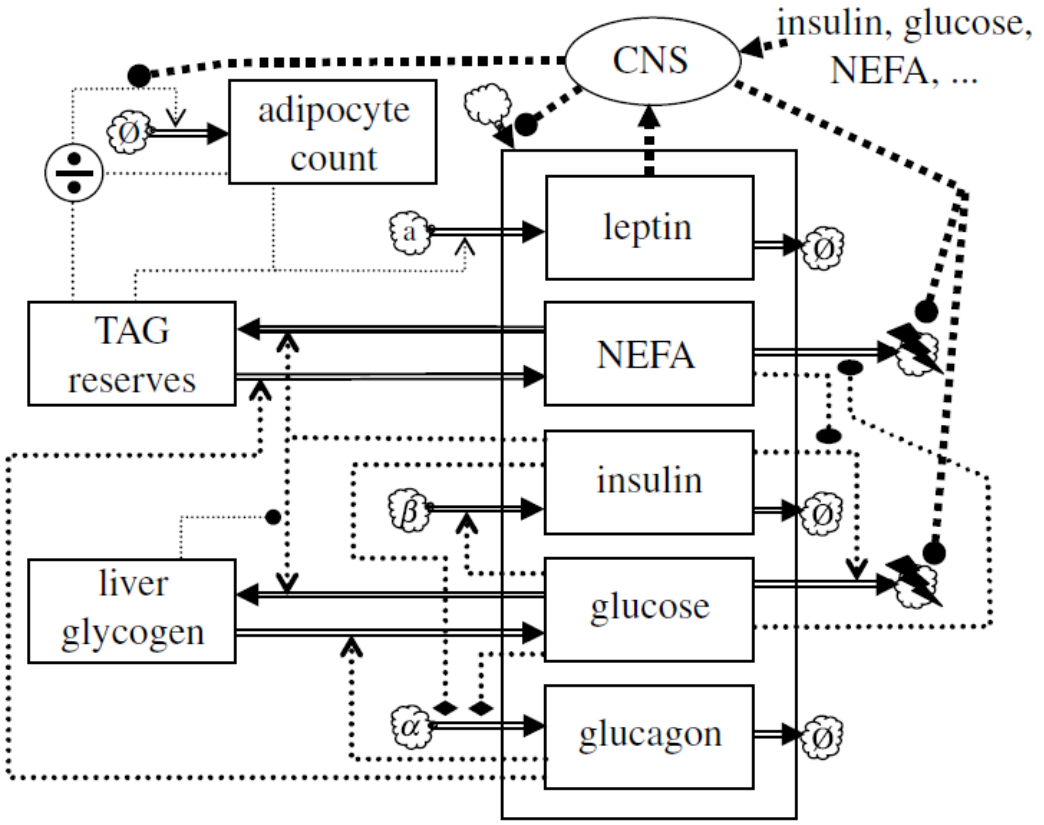

Figure 2.10: Glycæmic feedback model extended with fatty acid utilization, adipocyte proliferation, and central regulation of energy assimilation and expenditure. The empty cloud indicates endogenous sources. The cloud marked 'a' identifies adipocytes as the source of leptin. CNS, central nervous system.

Leptin as an adiposity signal

Leptin is secreted by adipocytes. The leptin plasma concentration $L^{[p]}$ correlates well with percentage body fat (Considine *et al.*, 1996; Friedman & Halaas, 1998), and is thus generally regarded as an adiposity signal (Benoit *et al.*, 2004). The long-term average $\left\langle L^{[p]} \right\rangle$ is proportional to the leptin secretion rate, which is a product of n_{Adip} and the secretion rate per adipocyte. If the latter is a basal value, independent of adipocyte size, we would have $\left\langle L^{[p]} \right\rangle \propto \frac{n_{Adip}}{V^{[p]}}$, where $V^{[p]}$ is the plasma volume. By contrast, we obtain $\left\langle L^{[p]} \right\rangle \propto \frac{Q_{TAG}}{V^{[p]}}$ if the leptin secretion rate is proportional to the size of the adipocyte (which is $\frac{Q_{TAG}}{n_{Adip}}$ on average).

Again, if each adipocyte signals in proportion to the assimilatory flux it is conducting, we would obtain $\left\langle L^{[p]} \right\rangle \propto \frac{\left((d/dt)Q_{TAG}\right)}{V^{[p]}}$. Which, if any, of these options is the most realistic model?

Leptin gene expression is regulated by the hexosamine pathway which converts fructose 6-phosphate (Fruc6P) into UDP-*N*-acetylglucosamine (UDP-GlcNac); this product donates GlcNac moieties to transcription factors thus promoting the transcription of leptin mRNA (Wang *et al.*, 1998). The flux into the hexosamine pathway is increased when Fruc6P accumulates due to NEFA availability (which slows down glycolysis) and/or hyperglycæmia (which promotes the influx of glucose). Larger adipocytes express more leptin (Maffei *et al.*, 1995). Leptin expression is also regulated at the posttranslational level via the mTOR-mediated pathway, which is activated by free amino acids (Roh *et al.*, 2003). The secretion of leptin is regulated by intracellular ATP (Levy *et al.*, 2000). In keeping with these nutrient-sensing regulatory mechanisms, plasma leptin levels decrease during dynamic weight loss (Rosenbaum *et al.*, 1997; Velkoska *et al.*, 2003), whereas leptin rises during hyperinsulinæmic clamp (Boden *et al.*, 1997) and following food intake (more markedly so in obese subjects). Plasma levels slowly fall during sleep (Yildiz *et al.*, 2004), yielding a diurnal rhythm that has been shown to be entrained to meal timing rather than an endogenous clock (Schoeller *et al.*, 1997). Collectively, these observations suggest, in general, that leptin secretion by adipocytes reflects assimilatory activity in these cells and, in particular, that adipocytes operating near their maximum storage capacity have high levels of leptin expression.

2.5.2.3 The Friedman adipostasis model

Friedman and Halaas (1998) proposed a conceptual model in which the CNS permits a positive energy balance to persist while $\left\langle L^{[p]} \right\rangle$ remains well below a critical value which he calls the *leptin set point*. As leptin levels start to approach this threshold, the modulatory effects on food intake and energy expenditure come into effect, so that a neutral energy balance is attained at plasma leptin levels in the vicinity of the set point.

The leptin set point in this model is equivalent to an adiposity set point provided that we have $\left\langle L^{[p]} \right\rangle \propto \frac{Q_{TAG}}{V^{[p]}}$. Thus the model explains the existence of an apparent "body weight set point" particular to the individual and subject to genetic variation in the population (Keesey & Hirvonen, 1997). Furthermore, the Friedman model predicts that obesity can be caused by a reduced ability of adipocytes to produce leptin, or an impairment of the transport of leptin to the brain; in either case the effect will be that the brain "perceives" adipose reserves to be smaller than they are. Alternatively, obesity can be caused by a reduced sensitivity to leptin in the CNS. In the first scenario, obesity with normal leptin levels ensues, whereas leptin levels will be elevated in the second scenario.

To represent the Friedman model mathematically, we start with the following expression for the energy balance:

$$\eta(x)\Phi_{ass}(u) = \Phi_{\exp}(x,v) + \frac{d}{dt}Q_{TAG}, \qquad (2.28)$$

where x represents an internal state of the hypothalamus, Φ_{ass} the assimilatory influx of energy and $\Phi_{\exp}$ is the expenditure of energy (expressed in the same units as Q_{TAG} to keep the notation as simple as possible). The multiplier $\eta \in [0,1]$ represents the hypothalamic modulation of food intake; u represents environmental factors such as food availability that codetermine the assimilatory flux; and v represents physiological or endocrinological variables that affect energy expenditure, such as the body growth rate, pregnancy, and physical exercise.

Suppose now that the hypothalamus receives inputs carrying information about (i) Q_{TAG} and/or $\left(\frac{d}{dt}\right)Q_{TAG}$, which is reasonable in view of the foregoing discussion; as well as (ii) v. Then, formally, u can be recovered from these inputs; say

$$u = \Gamma\left(Q_{TAG}, \frac{d}{dt}Q_{TAG}, v, x\right),$$

where Γ is at least locally uniquely defined by the balance equation (2.28). This shows that the hypothalamus can regulate Q_{TAG} towards an "adiposity set point" which can be, in general, any function of u and/or v. This is the *adipostasis property*. Two caveats apply: first, this regulatory ability is limited by obvious physiological constraints, namely, the maximum food intake rate and the minimum expenditure rate. Second, it should not be thought that the hypothalamus is supposed to solve algebraic equations. Our formal representation is simply intended to highlight the fact that the information inputs mentioned suffice to obtain the adipostasis property.

The above argument is fairly abstract; let us consider two simple examples. First, take x to be one-dimensional with first-order relaxation toward the leptin input:

$$\frac{d}{dt}x = \kappa_X \frac{Q_{TAG}}{V^{[p]}} - \lambda_X x, \tag{2.29}$$

where κ_X and λ_X are positive constants, and let the food intake multiplier η be a steeply descending Hill-type function of x (cf. (Velkoska *et al.*, 2003)) with mid-point parameter $\xi > 0$. Then, as long as the quantity $\frac{\Phi_{\exp}}{\Phi_{ass}}$ fluctuates in the interval [0, 1], adiposity $\frac{Q_{TAG}}{V^{[p]}}$ fluctuates around $\frac{\lambda_X \xi}{\kappa_X}$. The latter is the apparent set point. This pattern is typical: apparent set points arise as a compound of rate constants and sensitivity (coupling) constants.

Although very simple, this minimal implementation of the Friedman hypothesis already shows how one can make sense of Keesey and Hirvonen (1997) remarks about the "body weight set point" and variability of this set point within the population. The model states that individuals with a lower-than-average κ_X-value have a higher apparent adiposity set point. The coupling constant κ_X represents hypothalamic sensitivity to leptin. Thus, if the hypothalamic leptin receptor is knocked out, κ_X would be zero and the model predicts that the individual becomes massively obese (i.e. $\langle Q_{TAG} \rangle$ goes to its maximum $\left\langle \frac{\Phi_{\exp}}{\Phi_{ass}} \right\rangle$), in keeping with the findings of Maffei *et al.*, (1995).

In the simple model, the adiposity set point is $\frac{\lambda_X \xi}{\kappa_X}$, a constant independent of ambient conditions (u) such as food availability. Alternatively, one might propose that the set point proportional to the time-average caloric density of the available diet:

$$\frac{d}{dt}\frac{Q_{TAG}}{V^{[p]}} = \theta \frac{\langle \Phi_{ass}(u) \rangle}{V^{[p]}} - \rho \frac{Q_{TAG}}{V^{[p]}}, \tag{2.30}$$

where θ and ρ are empirical constants. This is an intuitively attractive and physiologically plausible model, at least qualitatively. The caloric-density set point model gives rise to first-order adipose density dynamics in times of positive energy balance (see Sousa *et al*., 2008, for a discussion of similar dynamics). The model can be justified on the basis of the adipostasis property. For example, the simple Friedman model can be extended by assuming that the midpoint parameter ξ is governed by the available inputs listed above. We can recover the functional dependence by solving the following equation for ξ:

$$\eta(x;\xi)\xi = \frac{\theta \kappa_X}{\rho \lambda_X} \cdot \frac{\Phi_{ass}(\Gamma(Q_{TAG}, \frac{d}{dt}Q_{TAG}, v, x)) + \frac{d}{dt}Q_{TAG}}{V^{[p]}} \tag{2.31}$$

Again, there is no suggestion that the hypothalamus explicitly carries out the algebra; the point is to show how it can nonetheless effect the equivalent mapping by showing how we can represent this mapping in terms of the our notation.

2.5.3 Negative energy balance and starvation

The Friedman model deals with the adaptation to positive energy balance. There are also adaptations to negative energy balance. This response consists of co-ordinated regulation of energy expenditure, the mobilisation of energy stores, and hyperphagia once food becomes available. Both hypothalamus and peripheral tissues partake in this response (Keesey & Hirvonen, 1997; Frayn, 2003).

Energy expenditure is reduced as leptin levels fall; peripherally, leptin affects insulin secretion (Lam *et al.*, 2004) and glucose utilisation (Haque *et al.*, 1999; Shiuchi *et al.*, 2001) while centrally, there is a shut-down of the leptin-TRH-TSH-thyroid axis (cf. Figure 2.9; (Rosenbaum *et al.*, 1997; Kim *et al.*, 2000)) as well as the leptin-growth hormone axis (Tannenbaum *et al.*, 1998). The shift in the insulin/glucagon ratio stimulates the Cori cycle (section 2.4.2).

The key problem in the mobilisation of energy stores is the co-ordinated use of the three types of energy reserve, *viz.* glycogen, fat and muscle protein. Hepatic glycogen stores are rapidly depleted (Nilsson & Hultman, 1973), leaving adipose stores and protein. Various adaptations favour the use of the former: gluconeogenesis from lactate via the Cori cycle allows obligatory glycolytic tissues to use energy derived from fatty acids, which are also converted into ketone bodies used by the CNS as an alternative to glucose, whereas residual obligatory utilisation of glucose is sustained by protein breakdown via the alanine cycle (section 2.4.2; Salway, 2004). The CRH-ACTH-cortisol axis regulates proteolysis in muscle, counteracting the effects of insulin and IGF-1 (Brook & Marshall, 2001); this axis governs the terminal phase of starvation, when adipose stores have run out.

The long-term dynamics of Q_{TAG} is thus governed by (minimised) obligatory energy requirements, and the phenomenological approach that led to equation (2.30) may therefore be inappropriate, although Kooijman (2000) argues that this equation can be used to describe starvation as well as energy-surplus.

2.6 Conclusion & outlook

Since the purpose of this paper was to survey the existing literature, we have followed the literature's glucocentric bias, starting with basic models of glucostasis and the various ways in which these models are extended with additional dynamic degrees of freedom. However, the problems presented by diabetes, obesity, and controlled nutrition of e.g. cachexic subjects call for models which integrate glucostasis with adipostasis and myostasis at the long-term time scale (the 'developmental' or 'life history' time scale). We have focused attention here on the interplay of glucostat and adipostat. Other aspects which are important on the developmental time scale, but which have not been emphasised in this review include interactions with lipoprotein metabolism and cholesterol homeostasis and the

interplay between amino acid metabolism, glucoplastic carbon metabolism, myostasis and the regulation of the overall growth rate.

An open question is how one can include all these aspects in one over-arching model, and, indeed, whether one should. The 16-state variable model shown in Figure 2.1 is already prohibitive in terms of parameter identifiability, and could easily be extended with many more humoral factors and compartments. Perhaps the approach taken in the analysis of the Friedman model and the adipostasis property (section 2.5.2.3) will prove to be fruitful in general. Thus, to describe dynamics on the life-history time scale, one starts with balance equations, augmented with a minimum of additional physiological state variables needed to describe the regulation of the flux terms in response to e.g. dietary challenges. What is as yet missing is a systematic way of deriving the dynamics of these additional state variables at the slow time scale from the underlying detailed dynamics at the fast physiological time scales.

Table 2.1 Summary of notation

State variables

$G^{[p]}$	glucose concentration in blood plasma
$I^{[p]}$	insulin concentration in blood plasma
$A^{[p]}$	glucagon concentration in blood plasma
$I_l^{[is]}$	interstitial fluid concentration of insulin in the l th tissue compartment
$F^{[p]}$	non-esterified fatty acids concentration in blood plasma
M_β	β-cell mass
Q_{TAG}	total TAG content of adipocytes
$L^{[p]}$	leptin concentration in blood plasma

Fluxes

Φ_I	insulin secretion rate by the pancreatic β-cells
ϕ_I	insulin secretion rate per pancreatic β-cell
Φ_G	glucose assimilation
Ψ_G	glucose clearance
$\Phi_G^{[exo]}$	exogenous glucose input
$\Phi_G^{[endo]}$	endogenous glucose input
Φ_A	glucagon secretion rate
Φ_0	baseline glucose release rate from the liver
Φ_{ass}	assimilatory influx of energy
$\Phi_{\exp}$	expenditure influx of energy

Rate constants

λ_I	insulin clearance rate constant
λ_A	glucagon clearance rate constant
$\kappa_{I,l}$	passive transport parameter of interstitial insulin
$\kappa_{I,l}^{out}$	transport coefficient for transport out of the interstitial insulin compartment

$\kappa_{I,l}^{in}$ transport coefficient for transport into the interstitial insulin compartment

α inhibitory effect coefficient of insulin on gluconeogenesis

β insulin-independent glucose usage

γ insulin-dependent glucose usage

μ_β β-cell proliferation function

α_β β-cell death rate

Miscellaneous

t time

$\tau_{I,d}$ response-time delay by the pancreatic β-cells as they respond to changes in the plasma glucose levels

$\tau_{G,d}$ response-time delay for hepatic glucose production

n_{Adip} number of adipocytes in the body

$V^{[p]}$ plasma volume

η hypothalamic modulation of food intake

x internal state of the hypothalamus

u environmental factors

v physiological or endocrinological variables that affect energy expenditure

f_Q forcing function describing long-term evolution of adiposity function

Chapter 3

Experimental procedures

3.1 Electrophysiology - Whole-cell patch-clamp: The arcuate nucleus

3.1.1 Experimental groups and animal care

Male Wistar rats, aged 5 to 8 weeks old, were used throughout this study. All experiments were carried out in accordance with national ethical guidelines and in accordance with the UK Animal Scientific Procedures Act (1986). All animals were normally housed in groups of 4 in individually ventilated cages (IVCs) manufactured by Techniplast (dimensions: 1500U; 64.65 x 26.77 x 73.23 inch) and fed a commercially available pelleted rodent maintenance diet (RM1 diet supplied by Special Diet Services (SDS)). Animals were housed under a 12/12 hour light/dark cycle and food and water were provided *ad libitum*, except where otherwise indicated. Several experimental groups were used over the course of these studies in addition to the normal, fed *ad libitum* group as outlined above. Rats were also fasted for 24 hours. This group was housed individually on an elevated metal grid floor, to capture and isolate waste material, with water available *ad libitum*. A control group for the fasted animals was also used. These animals were housed, as the fasted group, with an elevated metal grid flooring, but with food and water available *ad libitum*.

3.1.2 Slice preparation

Hypothalamic slice preparations were obtained from adult male rats maintained as outlined above. Rats were killed by cervical dislocation and decapitated. The brain was then immediately removed from the cranial cavity and placed in freshly prepared oxygenated (95% O_2, 5% CO_2), ice-cold (2°C - 4°C) artificial cerebrospinal fluid (aCSF), the composition of which is shown in Table 3.1. The brain was trimmed to a hypothalamic block which was subsequently glued onto the plate of a vibratome (Intracell series 1000, Royston, UK or Leica VT1000S, Leica Microsystems Nussloch GmbH, Nussloch, Germany). Transverse slices containing the arcuate nucleus (ARC), identified in the slices as the area directly above the median eminence (ME) surrounding the third ventricle on both sides, were cut at a thickness of 300 μm on a vibratome. During the process of slicing, the hypothalamic block was constantly bathed in oxygenated, ice-cold aCSF. Slices were transferred to and maintained in a 250 ml beaker containing oxygenated aCSF at room temperature for at least one hour prior to whole cell recording.

Table 3.1: aCSF composition

Composition of aCSF (in mM) utilised in this study. Changes in glucose concentration were compensated by equimolar changes of D-mannitol

	10 mM	**5 mM**	**2 mM**	**1 mM**	**0.5 mM**	**0.2 mM**	**0 mM**
NaCl	127.0	127.0	127.0	127.0	127.0	127.0	127.0
KH_2PO_4	1.2	1.2	1.2	1.2	1.2	1.2	1.2
KCL	1.9	1.9	1.9	1.9	1.9	1.9	1.9
$NaHCO_3$	26.0	26.0	26.0	26.0	26.0	26.0	26.0
Glucose	**10.0**	**5.0**	**2.0**	**1.0**	**0.5**	**0.2**	**0.0**
D-Mannitol	**0.0**	**5.0**	**8.0**	**9.0**	**9.5**	**9.8**	**10.0**
$CaCl_2$	2.4	2.4	2.4	2.4	2.4	2.4	2.4
$MgCl_2$	1.3	1.3	1.3	1.3	1.3	1.3	1.3

3.1.3 Solutions and drugs

The medium aCSF was prepared fresh daily, of ionic composition shown in Table 3.1. The aCSF had a pH of 7.3-7.4 and an osmolarity of 315 mOsm kg^{-1}. For experiments where the concentration of glucose was manipulated (0.0, 0.2, 0.5, 1.0, 2.0, 5.0 mM), glucose was replaced in equimolar quantities with D-mannitol to maintain osmolarity.

Intracellular solution (pipette solution) was prepared daily for each experiment as a 1 ml volume from stock solutions; the composition of intracellular solutions is shown in Table 3.2. Stock solutions were prepared in advance and stored at 4°C excluding Na_2ATP which was kept at -20°C. The concentration of intracellular ATP was manipulated in a specific series of experiments without significant effect on osmolarity. Thus the volume of ATP used was appropriately compensated with distilled water. The osmolarity of the intracellular solution was adjusted with sucrose to maintain close to that of the aCSF whilst the pH was adjusted to 7.4 KOH.

Table 3.2: Composition of intracellular solutions used in this study

	(in mM)				
K-gluconate	140	140	140	140	140
HEPES	10	10	10	10	10
KCL	10	10	10	10	10
EGTA	1	1	1	1	1
Na_2ATP	10	5	2	1	0

Drugs used in the present study included tetrodotoxin (TTX; Alomone labs, Jerusalem, Israel), prepared in distilled water and Tolbutamide (Sigma). Tolbutamide was dissolved in 100% dimethylsulphoxide (DMSO; Sigma). All drugs were prepared as a stock solution as appropriate and then further diluted to the required concentration in aCSF prior to use. Drugs were then applied to the slice by a gravity feed perfusion system from a series of 60 ml syringes with manually operable three-way taps connected to the main aCSF reservoir.

3.1.4 Electrophysiological recording and data analysis

The whole-cell patch-clamp recording was used to obtain the electrophysiological recordings. Hypothalamic slices containing the ARC were transferred to a custom-made recording chamber and secured between two nylon grids where the top which was secured to a chloride-coated silver wire, acted as the bath-earth. These slices were superfused with oxygenated aCSF at room temperature through a gravity-fed system at a continuous flow rate of 5-10 ml min^{-1}. Recording electrodes (pipettes) were made of thin-walled borosilicate glass capillaries (GC150TF-10, Harvard Apparatus LTD, Edenbridge, Kent, UK) and were pulled using a horizontal puller (P-97, Sutter Instrument Co, Novato, CA, USA) with a resistance between 4-8 MΩ. These pipettes were filled with the intracellular solutions as shown in Table 3.2 while recording.

All recordings were obtained using an Axopatch-1D amplifier (Axon Instruments, Foster City, CA, USA). The series resistance of the recording was in the range of 8-20 MΩ and compensated as appropriate. All recordings were displayed online via a digital oscilloscope (Gould DSO1602, Gould Instrument Systems). Current traces were then sampled at 10 kHz and were directly recorded and stored on computer running the pCLAMP 9 data acquisition software (Axon Instruments) for subsequent offline analysis. Data was also digitised at 20 kHz and analysed using Clampex 8.2 software (Axon Instruments) on a personal computer. Current-voltage relationships were also produced using Clampex 8.2, sampled at 20 kHz

Resting membrane potential of silent cells and slowly active cells were obtained from the recorded trace in Clampex. The accurate measurement of the resting membrane potential of these cells could be taken at a period of quiescence with little or no sub- and supra-threshold activity. However, for active cells, for which this type of measurement was impossible, the low-pass readout of the recording amplifier was used instead. The recorded membrane potentials were not corrected for off-sets related to the occurrence of liquid junction potentials. Input resistance was calculated using Ohm's law (V= I x R) at steady-state membrane potential by injecting small negative rectangular-wave current pulses in the current-voltage protocol (step: amplitude -5 to -20 pA, duration 1000 ms, 0.2 Hz). The inter-pulse interval between each negative current injection was set at a magnitude sufficient to detect changes in input resistance whilst limiting the

activation of active conductances. Firing frequency was calculated in Hz (the number of firing spikes discharged per second) from the recorded current trace.

3.1.5 Statistical analysis

Statistical analysis was performed using Microsoft Excel with all values expressed as the mean ± SEM. Statistical significance ($P < 0.05$) between two related populations was determined using the two-tailed student's *t*-test using paired or unpaired as appropriate. Statistical significance ($P < 0.05$) among related populations of more than two groups was determined using ANOVA test from Instat 3. The number of observations is stated as *n* values referring to the number of neurones from which observations were made.

Table 3.1: aCSF composition

Composition of aCSF (in mM) utilised in this study. Changes in glucose concentration were compensated by equimolar changes of D-mannitol

	10 mM	**5 mM**	**2 mM**	**1 mM**	**0.5 mM**	**0.2 mM**	**0 mM**
NaCl	127.0	127.0	127.0	127.0	127.0	127.0	127.0
KH_2PO_4	1.2	1.2	1.2	1.2	1.2	1.2	1.2
KCL	1.9	1.9	1.9	1.9	1.9	1.9	1.9
$NaHCO_3$	26.0	26.0	26.0	26.0	26.0	26.0	26.0
Glucose	**10.0**	**5.0**	**2.0**	**1.0**	**0.5**	**0.2**	**0.0**
D-Mannitol	**0.0**	**5.0**	**8.0**	**9.0**	**9.5**	**9.8**	**10.0**
$CaCl_2$	2.4	2.4	2.4	2.4	2.4	2.4	2.4
$MgCl_2$	1.3	1.3	1.3	1.3	1.3	1.3	1.3

Chapter 4

The effects of food withdrawal (fasting) on the electrophysiological properties of rat hypothalamic arcuate nucleus neurones in vitro

4.1 Introduction

The hypothalamic arcuate nucleus (ARC) is located in the basal hypothalamus, adjacent to the third ventricle directly above the median eminence (ME). It is a major hypothalamic nucleus, consisting of heterogeneous sets of neurones involved in the control of energy homeostasis (Chronwall, 1985; Bell *et al.*, 2000; Williams *et al.*, 2000; Cone *et al.*, 2001; Williams *et al.*, 2001), adaptations to stress (Bell *et al.*, 2000), pain, reproduction (Gottsch *et al.*, 2004) and other functions (Chronwall, 1985).

ARC neurones receive inputs from a range of central areas and are innervated by neurones of multiple neurotransmitter and neuropeptide phenotypes, including orexin, GABA, dopamine, glutamate, noradrenaline and serotonin, hence it is a key integrative centre which receives a variety of afferent inputs from multiple hypothalamic and brainstem nuclei (Chronwall, 1985). These afferent inputs arise from the hypothalamic ventromedial nucleus (VMN), the paraventricular nucleus (PVN), the lateral hypothalamus (LH), the suprachiasmatic nucleus (SCN) and the brain stem nuclei such as nucleus of tractus solitarius (NTS) (Chronwall, 1985). ARC neurones themselves project outputs to second-order neurones in several brain areas, including PVN, LH, perifornical area (PFA), and ME and more (Chronwall, 1985; Baker & Herkenham, 1995). Some areas in the hypothalamus send and receive information to and from the ARC via reciprocal connections.

The ARC plays an important role in controlling both feeding and energy metabolism, through two main interconnected groups of first-order neurones that release orexigenic (anabolic) and anorexigenic (catabolic) neuropeptides. Orexigenic neuropeptides include neuropeptide Y (NPY), agouti-related peptide (AgRP) and galanin (GAL), whilst anorexigenic neuropeptides include pro-opiomelanocortin (POMC) derived α-melanocyte stimulating hormone (α-MSH), cocaine and amphetamine regulated transcript (CART), and Galanin-like peptide (GALP) amongst others (Chronwall, 1985; Koylu *et al.*, 1997; Cone *et al.*, 2001).

The ARC is situated directly above the ME, which has been reported to have a compromised blood-brain-barrier (BBB), permitting passage of essential nutrients and hormones indicating shifts in energy balance (Broadwell *et al.*, 1983; Fry *et al.*, 2007). Thus the ARC represents an area where both central and peripheral signals converge (Cone *et al.*, 2001). In addition, it has been reported that the individual neurones within the ARC are sensitive to multiple peptides involving in the control

of food intake and energy balance, including insulin (Spanswick *et al.*, 2000; van den Top *et al.*, 2004; Wang *et al.*, 2004), leptin (Spanswick *et al.*, 1997; van den Top *et al.*, 2004) and nutrients as glucose (van den Top *et al.*, 2007). Hence, understanding how ARC neurones sense or respond to these multiple peptide hormone and nutrient signals is fundamental to our understanding of the central control of body weight.

Despite numerous studies on the responsiveness of ARC neurones to specific neuropeptides and neurotransmitters and nutrients such as glucose, the mechanisms by which these neurones detect, integrate and respond to these signals remains unclear. Several key features of neuronal function need to be recognised when addressing issues related to the functional operation of neural circuits and how they respond to central neural and peripheral hormonal signals to produce appropriate outputs, including the passive and active suprathreshold active conductances expressed by neurones, subthreshold active conductances, synaptic inputs, chemical phenotype and target projection.

This study is focused on the mechanisms by which ARC neurones are able to detect and respond to changes in extracellular glucose levels and how such mechanisms may adapt depending on the energy status of the organism. To address this issue the electrophysiological properties of ARC neurones and their responsiveness to changes in extracellular glucose were investigated in rats fed *ad libitum* and 24-hour fasted rats (with water *ad libitum*). Fasted rats were isolated from any source of food, including excrement, by placing rats in cages with raised metal grid floors. Appropriate controls for this experimental manipulation included rats in similar housing but with food available *ad libitum.* Differences in rat housing can cause stress and affect the level of some hormones, body weight and muscle performance (Brown & Grunberg, 1995; Spangenberg *et al.*, 2005). The housing of rats in isolation alone can cause changes in behaviour, neurochemistry and anatomy (Globus *et al.*, 1973; Sahakian *et al.*, 1975; Thoa *et al.*, 1977; Weinstock *et al.*, 1978; Garzon *et al.*, 1979; Jorgensen & Bock, 1979; Gentsch *et al.*, 1981). Hence the general membrane properties of ARC neurones were examined in three different groups of rats (1. rats fed *ad libitum*; 2. rats fed *ad libitum* housed in cages with a raised metal grid (control group for 3) and 3. rats fasted for 24 hours housed in cages with a raised metal grid).

Neuronal function, integrative and computational capability are a product of both active and passive membrane properties of neurones. Subthreshold active conductances also shape the electrical output and are responsible for integrating and translating synaptic inputs (Pape, 1996; van den Top *et al.*, 2004; Gulledge *et al.*, 2005).

There are many approaches which can be used to classify neurones into different subgroups/clusters. In the present study, neurones were distinguished into clusters based on an approach outlined by (Pennartz *et al.*, 1998), based on previous studies (Tasker & Dudek, 1991) whereby neurones were distinguished according to postsynaptic membrane properties, including subthreshold active conductances. Furthermore, this approach has revealed functional significance. In the present classification of neurones, cluster 2, characterised by a transient outward and an anomalous inward rectification, has been shown to respond to orexigenic inputs such as ghrelin and orexin with a stereotyped pacemaker-like activity (van den Top *et a l.,* 2004). No other cluster responds in this way suggesting classifying neurones in such a manner has functional significance. However, there are also other approaches to clustering neurones, for example, the work by (Toledo-Rodriguez *et al.*, 2004) revealed a consistent relationship between the co-expression of ion channel subunit and calcium binding protein genes and the electrical phenotype of individual neocortical neurones.

In the present study, electrophysiological recordings were undertaken in three different groups of rats, as mentioned above, to obtain both active and passive membrane properties of ARC neurones. The subthreshold active conductances expressed by ARC neurones were also observed and used as parameters to classify populations of ARC neurone into subgroups (termed clusters), following on from and building upon previous work undertaken in this lab (van den Top, 2002; Saker, 2009; Virdee, 2009). Electrophysiological properties were investigated and compared between rats fed *ad libitum* in normal housing; rats fed *ad libitum* housed in cages with a raised metal grid (control group for fasted rats) and rats fasted for 24 hours housed in cages with a raised metal grid.

4.2 Results

In the present study, hypothalamic ARC neurones from three groups of rats were investigated and general active and passive membrane properties compared. Male Wistar rats (5-8 weeks old) were provided with food and water *ad libitum* in an identical environment until 24 hours before experiments. Twenty-four hours prior to experiment rats were separated into three different groups mentioned above.

Whole cell recordings were obtained from 149 ARC neurones. All recordings were obtained in aCSF containing 2.0 mM glucose, suggested to indicate a physiological concentration (Levin *et al.*, 2004; Routh *et al.*, 2007) together with 2.0 mM intracellular ATP. Forty-seven neurones were recorded from rats fed *ad libitum* in normal rodent housing, 50 neurones from rats fed *ad libitum* housed on a raised metal grid and the remaining 52 neurones from rats fasted for 24 hours, housed on a raised metal grid. A comparison between general membrane properties of ARC neurones obtained from these three rat groups was firstly carried out. General membrane properties included: average membrane potential, input resistance and the firing frequency of the neurones. A comparison of other electrophysiological properties of ARC neurones were also obtained by investigating the subthreshold active membrane properties of these neurones from current-voltage (I-V) relationships, membrane-time constants (tau) and action potential wave-forms. ARC neurones expressed a range of subthreshold active conductances, and in many cells more than one conductance. In this study, subthreshold active conductances of individual ARC neurone were therefore used as indicators of function and to sub-classify neurones. Using these criteria, ARC neurones were separated into 8 subtypes, termed clusters.

4.2.1 Passive membrane properties of ARC neurones

The membrane potential, input resistance and firing frequency of all ARC neurones recorded in 2.0 mM extracellular glucose and 2.0 mM intracellular ATP were computed. An overall comparison of these properties for the three groups of rats studied is shown in Table 4.1. Figure 4.1 presents bar charts showing the mean and standard error of the mean of all passive membrane properties. The frequency histograms for each passive membrane property in three groups of rats are shown in Figure 4.2.

4.2.1.1 Resting membrane potential

The average resting membrane potential of ARC neurones recorded from rats fed *ad libitum* in normal housing was -48 ± 1 mV (range -40 and -71 mV, n = 47). The corresponding value for rats fed *ad libitum* housed on a raised metal grid was -48 ± 1 mV (range -39 and -62 mV, n = 50) and for rats following a 24 hours fasted housed on a raised metal grid amounted to -49 ± 1 mV (range -39 and -62 mV, n = 52) (Figure 4.1 A; Table 4.1). This data showed no significant difference in the resting membrane potentials of ARC neurones recorded from the three groups of rats. The range of resting membrane potentials recorded containing the highest proportion of neurones was -45 to -50 mV in rats fed *ad libitum* in normal housing (38.3%) and in 24-hour fasted rats (28.8%), and -40 to -45 mV in rats fed *ad libitum* rats housed on raised metal grid (30.0%; Figure 4.2 A). The median values for all three groups of rats were -48, -48 and -48 mV for rats fed *ad libitum* rats and housed normally, fed *ad libitum* on a raised metal grid and 24-hour fasted rats, respectively. The distribution plot for resting membrane potential of ARC neurones in rats fed *ad libitum* rats in normal housing (see Figure 4.2 A) was skewed to the right compared to the same plot for the other two groups of rats, indicating that neurones recorded from the rats housed on a raised metal grid, either fed *ad libitum* or fasted for 24 hours, generally expressed more positive resting membrane potentials.

4.2.1.2 Input resistance

In rats fed *ad libitum* in normal cages, the mean input resistance was 1606 ± 98 MΩ (range 400 to 3174 MΩ, n = 47), and amounted to 1440 ± 93 MΩ (range 536 to 3530 MΩ, n = 50) and 1452 ± 84 MΩ (range 655 to 3350 MΩ, n = 52) in rats fed *ad libitum* and rats fasted for 24 hours housed on raised metal grids, respectively (Figure 4.1 B; Table 4.1). This data also revealed no significant difference between the input resistances of ARC neurones recorded from three groups of rats. The median values for all three groups of rats were 1452, 1426 and 1337 MΩ in rats fed *ad libitum*, fed *ad libitum* housed on metal grids and 24-hour fasted rats, respectively. The range of input resistances containing the highest proportion of neurones was 1000-1500 MΩ (31.9%) for rats fed *ad libitum* in normal housing and (40.4%) in 24-hour fasted rats. In rats fed

ad libitum housed on metal grids, there were two ranges of input resistance recorded that contained the largest proportion of neurones, 1000-1500 MΩ (30.0%) and 1500-2000 MΩ (30.0%) (Figure 4.2 B). The frequency histograms plotted and shown in Figure 4.2 B showed that the input resistance values for rats fed *ad libitum* in the normal housing was skewed to the left compared to the other two groups of rats housed on the raised metal grid, suggesting that neurones recorded from rats fed *ad libitum* raised in normal housing, had lower input resistance.

Table 4.1 General membrane properties of ARC neurones recorded in fed, fasted and a fed control group for fasted rats.

All neurones				
Parameter	**Fed *ad libitum* in standard housing (solo)**	**Fed *ad libitum* housed as fasted**	**Fasted**	**Significance (*P*)**
Membrane potential (mV)	-48 ± 1 (n = 47)	-48 ± 1 (n = 50)	-49 ± 1 (n = 52)	0.8662
Input resistance (MΩ)	1606 ± 98 (n = 47)	1440 ± 93 (n = 50)	1452 ± 84 (n = 52)	0.3694
Spontaneous firing frequency (Hz)	1.2 ± 0.2 (n = 47)	0.9 ± 0.2 (n = 50)	0.9 ± 0.2 (n = 52)	0.4782
Spontaneous active neurones (%)	59.6 (n = 28)	72.0 (n = 36)	69.2 (n = 36)	-
Membrane time-constant (ms)	60 ± 7 (n = 47)	51 ± 6 (n = 50)	45 ± 4 (n = 52)	0.1680

4.2.1.3 Firing frequency

The average spontaneous action potential firing frequency of ARC neurones recorded from rats fed *ad libitum*, in normal housing, rats fed *ad libitum* as the fasted group control and 24-hour fasted rats was 1.2 ± 0.2 Hz (range 0.0 to 4.8 Hz, n = 47), 0.9 ± 0.2 Hz (range 0.0 to 5.6 Hz, n = 50) and 0.9 ± 0.2 Hz (range 0.0 to 4.1 Hz, n = 52), respectively (Figures 4.1 C and 4.2 C; Table 4.1). This data showed no significant differences between the spontaneous action potential firing frequencies of ARC neurones recorded from these groups of rats. 0.0-0.5 Hz was the range of spontaneous action potential firing frequency containing the largest proportion of neurones in all three groups of rats: 53.2% in fed, 56.0% in rats fed *ad libitum* housed on metal grids and 53.8% in fasted rats. Frequency histograms revealed neurones recorded from fed rats in normal cages and fed rats housed on the metal grid had a greater proportion of neurones with a higher firing frequency than those from fasted rats (Figure 4.2 C). The median values were 0.5, 0.5 and 0.4 Hz for fed, fasted control group and fasted rats, respectively. The data also showed higher proportions of neurones recorded from all three groups of rats that were spontaneously active. The percentage of spontaneous active neurones were 59.6% in fed rats, 72.0% in fed and housed on metal grids and 69.2% for fasted rats (Figure 4.3), indicating neurones recorded from rats housed on metal grids either fed or fasted showed a higher degree of spontaneous suprathreshold activity than neurones recorded from rats housed in normal rodent cages.

4.2.1.4 Membrane time-constant

The average membrane time-constant of neurones recorded from fed rats was 60 ± 7 ms (range 17 to 298 ms, n = 47), whilst it amounted to 51 ± 6 ms (range 8 to 275 ms, n = 50) and 45 ± 4 ms (range 9 to 111 ms, n = 52) for fed rats housed on metal grids and fasted rats, respectively (Figures 4.4 A and B, Table 4.1). The data revealed no significance different between the membrane time-constant of ARC neurones recorded from three groups of rats. The median value of membrane time-constant in fed rats was 49 ms, 40 ms in fed and housed on metal grids and 39 ms for fasted rats. The membrane time-constant ranges that contained the highest proportion of neurones were 40-60 ms (28.3%) in fed rats and 20-40 ms for the other two groups: 36.0% in fed (fasted control) and 44.2% in fasted rats (Figure 4.4 B).

Frequency histograms of membrane time-constant for the three groups of rats (see Figure 4.4 B) demonstrated that the plot for rats, housed normally, was skewed to the right and the plot for fasted rats skewed to the left.

Table 4.2 Changes in body weight in fed and fasted rats

Parameter	Weight of rats			
	24 hours before experiment	**15 minutes before experiment**	**Significance (*P*)**	**% change in body weight**
Fed *ad libitum* in standard housing (solo)	283.7 ± 7.7 (n = 11)	285.8 ±7.4 (n = 11)	0.85	0.8 ± 0.2 (n = 11)
Fed *ad libitum* housed as fasted	258.2 ± 10.5 (n = 11)	259.5 ± 10.2 (n = 11)	0.93	0.6 ± 1.5 (n = 11)
Fasted	270.3 ± 7.1 (n = 28)	242.8 ± 6.7 (n = 28)	***P* < 0.05**	(-)10.3 ± 0.2 (n = 28)

4.2.2 The effects of fasting and housing of rats on body weight

Rats from the three groups were initially weighed 24 hours before and subsequently 15 minutes prior to experiment to investigate changes in body weight. The average body weight of rats fed *ad libitum* housed conventionally, measured initially 24 hours and subsequently 15 minutes before experiment were 283.7 ± 7.7 g (range 240 to 330 g, n = 11) and 285.8 ± 7.4 g (range 246 to 331 g, n =11), respectively (Table 4.2). The average weight of fed rats housed on the metal grid were 258.2 ± 10.5 g (range 175 to 296 g, n = 11) and 259.5 ± 10.2 g (range 182 to 298 g, n = 11) at 24 hours and 15 minutes before experiments, respectively (Table 4.2). In fasted rats the mean body weight was 270.3 ± 7.1 g (range 180 to 324 g, n = 28) at 24 hours before experiments and 242.8 ± 6.7 g (range 158 to 292 g,

n = 28) at 15 minutes before experiments (Table 4.2). This data revealed that over a 24-hour period fed rats gained an average weight of 0.8 ± 0.2 % and gained 0.6 ± 1.5 % in weight when fed and housed on a raised metal grid. However, those rats fasted for 24 hours lost 10.3 ± 0.2 % of body weight (Table 4.2). Two-tailed student's *t*-test showed no statistically significant change in weight when fed, whereas rats fasted for 24 hours lost a statistically significant amount of body weight ($P < 0.05$;Table 4.2).

4.2.3 The effects of fasting on subthreshold active conductances expressed in ARC neurones

ARC neurones were classified into eight groups based on the differential expression of one or more subthreshold active conductances. Hyperpolarising and depolarising rectangular-wave current pulses of constant increment were used to generate I-V relations and neurones grouped into clusters (Pennartz *et al*., 1998) based upon the subthreshold active conductances they expressed. Conductances differentially expressed included: anomalous inward rectification; transient outward rectification, hyperpolarisation-activated non-selected cation conductances, low voltage-activated calcium conductance and expression of various combinations of these. This study aimed to investigate the effects of a negative energy state, fasted state, on the expression of these subthreshold active conductances. Properties of action potentials and active conductances were calculated as shown in Figure 4.5.

4.2.3.1 Cluster 1 - Expression of anomalous inward rectification

This group of ARC neurones were characterised by a reduction in input resistance at more negative/hyperpolarised membrane potential, showing a nonlinear I-V relationship (Figures 4.7 Ai and Aii). This decrease in input resistance was instantaneous and non-inactivating. This subthreshold active conductance, has been reported previously in other neurones and is most often called an anomalous inward rectification (Constanti & Galvan, 1983; Pickering *et al.*, 1991; Tasker & Dudek, 1991). In the present study, this group of neurones has been termed cluster 1. An overview of this data is shown in Table 4.3.

Cluster 1 neurones accounted for 6.4% of the ARC neuronal population recorded in the fed group and accounted for 2.0% of the fasted control group (i.e. fed *ad libitum* on a raised metal grid). However, no cluster 1 neurones were encountered in ARC of fasted animals (Figure 4.6) although the total number of neurones recorded was relatively low.

The average resting membrane potential of cluster 1 neurones was -42 ± 2 mV (range -40 to -46 mV, n = 3) in fed rats and -59 (n = 1) in the control for the fasted group (see Figures 4.10 Aii).

Table 4.3 Electrophysiological properties of cluster 1 neurones

Cluster 1				
Parameter	**Fed *ad libitum* in standard housing (solo) (n = 3)**	**Fed *ad libitum* housed as fasted (n = 1)**	**Fasted**	**Significance (*P*)**
Membrane Potential (mV)	-42 ± 2	-59	-	-
Input resistance (MΩ)	1244 ± 284	2119	-	-
Firing frequency (Hz)	2.3 ± 1.2	0.0	-	-
Membrane time-constant (ms)	37 ± 11	68	-	-
AP spike duration (ms)	4.2 ± 0.6	2.8	-	-
Holding membrane potential (mV)	-100 ± 1	-100	-	-
Reduction of input resistance induced by I_{an} (%)	18.8 ± 14.3	42.2	-	-

The mean input resistance of cluster 1 neurones of rats fed *ad libitum* was 1244 ± 284 MΩ (range 896 to 1806, n = 3), whereas it was 2119 MΩ (n = 1) in the control for the fasted group (i.e. fed *ad libitum* on a raised metal grid: Figures 4.10 Bii).

The average firing frequency of cluster 1 neurones was 2.3 ± 1.2 Hz (range 0.31 to 4.5 Hz, n = 3) in rats fed *ad libitum* in normal housing, whilst the neurone recorded in the fasting control group was silent. The mean membrane time-constant and action potential duration of cluster 1 neurones in fed rats were 37 ± 11 ms and 4.2 ± 0.6 ms (n = 3), respectively (see Table 4.3). In the fasted control group, the membrane time-constant was 68 ms and the action potential duration was 2.8 ms (n = 1) (Table 4.3). The magnitude of the anomalous inward rectification (I_{an}), was estimated by measuring input resistance at rest relative to input resistance of the neurone at around -100 mV. The mean relative rectification amounted to an 18.8 ± 14.3% decrease in input resistance at a mean membrane potential of -100 ± 1 mV (n = 3) in rats fed *ad libitum*. The corresponding value in the fasted control group (fed ad libitum on raised metal mesh) amounted to a reduction in input resistance of 42.2% at a holding membrane potential of -100 mV (n = 1; Table 4.3).

4.2.3.2 Cluster 2 – Expression of transient outward rectification and anomalous inward rectification (I_{an})

Cluster 2 neurones were characterised by the expression of two subthreshold active conductances: an anomalous inward rectification (I_{an}) (as expressed by cluster 1) and an A-like transient outward conductance (I_A; see Figures 4.7 Bi and Bii). I_A is characterised by a delayed return of the membrane response to resting levels, following negative current injections. I_A has been described in many neurones in the CNS (Connor & Stevens, 1971a, 1971b; Tasker & Dudek, 1991; Bouskila & Dudek, 1995; Miyazaki *et al.*, 1996). Cluster 2 neurones have been described in the ARC as NPY/AgRP conditional pacemaker neurones that can be characterised by their ability to generate burst firing patterns of activity in response to orexigenic inputs such as ghrelin (van den Top *et al.*, 2004). An overview of this data is shown in Table 4.4.

4.3% of the population of ARC neurones recorded from rats fed *ad libitum* were classified as cluster 2 neurones. The corresponding values for neurones recorded from fasted rats was 3.8% and the control group for fasted rats (fed *ad libitum* raised on metal grids) comprised of 2.0% of cluster 2 neurones (see Figure 4.6). However, all groups comprised of only 1 or 2 neurones, statistical analyses for cluster 2 under the range of conditions investigated was not possible.

The mean resting membrane potential of cluster 2 neurones in rats fed *ad libitum* was -49 ± 1 mV (range -48 to -50 mV, n = 2; see Figures 4.11 Aii) and in 24-hour fasted rats amounted to -47 ± 7 mV (range -40 to -53 mV, n = 2; see Figures 4.11 Aii). The resting membrane potential of the neurone recorded in fasted control group was -48 mV (Figures 4.11 Aii).

Cluster 2 neurones had an average input resistance at 1400 ± 418 MΩ (range 982 to 1817, n = 2) in rats fed *ad libitum* (Figures 4.11 Bii) and 2389 ± 650 MΩ (range 1739 to 3038, n = 2) in 24-hour fasted rats (Figures 4.11 Bii). The input resistance of the single cluster 2 neurone recorded in the fasted control group was 1568 MΩ (Figures 4.11 Bii).

The average firing frequency of cluster 2 neurones were 1.3 ± 0.3 Hz (range 0.93 to 1.6 Hz, n = 2) in fed rats and 0.6 ± 0.4 Hz (range 0.2 to 1 Hz, n = 2) in fasted rats. The firing frequency of the neurone recorded in the fasted control group was 0.2 Hz (see Figures 4.11 Cii).

The mean membrane time-constant and action potential duration of cluster 2 neurones were 51 ± 30 ms and 3.1 ± 1.0 ms (n = 2), respectively in fed rats, 94 ms and 2.5 ms (n = 1), respectively in the control group for fasted rats and 47 ± 7 ms and 2.3 ± 0.3 ms (n = 2), respectively in 24-hour fasted rats (Table 4.4). The anomalous inward rectification was also observed in this cluster. In fed rats (n = 2), the average reduction in input resistance induced by I_{an} was 31.2 ± 24.8% relative to input resistance at rest at a membrane potential of -95 ± 3 mV, the corresponding values for fasted rats amounting to a 41.5 ± 23.0% reduction in input resistance relative to input resistance at rest at a membrane potential of -100 ± 1 mV in 24-hour fasted rats (n = 2; see Table 4.4). However, the input resistance also decreased by 49.7% at a membrane potential of -98 mV in the fasted control group (n = 1; Table 4.4). Thus, given the small numbers of neurones recorded from this cluster and the apparent "stronger" anomalous inward rectification observed in fasted and the fasted control group (fed *ad libitum* on a

raised metal grid), it is too premature to suggest a significant effect of fasting on the apparent "strength" of the inward rectifier.

Table 4.4 Electrophysiological properties of cluster 2 neurones

Cluster 2				
Parameter	**Fed *ad libitum* in standard housing (solo) (n = 2)**	**Fed *ad libitum* housed as fasted (n = 1)**	**Fasted (n = 2)**	**Significance (*P*)***
Membrane Potential (mV)	-49 ± 1	-48	-47 ± 7	-
Input resistance (MΩ)	1400 ± 418	1568	2389 ± 650	-
Firing frequency (Hz)	1.3 ± 0.3	0.2	0.6 ± 0.4	-
Membrane time-constant (ms)	51 ± 30	94	47 ± 7	-
AP spike duration (ms)	3.1 ± 1.0	2.5	2.3 ± 0.3	-
Holding membrane potential (mV)	-95 ± 3	-98	-100 ± 1	-
Reduction of input resistance induced by I_{an} (%)	31.2 ± 24.8	49.7	41.5 ± 23.0	-
Amplitude I_A at ½ decay time (mV)	3.9 ± 0.2	3.9	7.3 ± 0.2	-
I_A duration (ms)	1584 ± 676	1920	1519 ± 189	-

Properties of I_A were also explored. The inactivation time of I_A was calculated as the time taken from cessation of the negative current injection until the membrane response returned back to the resting membrane potential. The amplitude of the membrane response induced by I_A was measured at the half time for inactivation as described above. The mean amplitudes of the responses induced by activation of I_A at half-decay time were 3.9 ± 0.2 mV (n = 2), 3.9 mV (n = 1) and 7.3 ± 0.2 mV (n = 2) in fed, fasted control group and 24-hour fasted rats, respectively with the corresponding average decay duration of 1584 ± 676 ms (n = 2), 1920 ms (n = 1) and 1519 ± 189 ms (n = 2), respectively. However, again the low numbers do not allow detailed conclusions to be drawn or meaningful statistics to be undertaken for this population of neurones. Thus, further recordings from cluster 2 neurones, are required to appreciate the impact of a negative energy status on the functional electrophysiological properties of these neurones.

4.2.3.3 Cluster 3 – No expression of any subthreshold active conductance

Cluster 3 neurones were identified as neurones which expressed no obvious subthreshold active conductance, therefore giving a linear current-voltage (I-V) relationship (Figures 4.7 Ci and Cii). This particular subclass of ARC neurone was only encountered once, in fed rats housed on a raised metal grid, with no neurones fitting these criteria in the other groups (see Figure 4.6). The membrane properties of this particular one are summarised in Table 4.5 and Figures 4.12. This neurone was recorded from a fed rat and had a resting membrane potential of -43 mV and input resistance of 911 MΩ. This neurone was rather active with a firing frequency of 3.4 Hz. The membrane time-constant was 18 ms and the action potential duration was 4.1 ms. Further recordings from this subclass of ARC neurone are required to explore the impact of fasting on the functional operation and properties of these neurones.

Table 4.5 Electrophysiological properties of cluster 3 neurones

Cluster 3				
Parameter	**Fed *ad libitum* in standard housing (solo)**	**Fed *ad libitum* housed as fasted (n = 1)**	**Fasted**	**Significance (*P*)**
Membrane Potential (mV)	-	-43	-	-
Input resistance (MΩ)	-	911	-	-
Firing frequency (Hz)	-	3.4	-	-
Membrane time-constant (ms)	-	18	-	-
AP spike duration (ms)	-	4.1	-	-

4.2.3.4 Cluster 4 – Expression of voltage- and time-dependent inward rectification (I_h)

Cluster 4 neurones were classified as neurones which expressed voltage- and time-dependent inward rectification. This subthreshold active conductance was seen as depolarising 'sag' in the membrane response to negative current injection, thus showing a non-linear I-V relationship (Figures 4.8 Ai and Aii). This 'sag' became more apparent when greater negative current injection was applied. This subthreshold active conductance, a voltage- and time-dependent hyperpolarisation-activated non-selective cation conductance (I_h), has been described in other neurones (Halliwell & Adams, 1982; McCormick & Pape, 1990; Akasu *et al.*, 1993; Pape, 1996). Data summarising the properties of cluster 4 neurones is shown in Table 4.6.

Cluster 4 neurones accounted for 4.3% of the ARC population in fed rats and 3.8% of the population recorded from 24-hour fasted rats. Unfortunately, no cluster 4

neurones were recorded in the fasted control group (fed *ad libitum*, housed on a metal grid).

Cluster 4 neurones in fed rats had an average resting membrane potential at -49 ± 7 mV (range -42 to -55 mV, n = 2; see Figures 4.13 Aii). The corresponding values in 24-hour fasted rats was -49 ± 4 mV (range -45 to -52 mV, n = 2; see Figures 4.13 Aii). The average input resistance of cluster 4 neurones in fed rats was 1332 ± 179 MΩ (range 1153 to 1511 MΩ, n = 2) and 1282 ± 231 MΩ in fasted rats (range 1051 to 1513 MΩ, n = 2; see Figures 4.13 Bii).

Table 4.6 Electrophysiological properties of cluster 4 neurones

Cluster 4				
Parameter	**Fed *ad libitum* in standard housing (solo) (n = 2)**	**Fed *ad libitum* housed as fasted**	**Fasted (n = 2)**	**Significance (*P*)***
Membrane Potential (mV)	-49 ± 7	-	-49 ± 4	-
Input resistance (MΩ)	1332 ± 179	-	1282 ± 231	-
Firing frequency (Hz)	0.0 ± 0.0	-	1.2 ± 1.2	-
Membrane time-constant (ms)	51 ± 33	-	27 ± 5	-
AP spike duration (ms)	4.3 ± 0.6	-	3.0 ± 0.1	-
Amplitude of depolarising 'sag' induced by activation of I_h (mV)	5.4 ± 1.1	-	3.0 ± 0.4	-
Reduction in input resistance induced by I_h (%)	9.1 ± 1.1	-	6.0 ± 0.3	-

In rats fed *ad libitum*, all cluster 4 neurones were silent showing no spontaneous suprathreshold activity (n = 2; Figures 4.13 Cii), whereas one cluster 4 neurone, out of two recorded neurones was active in the fasted population (1.2 ± 1.2 Hz; range 0.0 to 2.4 Hz, n = 2 see Figures 4.13 Cii).

The mean membrane time-constants of cluster 4 neurones were 51 ± 33 ms (n =2) and 27 ± 5 ms (n = 2) in fed and fasted rats, respectively with an action potential duration of 4.3 ± 0.6 ms (n = 2) and 3.0 ± 0.1 ms (n = 2) for fed and fasted cluster 4 neurones, respectively. Once again the numbers of neurones recorded for these different clusters were too low to generate meaningful comparisons between the fed and fasted states.

The amplitude of I_h was described by the difference in membrane potential between the instantaneous and steady-state responses to negative current injection. The input resistance ratio, as shown in Table 4.6, was calculated as a percentage decrease in input resistance (at the termination of negative current injection) relative to the peak input resistance prior to activation of I_h. In fed rats, the mean amplitude of the depolarising sag induced by I_h was 5.4 ± 1.1 mV at an average membrane potential of -109 ± 3 mV (n = 2). The reduction in input resistance reflecting I_h activation amounted to 9.1 ± 1.1% (n = 2). In contrast, in fasted rats, the average depolarising sag amplitude was 3.0 ± 0.4 mV at a mean membrane potential of -104 ± 3 mV (n = 2), and the input resistance decreased by 6.0 ± 0.3% (n = 2) relative to the peak input resistance. This data suggest a trend toward a reduction in the "strength" of I_h in 24-hour fasted rats. However, the number of recordings for this cluster was again too low to generate meaningful statistical comparisons between these groups of neurones.

4.2.3.5 Cluster 5 – Expression of voltage- and time-dependent inward rectification (I_h) and T-type calcium conductance

This group of neurones were classified by the expression of voltage- and time-dependent inward rectification (I_h) as in cluster 4 and the expression of a T-type calcium conductance (Figures 4.8 Bi and Bii). A rebound depolarisation after the end of negative current injection was used to describe this latter conductance. T-type calcium conductance has also been reported in other neurones (Llinas & Yarom, 1981). An overview of this data is shown in Table 4.7. 36.2% of the population of

ARC neurones recorded in fed rats, 30.0% in the fasted control group and 26.9% of ARC neurones in fasted were characterised by this electrophysiological phenotype (see Figure 4.6).

Table 4.7 Electrophysiological properties of cluster 5 neurones

Cluster 5				
Parameter	**Fed *ad libitum* in standard housing (solo) (n = 17)**	**Fed *ad libitum* housed as fasted (n = 15)**	**Fasted (n = 14)**	**Significance (*P*)**
Membrane Potential (mV)	-50 ± 2	-50 ± 1	-53 ± 1	0.3142
Input resistance (MΩ)	1516 ± 158	1528 ± 157	1363 ± 137	0.7116
Firing frequency (Hz)	0.7 ± 0.4	0.4 ± 0.1	0.5 ± 0.3	0.7137
Membrane time-constant (ms)	57 ± 7	46 ± 10	54 ± 7	0.5919
AP spike duration (ms)	4.4 ± 0.4	3.2 ± 0.2	2.7 ± 0.1	***P* < 0.001**
Amplitude of depolarising 'sag' induced by activation of I_h (mV)	6.3 ± 0.7	8.8 ± 0.9	10.0 ± 1.1	***P* < 0.05**
Reduction in input resistance induced by I_h (%)	11.5 ± 1.3	15.4 ± 1.4	17.9 ± 1.6	***P* < 0.05**
T-type amplitude (mV)	10.4 ± 1.4	12.8 ± 1.5	12.9 ± 1.5	0.5083

The average resting membrane potential of these neurones was -50 ± 2 mV (range -40 to -71 mV, n = 17) in fed rats (Figures 4.14 Aii), -50 ± 1 mV (range -42 to -59 mV, n = 15) in the fasted control group (Figures 4.14 Aii) and -53 ± 1 mV (range -44 to -62 mV, n = 14) in 24-hour fasted

rats on metal grids (Figures 4.14 Aii). Statistical analysis of these groups (ANOVA) revealed no significant differences in resting membrane potential among the three groups of rats. Figure 4.14 Ai shows the frequency histograms revealing the modes of resting membrane potential ranged from -45 to -50 mV (41.2%), -50 to -55 mV (40.0%) and -55 to -60 mV (35.7%) for fed, control group for fasted and fasted rats, respectively with corresponding median values of -49 mV, -51 mV and -53 mV, respectively. This data showed that rats fasted for 24 hours, had the most negative membrane potential of the three groups, whilst the fed rats were relatively more depolarised compared to the fasted group.

Cluster 5 neurones of rats fed *ad libitum* had a mean input resistance of 1516 ± 158 MΩ (range 690 to 3038 MΩ, n = 17; Figures 4.14 Bii), the corresponding values of the control group for fasted rats amounting to 1528 ± 157 MΩ (range 536 to 2863 MΩ, n = 15; Figures 4.14 Bii). In fasted rats the mean input resistance of cluster 5 neurones was relatively lower, amounting to 1363 ± 137 MΩ (range 660 to 2310 MΩ, n = 14; Figures 4.14 Bii). However, this apparent lower input resistance was not statistically significant when compared to either the fed group or the fasted control group. The ranges of input resistance containing the largest populations of neurones were 1500-2000 MΩ (46.7%) in the control group for fasted rats while the other two groups, fed and fasted, shared the same range from 1000 to 1500 MΩ, 35.3% in rats fed *ad libitum* in the normal housing and 42.9% in 24-hour fasted rats (Figure 4.14 Bi) with the median values being 1416 MΩ, 1505 MΩ and 1287 MΩ, respectively.

The mean firing frequency of cluster 5 neurones were 0.7 ± 0.4 Hz (range 0.0 to 4.2 Hz, n = 17), 0.4 ± 0.1 Hz (range 0.0 to 1.6 Hz, n = 15) and 0.5 ± 0.3 Hz (range 0.0 to 4.1 Hz, n = 14) in fed rats (Figures 4.14 Cii), control group for fasted rats (Figures 4.14 Cii) and 24-hour fasted rats (Figures 4.14 Cii), respectively. There was no statistically detectable difference in firing frequency between the groups of rats). All three groups of rats shared the same range of firing frequency containing the largest neurone population between 0.0 and 0.5 Hz, 76.5% in rats fed *ad libitum*, 53.3% in rats fed *ad libitum* (fasted control group) and 85.7% in 24-hour fasted rats, as illustrated in Figure 4.14 Ci. The median value for firing frequency in rats fed *ad libitum* was 0.0 Hz, the corresponding value in the control group for fasted rats and 24-hour fasted rats amounting to 0.2 Hz and 0.0 Hz.

Therefore, the data from all three groups of rats revealed that most neurones either were silent or had relatively low level of spontaneous activity.

The average membrane time-constant of neurones recorded in rats fed *ad libitum* was 57 ± 7 ms with action potential duration of 4.4 ± 0.4 ms (n = 17), whereas the corresponding value for the group fed *ad libitum* and housed on a metal grid was 46 ± 10 ms with action potential duration of 3.2 ± 0.2 ms (n = 15). In fasted rats these values amounted to 54 ± 7 ms with action potential duration of 2.7 ± 0.1 ms. ANOVA revealed no statistically detectable difference in membrane time-constant for those three groups of rats. However, statistically significant differences were detected in action potential duration ($P < 0.001$). This data revealed a significant reduction in action potential duration in rats fed *ad libitum* but housed on a metal grid compared to those rats housed normally and fed *ad libitum* ($P < 0.05$; two-tailed student's *t*-test). This indicates that the effect of housing on a metal grid alone may be sufficient to cause changes in ARC neurones. This may be due to a stress effect for example of the housing conditions. The action potential duration was further reduced in fasted rats compared to both fed groups although no statistically significance was observed between fasted rats and their control group. This suggests that cluster 5 neurones may be subject to functional electrophysiological re-organisation in terms of electrophysiological properties with changes in energy status.

The amplitude of the depolarising sag induced by I_h activation was also investigated. I_h in Cluster 5 neurones had a mean amplitude of 6.3 ± 0.7 mV at an average membrane potential of -106 ± 2 mV (n = 17) in fed rats. The corresponding value in the control group for fasted animals amounted to 8.8 ± 0.9 mV at an average membrane potential of -110 ± 3 mV (n = 15). In rats fasted for 24 hours, the magnitude of I_h reached a maximum value of 10.0 ± 1.1 mV at an average membrane potential of -109 ± 2 mV (n = 14) suggesting an increase in the apparent amplitude of I_h in fasted rats. Performing ANOVA revealed statistically detectable difference in the amplitude of the depolarising sag induced by I_h activation among three groups of rats ($P < 0.05$; ANOVA). Two-tailed student's *t*-test was further performed revealing that there was a statistically significant increase in the apparent amplitude of I_h in the control group of fasted rats compared to rats fed *ad libitum* in normal housing ($P = 0.0400$), whereas no statistically significant difference was detected in the amplitude of the depolarising

sag between the control group of fasted rats and 24-hour fasted rats. Thus this data suggests that some effects on I_h reflected a potential stress/behaviour-related effect of housing rats on a metal grid. The activation of I_h was associated with a reduction in input resistance of 11.5 ± 1.3%, 15.4 ± 1.4% and 17.9 ± 1.6% in rats fed *ad libitum*, rats fed *ad libitum* housed on a metal grid (fasted control) and 24-hour fasted rats, respectively ($P < 0.05$;ANOVA). Two-tailed student's *t*-test was further performed and revealed no statistically detectable difference in reduction in input resistance induced by I_h between rats fed *ad libitum* in normal housing and rats fed *ad libitum* housed on a metal grid (fasted control group). In addition, no statistically significant difference in reduction in input resistance induced by I_h was detected between fasted control group and 24-hour fasted rats, whereas a significant greater reduction in input resistance was detected in 24-hour fasted rats than in rats fed *ad libitum* in normal housing ($P < 0.01$; two-tailed student's *t*-test). This data suggests that an increase in both the amplitude and reduction in input resistance of activation of I_h is affected by both stress/behaviour-related effect of housing rats on a metal grid and fasted state in the ARC neurones.

The investigation of the properties of the T-type calcium conductance was undertaken in cluster 5 neurones. The amplitude of the rebound depolarisation peak, relative to the membrane potential at rest, was measured and used as an indicator of activation of this conductance. Activation of the T-type calcium conductance was associated with a mean membrane depolarisation of 10.4 ± 1.4 mV (n = 17) in rats fed *ad libitum*, with the corresponding values for the fasted control group and fasted group amounting to 12.8 ± 1.5 mV (n = 15) and 12.9 ± 1.5 mV (n = 14), respectively. However, these effects on this conductance were not statistically significant. However, additional recordings may be worth undertaking to address these properties of the T-type conductance.

4.2.3.6 Cluster 6 – Expression of T-type calcium conductance

Neurones in this group were characterised by the expression of one clear subthreshold active conductance, the T-type calcium conductance (Figures 4.8 Ci and Cii). An overview of data for cluster 6 neurones is summarised in Table 4.8. Of the total population of ARC neurones recorded, cluster 6 neurones accounted for 25.5%, 22.0% and 23.1% in the fed *ad libitum* group, fed group housed on a metal grid (fasted control group) and 24-hour fasted group, respectively (Figure 4.6).

Cluster 6 neurones had a mean resting membrane potential of -46 ± 1 mV (range -42 to -51 mV, n = 12) in rats fed *ad libitum* (Figures 4.15 Aii), with corresponding values of -46 ± 3 mV (range -40 to-62 mV, n = 11) for fed rats housed on the metal grid (Figures 4.15 Aii) and -46 ± 1 mV (range -41 to -55 mV, n = 12) for fasted rats (Figures 4.15 Aii). There was no statistically significant difference between these groups (ANOVA). The mode for resting membrane potential ranged from -40 to -45 mV in all three groups of rats, 50.0% in fed, 54.5% in fed housed on the metal grid and 50.0% in 24-hour fasted rats (Figure 4.15 Ai), with median values of -45, -42 and -45 mV, respectively.

The average input resistance of cluster 6 neurones was 1760 ± 206 MΩ (range 967 to 3021 MΩ, n = 12) in rats fed *ad libitum* (Figures 4.15 Bii) and 1242 ± 185 MΩ (range 645 to 2767 MΩ, n = 11) in rats fed *ad libitum* rats housed on a metal grid (Figures 4.15 Bii). The corresponding value in fasted rats was 1322 ± 146 MΩ (range 765 to 2450 MΩ, n = 12; Figures 4.15 Bii). These differences in input resistance between each group of rats were not a statistically detectable difference (ANOVA). The ranges of input resistance containing the highest percentage of neurones were 1000-1500 MΩ (33.3%) in fed rats and 500-1000 MΩ (45.5%) in the fed control group for fasted rats with median values of 1524 MΩ and 1063 MΩ, respectively (Figure 4.15 Bi). In 24-hour fasted rats, there were two ranges of input resistance that shared the largest proportion of neurones in this group (33.3%), 500-1000 MΩ and 1000-1500 MΩ with 1200 MΩ representing the median.

In fed rats the average firing frequency was 1.4 ± 0.4 Hz (range 0.0 to 4.5 Hz, n = 12; see Figures 4.15 Cii), whilst it was 0.6 ± 0.3 Hz (range 0.0 to 3.3 Hz, n = 11) in the fed, control group for fasted rats (Figures 4.15 Cii) and 0.8 ± 0.2 Hz (range 0.03 to 1.97 Hz, n = 12) in 24-hour fasted rats (Figures 4.15 Cii). ANOVA analysis revealed no statistically significant difference in firing frequency.

The majority of neurones in all three groups of rats had a firing frequency between 0.0 and 0.5 Hz, 41.7% in fed rats, 63.6% in fed (fasted control group) and 50.0% in 24-hour fasted rats (see Figure 4.15 Ci). The median values for firing frequency were 1.14 Hz, 0.13 Hz, and 0.50 Hz in fed rats, rats fed *ad libitum* housed on a metal grid and 24-hour fasted rats, respectively. Thus for cluster 6 neurones there appeared to be a tendency towards lower firing frequencies in fasted rats although this again may have reflected a change in the housing arrangement rather than a direct effect relating to changes in energy status.

Table 4.8 Electrophysiological properties of cluster 6 neurones

Cluster 6				
Parameter	**Fed *ad libitum* in standard housing (solo) (n = 12)**	**Fed *ad libitum* housed as fasted (n = 11)**	**Fasted (n = 12)**	**Significance (*P*)**
Membrane Potential (mV)	-46 ± 1	-46 ± 3	-46 ± 1	0.9593
Input resistance (MΩ)	1760 ± 206	1242 ± 185	1322 ± 146	0.1073
Firing frequency (Hz)	1.4 ± 0.4	0.6 ± 0.3	0.8 ± 0.2	0.1868
Membrane time-constant (ms)	39 ± 7	28 ± 5	23 ± 3	0.0910
AP spike duration (ms)	4.2 ± 0.3	3.3 ± 0.3	2.95 ± 0.1	***P* < 0.01**
T-type amplitude (mV)	9.9 ± 1.8	8.2 ± 1.2	7.7 ± 0.6	0.3055

The mean membrane time-constant was 39 ± 7 ms in rats fed *ad libitum*, 28 ± 5 ms in the fed control group for fasted rats and 23 ± 3 ms in 24-hour fasted rats. The membrane time-constant tended to decrease in neurones recorded from fasted rats, however, ANOVA analysis revealed no statistically significant difference. In contrast, statistical analysis revealed changes in action potential

duration ($P < 0.01$; ANOVA). The action potential duration of neurones recorded in rats fed *ad libitum* was 4.2 ± 0.3 ms, in the fed control group for fasted rats amounted to 3.3 ± 0.3 ms and 2.95 ± 0.1 ms in 24-hour fasted rats. Thus, both fasting and housing on a metal grid appeared to be factors contributing to changes in action potential duration.

Activation of the T-type calcium conductance gave an average membrane depolarisation (the amplitude of the rebound excitation observed at the termination of negative current injection) of 9.9 ± 1.8 mV, 8.2 ± 1.2 mV and 7.7 ± 0.6 mV in rats fed *ad libitum*, the fed control group for fasted rats and 24-hour fasted rats, respectively. There was no statistically significant difference in amplitude of the T-type calcium conductance among three groups of rats (ANOVA).

4.2.3.7 Cluster 7 – Expression of anomalous inward rectification (I_{an}) and T-type calcium conductance

Cluster 7 neurones were characterised by the expression of two subthreshold active conductances – anomalous inward rectification (I_{an}) and T-type calcium conductance (Figures 4.9 Ai and Aii). I_{an} was described as one of the subthreshold active conductances in cluster 1 and 2 neurones, whilst T-type calcium conductance was expressed in cluster 5 and 6 neurones. Table 4.9 summarises an overview of this data.

Cluster 7 neurones accounted for 8.5% of the ARC population of rats fed *ad libitum*, 14.0% of the fed control group for fasted rats and 15.4% of the population recorded from fasted rats. However, an insufficiency in recordings for these neurones in some groups made statistical analysis difficult, thus further recordings are needed to confirm or strengthen this data set.

Cluster 7 neurones had a mean resting membrane potential of -47 ± 4 mV (range -41 to -57 mV, n = 4) in rats fed *ad libitum* (Figures 4.16 Aii), -46 ± 1 mV (range -44 to -49 mV, n = 7) in the fed control group for fasted rats (Figures 4.16 Aii) and -45 ± 1 mV (range -39 to -51 mV, n = 8) in 24-hour fasted rats (Figures 4.16 Aii). Statistical analysis showed no statistically detectable difference in resting membrane potential among these three groups of rats (ANOVA). Frequency histogram plots (see Figure 4.16 Ai) revealed the majority of neurones had resting membrane potentials ranging from -40 to -45 mV (50.0%) and -45 to -50 mV

(57.1%) in rats fed *ad libitum* and the fed control group for fasted rats, respectively with the corresponding median values of -46 mV and -46 mV, respectively. In 24-hour fasted rats, two ranges of resting membrane potential accounted for the majority of cluster 7 neurones, -40 to -45 mV (37.5%) and -45 to -50 mV (37.5%) with a median value of -45 mV.

Table 4.9 Electrophysiological properties of cluster 7 neurones

Cluster 7				
Parameter	**Fed *ad libitum* in standard housing (solo) (n = 4)**	**Fed *ad libitum* housed as fasted (n = 7)**	**Fasted (n =8)**	**Significance (*P*)**
Membrane potential (mV)	-47 ± 4	-46 ± 1	-45 ± 1	0.6546
Input resistance (MΩ)	2376 ± 343	1544 ± 279	1485 ± 185	0.0860
Firing frequency (Hz)	1.9 ± 1.1	1.8 ± 0.7	1.7 ± 0.3	0.9722
Membrane time-constant (ms)	154 ± 75	39 ± 8	38 ± 4	***P* < 0.01**
AP spike duration (ms)	2.8 ± 0.3	3.3 ± 0.4	2.7 ± 0.2	0.2039
Holding membrane potential (mV)	-103 ± 2	-103 ± 3	-101 ± 2	0.6681
Reduction of input resistance induced by I_{an} (%)	22.7 ± 7.1	27.3 ± 4.8	11.8 ± 4.8	0.1042
T-type amplitude (mV)	4.2 ± 2.7	7.3 ± 1.9	5.6 ± 0.8	0.6085

The average input resistance of cluster 7 neurones in rats fed *ad libitum* was 2376 ± 343 MΩ (range 1566 to 3174 MΩ, n = 4; see Figures 4.16 Bii), and 1544 ± 279 MΩ (range 920 to 3094 MΩ, n = 7) for the fed control group for fasted

rats (Figures 4.16 Bii). The corresponding values for fasted rats were 1484 ± 185 MΩ (range 1017 to 2645 MΩ, n = 8; see Figures 4.16 Bii). The difference in input resistance of cluster 7 neurones between the groups was not statistically significant difference (ANOVA) although the data showed a trend toward a reduction in input resistance in the fed control group for fasted rats and 24-hour fasted rats. Figure 4.16 Bi revealed the range of input resistance containing the largest proportion of neurones, was shared by both the fed control group for fasted rats (42.9%) and 24-hour fasted rats (50.0%), and amounted to 1000-1500 MΩ. However, in rats fed *ad libitum* the numbers were too small to generate meaningful data. The median values were 2382 MΩ, 1353 MΩ and 1398 MΩ in rats fed *ad libitum*, fed control group for fasted rats and 24 hour fasted rats, respectively.

The mean firing frequency of neurones in rats fed *ad libitum* was 1.9 ± 1.1 Hz (range 0.0 to 4.8 Hz, n = 4; Figures 4.16 Cii), with corresponding values of 1.8 ± 0.7 Hz (range 0.05 to 5.1 Hz, n = 7) in the fed control group for fasted rats (Figures 4.16 Cii) and 1.7 ± 0.3 Hz (range 0.7 to 3.3 Hz, n = 8) in 24-hour fasted rats (Figures 4.16 Cii). There was no statistically significant difference in firing frequency between all three groups of rats (ANOVA). Figure 4.16 Ci shows that neurones recorded in fed rats and the fed control group for fasted rats had the same range of firing frequency containing the largest percentage of neurones in the range 0.0 and 0.5 Hz (50% in fed rats and 28.6% in the fed control group for fasted rats) with the corresponding median values of 1.5 Hz and 1.1 Hz, respectively. In 24-hour fasted rats, the majority of neurones had firing frequency in the range of 1.0 to 1.5 Hz (50.0%) with a median value of 1.4 Hz.

The mean membrane time-constant was 154 ± 75 ms in cluster 7 neurones from rats fed *ad libitum*, 39 ± 8 ms in the fed control group for fasted rats and 38 ± 4 ms in 24-hour fasted rats. Thus a statistically significant difference was observed between the fed control group for fasted rats and the fasted group when compared to rats housed normally and fed *ad libitum* ($P < 0.01$; ANOVA). This data suggest that changes in the housing of the animals alone, possibly inducing stress, is a factor contributing to changes in time-constant in these neurones. There was no statistically significant difference in action potential duration between the three groups of rats. The average action potential duration in rats fed *ad libitum* was

2.8 ± 0.3 ms with the corresponding value in the fed control group for fasted rats amounting to 3.3 ± 0.4 ms and 2.7 ± 0.2 ms in 24-hour fasted rats.

As described in the section on cluster 1, I_{an} activation induced a reduction in input resistance at more negative membrane potentials (around -100.0 mV) relative to input resistance at rest and this was calculated as a percentage decrease relative to rest. With activation of I_{an}, the input resistance of neurones recorded in rats fed *ad libitum* was reduced by 22.7 ± 7.1% at a mean membrane potential of -103 ± 2 mV, and amounted to a 27.3 ± 4.8% decrease and 11.8 ± 4.8% input resistance reduction at a mean holding membrane potential of -103 ± 3 mV and -101 ± 2 mV in the fed control group for fasted rats and 24-hour fasted rats, respectively. There was no statistically significant difference among these groups. However, two-tailed student's *t*-test revealed statistically significant weaker inward rectification in fasted rats compared to the fasted control group (rats fed *ad libitum* house on a metal grid; $P < 0.05$). Thus, the fasting state appeared to be a factor contributing to changes in an inward rectification of ARC neurones in this cluster.

Activation of the T-type calcium conductance induced a rebound depolarisation and the amplitude of this rebound potential was investigated. Neurones recorded in rats fed *ad libitum* had average rebound amplitude of 4.2 ± 2.7 mV, the corresponding values in the fed control group for fasted rats and the fasted group amounting to 7.3 ± 1.9 mV and 5.6 ± 0.8 mV, respectively. However, these differences were not statistically significant (ANOVA).

4.2.3.8 Cluster 8 – Expression of anomalous inward rectification (I_{an}), voltage- and time-dependent inward rectification (I_h) and T-type calcium conductance

This group of neurones were identified as having three subthreshold active conductances, anomalous inward rectification (I_{an}), voltage- and time-dependent inward rectification (I_h) and T-type calcium conductance (Figures 4.9 Bi and Bii). Due to the similar voltage-dependencies of these conductances all values for activation of each individual conductance can only be approximated. An overview of data describing cluster 8 neurones is shown in Table 4.10.

The percentage of neurones recorded from rats fed *ad libitum* and classified as cluster 8 was 14.9%, with the corresponding values for the fed control group for

fasted rats and fasted rats being 28.0% and 26.9%, respectively (Figure 4.6). Cluster 8 neurones had a mean resting membrane potential of -51 ± 4 mV (range -42 to -70 mV, n = 7) in rats fed *ad libitum* (Figures 4.17 Aii), -49 ± 2 mV (range -39 to -62 mV, n = 14) in the fed control group for fasted rats (Figures 4.17 Aii) and -50 ± 2 mV (range -40 to -62 mV, n = 14) for 24-hour fasted rats (Figures 4.17 Aii). There was no statistically significant difference in resting membrane potential for cluster 8 neurones between the groups (ANOVA). The majority of neurones had resting membrane potentials ranging from -40 to -45 mV (42.9%) in fed rats with a median of -48 mV, whereas those majority of neurones recorded from the fed control group for fasted rats and 24-hour fasted rats had resting membrane potentials ranging from -45 to -50 mV (28.6% and 35.7%, respectively) with the corresponding median values of -48 mV and -50 mV, respectively.

The mean input resistance of these neurones was 1426 ± 219 MΩ (range 486 to 2320 MΩ, n = 7) in rats fed *ad libitum* (Figures 4.17 Bii), 1417 ± 202 MΩ (range 653 to 3530 MΩ, n = 14) in the fed control group for fasted rats (Figures 4.17 Bii) and 1581 ± 200 MΩ (range 655 to 3350 MΩ, n = 14) in 24-hour fasted rats (Figures 4.17 Bii). There were no statistically significant differences in input resistance between all three groups (ANOVA). Frequency histograms revealed ranges of input resistance containing the largest populations of neurones (Figure 4.17 Bi): 500-1000 MΩ (35.7%) in fed control group for fasted rats with a median of 1438 MΩ and 1000-1500 MΩ for both rats fed *ad libitum* (42.9%) and 24-hour fasted rats (42.9%) with median values of 1440 MΩ and 1425 MΩ, respectively.

Spontaneous firing frequency in cluster 8 neurones recorded from all three groups did not vary significantly between the groups (ANOVA) although there was a trend toward a reduction in firing frequency in the fed control group for fasted rats and 24-hour fasted rats suggesting again, changes in housing had significant effects on the properties of these neurones. The mean spontaneous firing frequency was amounted to 1.6 ± 0.6 Hz (range 0.0 to 4.8 Hz, n = 7) in fed rats (Figures 4.17 Cii), 1.2 ± 0.4 Hz (range 0.0 to 5.6 Hz, n = 14) in the fed control group for fasted rats (Figures 4.17 Cii) and 1.1 ± 0.4 Hz (range 0.0 to 4.1 Hz, n = 14) in 24-hour fasted rats (Figures 4.17 Cii). The majority of neurones recorded from the fed control group for fasted rats (57.1%) and 24-hour fasted rats (57.1%) shared the same range of firing frequencies, between 0.0 to 0.5 Hz, with median values of 0.5 Hz and 0.2 Hz,

respectively. In rats fed *ad libitum*, the ranges of firing frequency containing the largest population of neurones (28.6%) were, 0.0 to 0.5 Hz and 1.0 to 1.5 Hz with a median value of 1.1 Hz.

Table 4.10 Electrophysiological properties of cluster 8 neurones

Cluster 8				
Parameter	**Fed *ad libitum* in standard housing (solo) (n = 7)**	**Fed *ad libitum* housed as fasted (n = 14)**	**Fasted (n = 14)**	**Significance (*P*)**
Membrane Potential (mV)	-51 ± 4	-49 ± 2	-50 ± 2	0.7240
Input resistance (MΩ)	1426 ± 219	1418 ± 202	1581 ± 200	0.8147
Firing frequency (Hz)	1.6 ± 0.6	1.2 ± 0.4	1.1 ± 0.4	0.7898
Membrane time-constant (ms)	81 ± 15	78 ± 16	61 ± 8	0.5317
AP spike duration (ms)	2.9 ± 0.4	2.5 ± 0.1	2.5 ± 0.1	0.2806
Holding membrane potential (mV)	-100 ± 1	-101 ± 1	-102 ± 2	0.5764
Reduction of input resistance induced by I_{an} (%)	32.6 ± 7.2	28.2 ± 4.7	33.1 ± 3.2	0.6895
T-type amplitude (mV)	12.9 ± 2.6	8.8 ± 1.6	5.2 ± 0.9	0.0718
Amplitude of depolarising ‘sag’ induced by activation of I_h (mV)	8.4 ± 1.4	5.4 ± 0.9	6.5 ± 0.8	0.1708
Reduction in input resistance induced by I_h (%)	19.2 ± 4.5	11.0 ± 1.9	20.0 ± 6.2	0.3103

The mean membrane time-constant of neurones recorded in rats fed *ad libitum* was 81 ± 15 ms, and 78 ± 16 ms and 61 ± 8 ms in the fed control group for fasted rats and 24-hour fasted rats, respectively. There were no statistically significant differences in time-constant between the three groups (ANOVA). The action potential duration was also measured and amounted to 2.9 ± 0.4 ms, 2.5 ± 0.1 ms and 2.5 ± 0.1 ms in fed rats, fed control group for fasted rats and 24-hour fasted rats, respectively. Again there was no statistically significant difference between these groups (ANOVA).

The activation of I_{an} induced a reduction in input resistance at more negative membrane potentials. In rats fed *ad libitum*, the input resistance decreased by 32.6 ± 7.2% at a mean membrane potential of -100 ± 1 mV. I_{an} activation accounted for a 28.2 ± 4.7% and 33.1 ± 3.2% reduction in input resistance at an average holding membrane potential of -101 ± 1 mV and -102 ± 2 mV in the fed control group for fasted rats and 24-hour fasted rats, respectively. Thus there was no statistically significant change in the strength of activation of this conductance in cluster 8 neurones between the three groups (ANOVA).

Activation of a T-type calcium conductance gave a mean membrane depolarisation of 12.9 ± 2.6 mV in rats fed *ad libitum*, with corresponding values of 8.8 ± 1.6 mV for the fed control group for fasted rats and 5.2 ± 0.9 mV for 24-hour fasted rats. Although this data exhibited a trend for a decrease in T-type amplitude in the fed control group for fasted rats and 24-hour fasted rats, statistical analysis revealed no significant difference (ANOVA). Increasing the numbers of neurones recorded for these groups may clarify this issue.

The size of I_h could be measured by taking the difference in peak amplitude between the steady-state and instantaneous membrane potential responses to negative current injection. The average amplitude of this depolarising sag induced by I_h was 8.4 ± 1.4 mV in rats fed *ad libitum*, 5.4 ± 0.9 mV in the fed control group for fasted rats and 6.5 ± 0.8 mV in 24-hour fasted rats. These differences in amplitude of this conductance were not statistically detectable difference (ANOVA). The input resistance ratio was also calculated as a percentage of the decrease in input resistance (at the termination of negative current injection) relative to the peak input resistance. In rats fed *ad libitum*, I_h activation induced a 19.2 ± 4.5% reduction in input resistance, 11.0 ± 1.9% reduction in the fed control group for fasted rats and 20.0 ± 6.2% in 24-hour fasted rats. This data yielded no statistically significant

changes either (ANOVA), although the apparent decrease in the fed control group for fasted rats again highlighted the effects of changes in housing alone on these properties.

4.2.3.9 Differential expression of ARC clusters in fed and fasted rats

Generally, clusters 1, 2, 3 and 4 were poorly represented across the population, generally accounting for low numbers (see Figure 4.6) whereas the majority of ARC neurones recorded from all three groups of rats (fed, fed control group for fasted rats and 24 hour fasted rats) were classified as cluster 5, 6, 7 and 8. The highest percentage of neurones recorded in rats fed *ad libitum* fell into cluster 5 (36.2%), and cluster 6 (25.5%). The fed control group for fasted rats was characterised by the majority of neurones falling into clusters 5 (30.0%) and 8 (28.0%). In 24-hour fasted rats, the majority of neurones fell approximately equally (26.9%) into clusters 5 and 8, and cluster 6 (23.1%). These data suggest both changing the housing environment and energy status (fasting) can affect intrinsic membrane properties regulating excitability and functional operation of ARC neurones and circuits.

4.2.3.10 Comparison of general membrane properties of neurones in individual clusters recorded from rats fed *ad libitum* housed in normal rodent housing

In rats fed *ad libitum*, cluster 1 neurones exhibited the most depolarised resting membrane potential -42 ± 2 mV whereas cluster 8 neurones showed the most negative at -51 ± 4 mV. Cluster 1 was characterised by the lowest input resistance (1244 ± 284 MΩ) among the eight clusters, whilst cluster 7 neurones showed the highest input resistance of 2376 ± 343 MΩ. Cluster 1 exhibited the highest spontaneous firing frequency (2.3 ± 1.2 Hz), and clusters 7 (1.9 ± 1.1 Hz) and 8 (1.6 ± 0.6 Hz) showed the second and third highest firing frequency, respectively. Cluster 4 neurones were silent displaying no spontaneous activity (0.0 Hz).

4.2.3.11 Comparison of general membrane properties of neurones in individual clusters recorded from rats fed *ad libitum* housed as a control for fasted rats (on a raised metal grid)

In this group of neurones, cluster 3 exhibited the most depolarised resting membrane potential of -43 mV, followed by -46 ± 1 mV for cluster 7, whilst the most negative resting membrane potential was -59 mV, associated with cluster 1. Cluster 1 was characterised by the highest input resistance (2119 MΩ), whilst cluster 3 neurone showed the lowest input resistance of 911 MΩ. Cluster 3 exhibited the highest spontaneous firing frequency (3.4 Hz) and clusters 7 (1.8 ± 0.7 Hz) and 8 (1.2 ± 0.4 Hz) showed the second and third highest firing frequency, respectively. However, the low 'n' values for clusters 1, 2 and 3 and none for cluster 4, make comparisons between clusters for this treatment group difficult.

4.2.3.12 Comparison of general membrane properties of neurones in individual clusters recorded from 24-hour fasted rats

In this group of rats, no neurones were detected that fell into the cluster 1 and 3 categories. The most negative resting membrane potential was -53 ± 1 mV, associated with cluster 5 neurones. The most depolarised resting membrane potential (-45 ± 1 mV) was associated with cluster 7.

Cluster 2 neurones displayed the highest input resistance, 2389 ± 650 MΩ, the remaining clusters having input resistances ranging from 1282 to 1581 MΩ, although cluster 4 showed the lowest input resistance of 1282 ± 231 MΩ.

Cluster 7 was the most active neuronal fasted group, 1.7 ± 0.3 Hz, followed by cluster 4 at 1.2 ± 1.2 Hz, whilst the lowest firing frequency was 0.5 ± 0.3 Hz, which was associated with cluster 5 and 0.6 ± 0.4 Hz associated with cluster 2 neurones.

4.3 Discussion

The aim of this study was to investigate the effects of a negative energy state (24 hours fast) on the intrinsic electrophysiological of ARC neurones. Data from three groups of rats were compared: fed *ad libitum* and fasted with a fed control group to control for the effects of housing animals on a raised metal grid, the latter required to prevent consumption of waste products as can occur in rodents following food withdrawal. Both active and passive subthreshold electrophysiological properties of ARC neurones were investigated and compared among the three groups of rats.

In this study, the effects of fasting were investigated on the general membrane properties (resting membrane potential, input resistance, spontaneous firing frequency and membrane time-constant) of ARC neurones. Other electrophysiological properties such as action potential duration and the consequences of subthreshold active conductance activation on ARC neurones were also investigated. Rat body weight was also monitored.

Neurones were classified into subgroups based upon the differential expression of subthreshold conductances. This approach led to the subclassification of ARC neurones into 8 groups (clusters 1 to 8). This work builds on previous work aimed at building a framework of the functional organisation of the ARC (van den Top, 2002; Saker, 2009; Virdee, 2009). However, over the course of the present study relatively low numbers of neurones were recorded for clusters 1, 2, 3 and 4, making detailed comparisons and statistical analysis of the effects of fasting on these clusters difficult. Further recordings are needed to take the present study further.

The major findings of this study revealed statistically significant differences in some active and passive membrane properties including the expression of subthreshold active conductances between fasted and fed groups. Cluster 2 neurones have been previously described (van den Top *et al*., 2004) and represent a subtype of orexigenic NPY/AgRP neurones capable of pacemaker-like activity when exposed to orexigenic signals such as ghrelin. The transient outward rectifier in these neurones was enhanced in 24-hour fasted rats compared to rats fed *ad libitum*. As the A-current in these neurones is thought to play a key role in setting the frequency of burst firing, the increased magnitude of the conductance in fasted rats suggests in a “hunger” state the dynamics of the burst firing may be subject to

modulation (van den Top *et al*., 2004). However, the lack of sufficient numbers, in particular for the fed control group for fasted rats, makes it difficult o determine if these changes in the A-current reflect energy status or "stress". Further work is required to clarify if this is the case.

Cluster 5 neurones displayed the most significant differences in membrane properties of all clusters when fasted and fed groups were compared. These included a significant reduction in action potential duration in cluster 5 and 6 neurones recorded from fasted rats compared to rats fed *ad libitum*. However, a reduction in action potential duration was also observed, although less significant, in both cluster 5 and 6 neurones from the fed control group for fasted rats (fed *ad libitum* but housed on the raised metal grid as was required for the fasted group) compared to rats fed *ad libitum*. Similarly, the magnitude of I_h in cluster 5 neurones was subject to modulation, being enhanced in terms of both its contribution to reducing input resistance upon activation and the amplitude of the depolarising 'sag' that characterises this conductance, in neurones from fasted rats compared to fed. However, once again, this enhancement of I_h in these neurones was also to some extent mirrored in the control group for fasted rats, suggesting some changes induced a response to the changes in housing conditions rather than entirely due to food withdrawal. Clusters 4, 5 and 8 expressed I_h, observed as a depolarising sag during the response to hyperpolarising current injections has been reported in many other neurones (Halliwell & Adams, 1982; Pape, 1996). It has been suggested this has a role in establishing the resting membrane potential of hypothalamic neurones (Akasu *et al.*, 1993), and together with a T-type calcium conductance work in tandem to generate rhythmic activity in thalamic relay neurones (for review see Huguenard, 1996). It has also been reported that this conductance is not found within the ARC of mice which is at odds to the study of rats (Burdakov & Ashcroft, 2002).

Cluster 7 neurones were characterised by a significantly greater membrane time-constant in neurones recorded from slices prepared from rats fed *ad libitum* than both fasted and its corresponding fed control group. As the time-constant indicates the surface-area of the neurone, this decrease in time constant in fasted and its control group suggests a possible functional, anatomical reorganisation of these neurones. However, once again the change in housing appears to be the main factor influencing this level of plasticity in ARC neurones.

When the whole population of ARC neurones were compared between the three groups, independent of clusters, the resting membrane potentials in neurones were relatively the same. However, input resistance in neurones recorded from 24-hour fasted rats and the corresponding fed control group on the metal grid was lower compared to rats fed *ad libitum*. Similarly, neurones recorded from rats fed *ad libitum* had a higher spontaneous firing frequency than neurones recorded from fasted animals and their control group. This data indicated that the housing of animals on a raised metal grid, either with or without fasting was a significant factor contributing to the changes in activity in ARC neurones. This notion is further supported by the fact that the number of active neurones in both groups of rats housed on the metal grid was comparable and higher than the number of active neurones in normally housed rats fed *ad libitum*. Housing conditions alone can affect rat behaviour and the level of corticosterone (a biochemical index of stress), body weight and muscle performance of animals (Gentsch *et al.*, 1981; Brown & Grunberg, 1995; Spangenberg *et al.*, 2005). Brown and Grunberg (2005) reported that rats caged or housed individually and overcrowded revealed differences in stress levels. Further evidence was also forwarded by Spangenberg and co-workers (2005) who showed differences in housing space area affected body weight, levels of stress and muscle performance due to changes in the rate of physical activity of rats. Fasting also causes stress and affects rat haematology and hormone levels, causes changes in cholesterol, triglycerides, urea nitrogen, calcium and decreases body weight and insulin secretion although the plasma glucose remains unchanged (Grey *et al.*, 1970; Maejima & Nagase, 1991; Matsuzawa & Sakazume, 1994; Young & Landsberg, 1997). However, in contrast to above finding, there were some evidences showed that fasting causes a decrease in plasma glucose level (De Boer *et al.*, 1989; Faggioni *et al.*, 2000; de Vries *et al.*, 2003; Palou *et al.*, 2009) compared to fed *ad libitum* state. Thus to address this issue, future experiments need to be better designed and should take into account the "housing effect." Studies should include housing of animals in groups on raised metal grids for longer periods of time to allow them to acclimatise. Wherever possible, animals should be housed in groups to prevent "stress" associated with being housed in isolation.

The membrane time-constant (tau), the product of membrane resistance and capacitance, is an indicator of neuronal surface area (and size). Comparing the entire population of neurones recorded, there appears to be no significant change among the

three groups. However, as mentioned above, in cluster 7 neurones, there was a highly significant change in membrane time-constant. The tau value in neurones recorded in normal rats, fed *ad libitum* was significantly higher than in the other two groups although the tau values in the latter two groups of rats on the metal grid were virtually indistinguishable. These results do suggest that cluster 7 neurones recorded from rats fed *ad libitum* rats expressed a greater surface area of membrane, suggesting a significant functional and anatomical reorganisation, although this did not appear to be a direct effect relating to energy status, more likely indicating a stress-like effect due to isolation or the change in environment.

Anomalous inward rectification (I_{an}), was a characteristic feature of clusters 1, 2, 7 and 8. This conductance manifests as a reduction in input resistance at more negative/hyperpolarised membrane potential which was also described in other neurones (Constanti & Galvan, 1983). However, the function of I_{an} remains unclear although the suggested role is to prevent neurones from becoming excessively hyperpolarised and keep them within a functional range (Wilson *et al.*, 2002; van den Top & Spanswick, 2006). Results described here provided no evidence for changes in this conductance between the various groups although the low numbers of recordings for clusters 1 and 2 make detailed conclusions regarding this conductance difficult. Interestingly, fasting in clusters 7 neurones showed a strong tendency to a reduction in the strength of activation of this conductance, an effect not mirrored in the fed control group. Further work in this area to increase the numbers of neurones may clarify this issue.

The T-type calcium conductance, a low-voltage activated and rapidly inactivating current, similar to that reported previously (Llinas & Yarom, 1981), was a feature of clusters 5, 6, 7 and 8. No significant change in the amplitude of this depolarising rebound conductance was observed, suggesting that stress due to the effects of changes in housing and fasting had no effect on T-type calcium conductance expression. However, the T-type calcium conductance has been reported crucial for the generation of bursting firing patterns in other neurones in the CNS (Huguenard & Prince, 1994; Huguenard, 1996) and involved in the pacemaker activity generation in the ARC (van den Top *et al.*, 2004). Hence, changes in neurones expressing T-type calcium conductance could play a key role in determining specific firing pattern in ARC neurones. Further work is required to clarify this.

Considering only clusters 5, 6, 7 and 8 neurones, given the small numbers of recordings obtained for clusters 1 to 4, data from rats fed *ad libitum* revealed a greater proportion of clusters 5 and 6 neurones than both the fasted and fed control group for fasted, both being housed on a metal grid. Both the fasted and its fed control group displayed a greater percentage of neurones expressing I_{an} and T-type calcium conductance (cluster 7) and cluster 8 than rats fed *ad libitum* with regular housing. However, distinguishing effects due to housing as opposed to effects due to fasting was difficult.

Body weight was measured and revealed rats lost approximately 10.3% of their body weight within 24 hours. This data is in agreement with previous studies showing that after 24 hours of fasting, the weight of male F344 rats was 91% of the initial body weight (Maejima & Nagase, 1991). The body weight in rats fed *ad libitum* both in regular housing and when housed on a metal grid showed no statistically significant difference in their body weight, gaining around 0.8% and 0.6 %, respectively over 24 hours.

In conclusion, the present study revealed changes in electrophysiological properties of ARC neurones between three different groups of rats: fed, fasted and a control group that were fed but housed in a manner similar to fasted rats. However, some of these changes in properties appear to reflect changes in housing conditions rather than as a result of a negative energy state induced by fasting. Further work is required to address this issue.

Chapter 5

Effects of intracellular adenosine triphosphate (ATP) on glucose-sensing neurones in the rat hypothalamic arcuate nucleus

5.1 Introduction

ATP (adenosine triphosphate) is a nucleotide which performs many important roles in the cell. Structurally it is composed of adenine, ribose and three phosphate groups. It serves as a convenient and multipurpose store, or currency, of energy to drive a variety of chemical reactions in cells. The formation of ATP is obtained from energy metabolism, providing energy for processes as diverse as building cell components, transmission of nerve impulses, excitability, cell motility and muscle contraction. The breakdown of ATP releases energy which is then used as fuel for all our bodily functions. ATP is the most abundant active carrier in cells, for example, it is used to supply energy for many pumps that transport substances and ions out of and into cells, and for ion channels to control the voltage gradient across the plasma membrane of cells. It also powers the nerve cells to transport materials from one end of their long axons to another.

ATP concentrations inside the cells are not stable, instead the local ATP level may depend on many factors, for example, the ATP production rate, ATP diffusion rate and ATP consumption rate (Jones, 1986). Hence, it is predicted that ATP concentration will be decreased as a function of distance from the mitochondria. ATP also has an important role in the direct regulation of ion channels and ion pumps.

Regulation of ion pumps by ATP

The ability of the cell to sustain ion gradients across biological membranes is a function of ion pumps and is the foundation for life. These pumps include various types of Ca^{2+}-ATPase, Na^+/K^+-ATPase, H^+-ATPase and Na^+/K^+ exchangers which all work by using the energy from ATP hydrolysis. High levels of ion pump activity indicates an increase in ATP turnover based on glycolysis (Wittam R & M., 1965). In this section, only Na^+/K^+-ATPase is described as it is relatively common and found in brain cells.

The Na^+/K^+-ATPase (Na^+/K^+ pump) is a transmembrane protein present in all eukaryotic cells that uses the energy of ATP hydrolysis to transport Na^+ and K^+ ions across the membrane against their electrochemical gradients (Dhar-Chowdhury *et al.*, 2007). This pump is a membrane protein, regulated by glycolytically-derived ATP (Dhar-Chowdhury *et al.*, 2007), identified in many studies in numerous tissues including brain synaptosomes, squid giant axon, kidney cells, skeletal muscle and smooth muscle with a variety of techniques (Caldwell *et al.*, 1960; Philipson &

Nishimoto, 1983; Hasin & Barry, 1984; Kennedy *et al.*, 1986; Takai & Tomita, 1986; Lynch & Balaban, 1987; MacLeod, 1989; Erecinska & Dagani, 1990; Campbell & Paul, 1992; Glitsch & Tappe, 1993; Okamoto *et al.*, 2001). Furthermore, the Na^+/K^+ pump can directly contribute to the electrical activity of cells since it translocates an unequal number of Na^+ and K^+ ions in each cycle (three Na^+ ions and two K^+ ions), leading to an electrogenic effect. Hence, through this pump, ATP regulates excitability of cells and may indirectly influence a large numbers of physiological processes, both in health and disease.

Regulation of ion channels by ATP and ion channels

Ion channels are transmembrane pores which control voltage gradients across the plasma membrane of all cells by allowing the passage of ions out and into the cell due to their electrochemical gradient. They are responsible for setting the resting membrane potential in both excitable and non-excitable mammalian cells and they also play a key role in a host of biological activities (Kandel *et al.*, 2000). Various ion channels are sensitive to glycolytic activity and therefore couple glucose metabolism directly to excitability (Kandel *et al.*, 2000; Dhar-Chowdhury *et al.*, 2007). Ion channels can be classified according to which physical or chemical modulator controls their gating activity, for example, ATP-sensitive K^+ (K_{ATP}) channels, Ca^{2+}-activated potassium channels etc. In this section, only ATP-sensitive K^+ (K_{ATP}) channels are described due to their regulation by glycolysis-derived ATP.

K_{ATP} channels were first described as being blocked by cytosolic ATP (Noma, 1983) and activated by Mg-ADP (Lederer & Nichols, 1989). Their functional opening is controlled by the ATP:ADP ratio, classically described in the pancreatic β-cell, where an increase in ATP production following an increase in glucose results in K_{ATP} channel closure, leads to membrane depolarisation with an increase in intracellular Ca^{2+}, resulting in insulin secretion (Minami *et al.*, 2004). Many studies have shown various roles of K_{ATP} channels in several cells, for example, in the cardiac myocyte, K_{ATP} channels have been shown to be involved in protection of the heart against stress responses (Kane *et al.*, 2005; Tong *et al.*, 2006) and in the hypothalamus, K_{ATP} channels are strongly expressed in glucose-sensing neurones which alter their firing frequency in response to blood glucose levels (Miki *et al.*, 2001). Furthermore, a number of studies also confirmed that K_{ATP} channels are regulated by glycolysis, for example, an action potential shortening

during metabolic inhibition and hypoxia, which resulted from an opening of K_{ATP} channels, is rapidly reversed by glucose (Van der Heyden *et al.*, 1985; Nakamura *et al.*, 1989).

Glucose-sensing neurones in the rat hypothalamic arcuate nucleus and the underlying mechanism(s) by which they respond to changes in extracellular glucose concentration were studied in this project. Two different energy states were induced in rats and subsequently studies *in vitro* using whole-cell recording techniques: rats fed *ad libitum* housed normally and rats fasted for 24 hours housed on a raised metal grid. Plasma glucose levels in 24-hour fasted rats have been reported as being lower than those *ad libitum* fed rats (De Boer *et al.*, 1989; Faggioni *et al.*, 2000; de Vries *et al.*, 2003; Palou *et al.*, 2009) and the majority of ATP production takes place in mitochondria whereas some ATP are produced through the glycolysis pathway in which two molecules of ATP are produced for each glucose molecule breakdown. Thus, as intracellular ATP levels correlate with that of extracellular glucose, we hypothesised that the intracellular ATP concentration in neurones of rats fed *ad libitum* and 24-hour fasted rats is different and that this will lead to changes in both basal levels of activity in glucose-sensing neurones and their sensitivity to changes in extracellular glucose. In addition, the mechanisms of glucose-sensing in neurones have strongly implicated the involvement of ion channels especially K_{ATP} channels (Song *et al.*, 2001; Wang *et al.*, 2004; Song & Routh, 2005; van den Top *et al.*, 2007) and ion pumps (Na^+/K^+) (Oomura, 1983; Silver & Erecinska, 1998) both of which are regulated by ATP.

The specific aim of the present study was to investigate the effects of intracellular ATP concentration on ARC glucose-sensing neurones to determine the levels of ATP required to maintain resting membrane potential and input resistance, thus providing an estimate of intracellular ATP levels and how this changes depending on energy status, fed versus fasted. The second aim was to determine the levels of intracellular ATP required to maintain glucose-sensing capability. To do this, extracellular glucose levels were manipulated from 2.0 to 0.0 mM whilst intracellular ATP was manipulated by changing intracellular ATP levels in the pipette solution (0.0, 1.0, 2.0, 5.0 and 10.0 mM) using whole-cell patch-clamp recording techniques. For this and the subsequent chapter, neurones in which firing frequency increased when glucose was raised, are referred to as glucose-excited (GE) neurones, and neurones in which firing frequency decreased when glucose was

raised, are called glucose-inhibited (GI) neurones. In neurones in which effects of changes in glucose levels induced transient effects on membrane excitability, the term rapidly adapting was used to describe these neurones (glucose rapidly adapting: GRA). Putative mechanisms involving K_{ATP} channels were also explored.

5.2 Results

The effects of intracellular ATP concentration (0.0, 1.0, 2.0, 5.0 and 10.0 mM) on baseline membrane properties and responsiveness to a 2.0 to 0.0 mM change in extracellular glucose concentration were investigated in hypothalamic brain slices prepared from rats fed *ad libitum* housed normally and rats fasted for 24 hours housed on a raised metal grid.

5.2.1 Effects of intracellular ATP on resting membrane properties of ARC neurones

Baselines, resting membrane properties or spontaneous activity of ARC neurones were recorded in both slices, maintained in 2.0 mM extracellular glucose, from rats fed *ad libitum* and 24-hour fasted rats. The level of intracellular ATP was investigated by determining the ability of these neurones to maintain resting membrane properties and to sustain a stable spontaneous firing frequency in active cells.

In recordings with 0.0 mM intracellular ATP in the pipette, 87.5% of neurones recorded from rats fed *ad libitum*, maintained a stable baseline level of activity whereas a further 12.5% were subject to spontaneous inhibition of activity characterised by membrane hyperpolarisation and/or a reduction or cessation of action potential firing. Similarly in slices prepared from fed animals with 1.0 or 2.0 mM intracellular ATP in the patch pipette, 50.0% of neurones were characterised by the maintenance of a stable baseline resting membrane potential or level of spontaneous firing whereas the remaining 50.0% were subject to a spontaneous inhibition over the time-course of recording. In the presence of 5.0 mM intracellular ATP 78.6% of recorded neurones maintained resting membrane potential and/or firing frequency with only 21.4% of neurones being inhibited.

In slices prepared from rats fasted for 24 hours, whole-cell recordings from ARC neurones with 0.0 mM intracellular ATP revealed the majority of neurones to be spontaneously inhibited (77.8%) with only 22.2% of neurones maintaining a stable baseline resting membrane potential and/or firing frequency. However, neurones recorded from slices prepared from fasted rats with 1.0 or 2.0 mM intracellular ATP were more stable maintaining resting membrane potential and/or input resistance in 62.5% and 70.0% of neurones, respectively, whereas the baseline in the remaining neurones 37.5% in 1.0 mM ATP and 30.0% in 2.0 mM ATP was subject to spontaneous inhibition. With 5.0 mM ATP in the patch pipette in slices from fasted rats, 45.5% of neurones remained electrophysiologically stable, and 45.5% were subject to spontaneous inhibition and 9.0% were subject to a spontaneous increase in activity with this level of intracellular ATP. In 10.0 mM intracellular ATP, baseline activity was maintained stable in 70.6% of neurones, none were subject to inhibition, and 29.4% were characterised by an increase in spontaneous activity.

Table 5.1 Effects of intracellular ATP in the patch pipette on spontaneous activity and resting membrane properties of ARC neurones in slices from rats fed *ad libitum*

Intracellular ATP concentration (mM)	Percentage of baseline behaviour of ARC neurones recorded in *ad libitum* fed rats (%)			
	Stable	Inhibited	Excited	Total
0.0	87.5 (n = 7)	12.5 (n = 1)	0.0 (n = 0)	100.0 (n = 8)
1.0	50.0 (n = 5)	50.0 (n = 5)	0.0 (n = 0)	100.0 (n = 10)
2.0	50.0 (n = 3)	50.0 (n = 3)	0.0 (n = 0)	100.0 (n = 6)
5.0	78.6 (n = 11)	21.4 (n = 3)	0.0 (n = 0)	100.0 (n = 14)
10.0	-	-	-	-

This data is summarised in Tables 5.1 and 5.2, respectively. Figures 5.1 to 5.5 show examples of baseline levels of activity recorded in different concentrations of intracellular ATP from slices prepared from rats fed *ad libitum* and fasted for 24 hours.

Table 5.2 Effects of intracellular ATP in the patch pipette on spontaneous activity and resting membrane properties of ARC neurones in slices from 24-hour fasted rats

Intracellular ATP concentration (mM)	Percentage of baseline behaviour of ARC neurones recorded in 24-hour fasted rats (%)			
	Stable	Inhibited	Excited	Total
0.0	22.2 (n = 2)	77.8 (n = 7)	0.0 (n = 0)	100.0 (n = 9)
1.0	62.5 (n = 5)	37.5 (n = 3)	0.0 (n = 0)	100.0 (n = 8)
2.0	70.0 (n = 7)	30.0 (n = 3)	0.0 (n = 0)	100.0 (n = 10)
5.0	45.5 (n = 5)	45.5 (n = 5)	9.0 (n = 1)	100.0 (n = 11)
10.0	70.6 (n = 12)	0.0 (n = 0)	29.4 (n = 5)	100.0 (n = 17)

5.2.2 A comparison of the effects of intracellular ATP concentration ($[ATP]_i$) on responses to a reduction in extracellular glucose in ARC neurones from rats fed *ad libitum* and rats fasted for 24 hours

Different concentrations of intracellular ATP (0.0, 1.0, 2.0, 5.0 and 10.0 mM) were used to investigate the responses of ARC neurones from rats fed *ad libitum* and rats fasted for 24 hours *in vitro* to a change in extracellular glucose concentration from 2.0 to 0.0 mM. Figures 5.26 and Figure 5.27 show overviews of the proportion of neurones and their responses in each concentration of intracellular ATP in fed and fasted rats, respectively.

5.2.2.1 Effects of 0.0 mM ($[ATP]_i$) on responses to a reduction in extracellular glucose in ARC neurones from rats fed *ad libitum* and rats fasted for 24 hours

Whole-cell recordings were obtained from 11 ARC neurones in slices from rats fed *ad libitum* using an electrode solution from which ATP was omitted. In the presence of 2.0 mM glucose, for at least 5.0 minutes prior to applying glucose-free aCSF, these neurones were usually spontaneously active and showed stable input resistance. The initial resting membrane potential of these neurones was -45 ± 2 mV (n = 8), whilst the input resistance was 1460 ± 297 MΩ (n = 8) and the firing frequency was 1.3 ± 0.7 Hz (n = 8). Of these 11 neurones, 72.7% were characterised as GE, 18.2% GI neurones and 9.1% of neurones did not respond to 0.0 mM glucose (Figure 5.26 A). No neurone was found to be a GRA neurone in fed rats. In 24-hour fasted rats (n = 9 ARC neurones) in which ATP was omitted from the pipettes solution, neurones were usually spontaneously active and showed stable input resistance. The initial resting membrane potential of these neurones in 24-hour fasted rats was -43 ± 1 mV (n = 6), whilst the input resistance was 1057 ± 120 MΩ (n = 6) and the firing frequency was 0.6 ± 0.3 Hz (n = 6). Of these 9 neurones, 33.3% (n = 3) were characterised as GE, 22.3% (n = 2) as GI, 11.1% (n = 1) were GRA and 33.3% (n = 3) of neurones did not respond to 0.0 mM glucose (see Figure 5.27 A).

Removal of extracellular glucose from the bathing solution revealed the majority of ARC neurones (8/11, 72.7%) to be GE neurones in fed rats. These GE neurones were characterised by membrane hyperpolarisation from -45 ± 3 mV in 2.0 mM extracellular glucose to -53 ± 4 mV in glucose-free aCSF (n = 6, Figure 5.6). The response was associated with a reduction in input resistance from 1540 ± 398 MΩ in control to 770 ± 166 MΩ and a marked decrease in firing frequency from 1.6 ± 1.0 Hz to 0.0 ± 0.0 Hz (n = 6, Figure 5.6). The time taken for the response to peak (from onset of addition of glucose-free aCSF) was 25 ± 2 minutes (n = 8; see Figure 5.25 A and Table 5.5). The corresponding values for GE neurones in fasted rats were: membrane hyperpolarisation from -42 ± 1 mV to -47 ± 1 mV (n = 3), a response associated with a decrease in input resistance from 1005 ± 174 MΩ to 773 ± 133 (n = 3), and firing frequency from 0.9 ± 0.7 Hz to 0.0 ± 0.0 Hz in 0.0 mM glucose (Figure 5.7). The mean time to peak for this response was 17 ± 1 minutes (n = 3; Figure 5.25 A and Table 5.5). An example of current-clamp recording of these neurones is shown in Figure 5.7 A, with a

corresponding current-voltage relationship in Figure 5.7 B. This effect was reversed upon reintroduction of 2.0 mM glucose-containing aCSF in 2/3 GE neurones restoring membrane potential to -43 ± 1 mV (n = 2), input resistance to 1068 ± 10 MΩ (n = 2) and firing frequency to 0.1 ± 0.1 Hz (n = 2; Figure 5.7). The time taken to reverse the effects of glucose-free in GE neurones from 24-hour fasted rats amounted to 13 ± 1 minutes (n = 2, Table 5.6). In GE neurones from fed rats the effects of glucose-free bathing medium were reversed in 4/5 cells upon reintroduction of 2.0 mM extracellular glucose (Figure 5.6), depolarising and restoring membrane potential to -48 ± 9 mV (n = 3) and increasing input resistance to 1398 ± 358 (n = 3) and firing frequency to 0.6 ± 0.5 Hz (n = 3), with a mean time to peak recovery of 12 ± 1 minutes (n = 4, Table 5.6). The effects of glucose-free aCSF was maintained in the presence of TTX (500 nM), suggesting a direct effect on the cell and reversed in the presence of the ATP-sensitive potassium channel blocker tolbutamide (n = 3; see section 5.2.3.1).

2/11 (18.2%) ARC neurones recorded in glucose-free bathing medium responded with depolarisation in fed rats. These GI neurones gradually depolarised from an initial membrane potential of -44 ± 2 mV to -38 ± 2 mV in glucose-free aCSF (n = 2, Figure 5.8), a response associated with a reduction in input resistance, from 1219 ± 159 MΩ in control to 1017 ± 33 MΩ in glucose-free bathing medium. Under these conditions the spontaneous firing rate also increased from 0.3 ± 0.2 Hz in control to 1.6 ± 0.6 Hz under glucose-free conditions (n = 2, Figure 5.8). This depolarisation had a peak response time of 12 ± 1 minutes (n = 2; see Figure 5.25 B and Table 5.5) from the onset of glucose-free application. This glucose free-induced response was reversed in 2/2 cells upon reapplication of 2.0 mM glucose to the bathing solution (Figure 5.8), restoring membrane potential to -41 ± 4 mV and firing frequency to 0.4 ± 0.0 Hz although input resistance apparently increased to 1336 ± 45 MΩ (n = 2), higher than the control value initially recorded. The time to peak of this response was 12 ± 2 minutes (n = 2; see Table 5.6). In 24-hour fasted rats 2/9 (22.3%) ARC neurones, classified as GI neurones responded to 0.0 mM glucose, from 2.0 mM, with membrane depolarisation from -43 ± 0 mV (n = 2) in 2.0 mM glucose to -38 ± 1 mV (n = 2) in 0.0 mM (Figure 5.9). This response was associated with an increase in input resistance from 1049 ± 324 MΩ to 1059 ± 22 MΩ in 0.0 mM glucose (n = 2), and firing frequency from 0.2 ± 0.2 Hz in the presence of 2.0 mM to 1.1 ± 0.9 Hz in 0.0 mM extracellular glucose (n = 2;

Figure 5.9). The time taken for this response to peak amounted to 18 ± 3 minutes (n = 2; Figure 5.25 B and Table 5.5). An example of a current-clamp recording from these neurones is shown in Figure 5.9 A, with a corresponding current-voltage relationship in Figure 5.9 B.

One ARC neurone recorded in fasted rats in the absence of intracellular ATP was classified as a GRA neurone. This neurone responded to application of glucose-free aCSF with membrane depolarisation from -45 mV to -39 mV and an increase in firing frequency from 0.6 Hz to 2.0 Hz in 0.0 mM glucose. The input resistance was also increased from 1229 MΩ to 1625 MΩ in 0.0 mM glucose (Figure 5.10). The time to peak for this response was 8 minutes. Upon returning 2.0 mM glucose to the bathing medium, a biphasic response was observed characterised by a rapid membrane hyperpolarisation, within the first 2 minutes, to a membrane potential of -57 mV, associated with a cessation of spontaneous action potential discharge and a reduction in input resistance from 1625 MΩ in 0.0 mM glucose to 1001 MΩ. This initial inhibition was however relatively transient and was subsequently superseded by membrane depolarisation to -46 mV associated with an increase in neuronal input resistance to 1401 MΩ and spontaneous firing rate up to 0.2 Hz (Figure 5.10). The time taken for the depolarisation to peak from the peak of the transient inhibition amounted to 8 minutes. This response was repeatable upon subsequent exposure to 0.0 mM followed by 2.0 mM applications of glucose (Figure 5.10).

One ARC neurone (1/11; 9.1%) in slices from fed rats and three neurones recorded in slices from fasted rats with no intracellular ATP were insensitive to 0.0 mM glucose..

5.2.2.2 Effects of 1.0 mM $[ATP]_i$ on responses to a reduction in extracellular glucose in ARC neurones from rats fed *ad libitum* and rats fasted for 24 hours

The effects of glucose-free bathing medium were tested on 14 ARC neurones recorded in slices prepared from rats fed *ad libitum* and 8 ARC neurones from 24-hour fasted rats with 1.0 mM ATP in the pipette solution. In 2.0 mM extracellular glucose, the mean resting membrane potential was -41 ± 1 mV (n = 5), with a mean input resistance of 1185 ± 125 MΩ and spontaneous firing frequency of 1.3 ± 0.6 Hz

(n = 5) in neurones recorded from slices prepared from fed rats. The corresponding values for ARC neurones from fasted rats were -42 ± 1 mV, 1625 ± 109 MΩ (n = 6) and 1.2 ± 0.3 Hz (n = 6), respectively.

In glucose-free aCSF 64.3% of these neurones recorded in slices from fed rats were characterised as GE neurones, 7.1% GRA neurones and 28.6% showed no response (Figure 5.26 B). No GI neurones were apparent in this group recorded from brain slices of fed rats. In 24-hour fasted rats recorded with 1.0 mM ATP in the patch pipette, 75.0% (n = 6) were characterised as GE, and 25.0% (n = 2) as GI neurones (see Figure 5.27 B).

In neurones recorded from slices prepared from fed rats, GE neurones responded to a switch from 2.0 mM to 0.0 mM glucose-containing aCSF with membrane hyperpolarisation from a mean resting membrane potential of -42 ± 1 mV in 2.0 mM glucose-containing aCSF to -48 ± 3 mV in the absence of glucose (n = 4, Figure 5.11), a response associated with a reduction in firing frequency from 0.7 ± 0.4 Hz to 0.0 ± 0.0 Hz (n = 4) and input resistance from 1258 ± 132 MΩ in 2.0 mM glucose to 753 ± 74 MΩ (n = 4) in glucose-free aCSF. The time to peak of this response was 28 ± 2 minutes (n = 9; see Figure 5.25 A and Table 5.5). These effects of glucose-free aCSF were reversed in 4/5 GE neurones on a return to 2.0 mM extracellular glucose. In 2.0 mM glucose membrane potential was restored to -42 ± 3 mV (n = 3), accompanied by an increase in firing frequency to 0.2 ± 0.2 Hz (n = 3) and input resistance to 814 ± 112 MΩ (Figure 5.11). The time taken to at least partially reverse these effects with 2.0 mM extracellular glucose amounted to 13 ± 4 minutes (n = 4, Table 5.6). GE neurones recorded from slices in fasted rats, with 1.0 mM ATP in the pipette solution, responded to glucose-free aCSF with membrane hyperpolarisation from -41 ± 2 mV to -48 ± 2 mV (n = 4; Figure 5.12). This inhibition of membrane potential was associated with a reduction in input resistance from 1495 ± 71 MΩ in 2.0 mM to 820 ± 275 MΩ in 0.0 mM glucose (n = 2), and a complete cessation of firing from a baseline firing frequency in 2.0 mM glucose of 0.8 ± 0.3 Hz (n = 4; see Figure 5.12). The time taken for this response to peak amounted to 27 ± 4 minutes (n = 6; Figure 5.25 A and Table 5.5). These effects of glucose-free aCSF were reversed on restoring 2.0 mM glucose as the bathing medium in 5/6 GE neurones, with membrane potential being restored to -41 ± 2 mV (n = 3) and firing frequency to 0.1 ± 0.1 Hz (n = 3) although the input resistance remained unchanged with a value

of 820 MΩ (n = 1). The time taken for this reversal of effects of glucose-free was 12 ± 2 minutes (n = 5, Table 5.6). Examples of current-clamp recordings from these neurones are shown in Figure 5.11 A and 5.12 A, with a corresponding current-voltage relationship in Figures 5.11 B and 5.12 B.

In 2/4 GE neurones, in the presence of TTX (500 nM) membrane hyperpolarisation induced by 0.0 mM glucose persisted and was reversed by subsequent application of tolbutamide suggesting an effect mediated through ATP-sensitive potassium channels (see section 5.2.3.1).

In experiments with 1.0 mM intracellular ATP, no GI neurones were encountered in slices from fed rats whereas 2/8 (25.0%) neurones from 24-hour fasted rats responded to the switch from 2.0 to 0.0 mM glucose with membrane depolarisation from -44 ± 2 mV to -42 ± 1 mV (see Figure 5.13), thus classified as GI. This response was associated with a decrease in input resistance from 1756 ± 180 MΩ to 1100 ± 367 MΩ in 0.0 mM glucose (n = 2), and increase in firing frequency from 1.9 ± 0.5 Hz to 2.8 ± 1.4 Hz (n = 2; see Figure 5.13), with a mean time to peak of 23 ± 4 minutes (n = 2; Figure 5.25 B and Table 5.5). On restoring 2.0 mM extracellular glucose to the bathing medium the depolarisation induced by glucose-free aCSF was partly reversed in 1/2 of the GI neurones with time to peak recovery of 26 minutes (Table 5.6) for restoration of the membrane potential to -47 mV (n = 1; Figure 5.13).

1/14 (7.1%) ARC neurones investigated here was characterised as a rapidly adapting (GRA) neurone, recorded in a slice from a fed rat whereas no GRA neurone was detected in the fasted rat group. This neurone hyperpolarised from a membrane potential of -37 mV in the presence of 2.0 mM glucose-containing aCSF to -37 mV (n = 1) in glucose-free aCSF with a peak response of around 28 minutes following exposure to glucose-free aCSF. Membrane hyperpolarisation was associated with a reduction in firing frequency from 3.5 Hz to 0.3 Hz and decrease in input resistance from 895 MΩ to 740 MΩ (n = 1), see Figure 5.14. Upon reintroduction of 2.0 mM glucose, a biphasic response was observed. This neurone exhibited an initial hyperpolarisation to -41 mV, within 6 minutes of the 2.0 mM glucose application, with an associated cessation of firing and further decrease in input resistance to 705 MΩ (n = 1; see Figure 5.14). However, subsequently, this neurone depolarised to -35 mV, firing frequency increased to 0.2 Hz and input resistance increased to 832 MΩ, suggesting a relatively transient adapting response of this neurone to the

presence of 2.0 mM glucose. A further 4/14 (28.6%) of ARC neurones recorded in 1.0 mM ATP in slices from fed rats did not respond to changes in extracellular glucose.

5.2.2.3 Effects of 2.0 mM $[ATP]_i$ on responses to a reduction in extracellular glucose in ARC neurones from rats fed *ad libitum* and rats fasted for 24 hours

The effects of glucose-free bathing medium were tested on 9 ARC neurones recorded in slices prepared from rats fed *ad libitum* and from 10 neurones in slices recorded from 24-hour fasted rats with 2.0 mM ATP in the pipette solution. In slices from fed rats, in 2.0 mM glucose-containing aCSF, the mean resting membrane potential of these neurones was -42 ± 2 mV (n = 6), with input resistance and firing frequency of 1433 ± 263 MΩ (n = 6) and 2.2 ± 1.3 Hz (n = 6), respectively. The corresponding values for ARC neurones recorded in slices from 24-hour fasted rats were -43 ± 3 mV (n = 6), 1176 ± 230 MΩ (n = 5) and 0.1 ± 0.1 Hz (n = 6). Of these 10 neurones, 40.0% (n = 4) were characterised as GE, and 60.0% (n = 6) were insensitive to 0.0 mM glucose (see Figure 5.27 C).

Reducing extracellular glucose from 2.0 to 0.0 mM in these neurones revealed: 77.8% (7/9) in slices from fed and 40.0% (4/10) in slices from fasted were GE neurones; 22.2% of neurones in slices from fed rats were GI neurones whereas no GI neurone was detected in slices from fasted rats, the remaining 60.0% (6/10) of neurones in slices from fasted rats failing to respond to the change in glucose (Figure 5.26 C).

GE neurones in slices from fed rats responded to a switch from 2.0 to 0.0 mM extracellular glucose with membrane hyperpolarisation from -40 ± 1 mV to -48 ± 2 mV (n = 5) in glucose-free aCSF (Figure 5.15). This response was associated with a decrease in input resistance from 1463 ± 320 MΩ to 647 ± 117 MΩ (n = 5) in 0.0 mM glucose, and cessation of spontaneous firing from a baseline level of 2.6 ± 1.4 Hz (n = 5). 0.0 mM glucose-induced hyperpolarisation reached a peak around 23 ± 3 minutes (n = 7, Figure 5.25 A and Table 5.5) after exposure to 0.0 mM glucose. In 3/4 GE neurones tested, subsequent reintroduction of 2.0 mM extracellular glucose reversed the effects of glucose-free aCSF with a time to peak of 13 ± 1 minutes (n = 3, Table 5.6). Glucose-induced recovery was associated with

membrane depolarisation and increases in input resistance and firing frequency to -41 ± 1 mV, 1038 ± 93 MΩ and 1.1 ± 0.6 Hz, respectively (Figure 5.15). GE neurones from 24-hour fasted rat slices, with 2.0 mM ATP in the pipette solution, responded to glucose-free aCSF with membrane hyperpolarisation from -44 ± 4 mV to -45 ± 3 mV (n = 4; Figure 5.16), associated with a reduction in input resistance from 1176 ± 297 MΩ to 1000 ± 456 MΩ (n = 3) and firing frequency from 0.2 ± 0.2 Hz to 0.0 ± 0.0 Hz (n = 4; Figure 5.16). This hyperpolarisation of GE neurones reached a peak around 23 ± 2 minutes after exposure to glucose-free aCSF (n = 4; Figure 5.25 A and Table 5.5). An example of a current-clamp recording from these neurones is shown in Figure 5.16. These effects on all 4 GE neurones were reversible upon reapplication of 2.0 mM glucose, taking 11 ± 1 minutes (n = 4, Table 5.6) to recover membrane potential to -43 ± 4 mV (n = 4), input resistance and firing frequency to 1118 ± 469 MΩ (n = 3) and 0.3 ± 0.3 Hz (n = 4), respectively (Figure 5.16). Examples of current-clamp recording from GE neurones recorded from fed and fasted rats are shown in Figure 5.15 A and 5.16 A, with corresponding current-voltage relationship in Figure 5.15 B. The effects of 0.0 mM glucose were also repeatable (see Figure 5.16).

In 2/3 GE neurones, in the presence of TTX (500 nM) membrane hyperpolarisation induced by 0.0 mM glucose persisted and was reversed by subsequent application of tolbutamide suggesting an effect mediated through ATP-sensitive potassium channels (see section 5.2.3.1).

2/9 ARC neurones recorded in slices from fed rats with 2.0 mM ATP in the pipette were GI neurones that responded to a reduction in glucose from 2.0 to 0.0 mM with membrane depolarisation from -53 mV to -42 mV (n = 1), and increase in input resistance from 1282 MΩ to 1532 MΩ and firing frequency from 0.0 Hz to 0.3 Hz (n = 1, Figure 5.17) with a mean time to peak of response of 16 ± 2 minutes (n = 2, Figure 5.25 B and Table 5.5). These effects were partly reversible in one neurone and not reversed in the other over the time course of recording with a peak time response of 8.2 minutes (n = 1, Table 5.6). An example of a current-clamp recording from these GI neurones is shown in Figure 5.17 A, with a corresponding current-voltage relationship in Figure 5.17 B. No GI neurone was detected in this group of slices from fasted animals.

5.2.2.4 Effects of 5.0 mM $[ATP]_i$ on responses to a reduction in extracellular glucose in ARC neurones from rats fed *ad libitum* and rats fasted for 24 hours

The effects of glucose-free bathing medium were tested on 18 ARC neurones recorded in slices prepared from rats fed *ad libitum* and 11 ARC neurones from fasted rats, with 5.0 mM ATP in the pipette solution. The group of neurones from fed rats had a mean resting membrane potential of -46 ± 2 mV (n = 5), and input resistance and firing frequency of 1202 ± 232 MΩ and 0.2 ± 0.1 Hz, respectively. The corresponding values for neurones from fasted rats were -43 ± 1 mV (n = 5), 1384 ± 345 MΩ (n = 4), and 0.4 ± 0.2 Hz (n = 5), respectively.

Reducing extracellular glucose from 2.0 to 0.0 mM revealed 55.6% (10/18) and 27.3 % (n = 3) to be GE in fed and fasted rats, respectively. 11.1% (2/18) and 18.2% (n = 2) were classified as GI in fed and fasted tissue, respectively. 33.3% (6/18) and 54.5% (6/11) of fed and fasted ARC neurones, respectively were insensitive to 0.0 mM glucose (see Figures 5.26 D and 5.27 D).

GE neurones in slices from fed rats, with 5.0 mM ATP in the pipette solution, responded to a reduction in extracellular glucose with membrane hyperpolarisation from -46 ± 2 mV to -52 ± 4 mV (n = 4). Input resistance simultaneously decreased from 1727 ± 505 MΩ to 720 ± 120 MΩ (n = 4) at the peak of the response, and spontaneous firing from 0.2 ± 0.1 Hz in 2.0 mM glucose was completely inhibited (n = 4; see Figure 5.18). The average time to peak for this response was 21 ± 2 minutes (n = 10), Figure 5.25 A and Table 5.5. The hyperpolarisation induced by glucose-free aCSF in 3/8 GE neurones was reversed on restoring 2.0 mM extracellular glucose, with membrane potential depolarising to -44 mV and input resistance and firing frequency increasing to 1123 MΩ and 0.1 Hz (n = 1), respectively, and an average time to peak of recovery of 10 ± 1 minutes (n = 3; see Figures 5.18 A and B and Table 5.6). However, 5/8 GE neurones in this group of neurones from fed rats, failed to recover upon reintroduction of 2.0 mM glucose. In 2 GE neurones, membrane hyperpolarisation induced by 0.0 mM glucose did not persist in the presence of TTX (500 nM). GE neurones recorded in slices from fasted rats, with 5.0 mM ATP in the pipette solution, responded to glucose-free aCSF with membrane hyperpolarisation from -43 ± 1 mV (n = 2) in the presence of 2.0 mM glucose to -46 ± 1 mV (n = 2) in 0.0 or 0.2 mM glucose, a response associated with a reduction in neuronal input resistance from 938 ± 203 MΩ to 733 ± 265 MΩ (n = 2;

Figure 5.19) and complete inhibition of firing frequency from a baseline level of 0.1 ± 0.1 Hz (n = 2). The time to peak for these responses amounted to 17 ± 0 minutes (n = 3; Figure 5.25 A and Table 5.5). An example of a current-clamp recording from these neurones is shown in Figure 5.19 A, with a corresponding current-voltage relationship in Figure 5.19 B.

GI neurones in this population (2/18; 11.1%) of ARC neurones responded to 0.0 mM glucose-containing aCSF, with membrane depolarisation from -48 ± 6 mV in the presence of 2.0 mM to -42 ± 2 mV in 0.0 mM glucose (Figures 5.20 and 5.21). The response was associated with a decrease in input resistance from 1575 MΩ (n = 1) to 693 MΩ (n = 1) in 0.0 mM glucose, and firing frequency increased from 0.3 to 1.4 Hz in 0.0 mM glucose (n = 1; see Figure 5.21 A) taking 21 ± 5 minutes to reach a peak response (n = 2; Figure 5.25 B and Table 5.5). With reintroduction of 2.0 mM glucose, these effects were reversed returning membrane potential to -46 ± 4 mV (n = 2) and firing frequency to 0.2 Hz (n = 1) although input resistance was not recovered (Figures 5.20 and 5.21). The time to peak of this response was 11 ± 1 minutes (n = 2, Table 5.6). Current-voltage relations in one of these neurones revealed a reversal potential of -44 mV, suggesting a mechanism involving the opening of one or more non-selective cation channels (Figures 5.20 A, B and C). GI neurones (2/11; 18.2%) recorded in slices from fasted rats responded to 0.2 mM extracellular glucose with membrane depolarisation from -43 ± 3 mV (n = 2) to -41 ± 2 mV (n = 2), a response associated with a decrease in neuronal input resistance from 2355 MΩ to 1911 MΩ (n = 1) and increased firing frequency from 1.0 ± 0.2 Hz to 2.2 ± 0.4 Hz (n = 2; Figure 5.22). The time taken to reach a peak effect amounted to 16 ± 1 minutes (n = 2; Figure 5.25 B, Table 5.5). An example of a current-clamp recording from these neurones is shown in Figure 5.22 A, with a corresponding current-voltage relationship in Figure 5.22 B.

A further 6/18 (33.3%) ARC neurones recorded in slices from fed rats and 6/11 (54.5%) of neurones recorded in slices from fasted rats were insensitive to lowering extracellular glucose concentration.

5.2.2.5 Effects of 10.0 mM $[ATP]_i$ on responses to a reduction in extracellular glucose in ARC neurones from rats fed *ad libitum* and rats fasted for 24 hours

The effects of glucose-free bathing medium were tested on 11 ARC neurones recorded in slices prepared from rats fed *ad libitum* and 17 neurones in slices from 24-hour fasted rats with 10.0 mM ATP in the pipette solution. Neurones recorded from fed rats had a mean resting membrane potential of -45 ± 1 mV (n = 5), and input resistance and firing frequency of 1805 ± 298 MΩ and 0.2 ± 0.1 Hz (n = 5), respectively. The corresponding values for neurones in slices from fasted rats were -44 ± 2 mV; 1324 ± 71 MΩ and 0.3 ± 0.2 Hz (n = 6), respectively.

Reducing extracellular glucose from 2.0 to 0.0 mM revealed 9.1% (1/11) to be GE, 72.7% were GI (8/11) and 18.2% (2/11) failed to respond (Figure 5.26 E). Further details are described below. Of these 17 neurones, 41.2 % (n = 7) were characterised as GE and 58.8% (n = 10) were insensitive to 0.0 mM glucose (see Figure 5.27 E).

Of these neurones only one GE neurone (9.1%) was recorded in slices from fed animals whereas 41.2 % (n = 7) were characterised as GE in slices from fasted animals. In the single GE neurone in a slice from a fed rat, changing extracellular glucose from 2.0 to 0.0 mM induced membrane hyperpolarisation from -48 mV to -56 mV, a response associated with a reduction in input resistance from 2533 MΩ in 2.0 mM glucose to 1269 MΩ in glucose-free aCSF and complete inhibition of action potential firing from a baseline level of 0.3 Hz. The response took 24 minutes to reach a peak (n = 1; Figure 5.25 A and Table 5.5). GE neurones recorded in slices from fasted rats, with 10.0 mM ATP in the pipette solution, responded to glucose-free aCSF with membrane hyperpolarisation from -44 ± 2 mV to -46 ± 2 mV (n = 6; see Figure 5.23). The response was associated with a reduction in neuronal input resistance from 1324 ± 71 MΩ to 854 ± 67 MΩ (n = 6) and complete cessation of firing from a baseline level of 0.4 ± 0.1 Hz (n = 6). The time to peak for these responses amounted to 22 ± 2 minutes (n = 7) after the onset of 0.0 mM glucose application. An example of a current-clamp recording from these neurones is shown in Figure 5.23 A, with a corresponding current-voltage relationship in Figure 5.23 B. The effects of 0.0 mM glucose were reversed in 4/7 GE neurones after restoring 2.0 mM glucose. Membrane potential recovered to -42 ± 3 mV (n = 4), accompanied by an increase in input resistance and firing frequency to 967 ± 89 MΩ

and 0.4 ± 0.2 Hz (n = 4), respectively (see Figures 5.23 A and B). The time taken to achieve reversal amounted to 10 ± 2 minutes (n = 4).

GI neurones were the most predominant type of glucose-sensing neurone in slices from fed rats with 10.0 mM ATP in the pipette (8/11, 72.7%) whereas no GI neurone was observed in the corresponding group of neurones recorded in slices from fasted rats. GI neurones, in slices from fed rats, responded to 0.0 mM extracellular glucose with membrane depolarisation from -44 ± 1 mV to -40 ± 2 mV (n = 4) associated with an increase in neuronal input resistance from 1623 ± 304 MΩ to 1774 ± 304 MΩ (n = 4) and firing frequency from 0.2 ± 0.1 Hz to 0.9 ± 0.1 Hz (n = 4; Figures 5.24 A and B). The time to the peak of this response was 28 ± 2 minutes (n = 8, Table 5.5).

A further 2/11 (18.2%) ARC neurones in fed slices from fed rats and 10/17 (58.8%) of ARC neurones in slices from fasted rats, were insensitive to 0.0 mM extracellular glucose.

5.2.3 Mechanisms of action of ARC glucose-sensing neurones in hypothalamic slices from rats fed *ad libitum*

In rats fed *ad libitum*, the mechanisms of three different groups of ARC glucose-sensing neurones (GE, GI and GRA neurones) in response to changes in extracellular glucose were investigated and are described below.

5.2.3.1 Mechanism of action underlying GE neurone responses to changes in extracellular glucose

In rats fed *ad libitum*, the mechanisms of action by which GE neurones respond to changes in extracellular glucose were investigated. As already mentioned earlier, membrane hyperpolarisation induced in response to a switch from 2.0 to 0.0 mM persisted in the presence of TTX suggesting a direct effect on the cell and was associated with a reduction in neuronal input resistance consistent with activation of one or more conductances and opening of ion channels (see earlier sections for details). To further clarify the mechanism underlying these responses voltage clamp protocols and the effects of the ATP-sensitive channel blocker

tolbutamide were investigated. Note due to the similar nature of responses regardless of the intracellular ATP concentration, data from all GE neurones were pooled.

Following membrane hyperpolarisation induced by glucose-free bathing medium in GE neurones the effects of tolbutamide were investigated. Bath application of tolbutamide (200 μM) reversed the effects of glucose-free bathing medium inducing membrane hyperpolarisation in 7 out of the 10 neurones tested from -58 ± 2 mV to -46 ± 4 mV (n = 6) at the peak of the response. Tolbutamide-induced excitation was associated with an increase in neuronal input resistance from 463 ± 111 MΩ to 718 ± 136 MΩ (n = 5). Responses to tolbutamide persisted in TTX (500 nM, n = 7, Figures 5.28 A and B) suggesting a direct effect on the cell. To further characterise the mechanism a series of voltage-clamp ramps were utilised to determine the likely ionic mechanism underlying these responses. Ramp protocols to drive the holding potential from -120.0 mV to -40.0 mV, at a rate of 10.0 mV per second were utilised from an initial holding potential of -60.0 mV. The voltage clamp at a holding potential of -60.0 mV, in the presence of TTX (500 nM), tolbutamide (200 μM) induced an inward current of 31.1 ± 7.1 pA (n = 6) in neurones previously hyperpolarised in glucose-free aCSF. Voltage-clamp ramps in the absence and presence of tolbutamide revealed a reduction in membrane conductance and a reversal potential of the tolbutamide inhibited conductance of -85 ± 2 mV (n = 7, Figure 5.28 C), close to the predicted reversal potential for potassium ions under our recording conditions. Taken together these data suggest GE neurones respond to a reduction in extracellular glucose by opening K_{ATP} channels.

5.2.3.2 Mechanism of action underlying GI neurone responses to changes in extracellular glucose

GI neurones responded to a reduction in extracellular glucose with membrane depolarisation from -46 ± 2 mV (n = 9) to -40 ± 1 mV (n = 9), a response associated with an increase in firing frequency from 0.2 ± 0.1 Hz to 0.9 ± 0.2 Hz (n = 9). In 4 GI neurones the reduced extracellular glucose-induced response was associated with a decrease in neuronal input resistance from 1257 ± 217 MΩ to 753 ± 185 MΩ (n = 4). Current-voltage relations in one of these neurones revealed a reversal potential of -44 mV, suggesting a mechanism involving opening of one or

more non-selective cation channels. Interestingly, in slices from fed rats in the presence of 10.0 mM intracellular ATP, GI neurones responded to a reduction in extracellular glucose with excitation associated with an increase in neuronal input resistance suggesting a different mechanism involving blocking of one or more conductances, presumably potassium or chloride ions. The reduced extracellular glucose-induced response of some GI neurones was associated with no change in input resistance, suggesting other mechanisms may be involved, for example modulation of electrogenic ion pumps or ion exchangers. Further work is required to clarify the ionic mechanism underlying the mechanisms of action by which GI neurones respond to glucose.

5.2.3.3 Mechanism of action underlying GRA neurone responses to changes in extracellular glucose

GRA neurones responded to a reduction in extracellular glucose with a transient change in membrane potential that subsequently adapted following the change in glucose. Two ARC neurones in this group were classified as GRA neurones. Changing glucose concentration from 0.0 mM to 2.0 mM induced a biphasic response characterised by a rapid membrane hyperpolarisation, associated with a cessation of spontaneous action potential discharge and a reduction in input resistance, suggesting activation of a conductance, most likely potassium or chloride ion mediated. However, this initial inhibition was relatively transient and subsequently superseded by membrane depolarisation associated with an increase in neuronal input resistance and spontaneous firing rate with no further changes in glucose (see Figure 5.14), consistent with inhibition or inactivation of the conductance previously activated following the initial change in extracellular glucose. Further work is needed to clarify the ionic mechanism underlying GRA neurones in the ARC.

5.3 Discussion

One of the key aims of the work outlined in this thesis was to investigate the mechanisms by which neurones in the ARC detect and respond to perturbations in glucose levels and if these mechanisms are subject to modulation or changes in sensitivity depending on the energy status of the organism. To achieve this aims, whole-cell patch-clamp recordings in hypothalamic slices were used, the brain slices being prepared from both rats fed *ad libitum*, and rats in a negative state of energy balance i.e. fasted for 24 hours. Before experiments to address glucose-sensing mechanisms in these neurones, two important variables needed to be clarified. Firstly, what levels of extracellular glucose should be utilised in aCSF to mimic physiological levels in the brain. Secondly, as glucose-sensing neurones rely on glycolytic activity and couple glucose metabolism directly to excitability through ATP-dependent mechanism, what levels of ATP should be utilised for whole-cell recording (Dhar-Chowdhury *et al.*, 2007).

Plasma glucose levels are well documented to fluctuate between 4.0 to 7.0 mM under normal conditions and can become much higher in pathophysiological states such as diabetes. However, the level of glucose to which the brain is exposed is far from clear. With a plasma glucose range of 5.0 – 8.0 mM, brain glucose levels in rats are detected to be between 1.0 - 2.5 mM (Silver & Erecinska, 1994). Under pathophysiological conditions, plasma glucose levels of 2.0 - 18.0 mM translate into brain glucose levels ranging between 0.2 to 4.5 mM, respectively (Silver & Erecinska, 1994). At the level of the hypothalamus, basal levels of glucose are suggested to be around a concentration of 1.4 mM (de Vries *et al.*, 2003; Mayer *et al.*, 2006) and brain glucose levels correlate with 10-30 % of plasma levels (Silver & Erecinska, 1994; de Vries *et al.*, 2003). However, areas of the brain such as the ARC, which sits in close proximity to the median eminence where the blood-brain-barrier is suggested compromised, are both well sited to detect changes in glucose levels and may be exposed to levels that more closely approximate that observed in the blood. In reality, therefore, the exact concentrations of extracellular glucose at the level of the ARC remain unclear and require further investigation. Thus, based on the published data outlined above, we selected a concentration of 2.0 mM glucose to constitute as close an estimate to physiological levels as possible and this was used as the basal control level in the present study.

The role of ATP in regulating ion channel and pump activity, and thereby contributing to regulation of electrical activity is extremely well documented. However, exactly what the physiological levels are and if and how they change depending on the status of the cell is less well understood. Previous work on hypothalamic neurones suggested GE neurones operate through closure of K_{ATP} channels but do so independent of cytosolic ATP concentration (Ainscow *et al.*, 2002). Furthermore, previous whole-cell recording studies investigating functions of hypothalamic ATP-sensitive potassium channels challenged neurones with large non-physiological shifts in extracellular glucose concentration (10.0 to 0.0 mM) with 2.0 – 4.0 mM ATP in the patch pipette, and were able to produce tolbutamide-sensitive membrane hyperpolarisation in neurones, effects that were readily reversed upon restoring 10.0 mM glucose (e.g. Spanswick *et al*., 1997; Spanswick *et al*., 2000). Again consistent with the idea that cytosolic ATP has little effect on maintaining electrical excitability. Thus other factors, such as magnesium concentration, second messenger molecules, or local mechanisms may act to maintain ATP levels or change ATP-sensitivity of ion channels appropriately to regulate functional operation of ion channels/pumps needed to maintain electrophysiological integrity of cells. However, ATP concentrations in the rat brain have been shown to change both seasonally and during stress (Rozhanets *et al.*, 1974), and the effects of fasting, in itself a stressful phenomena, on the functional operation of these neurones, circuits and ATP levels are unknown. Thus, this study to investigate the role of intracellular ATP levels on the electrophysiological integrity of ARC glucose-sensing neurones and their ability to sense changes in extracellular glucose was undertaken. The specific experiments were designed to: 1. determine the levels of ATP required to maintain resting membrane potential of glucose-sensing neurones in fed and fasted rats and 2. determine the effects of intracellular ATP on the ability of glucose-sensing neurones to detect a 2.0 to 0.0 mM shift in extracellular glucose concentrations. This was achieved through a titration-type experiment where levels of ATP were progressively increased and the basal levels of activity and glucose-sensitivity of neurones monitored. A key output of this study was to identify and inform of the levels of intracellular ATP required for subsequent studies investigating the effects of physiological shifts in extracellular glucose concentration on glucose-sensing neurones and how they change depending on the energy status of the organism.

Several parameters were utilised to determine if changes in cytosolic ATP concentration play a role in glucose sensing and what the approximate levels of ATP are in glucose-sensing neurones. Thus, the stability of recordings was monitored, with different levels of ATP in the pipette, over a period of time to determine if resting membrane potential, input resistance and firing frequency could be maintained. Secondly, the ability to generate reproducible, reversible responses to reduced (2.0 to 0.0 mM) extracellular glucose was also investigated. In this instance, reversibility of response, time taken to peak response, recovery on restoring glucose, amplitude of peak response and associated change in input resistance were all monitored. Of the neurones tested, GE, GI and GRA were identified. However, the most consistent and reproducible type of glucose-sensing cell encountered with the majority of ATP concentrations, was GE. Thus we focussed on data from these cells. In fed rats, GE neurones responded in a consistent and reproducible manner with ATP concentrations up to 5.0 mM. Beyond 5.0 mM, GE neurones recorded from slices from fed rats were hardly encountered suggesting this level of ATP was more than sufficient to block ATP-sensitive potassium channels. In the presence of 1.0 or 2.0 mM intracellular ATP, reproducible responses to reduced glucose were readily obtained. However, many of the neurones recorded under these conditions showed a tendency for an unstable baseline and for spontaneous hyperpolarisation suggesting cytosolic ATP in this instance was not sufficient to maintain electrophysiological integrity. However, with 5.0 mM intracellular ATP, the stability of the resting membrane potential and firing properties was considerably improved for the majority of neurones recorded. Furthermore, GE neurones produced reproducible and reversible responses to a reduction in extracellular glucose with the time to peak response shown in Tables 5.5 and 5.6. Other factors, as outlined above, did not significantly change. Thus, from this data in slices from fed rats, we concluded that the concentration of intracellular ATP required to maintain cell membrane properties and functional capability for glucose-sensing lay between 4.0 to 5.0 mM.

Similar criteria were applied to neurones recorded from 24-hour fasted rats subject to the same titration experiment with intracellular ATP. In neurones recorded from slices prepared from 24-hour fasted rats, similar data were observed in terms of the types of glucose-sensing neurones encountered. In both 1.0 and 2.0 mM intracellular ATP the majority of GE neurones in fasted rats showed stable resting membrane properties with little or no change in firing frequency and thus little

evidence of spontaneous "run-up" due to lack of or washout of ATP. With 0.0 mM or 1.0 mM ATP in the pipette, GE neurones showed a reliable and reproducible inhibition when challenged with a reduction in extracellular glucose from 2.0 to 0.0 mM. However, at concentrations of intracellular ATP of 2.0 mM and above, the peak amplitude of responses of GE neurones was markedly reduced (Tables 5.3 and 5.4). Thus, from this data in slices from fasted rats, we concluded that the concentration of intracellular ATP required to maintain cell membrane properties and functional capability for glucose-sensing lay between 1.0 to 2.0 mM. Taken together, two key important findings are highlighted here. Firstly, cytosolic ATP levels are important for glucose-sensing in ARC neurones, thus our findings are at odds with those reported by Ainscow and colleagues (Ainscow *et al.*, 2002). The second important finding related to the differences in ATP levels required to maintain electrophysiological and glucose-sensing integrity with neurones recorded in fasted rats being characterised by either lower levels of intracellular ATP, changes in sensitivity to ATP or a combination of both compared to their fed, age-matched counterparts. Although the numbers of neurones included in this study were in some instances low, work from other colleagues in the lab (data not submitted as part of the thesis) have subsequently confirmed this to be the case and the levels of ATP needed to maintain glucose sensing cell function amount to around 1.0 mM for fasted rats and 4.0 mM for fed rats (Spanswick & van den Top, unpublished data). These data have driven the protocol described in the subsequent Chapter 6 where 1.0 mM and 5.0 mM intracellular ATP were used to explore glucose-sensing mechanism in ARC neurones from fasted and fed rats, respectively. The mechanism by which this apparent change in sensitivity to ATP is bought about in these neurones requires further investigation. Possible mechanisms and future experiments should address whether intracellular ATP levels are subject to a decrease in fasted rats, as has been suggested from models of stress where brain ATP levels decrease (Rozhanets *et al.*, 1974), a notion supported by data shown in Chapter 4 where stress may have been a factor involved in electrophysiological effects after fasting. Other factors may be changes in sensitivity of ion channels to ATP. For example the sensitivity and function of ATP-sensitive potassium channels can be modulated by a range of factors (for further details see Wang & Giebisch, 1991; Inagaki & Seino, 1998; Hu *et al*., 2003). Thus changes in the release of hormones, such as ghrelin released following content depletion from the stomach, may act through second

messenger pathways to modulate the functional activity and sensitivity of ion channels such as ATP-sensitive potassium channels. Alternatively, changes in energy status may in themselves lead to changes in the sensitivity of the glucose-sensing machinery. Further work is required to clarify this issue.

Over the course of this aspect of the study, three types of glucose-sensing neurone were identified based upon their responsiveness to a reduction in extracellular glucose from 2.0 to 0.0 mM and 0.0 to 2.0 mM. These were GE neurones characterised by inhibition when glucose was reduced and subsequent excitation in response to an increase in extracellular glucose. GI neurones were characterised by their opposing effects, i.e. excited when glucose was reduced and inhibited on raising extracellular glucose. However, a third type was also identified which is to author's knowledge, the first report of such a response. These were neurones that responded electrophysiologically but subsequently adapted to a change in extracellular glucose concentration. Thus we termed these neurones glucose-rapidly adapting or GRA. These types of neurone have been described previously to occur in the lateral hypothalamus in orexigenic neurones (Williams *et al*., 2008).

Table 5.3 Effects of intracellular ATP levels on peak membrane hyperpolarisation induced in GE neurones following a shift from 2.0 to 0.0 mM extracellular glucose

Intracellular ATP concentration (mM)	Peak amplitude of membrane response to a 2.0 to 0.0 mM shift in extracellular glucose (mV)	
	GE fed	GE fasted
0.0	-7.8 ± 1.7 mV (n = 6)	-5.2 ± 0.3 mV (n = 3)
1.0	-6.4 ± 2.8 mV (n = 4)	-6.8 ± 1.2 mV (n = 4)
2.0	-7.7 ± 1.9 mV (n = 5)	-1.3 ± 1.2 mV (n = 4)
5.0	-6.1 ± 2.2 mV (n = 4)	-3.7 ± 2.1 mV (n = 2)
10.0	-8.6 mV (n = 1)	-1.6 ± 1.7 mV (n = 6)

Table 5.4 Effects of intracellular ATP levels on peak reduction in input resistance induced in GE neurones following a shift from 2.0 to 0.0 mM extracellular glucose

Intracellular ATP concentration (mM)	Peak reduction in input resistance to a 2.0 to 0.0 mM shift in extracellular glucose (MΩ)	
	GE fed	GE fasted
0.0	-770 ± 253 MΩ (n = 6)	-232 ± 209 MΩ (n = 3)
1.0	-506 ± 201 MΩ (n = 4)	-675 ± 204 MΩ (n = 2)
2.0	-815 ± 309 MΩ (n = 5)	-177 ± 236 MΩ (n = 3)
5.0	-1008 ± 424 MΩ (n = 4)	-206 ± 63 MΩ (n = 2)
10.0	-1264 MΩ (n = 1)	-470 ± 57 MΩ (n = 6)

Table 5.5 Time to peak response to a reduction in extracellular glucose of glucose-sensing neurones in rats fed *ad libitum* and rats fasted for 24 hours

Intracellular ATP concentration (mM)	Time to peak response to a 2.0 to 0.0 mM shift in extracellular glucose (mins)			
	GE fed	GE fasted	GI fed	GI fasted
0.0	25 ± 2 (n = 8)	17 ± 1 (n = 3)	12 ± 1 (n = 2)	18 ± 3 (n = 2)
1.0	28 ± 2 (n = 9)	27 ± 4 (n = 6)	No data	23 ± 4 (n = 2)
2.0	23 ± 3 (n = 7)	23 ± 2 (n = 4)	16 ± 2 (n = 2)	No data
5.0	21 ± 2 (n = 10)	17 ± 0 (n = 3)	21 ± 5 (n = 2)	16 ± 1 (n = 2)
10.0	24 (n = 1)	22 ± 2 (n = 7)	28 ± 2 (n = 8)	No data

Table 5.6 Time to peak response to an increase in extracellular glucose of glucose-sensing neurones in rats fed *ad libitum* and rats fasted for 24 hours

Intracellular ATP concentration (mM)	Time to peak response to a 0.0 to 2.0 mM shift in extracellular glucose (mins)			
	GE fed	GE fasted	GI fed	GI fasted
0.0	12 ± 1 (n = 4)	13 ± 1 (n = 2)	12 ± 2 (n = 2)	No data
1.0	13 ± 4 (n = 4)	12 ± 2 (n = 5)	No data	26 (n = 1)
2.0	13 ± 1 (n = 3)	11 ± 1 (n = 4)	8 (n = 1)	No data
5.0	10 ± 1 (n = 3)	No data	11 ± 1 (n = 2)	No data
10.0	No data	10 ± 2 (n = 4).	No data	No data

GE neurones were the most common glucose-sensing neurones encountered in this study. GE neurones were subject to a membrane hyperpolarisation and a decrease in neuronal input resistance following decreases in extracellular glucose concentration. Subsequent increases in extracellular glucose reversed these effects. Voltage-clamp studies revealed a glucose-induced decrease in conductance and reversal potential around -85 mV, close to the reversal potential for potassium ions under our recording conditions. Following inhibition induced by glucose-free bathing medium, the ATP-sensitive potassium channel blocker reversed this effect inducing, as glucose itself, depolarisation or an inward current associated with a decrease in conductance. Taken together, these data indicate that changes in glucose levels in ARC GE neurones is mediated through the activity of ATP-sensitive potassium channels. Thus, these data are in broad agreement with numerous previous studies showing such a phenomena in ARC, VMN and brainstem neurones (e.g. Ashford *et al.*, 1990; Rowe *et al.*, 1996; Spanswick *et al.*, 1997; Lee *et al.*, 1999; Spanswick *et al.*, 2000; Miki *et al.*, 2001; Balfour *et al*., 2006). Within the ARC there are two principal populations of neurones, neuropeptide Y/ agouti related peptide

(NPY/AgRP) neurones form the main anabolic drive and pre-pro-opiomelanocortin /cocaine and amphetamine regulated transcript (POMC/CART) neurones form the main catabolic drive (Schwartz *et al.*, 1991; Guan *et al.*, 1998; Howard *et al.*, 2000). NPY/AgRP neurones are suggested to be GI neurones (Muroya *et al.*, 1999) that are also inhibited by leptin, whereas POMC/CART neurones are suggested to be GE neurones (Ibrahim *et al.*, 2003). Both of these neurones express functional ATP-sensitive potassium channels (K_{ATP} channels; Ibrahim *et al*., 2003; van den Top *et al*., 2007). These channels have been shown to be pivotal for glucose-sensing in the CNS by the use of knock-out studies and pharamacology (Ashford *et al.*, 1990; Rowe *et al.*, 1996; Spanswick *et al.*, 1997; Lee *et al.*, 1999; Spanswick *et al.*, 2000; Miki *et al.*, 2001). K_{ATP} channels are composed of two different components: pore forming inward rectifiers K^+ channel (KIR; KIR6.1 or KIR6.2) and sulfonylurea receptor (SUR) subunits arranged in a 4:4 stoichiometry (Ashcroft & Gribble, 1999). Thus GE neurones are proposed to use functional K_{ATP} channels to sense glucose much like the pancreatic β-cells (Ashford *et al.*, 1990; Yang *et al.*, 1999; van den Top *et al.*, 2007). In brief GLUT 3 transporters on the membrane surface of hypothalamic neurones permit glucose influx at a rate dependent on extracellular plasma glucose concentration (Kang *et al.*, 2004). Within the cell, glucose is phosphorylated by glucokinase (GK), a key rate-limiting step for glucose metabolism and considered the major mechanism for glucose sensing (Dunn-Meynell *et al.*, 2002). Glucose metabolism increases the intracellular ATP/ADP ratio causing the K_{ATP} channel to close and subsequent membrane depolarisation (Yang *et al.*, 1999; Levin *et al.*, 2001; Dunn-Meynell *et al.*, 2002; Kang *et al.*, 2004).

GI neurones were also observed in ARC neurones in this study and have been suggested to be orexigenic NPY/AgRP neurones (Muroya *et al.*, 1999), presumably functionally inhibited following a meal due to the transient increase in glucose reflecting food consumption. GI neurones were in the present study shown to increase activity in response to a reduction in extracellular glucose, associated with a reduction in input resistance, at least for the main part. This data, and given that a reversal potential around -44 mV was obtained in one cell, suggests a mechanism involving opening of one or more non-selective cation conductances. Parallel shifts in I-V relationships were also obtained in some GI neurones, suggesting other mechanisms such as modulation of electrogenic ion pumps or ion exchangers maybe

involved. The mechanism by which GI neurones respond to changes in extracellular glucose remains however, unclear with activation of a hyperpolarising chloride current (Song *et al.*, 2001; Routh, 2002; Fioramonti *et al.*, 2007) and a mechanism change in activity of the electrogenic Na^+/ K^+ pump (Oomura *et al.*, 1974) being suggested. Further work is needed here to fully characterise the mechanism involved in GI neurone glucose sensing described here.

The final subtype of glucose-sensing neurone described here were the GRA neurones which responded to an increase in extracellular glucose with an initial inhibition or membrane hyperpolarisation, a response that was transient and that subsequently appeared to adapt. This is the first description of these neurones in the ARC. However, they share distinct similarities to adapting sugar-sensing neurones described in the orexigenic orexin-containing neurones of the lateral hypothalamus (LH; Williams *et al*., 2008). The initial hyperpolarisation observed in the studies described here was associated with a reduction in neuronal input resistance, similar to those neurones in the LH where the initial inhibition is thought to involve activation of a leak potassium conductance that subsequently adapts (Williams *et al*., 2008). These adapting neurones, together with GE and GI, have been suggested to function in combined transient and sustained glucosensing manner allowing the glucose-sensing neurones to maintain sensitivity to small fluctuations in glucose levels whilst simultaneously encoding a larger range of baseline glucose concentrations (Williams *et al*., 2008). Further work is required to determine the mechanism underlying these GRA neurones and their ability to sense changes in glucose, to determine their chemical phenotype and where they project before the functional significance of these neurones can be realised.

In summary, data presented here suggest a key role for cytosolic ATP in glucose sensing in ARC neurones and that either the levels or sensitivity to ATP are key factors contributing to the maintenance of electrical activity in these neurones. Levels of or sensitivity to ATP is subject to modulation depending on the energy status of the organism. Finally, both GE and GI neurones were identified in the ARC and for the first time, neurones that detect and adapt to changes in extracellular glucose at the level of the ARC were reported.

Chapter 6

Glucose-sensing neurones in the rat hypothalamic arcuate nucleus in vitro in fed and fasted rats

6.1 Introduction

In order to survive, living animals need to alter their behaviour depending on their energy stores and to ensure that nutrient levels are sufficient to maintain normal cellular, tissue and body function. The central nervous system, especially the hypothalamus, stands out as a key central neural area responsible for the coordination and regulation of intracellular metabolic processes and for sensing, integrating and effecting signals to control energy homeostasis (Cone *et al.*, 2001). Glucose is an important nutrient and the primary fuel for the brain which must receive an adequate amount of glucose in order to function effectively. Glucose levels are maintained, under normal conditions, within narrow limits through a homeostatic feedback system that includes function-specific areas of the brain, including hypothalamus and brainstem, responsible for glucose homeostasis, the pancreas and liver (Penicaud *et al.*, 2002). After a meal, glucose levels are sufficient to meet the immediate energy requirements of the body, thus it is stored as glycogen through glycogenesis in the liver and muscle. This storage of glucose as glycogen can be mobilised at a later time through glycogenolysis. The liver also produces glucose by gluconeogenesis, subsequently releasing glucose into the bloodstream, to supply the glucose-dependent needs of tissues. Two main hormones (insulin and glucagon) are required to maintain the levels of plasma glucose in the body. Insulin and glucagon are secreted from β-cells and α-cells, respectively, which reside in the islets of Langerhans of the pancreas (Dow *et al.*, 1996). When the plasma glucose concentration level is low, glucagon released from α-cells acts on liver cells, causing release of glucose into the plasma. When plasma glucose is high, insulin is released from β-cells and simultaneously inhibits hepatic glucose production and induces uptake of excess glucose by the liver and other cells, thus reducing plasma glucose concentration to maintain glucose levels within narrow limits. Disruption or dysfunction to this homeostatic system, gives rise to extreme elevated or reduced levels of plasma glucose, can be devastating leading to conditions such as diabetes mellitus (type 1 and type 2) and hypoglycaemia. Type 1 or “insulin-dependent” diabetes mostly occurs early in life and is caused by insulin deficiency due to β-cells failure in the pancreatic islets of Langerhans. Type 2 or “insulin-independent” diabetes is more common, the primary cause being insulin resistance. The study of the development of insulin resistance in type 2 diabetes is reviewed in more detail elsewhere (Kahn, 2003; Pattaranit *et al.*, 2008).

In the periphery, normal plasma glucose levels (euglycaemia) are considered to be 80-100 mg/dL (4.4-5.5 mM). Hypoglycaemia is considered to represent glucose levels below 60-70 mg/dL (~3.6 mM). Plasma glucose levels between 100 and 120 mg/dL (5.5-6.7 mM) are defined as the levels for the prediabetic state and for plasma glucose levels above 120 mg/dL are defined for diabetes which sometimes can rise to 400 mg/dL (22 mM) in some severe cases (American Diabetes Association). However, the physiological levels for brain glucose have to-date remained unclear. Silver and Erecinska were the first group to measure extracellular brain glucose concentration using the glucose clamp technique in rats (Silver & Erecinska 1994, 1998). Their studies showed that plasma glucose levels ranging from 2-18 mM, corresponded with brain (CSF) glucose levels between 0.2 and 4.5 mM. This data was supported by other studies (de Vries *et al.*, 2003) using the zero net flux method and microdialysis, reporting glucose levels in the ventromedial hypothalamus (VMH) around 1.5 mM in fed rats, reduced to 0.7 mM in overnight fasted rats, with basal levels in hypothalamus suggested to be around 1.4 mM (de Vries *et al.*, 2003; Mayer *et al.*, 2006). Thus, glucose levels in the brain appear much lower than that of the plasma, approximating to 10-30% of plasma levels (Silver & Erecinska, 1994; de Vries *et al.*, 2003). However, brain glucose levels have been shown to be dependent on the brain region, neuronal activity and rat strain (McNay & Gold, 1999; McNay *et al.*, 2000; McNay *et al.*, 2001). Therefore certain brain regions such as the arcuate nucleus (ARC) are suggested to have higher extracellular glucose levels than other areas in the hypothalamus reflecting their proximal location to the median eminence (ME) where the blood-brain-barrier (BBB) is thought to be compromised (Ganong, 2000; Peruzzo *et al.*, 2000). However, the precise glucose concentration in this area has not yet been directly demonstrated.

For many years, it has been known that the brain uses glucose to regulate the neuronal activity. Over 50 years ago, Mayer proposed the glucostat hypothesis, whereby plasma glucose levels were hypothesised to be sensed by hypothalamic glucoreceptors to regulate food intake (Mayer, 1953 and 1955). Subsequently, in 1964, both Anand and Oomura discovered glucose-sensing neurones in the rat brain that could change their electrical activity and function in response to changes in extracellular glucose concentrations (Anand *et al.*, 1964; Oomura *et al.*, 1964). Two types of glucose-sensing neurone have been proposed: one termed

glucose-responsive (GR) which increases firing frequency as brain glucose levels rise and the other termed glucose-sensitive (GS) decreases firing frequency when glucose levels rise (Oomura *et al.*, 1969; Mizuno & Oomura, 1984; Levin *et al.*, 1999; Song *et al.*, 2001). These terms for glucose-sensing neurones were deemed confusing as they give no clear indication of the nature of the response to glucose, so several recent studies have suggested a change in nomenclature with glucose-responsive (GR) neurones being termed "glucose-excited (GE) neurones" and glucose-sensitive (GS) neurones being termed "glucose-inhibited (GI) neurones." Glucose-sensing neurones (both GE and GI neurones) are found in many regions of the brain including areas associated with the control of food intake and energy balance, including the paraventricular nucleus (PVN; Kow & Pfaff, 1989), the nucleus of the solitary tract (NTS; Mizuno & Oomura, 1984; Dallaporta *et al*., 2000; Ferreira *et al*., 2001), the ARC (Spanswick *et al.*, 1997; Spanswick *et al.*, 2000), the ventromedial hypothalamic nucleus (VMN; Ashford *et al*., 1990b; Spanswick *et al*., 1997; Song *et al*., 2001) and the hindbrain (Ritter *et al.*, 1998; Ritter *et al.*, 2000; Balfour *et al.*, 2006). GE neurones are commonly found in the VMH and GI neurones in lateral hypothalamus (LH; Oomura *et al*., 1969). In recent years glucose-sensing neurones in the ARC have become a focus of interest. These three glucose-sensing areas, ARC, VMN and LH along with the PVN are reciprocally connected, regulating food intake and controlling energy balance and thus may represent the key hypothalamic circuits involved in the control of glucose homeostasis.

The mechanisms by which neurones sense changes in glucose was investigated by Ashford and colleagues (Ashford *et al.*, 1988; Ashford *et al.*, 1990a, 1990b). GE neurones in VMH were shown to sense glucose via an ATP-sensitive K^+ (K_{ATP}) channel-dependent mechanism, very much analogous to the mechanism proposed for glucose-stimulated insulin release in pancreatic β-cells (Ashcroft & Gribble, 1999). In the pancreas, glucose enters the cell through a glucose transporter (GLUT 2), elevating glucose levels leading to an increase in the ratio of ATP/ADP, the closure of K_{ATP} channels and membrane depolarisation. This resulting depolarisation gives rise to activation of voltage-sensitive calcium channels that mediate the secretion of insulin. An important role for K_{ATP} channels in glucose homeostasis and glucose-sensing in the hypothalamus has been suggested by several studies using selective K_{ATP} channel blockers, for example tolbutamide and

glibenclamide, and from transgenic mice studies (Ashford *et al.*, 1990a, 1990b; Rowe *et al.*, 1996; Spanswick *et al.*, 1997; Lee *et al.*, 1999; Spanswick *et al.*, 2000; Miki *et al.*, 2001; Zhang *et al.*, 2004; van den Top *et al.*, 2007).

The K_{ATP} channel is an octomeric structure containing four inwardly rectifying pore-forming units (KIR) and four sulfonylurea receptors (SUR; Aguilar-Bryan *et al*., 1998). SUR1 is a high-affinity receptor found in β-cells and some neurones (Karschin *et al.*, 1997; Aguilar-Bryan *et al.*, 1998; Levin *et al.*, 1999). In addition, K_{ATP} channels in the ARC are most likely composed of Kir 6.2 and SUR1 which are similar to those found in β-cells (Miki *et al.*, 2001; van den Top *et al.*, 2007). Furthermore, the hypothalamic K_{ATP} channels have also been reported to be crucial in hepatic glucose production whereby K_{ATP} channel activation in the hypothalamus *in vivo* inhibits hepatic gluconeogenesis leading to lower plasma glucose levels (Pocai *et al.*, 2005). Furthermore, inhibition of these channels also leads to the impairment of insulin and fatty acids in inhibiting glucose production (Obici *et al.*, 2002a; Obici *et al.*, 2002b), suggesting another important role of K_{ATP} channels in the regulation of glucose production.

The mechanism by which GI neurones sense glucose is less clear. To-date, four mechanisms have been proposed; (i) activation of chloride channels (Song *et al.*, 2001; Routh, 2002; Fioramonti *et al.*, 2007); (ii) Na^+/K^+ ATPase pump activity in which glucose stimulates the Na^+/K^+ ATPase pump, leading to electrogenic ion exchange ($3Na^+$ per $2K^+$), leading to hyperpolarisation and inhibition of cells (Oomura *et al.*, 1974); (iii) activation of potassium channels, whereby glucose-inhibited orexin neurones in the LH were revealed to signal through the involvement of tandem-pore potassium channels (TASK; Burdakov *et al*., 2006) although these findings have subsequently come under severe criticism and scrutiny (Burdakov & Gonzalez, 2009); (iv) activation of a K^+-selective current by glucose (Williams & Burdakov, 2009). The involvement of tandem-pore K^+ (K_{2P}) channels, has been questioned, as glucose-induced inhibition in hypothalamic neurones in mice lacking tandem-pore K^+ channels was shown to persist, suggesting other channels are involved (Guyon *et al.*, 2009).

A major criticism of work on glucose-sensing neurones has been the historical persistent use of non-physiological glucose levels and glucose challenges delivered to putative glucose-sensing neurones (0.0 to 10.0 or 20.0 mM). However, several early and more recent studies addressed this issue. VMH (43%)

and LH (33%) neurones in anesthetised rats *in vivo* were shown sensitive to small changes in plasma glucose with GE neurones mostly found in VMH and GI neurones in LH (Oomura, 1983; Silver & Erecinska, 1998). More recently, at least five subtypes of glucose-sensing neurones were suggested in VMH and ARC neurones based upon their sensitivity to a 0.1 to 5.0 mM glucose challenge (Song *et al.*, 2001; Wang *et al.*, 2004). Two of these were similar to previously described GE and GI neurones and directly sensed changes in extracellular glucose concentration, whilst the other three subtypes were modulated by glucose at the presynaptic level (Song *et al.*, 2001). High extracellular glucose concentrations (5.0 to 20.0 mM) have also been investigated (Fioramonti *et al.*, 2004) and suggested a further two subtypes of glucose-sensing neurone. High-glucose-excited (HGE) neurones activated in response to high glucose levels are potentially mediated through activation of non-selective cation conductances, in a K_{ATP}-independent manner. High-glucose-inhibited (HGI) neurones respond in an opposing manner via a mechanism that remains unknown (Fioramonti *et al.*, 2004).

Glucose-sensing neurones located in areas controlling energy homeostasis, in particular in ARC, appear to respond to many metabolites, including lactate, free fatty acids and ketone bodies (Oomura *et al.*, 1975; Minami *et al.*, 1990; Yang *et al.*, 1999). Furthermore, GE neurones have been suggested responsive to peripheral hormones such as insulin and leptin through activation of K_{ATP} channels (Spanswick *et al.*, 1997; Spanswick *et al.*, 2000). Orexigenic NPY/AgRP neurones in the ARC have been suggested to be GI neurones (Muroya *et al.*, 1999) and inhibited by leptin (van den Top *et al.*, 2004) whereas anorexigenic POMC neurones were suggested to be GE neurones (Ibrahim *et al.*, 2003) and excited by leptin (Cowley *et al.*, 2001). Both of these neuronal subtypes express K_{ATP} channels (van den Top *et al.*, 2007).

The effects of a negative energy state on glucose-sensing neuronal function has been little studied to-date. Both plasma glucose and leptin levels in fasted rats are lower than those observed in rats fed *ad libitum* (De Boer *et al.*, 1989; Faggioni *et al.*, 2000; de Vries *et al.*, 2003; Palou *et al.*, 2009). However, if and how long-term changes in basal glucose levels leads to changes in sensitivity of glucose-sensing neurones, remains unknown. Recent studies have begun to address this issue by showing that in a fasted state, with reduced leptin and glucose levels, ARC NPY-GI neurones showed an enhanced response to a decrease in extracellular glucose

concentration (Murphy *et al.*, 2009). However, at the cellular level, details of the mechanisms of glucose sensing in hypothalamic neurones and how they change with energy status remain relatively unexplored.

The aim of the present study was to investigate the subtypes of ARC neurones involved in sensing physiological changes in extracellular glucose in the ARC and the mechanisms by which these neurones detect these physiological changes in glucose. In addition, the effects of a negative state of energy balance, a fasted state, on the ability of ARC neurones to sense glucose and the effects of fasting on the sensitivity of ARC neurones to changes in extracellular glucose were investigated.

6.2 Results

In the present study, the responses of ARC neurones to physiological changes in extracellular glucose concentrations were investigated using the whole-cell patch clamp recording technique *in vitro* in slices prepared from rats fed *ad libitum* housed normally and 24-hour fasted rats hoursed on a metal grid. As mentioned in Chapter 4, all 24-hour fasted rats had water available *ad libitum*.

6.2.1 Effects of physiological changes in extracellular glucose on ARC neurones in slices prepared from rats fed *ad libitum*

The responses to physiological changes in extracellular glucose concentration of 41 ARC neurones recorded *in vitro* from rats fed *ad libitum* were obtained. Hypothalamic slices were initially prepared and maintained in 2.0 mM glucose-containing aCSF and recordings made with an electrode solution containing 5.0 mM ATP, the estimated physiological levels of intracellular ATP for neurones from rats fed *ad libitum* (see Chapter 5). In the presence of 2.0 mM extracellular glucose, the mean resting membrane potential of these neurones was -46 ± 1 mV (n = 41), with input resistance 1336 ± 93 MΩ (n = 41) and firing frequency 0.68 ± 0.17 Hz (n = 41; see Table 6.1 and Figures 6.1 A, B and C, respectively). Following establishment of a stable baseline in 2.0 mM extracellular glucose, the neurones were subsequently expose to 0.2 mM extracellular glucose, followed by progressive increases to 0.5, 1.0, 2.0 and 5.0 mM extracellular glucose.

The application time for each concentration of extracellular glucose was varied depending on the period of time taken for a response to peak. As these experiments could last hours, recordings were lost in some instances, thus measurements for all glucose concentrations from the same neurones was not always possible. Thus numbers used for calculations of responses and membrane properties are stated in parenthesis. A summary of the membrane properties of all 41 ARC neurones recorded from rats fed *ad libitum* is shown in Table 6.1.

ARC neurones were classified according to their differential expression of subthreshold active conductances (cluster 1 - I_{an}, cluster 2 - I_{an} and I_A, cluster 3 – no subthreshold active conductance, cluster 4 - I_h, cluster 5 - I_h and T-type, cluster 6 – T-type, cluster 7 - I_{an} and T-type and cluster 8 - I_{an}, I_h and T-type, see Chapter 4 for more details). In 2.0 mM glucose, the 41 ARC neurones recorded in this study were classified as cluster 1 (4.9% of the population), cluster 2 (7.3%); cluster 4 (2.4%), cluster 5 (31.7%), cluster 6 (17.1%), cluster 7 (12.2%) and cluster 8 (24.4%; see Figure 6.2). Of these 41 neurones recorded in slices from rats fed *ad libitum*, no neurone fell into the cluster 3 category.

The responses of ARC neurones (n = 41) to changes in extracellular glucose concentrations from 2.0 to 0.2 mM were used to classify neurones into groups based upon their characteristic response to this reduction in glucose (see Chapter 5; GE neurones are inhibited in response to reduced extracellular glucose and depolarise following an increase; GI neurones depolarise in response to reduced glucose and vice-versa; GRA neurones are characterised by a rapidly adapting inhibitory response to an increase extracellular glucose). Of the population of neurones studies 56.1% (23/41) were classified as GE, 9.7% (4/41) were GI and 4.9% (2/41) were GRA neurones. The remaining neurones, 29.3% (12/41) did not respond to changes in extracellular glucose concentration (see Figures 6.3 A and B).

6.2.1.1 Reducing extracellular glucose from 2.0 to 0.2 mM induced inhibition in a subset of ARC (GE) neurones recorded in hypothalamic slice preparations from rats fed *ad libitum*

23/41 (56.1%) of neurones responded with a decrease in electrical excitability and membrane hyperpolarisation upon reducing extracellular glucose concentration from 2.0 to 0.2 mM, and were therefore classified as GE neurones. This response was characterised by a decrease in spontaneous action potential firing from a mean firing frequency of 0.75 ± 0.22 Hz in 2.0 mM glucose-containing aCSF to 0.20 ± 0.07 Hz in 0.2 mM glucose-containing aCSF, with a mean peak statistically significant reduction in firing frequency of 0.55 ± 0.17 Hz (n = 23; $P < 0.05$ (two-tailed student's *t*-test); see Figures 6.4 Ci and Cii, 6.5 A and 6.6 A). The spontaneous firing frequency remained suppressed upon a subsequent increase in extracellular glucose to 0.5 mM (0.13 ± 0.06 Hz; n = 23). However, further progressive increases in extracellular glucose to 1.0, 2.0 and 5.0 mM glucose were associated with notable increases in firing frequency compared to 0.2 mM glucose. Thus firing frequency increased to 0.26 ± 0.13 Hz (n = 23), 0.36 ± 0.16 Hz (n = 21) and 0.34 ± 0.18 Hz (n = 17), in the presence of 1.0, 2.0 and 5.0 mM glucose, respectively (Figures 6.4 Ci and Cii, 6.5 A and 6.6 A), although these increases were not statistically significant.

Application of 0.2 mM glucose-containing aCSF induced membrane hyperpolarisation from a mean resting potential of -46 ± 1 mV to -49 ± 1 mV, amounting to a mean peak membrane hyperpolarisation of -2.6 ± 0.8 mV (n = 23; Figures 6.4 Ai and Aii, 6.5 A and 6.6 A). The membrane potential in 0.2 mM was little affected upon increasing extracellular glucose to 0.5 mM, resting membrane potential amounting to -49 ± 1 mV (n = 23). Upon subsequent exposure to 1.0, 2.0 and 5.0 mM extracellular glucose, membrane potential depolarised to -48 ± 1 mV (n =23), -47 ± 1 mV (n = 21) and -48 ± 2 mV (n = 17), respectively (see Figures 6.4 Ai and Aii and 6.5 A). However, these changes in membrane potential were not statistically significant among the five concentrations of extracellular glucose (see Table 6.2).

Membrane hyperpolarisation induced by lower extracellular glucose concentration from 2.0 to 0.2 mM was associated with a significant reduction in input resistance from 1305 ± 90 MΩ to 782 ± 61 MΩ ($P < 0.001$; two-tailed student's *t*-test) with a mean peak reduction in input resistance of 523 ± 69 MΩ

(n = 23; Figures 6.4 Bi and Bii, 6.5 A and 6.6 A). Subsequent progressive increases in extracellular glucose concentration induced an increase in neuronal input resistance to 806 ± 74 MΩ (n = 23), 882 ± 84 MΩ (n = 22), 838 ± 105 MΩ (n = 19) and 852 ± 110 MΩ (n = 16) in the presence of 0.5, 1.0, 2.0 and 5.0mM extracellular glucose, respectively (Figures 6.4 Bi and Bii, 6.5 A and 6.6 A; see Table 6.2). The time taken to reach the peak response to 0.2 mM glucose was estimated to be 11.8 ± 0.7 minutes (n = 23).

Current-voltage relationships were generated to investigate the ionic mechanism underlying the responses of ARC neurones to physiological changes in extracellular glucose concentrations. Reducing extracellular glucose from 2.0 to 0.2 mM, revealed a reversal potential of -62 ± 1 mV in 12 GE neurones (see Figures 6.5 B and C (i)), close to the predicted reversal potential for chloride ions under our recording conditions, suggesting activation of one or more chloride conductances. This was further supported from I-V data generated in the presence of 2.0 and 5.0 mM glucose which revealed a decrease in input resistance associated with a reversal potential around -58 mV, data consistent with closing chloride conductances.

In a further two GE, reversal potential of -79 ± 2 mV was observed (n = 2; Figure 6.6 B and C), close to the predicted reversal potential for potassium ions under our recording conditions, suggesting activation of potassium conductances underlies these effects of reducing extracellular glucose.

Two Cluster 2 neurones were included in this group and characterised as GE. Previous data has suggested that these neurones are NPY/AgRP neurones (van den Top *et al*., 2004). These neurones responded to lowering of extracellular glucose with membrane hyperpolarisation associated with a reduction in neuronal input resistance, an effect reversed upon increasing extracellular. Current-voltage relationships revealed that lower glucose extracellular glucose concentration from 2.0 to 0.2 mM induced an apparent inhibition or suppression of the A-like transient outward rectifier, an effect reversed following subsequent increases in extracellular glucose to 2.0 and 5.0 mM.

6.2.1.2 Reducing extracellular glucose from 2.0 to 0.2 mM induced excitation in a subset of ARC (GI) neurones recorded in hypothalamic slice preparations from rats fed *ad libitum*

Bath application of low extracellular glucose (from 2.0 to 0.2 mM) to the hypothalamic slice induced an increased in electrical excitability and a membrane depolarisation in 4/41 (9.7%) ARC GI neurones. This response was characterised by an increase in firing frequency from a mean of 0.13 ± 0.10 Hz in 2.0 mM glucose-containing aCSF to 0.33 ± 0.20 Hz in 0.2 mM, with a mean increase of 0.20 ± 0.10 Hz (n = 4; Figures 6.7 Ci and Cii and 6.8 A), although this effect was not statistically significant, most likely reflecting the low n values (two-tailed student's *t*-test). Subsequent progressive increases in extracellular glucose concentration to 0.5 mM glucose induced a further increase in firing frequency to 0.48 ± 0.19 Hz (n = 4), 0.42 ± 0.31 Hz in 1.0 mM, 0.83 ± 0.70 Hz in 2.0 mM and finally being inhibited by elevated extracellular glucose when the concentration was increased from 2.0 to 5.0 mM leading to a firing frequency of 0.73 ± 0.67 Hz. These changes in firing frequencies yielded no statistically significant effects, reflecting the high variation in firing rates and low n values (see Table 6.3).

Low extracellular glucose concentration (from 2.0 to 0.2 mM) induced membrane depolarisation from a mean resting membrane potential of -46 ± 4 mV to -43 ± 5 mV, with a mean peak membrane depolarisation of 2.4 ± 0.9 mV (n = 4; Figures 6.7 Ai and Aii and 6.8 A). The membrane potential continued to increase to -41 ± 4 mV, -38 ± 4 mV and -36 ± 4 mV in 0.5, 1.0, and 2.0 mM glucose-containing aCSF, corresponding to peak depolarisations of 2.1 ± 1.3 mV (n = 4), 0.4 ± 0.7 mV (n = 3) and 1.9 ± 1.4 mV (n = 3), respectively. However, when the extracellular glucose concentration reached 5.0 mM, membrane potential hyperpolarised to a mean of -39 ± 4 mV, amounting to a mean peak hyperpolarisation of -2.6 ± 0.8 mV (n = 3; see Figures 6.7 Ai and Aii and 6.8 A). Once again this data was not statistically significant (see Table 6.3).

Membrane depolarisation in response to reduced extracellular glucose concentration was associated with a small increase in input resistance from a mean of 1603 ± 381 MΩ to 1687 ± 350 MΩ, amounting to a peak increase in input resistance of 84 ± 215 MΩ (n = 4; Figures 6.7 Bi and Bii and 6.8 A). Upon exposure to 0.5, 1.0, 2.0 and 5.0 mM extracellular glucose, input resistance changes were variable with both increases and decreases with consecutive increases in glucose concentration

(1660 ± 364 MΩ in 0.5 mM, 1773 ± 532 MΩ in 1.0 mM, 1552 ± 356 MΩ in 2.0 mM and 1617 ± 329 MΩ in 5.0 mM; see Figures 6.7 Bi and Bii and 6.8 A). These effects on input resistance were not statistically significant (see Table 6.3). The time taken to reach a peak effect following a reduction in extracellular glucose from 2.0 to 0.2 was 10.3 ± 0.9 minutes (n = 4).

To determine the ionic mechanism underlying the depolarisation induced by lower extracellular glucose concentration, current-voltage relationships were generated in 2.0 mM glucose and at the peak of the depolarising response to 0.2 mM glucose. However, the low n values gave little scope to explore this in detail (data not shown).

6.2.1.3 Reducing extracellular glucose from 2.0 to 0.2 mM induced a transient, rapidly adapting effect in a subset of ARC (GRA) neurones recorded in hypothalamic slice preparations from rats fed *ad libitum*

2/41 (4.9%) of neurones in this aspect of the study were characterised as GRA based on their transient inhibitory response to a change in extracellular glucose that subsequently relatively rapidly adapted to the new level of bathing glucose.

Reducing extracellular glucose levels from 2.0 to 0.2 mM, induced in 2 neurones, a reduction in firing frequency from 0.46 ± 0.26 Hz to 0.02 ± 0.02 Hz with a mean time to peak response of 6.7 ± 2.2 minutes (n = 2). However, this effect was transient, the neurone adapting to the new level of extracellular glucose leading to an increase in firing frequency to 0.16 ± 0.04 Hz with an increase of 0.14 ± 0.06 Hz. The time taken to reach a peak effect of this adapting response was 14.2 ± 1.0 minutes (n = 2; see Figures 6.9 Ci and Cii and 6.10 A). Subsequently increasing extracellular glucose to 0.5 mM led to a further increase in firing frequency to 0.25 ± 0.02 Hz, a peak increase of 0.09 ± 0.06 Hz (n = 2). Further increases in extracellular glucose led to further increases in firing frequency in response to 1.0 mM and 2.0 mM glucose to 0.39 ± 0.01 Hz and 0.47 ± 0.24 Hz, respectively. At 5.0 mM glucose the firing frequency began to diminish to and 0.38 ± 0.30 Hz (n = 2; see Figures 6.9 Ci and Cii and 6.10 A), respectively. A two-tailed student's *t*-test showed the increase in firing frequency following an increase in extracellular glucose from 0.5 mM glucose to 1.0 mM glucose was

significant ($P < 0.05$), although the low n values made meaningful statistics here impossible (see Table 6.4).

These GRA neurones were further characterised by an initial membrane hyperpolarisation from a mean resting membrane potential of -40 ± 1 mV to -44 ± 2 mV, a peak response amounting to -4.3 ± 0.6 mV. Subsequently the neurone adapted to the new level of extracellular glucose (from 2.0 to 0.2 mM) the hyperpolarisation leading to a depolarisation to -40 ± 2 mV, with a peak depolarisation of 4.0 ± 0.5 mV (n = 2). Subsequent increases in extracellular glucose gave rise to progressive membrane depolarisation to -39 ± 1 mV, -38 ± 1 mV and -38 ± 0 mV in response to 0.5, 1.0 and 2.0 mM extracellular glucose, respectively (n = 2). At a concentration of 5.0 mM membrane potential stabilised around -38 ± 2 mV (n =2; see Figures 6.9 Ai and Aii and 6.10 A).

The initial transient hyperpolarisation induced by reducing glucose-containing aCSF from 2.0 to 0.2 mM was associated with a decrease in input resistance from 876 ± 101 MΩ to 713 ± 93 MΩ, a peak decrease of 164 ± 8 MΩ (n = 2). The subsequent adaptation to the new concentration of glucose led to depolarisation associated with a small increase in input resistance to 799 ± 101 MΩ with the mean peak increase of 86 ± 8 MΩ (n = 2; see Figures 6.9 Bi and Bii and 6.10 A). Neuronal input resistance in these GRA neurones progressively increased with increased glucose concentration, to 833 ± 103 MΩ and 1003 ± 127 MΩ in 0.5 mM and 1.0 mM extracellular glucose, respectively (n = 2; see Figures 6.9 Bi and Bii and 6.10 A). Further increases in extracellular glucose gave rise to stabilisation of the neuronal input resistance around 846 ± 19 MΩ and 909 ± 51 MΩ for 2.0 and 5.0 mM glucose (n = 2; see Table 6.4).

Current-voltage relationships were generated in these GRA neurones only in the secondary response (depolarisation) following glucose from 2.0 to 0.2 mM, thus the mechanism of the transient inhibition is unknown. I-V relations from one of these neurones revealed a reversal potential of -64 mV (Figures 6.10 B and C), close to the predicted reversal potential for chloride ions under recording conditions, suggesting that the response in this neurone was mediated through an opening of chloride channels.

The remaining 12/41 (29.3%) ARC neurones recorded in hypothalamic slices from rats fed *ad libitum* showed no response to changes in extracellular glucose at any concentrations and were thus considered non glucose-sensing neurones.

6.2.2 Effects of physiological changes in extracellular glucose on ARC neurones in slices prepared from 24-hour fasted rats

In this study, 38 ARC neurones were recorded from hypothalamic slices prepared from rats fasted for 24 hours (water *ad libitum*) and their responses to physiological changes in extracellular glucose concentration (2.0 – 0.2 – 0.5 – 1.0 - 2.0 and 5.0 mM) were investigated. Slices were prepared and maintained in 2.0 mM glucose-containing aCSF and recordings made with an electrode solution containing 1.0 mM ATP, the estimated physiological levels of intracellular ATP for neurones from 24-hour fasted rats (see Chapter 5). In the presence of 2.0 mM extracellular glucose, 33/38 (86.8%) ARC neurones were characterised as active based on observations of suprathreshold activity recorded at baseline levels with no current injection. The mean resting membrane potential of these ARC neurones was -43 ± 1 mV (n = 38), with input resistance of 1231 ± 85 MΩ (n = 38) and mean firing frequency of 1.11 ± 0.23 Hz (see Table 6.5 and Figures 6.1 A, B, and C). The application time for each extracellular glucose concentration was varied depending on the period of time taken to reach a peak response/steady state. As these experiments could last hours, recordings were lost in some instances, thus measurements for all glucose concentrations from the same neurones was not always possible. Thus numbers used for calculations of responses and membrane properties are stated in parenthesis. A summary of the membrane properties of all 38 ARC neurones recorded from 24-hour fasted rats is shown in Table 6.5.

In 2.0 mM glucose, the 38 ARC neurones recorded in this study were classified as cluster 3 (2.6%), cluster 5 (26.3%), cluster 6 (15.8%), cluster 7 (15.8%) and cluster 8 (39.5%; see Figure 6.2). No neurones recorded in this population fell into the clusters 1, 2 or 4 categories (Figure 6.2).

These neurones were investigated for their potential as glucose-sensing neurones. Of the 38 neurones included in this aspect of the study 36.9% were identified as GE neurones, 18.4% GI neurones and 44.7% non glucose-sensing

(see Figures 6.3 A and C). GRA neurones were not found in this aspect of the study on fasted rats.

6.2.2.1 Reducing extracellular glucose from 2.0 to 0.2 mM induced inhibition in a subset of ARC (GE) neurones recorded in hypothalamic slice preparations from rats fasted for 24 hours

14/38 (36.9%) neurones responded to a reduction in extracellular glucose concentration, from 2.0 to 0.2 mM, with membrane hyperpolarisation and were therefore classified as GE neurones. GE neurones responded to reduced extracellular glucose with a reduction in spontaneous firing frequency from 0.56 ± 0.23 Hz in 2.0 mM extracellular glucose to 0.11 ± 0.06 Hz in the presence of 0.2 mM glucose, with a mean peak decrease in firing frequency of 0.45 ± 0.23 Hz (n = 14; Figures 6.4 Ci and Cii, 6.11 A), although this effect was not statistically significant. Subsequent progressive increases in extracellular glucose reversed this effect leading to a glucose concentration-dependent increase in spontaneous firing frequency to 0.25 ± 0.10 Hz (n = 14), 0.35 ± 0.18 Hz (n = 14), 0.41 ± 0.26 Hz (n = 11), and 0.67 ± 0.37 Hz (n = 9) in the presence of 0.5, 1.0, 2.0, and 5.0 mM extracellular glucose, respectively. This amounted to a mean peak increase in firing frequency of 0.15 ± 0.05 Hz, 0.10 ± 0.13 Hz, 0.02 ± 0.06 Hz and 0.20 ± 0.13 Hz, respectively (see Figures 6.4 Ci and Cii and 6.11 A) although again these effects were not statistically significant (Table 6.6).

Decreased firing rate in reduced extracellular glucose, from 2.0 to 0.2 mM, was associated with membrane hyperpolarisation from a resting potential of -45 ± 1 mV to -48 ± 2 mV, a mean peak hyperpolarisation of -3.0 ± 1.3 mV (n = 14; Figures 6.4 Ai and Aii and 6.11 A). Subsequent increases in extracellular glucose induced membrane depolarisation to -47 ± 2 mV (n = 14), -45 ± 2 mV (n = 14), -45 ± 2 mV (n = 12) and -45 ± 2 mV (n = 9) in 0.5, 1.0, 2.0 and 5.0 mM glucose, respectively (Figures 6.4 Ai and Aii and 6.11 A). This amounted to a mean peak increase in resting membrane potential of 1.0 ± 0.9 mV, 2.5 ± 1.0 mV, 0.7 ± 0.5 mV and 1.7 ± 1.4 mV, respectively. Thus, increasing extracellular glucose induced a concentration-dependent depolarisation in these GE neurones although these effects did not reach statistically significance (ANOVA; Table 6.6).

Inhibition in reduced glucose in GE neurones was associated with a decrease in input resistance from a mean of 1267 ± 117 MΩ (n = 14) in 2.0 mM glucose to 945 ± 102 MΩ (n = 14) in 0.2 mM glucose with a mean peak reduction of 322 ± 141 MΩ (see Figures 6.4 Bi and Bii and 6.11 A). This effect was reversed following subsequent increases in extracellular glucose to 988 ± 108 MΩ (n = 14) and 1020 ± 108 MΩ (n = 11) in 0.5 mM and 1.0 mM extracellular glucose, respectively. However, further increases in glucose to 2.0 and 5.0 mM yielded reductions in input resistance to 950 ± 118 MΩ (n = 10) and 968 ± 106 MΩ (n = 9), respectively (see Figures 6.4 Bi and Bii and 6.11 A). These effects did not reach statistically significant difference (ANOVA). The time taken for the reduced glucose to reach a peak response in these neurones amounted to 17.5 ± 1.0 minutes (n = 14). Interestingly, this effect was statistically significant compared to the corresponding time to peak response of GE neurones in fed rats (11.8 ± 0.7 minutes; $P < 0.01$; two-tailed student's *t*-test).

To determine the ionic mechanism of GE neurones underlying the responses to physiological changes in extracellular glucose concentration, current-voltage relationships were generated. Reducing extracellular glucose from 2.0 to 0.2 mM, revealed a reduction in neuronal input resistance associated with a reversal potential of -85 ± 2 mV (n = 3; Figures 6.11 B and C), closed to the predicted reversal potential for potassium ions under our recording conditions, suggesting inhibition of neurones by low concentrations of extracellular glucose was mediated through the opening of one or more resting potassium conductances. In one neurone, subsequent increases in extracellular glucose to 0.5 mM induced an increase in input resistance and reversal potential around -82 mV, and further increasing glucose to 1.0 mM induced a further increase in input resistance and reversal potential around -81 mV, consistent with closure of one or more potassium conductances (see Figure 6.11 C) Higher concentrations of glucose, 2.0 mM, revealed parallel shifts in the I-V, suggesting other mechanisms may be involved in glucose sensing in higher levels of glucose.

6.2.2.2 Reducing extracellular glucose from 2.0 to 0.2 mM induced excitation in a subset of ARC (GI) neurones recorded in hypothalamic slice preparations from rats fasted for 24 hours

7/38 (18.4%) of ARC neurones were electrically excited in a subset of ARC neurones upon reducing extracellular glucose concentration from 2.0 to 0.2 mM, hence these neurones were classified as GI neurones. Reducing extracellular glucose from 2.0 to 0.2 mM, induced an increase in firing frequency from 0.92 ± 0.48 Hz (n = 7) to 1.39 ± 0.69 Hz (n = 7), with a mean peak increase of 0.46 ± 0.21 Hz (Figures 6.7 Ci and Cii). This increase in firing frequency persisted following subsequent increases in extracellular glucose, firing frequency amounting to 1.44 ± 0.60 Hz (n =7), 1.31 ± 0.70 Hz (n = 6), 2.42 ± 1.20 Hz (n = 4) and 2.69 ± 1.92 Hz (n = 4) in 0.5, 1.0, 2.0 and 5.0 mM glucose, respectively (Figures 6.7 Ci and Cii and Table 6.7).

In these neurones, reduced glucose-induced excitation was associated with membrane depolarisation from -43 ± 2 mV (n = 7) to -40 ± 1 mV (n = 7), amounting to a mean peak depolarisation of 3.07 ± 1.83 mV, although this effect did not reach statistically significant difference (two-tailed student's *t*-test). The depolarised membrane potential in low glucose persisted upon increasing extracellular glucose to 0.5, 1.0 and 2.0 mM, amounting to -38 ± 1 mV (n = 7), -38 ± 2 mV (n = 6) and -36 ± 2 mV (n = 4), respectively, although at a level of 5.0 mM extracellular glucose, the membrane potential began to recover to -37 ± 2 (n = 4; see Figures 6.7 Ai and Aii). However, these data were not statistically significant (see Table 6.7).

Neuronal input resistance was reduced in GI neurones from 1297 ± 173 MΩ (n = 7) to 1195 ± 100 MΩ, following a reduction in glucose from 2.0 to 0.2 mM, with a mean peak reduction in input resistance of 102 ± 166 MΩ, (Figures 6.7 Bi and Bii). This change in input resistance persisted upon subsequent increases in extracellular glucose to 0.5, 1.0, 2.0 and 5.0 mM with corresponding input resistances of 1202 ± 120 MΩ (n = 7), 1233 ± 94 MΩ (n = 6), 1233 ± 187 MΩ (n = 4) and 1045 ± 169 MΩ (n = 4), respectively (Figures 6.7 Bi and Bii). The time to peak response of these neurones, in slices from fasted rats, to a decrease in extracellular glucose was 16.3 ± 2.1 minutes (n = 7). This was longer in duration than the corresponding value in GI neurones from fed rats (10.3 ± 0.9 minutes), although this effect did not reach statistically significance (two-tailed student's *t*-test).

To investigate the ionic mechanism underlying the depolarisation induced by 0.2 mM extracellular glucose in these GI neurones, current-voltage relationships were obtained in control of 2.0 mM glucose and 0.2 mM glucose. I-V plots in 4/7 GI neurones revealed a reduction in neuronal input resistance associated with a reversal potential of -42 ± 1 mV, suggesting activation of one or more non-selective cation conductances underlies the glucose-induced inhibition of some ARC GI neurones. In 3/7 neurones low glucose-induced excitation was associated with no change in neuronal input resistance giving rise to parallel shifts in the I-V relationships. These latter data suggest other mechanisms, for example, electrogenic pumps and ion exchangers, may be important for glucose sensing in some ARC GI neurones.

The remaining 17/38 (44.7%) ARC neurones recorded in hypothalamic slices from fasted rats showed no response to changes in extracellular glucose at any concentration and were thus considered non glucose-sensing neurones.

.

6.2.5 Effects of physiological increases in extracellular glucose on ARC neurones in slices prepared from 24-hour fasted rats

The levels of extracellular glucose, as indicated earlier, to which ARC neurones are exposed in a fasted state are unknown but at the level of the hypothalamus, can be low (see introduction). Following a period of fasting, food intake would be expected to lead to transient increases in glucose levels, at the plasma and CSF levels. Furthermore, sudden rapid decreases in glucose are unlikely to occur under physiological conditions, whereas transient, rapid increases, for example following a meal, are more likely to occur. Thus a series of experiments were undertaken whereby extracellular glucose was maintained at a low level (0.2 mM) and the effects of increases in extracellular glucose investigated. Hypothalamic slices from 24-hour fasted rats were therefore prepared and maintained in 0.2 mM extracellular glucose. Subsequently after a period of recovery, the effects of progressive increases in extracellular glucose were investigated. As these experiments could last hours, recordings were lost in some instances, thus measurements for all glucose concentrations from the same neurones was not always

possible. Thus numbers used for calculations of responses and membrane properties are stated in parenthesis.

The responses to physiological changes in extracellular glucose concentrations of 16 ARC neurones were included in this study. A summary of the membrane properties of all 16 ARC neurones was shown in Table 6.8. 25.0% (4/16) of this population were identified as GE neurones, 25.0% (4/16) were GI neurones and 50.0% non glucose-sensing neurones (Figures 6.12 A and B). Note GRA neurones were not found in this series of experiments.

6.2.5.1 Increasing extracellular glucose induced excitation in a subset of ARC (GE) neurones recorded in hypothalamic slice preparations from rats fasted for 24 hours

4/16 (25%) of neurones responded to an increase in extracellular glucose concentration, from 0.2 to 0.5, 1.0, 2.0 and 5.0 mM, with membrane depolarisation and were therefore classified as GE neurones. These GE neurones were all silent at rest showing no spontaneous activity. Progressive increases in extracellular glucose induced increases in spontaneous firing rate from 0.00 ± 0.00 Hz (n = 4) in 0.2 mM glucose to 0.04 ± 0.04 Hz (n = 4), 0.22 ± 0.19 Hz (n = 4), 0.09 ± 0.07 Hz (n = 4) and 0.20 ± 0.20 Hz (n = 2) in the presence of 0.5, 1.0, 2.0 and 5.0 mM glucose, respectively (Figure 6.13 and Table 6.9). However, no statistically significant effects were observed, most likely reflecting the low n values in this study.

Increasing concentration of extracellular glucose-containing aCSF from 0.2 to 0.5, 1.0, 2.0 and 5.0 mM induced responses associated with membrane depolarisation from a mean resting membrane potential of -48 ± 3 mV (n = 4) in 0.2 mM to -48 ± 3 mV (n = 4), -43 ± 2 mV (n = 4), -42 ± 1 mV (n = 4) and -40 ± 2 mV (n = 4) in 0.5, 1.0, 2.0 and 5.0 mM glucose, respectively (see Figure 6.13 A; Table 6.9). Thus these responses were associated with a concentration-dependent depolarising effect to increasing extracellular glucose concentration.

Depolarisation induced by increasing extracellular glucose concentration was associated with a concentration-dependent increase in neuronal input resistance, from 867 ± 194 MΩ (n = 4) in 0.2 mM extracellular glucose to 1083 ± 176 MΩ (n = 4), 1099 ± 198 MΩ (n = 4), 1108 ± 223 MΩ (n = 4) and

1443 ± 361 MΩ, in the presence of 0.5, 1.0, 2.0 and 5.0 mM extracellular glucose, respectively (Figure 6.13). Comparing responses to neighbouring glucose concentrations revealed the effect to be statistically insignificant, again probably reflecting the low n values (ANOVA; see Table 6.9). The mean time to peak response of the 0.5 mM glucose-induced depolarisation amounted to 9.3 ± 1.7 minutes (n = 4).

6.2.5.2 Increasing extracellular glucose induced inhibition in a subset of ARC (GI) neurones recorded in hypothalamic slice preparations from rats fasted for 24 hours

4/16 (25.0%) of ARC neurones underwent a reduction in electrical excitability and hyperpolarisation in membrane potential following an increase in extracellular glucose concentration from 0.2 mM to 0.5 mM. GI neurones were characterised by a decrease in firing frequency from 0.14 ± 0.07 Hz in 0.2 mM glucose to 0.03 ± 0.03 Hz (n =4) in 0.5 mM glucose, 0.01 ± 0.01 Hz (n = 4) in 1.0 mM extracellular glucose and remained at this frequency in 2.0 mM (n = 4) and 5.0 mM extracellular glucose (n = 3, Table 6.10).

Increasing extracellular glucose concentrations from 0.2 to 0.5 mM induced membrane hyperpolarisation from a mean resting membrane potential of -42 ± 1 mV to -46 ± 2 mV (n = 4). However, on reaching this new steady-state membrane potential, subsequent increases in extracellular glucose had no significant effect on membrane potential, amounting to -46 ± 2 mV in 1.0 mM and 2.0 mM and -47 ± 3 mV (n = 3) in 5.0 mM glucose (Table 6.10).

Hyperpolarisation, induced in GI neurones, by increased glucose concentration was associated with a decrease in neuronal input resistance from a mean of 1492 ± 142 MΩ in 0.2 mM to 1362 ± 387 MΩ (n = 4), 1052 ± 315 MΩ (n = 4), 1031 ± 266 MΩ (n = 4) and 978 ± 312 MΩ (n = 3) in the presence of 0.5, 1.0, 2.0 and 5.0 mM glucose, respectively (Table 6.10). The mean time to peak response of the 0.5 mM glucose-induced depolarisation amounted to 10.5 ± 1.8 minutes (n = 4).

Current-voltage relationships were generated to determine the ionic mechanism underlying these responses. I-V plots were obtained for control in 0.2 mM extracellular glucose and at the peak of hyperpolarisation in 0.5 mM glucose-containing aCSF. These responses in 3/4 GI neurones were associated with a reduction in neuronal input resistance associated with a reversal potential of -60 ± 4 mV, close to the predicted reversal potential for chloride ions under our recording conditions, suggesting that this response was mediated through opening of one or more chloride conductances.

One cluster 2 neurone, previously described as a subtype of NPY/AgRP neurone (van den Top *et al*., 2004) was found in this group of GI neurones. This neurone had a firing frequency in 0.2 mM extracellular glucose of 0.3 Hz, and became completely silent in the presence of 0.5 mM glucose and remained silent thereafter (see Figure 6.14 A). The resting membrane potential of this cluster 2 neurone was also hyperpolarised from -38 mV in 0.2 mM glucose to -49 mV in 0.5 mM glucose (see Figure 6.14 A) and persisted, in 1.0 and 2.0 mM glucose, to rest around -52 mV and -51 mV, respectively. This hyperpolarisation was associated with a reduction in input resistance from 1144 MΩ in the presence of 0.2 mM glucose to 641 MΩ in 0.5 mM glucose (see Figure 6.14 A), with a reversal potential of -57 mV, closed to the predicted reversal potential for chloride ions under our recording conditions. These data suggest GI neurones, including orexigenic NPY/AgRP neurones respond to increased glucose with hyperpolarisation mediated through a chloride-dependent mechanism (see Figures 6.14 B and C).

6.3 Discussion

The aims of the investigation described here were to determine whether neurones in the ARC can sense physiological changes in glucose; the cellular mechanisms underlying these responses and how glucose-sensing neurones adapt to changes in energy status, in the latter instance during a negative state of energy balance induced by fasting. The principal findings of this study were that three types of glucose-sensing neurone were identified: neurones inhibited by a reduction in extracellular glucose within a physiological range and excited by increases in glucose, thus termed glucose-excited (GE) neurones; neurones excited by a reduction and inhibited following elevation of extracellular glucose, thus termed

glucose-inhibited (GI) neurones; finally neurones that showed an adaptive response to a change in extracellular glucose characterised by a transient change in membrane potential and firing rate before adaptation to the new level of extracellular glucose concentration. These latter neurones were therefore termed glucose-rapidly adapting (GRA) neurones, which are reported here in the ARC for the first time.

From normal animals, fed *ad libitum*, recordings in hypothalamic slice preparations revealed around 56% of neurones were GE. In these neurones reducing extracellular glucose from 2.0 to 0.2 mM induced membrane hyperpolarisation associated with a reduction in firing rate and input resistance. Subsequent increases in extracellular glucose to 0.5 mM had little effect but at 1.0 mM extracellular glucose, neurones responded with membrane depolarisation, increased firing rate and increased neuronal input resistance, and continued to respond in a glucose concentration-dependent manner with subsequent increases in glucose concentration to 2.0 and 5.0 mM. Thus the threshold concentration for detection of extracellular glucose in ARC GE neurones was around 1.0 mM. In rats that had been subject to a 24-hour fast, this sensitivity to extracellular glucose was increased. An increase in extracellular glucose, from 0.2 to 0.5 mM, induced membrane depolarisation, increased firing rate and increased input resistance suggesting increased sensitivity to extracellular glucose and decreased threshold for detection in GE neurones from fasted rats. This increased sensitivity to increased glucose concentration following induction of a negative state of energy balance was also observed in recordings where the bathing glucose levels were maintained low from the onset (0.2 mM) as opposed to 2.0 mM followed by a reduction to 0.2 mM. Furthermore, in this latter series of experiments, 5.0 mM intracellular ATP was utilised to allow direct comparison with slices from fed animals. Thus this change in sensitivity appears to be directly related to the energy status of the organism and relatively independent of the intracellular ATP concentration. These data therefore have several important implications. Firstly, GE neurones in the ARC are “true” glucose-sensing neurones capable of detecting physiological changes in extracellular glucose. Thus this data is in agreement with previous studies showing GE neurones in the ARC (Song *et al.*, 2001; Wang *et al.*, 2004) that have been suggested to be anorexigenic POMC neurones (Ibrahim *et al.*, 2003). Furthermore, changing the energy status of the organism appeared to change the sensitivity of glucose-sensing neurones to extracellular glucose, fasting effectively leading to an enhanced sensitivity.

The second key observation in this study is the change in sensitivity of ARC GE neurones to extracellular glucose, in terms of the threshold levels of glucose they detect. This is the first report of such a change in sensitivity with neurones in slices from fasted rats showing increased sensitivity to increased glucose concentration. An increase in glucose from 0.2 to 1.0 mM, but not 0.5 mM, was detected in GE neurones from slices from fed rats whereas in fasted, an increase to 0.5 mM was clearly detected. This sensitivity was independent of the bathing glucose concentration and intracellular ATP levels, suggesting other mechanisms were responsible for this change in sensitivity to extracellular glucose. Fasting rats for 24-hours reduces plasma glucose levels in rat (De Boer *et al.*, 1989; Faggioni *et al.*, 2000; de Vries *et al.*, 2003; Palou *et al.*, 2009), and plasma glucose levels ranging between 2-18 mM, correspond with brain (CSF) glucose levels between 0.2 and 4.5 mM (de Vries *et al.*, 2003), in VMH amounting to 1.5 mM in fed rats, reduced to 0.7 mM in overnight fasted rats (de Vries *et al.*, 2003; Mayer *et al.*, 2006). Thus, the range of glucose levels tested here in fed and fasted rats appears to be within the physiological range, given the available data. A further change in sensitivity was also noted in terms of the time taken for GE neurones to respond to a decrease in extracellular glucose. In slices from fed rats, the time taken to reach a peak response to reduced extracellular glucose from 2.0 to 0.2 mM amounted to approximately 12 minutes, whereas the corresponding time for the same response in GE neurones from fasted rats was considerably longer, amounting to approximately 18 minutes, irrespective of the higher concentration of intracellular ATP which may have been expected to delay inhibition to reduced glucose in neurones from fed animals. These data strongly suggest a shift in the sensitivity of the glucose-sensing machinery in these GE neurones. The functional significance of this is unclear but may reflect a number of functional adaptations to energy status. For example, the relative insensitivity to further reductions in glucose in the fasted state could represent an adaptation to the lack of food and glucose availability, thus providing a potential "safety" mechanism. The increase in sensitivity to elevations in extracellular glucose may be multi-functional in terms of preparing the brain glucose-sensing machinery to orchestrate appropriate behaviours to maximise utilisation and/or storage of glucose when it becomes available, the increased sensitivity representing an adaptation to the energy status of the organism. Further work is required to address these issues.

Whilst this is the first report of such an adaptation in GE neurones, a similar change in sensitivity has recently been reported for orexigenic NPY GI neurones in the ARC where fasting was shown to enhance the response of ARC NPY-GI neurons to decreased extracellular glucose (Murphy *et al*., 2009). The mechanism underlying this adaptation was suggested to be leptin and AMPkinase-dependent, whereby decreased extracellular glucose and leptin associated with fasting was suggested to activate AMPK in NPY-GI neurons leading to NPY-GI neurones becoming depolarized in response to smaller glucose fluctuations (Murphy *et al*., 2009). Whether such a leptin and AMPkinase-dependent mechanism operates in the GE neurones described here remains to be clarified. Furthermore, in relation to the study by Murphy *et al*., GI neurones were also investigated here. GI neurones were characterised by an increase in excitability upon a reduction in extracellular glucose and a decrease in excitability with an increase in glucose. GI neurones in fed rats were generally associated with lower spontaneous firing rates and more hyperpolarised resting membrane potentials compared to GI neurones from fasted rats suggesting these neurones were indicating a "hunger" state, if as previous reports suggest, subpopulations of orexigenic NPY neurones are also GI neurones. In ARC GI neurones from both fed and fasted tissue, reducing extracellular glucose from 2.0 to 0.2 mM induced clear increases in spontaneous action potential firing and membrane potential depolarisation. Subsequent increases in extracellular glucose induced a suppression of activity around 1.0 mM for fasted and fed rats. Interestingly further increases in extracellular glucose induced increases, not decreases in firing rate except in the fed group where 5.0 mM glucose induced a reduction in neuronal activity compared to 2.0 mM. As numbers for these higher concentrations of glucose were lower than those for 0.2, 0.5 and 1.0 mM glucose, the significance of this, if any, is unclear. The data suggest GI neurones are sensitive to reduced extracellular glucose and have a threshold for response or detection to increased glucose of around 1.0 mM in fasted and fed states. A second population of ARC GI neurone in slices from fasted rats were also investigated where they were only subject to increases in extracellular glucose from a fasted state mimicked with a control glucose bathing medium concentration of 0.2 mM. In these neurones, increasing extracellular glucose from 0.2 to 0.5 mM glucose induced a clear decrease in firing rate and membrane hyperpolarisation suggesting a high degree of sensitivity to extracellular glucose. Subsequent increases in extracellular glucose were without further significant effect.

These latter experiments were undertaken in higher intracellular ATP concentrations, thus a higher reliance of glucose sensing GI neurones for intracellular ATP, than GE neurones, may explain these data. Alternatively the basal level of extracellular glucose itself may be the key driver dictating sensitivity of GI neurones to changes in extracellular glucose levels. Nevertheless, the sensitivity of GI neurones to changes in extracellular glucose appears to depend on separate mechanisms and intracellular and extracellular factors than their counterparts, the GE neurones. Functionally this may relate to different roles whereby GI neurones couple and relate more to different functions, for example feeding, than GE neurones. Further work is required, in particular on GI neurones, to address these issues.

In relation to changes in sensitivity of glucose-sensing neurones depending on energy status, i.e. fed versus fasted, a number of other interesting observations were made over the course of this study. Firstly, the proportions of ARC GE and GI neurones detected in fed and fasted tissues varied considerably with around 56% of the population recorded in tissue from fed rats being identified as GE and only around 10% being GI. In the fasted scenario, this changed with around double the number of GI neurones detected (18%) compared to fed rats and the GE population reduced to around 37%. In the study of neurones maintained in 0.2 mM glucose and only subject to increases in extracellular glucose, this balance shifted further to 25% of neurones identified as GE and 25% of GI neurones. Whilst the numbers for all of these populations, particularly fasted, were not as high as would be ideally required, it is interesting to speculate that other levels of plasticity operate within the ARC glucose-sensing network. Thus it is tempting to speculate that glucose-sensing neurones may be modulated and in effect switched “on” or “off” depending on energy status. For example, in a fasted or hunger state, GI neurones are activated or recruited, reflecting low levels of extracellular glucose and negative energy balance, whereas GE neurones, required for co-ordinated behavioural responses to conserve and manage glucose fuel supplies, are “switched off” during this period of low glucose availability. Subsequently, upon food intake and increased glucose availability, GI neurones are switched off as the hunger and fasted state is alleviated and energy shortages restored. Conversely, upon food intake, GE neurones, required to co-ordinate behaviours to manage glucose stores and availability for the CNS, organs and tissues of the body, are recruited or “switched on.” Further work is required to address these issues which at this point can only be speculation.

A second interesting observation made over the course of this study and worthy of speculation relates to NPY/AgRP neurones. As already pointed out above, ARC NPY neurones, at least a subpopulation of them, have been reported to be GI neurones (Muroya *et al*., 1999; Murphy *et al*., 2009; Fioramonti *et al.*, 2007). A subpopulation of ARC NPY/AgRP neurones in rat have also been previously described and characterised by their electrophysiological properties and responsiveness to orexigenic and anorexigenic signals (van den Top *et al*., 2004) and classified as cluster 2 neurones in the present and previous theses (van den Top, 2002; Lyons, 2005; Saker, 2009; Virdee, 2009). In the present work, the effects of physiological changes in extracellular glucose were investigated in three cluster 2 neurones, two of which were recorded in slices prepared from fed rats and one from a fasted rat. Both cluster 2 NPY/AgRP neurones recorded in fed rats were classified as GE neurones as lowering of extracellular glucose from 2.0 to 0.2 mM yielded membrane hyperpolarisation associated with a reduction in neuronal input resistance, an effect reversed upon increasing extracellular glucose. Current-voltage relationships revealed that lowering extracellular glucose concentration from 2.0 to 0.2 mM induced an apparent inhibition or suppression of the A-like transient outward rectifier, an effect reversed following subsequent increases in extracellular glucose to 2.0 and 5.0 mM. Thus these characteristic neurones showed all traits consistent with being GE neurones capable of detecting physiological changes in glucose. However, the cluster 2 NPY/AgRP neurone recorded in tissue from a fasted rat showed characteristic features consistent with being a GI neurone. In tissue from a fasted rat, prepared and maintained in 0.2 mM extracellular glucose, subsequent increases in extracellular glucose led to a complete cessation in firing, associated with membrane hyperpolarisation from -38 mV in 0.2 mM to -49 mV in 0.5 mM glucose and persisted, in 1.0 and 2.0 mM glucose, to rest around -51 mV. These data are consistent with these neurones being GI. Taken together, these data raise an interesting possibility: specifically, glucose-sensing orexigenic NPY/AgRP neurones, or at least a subpopulation of them, can switch glucose sensing function depending on energy status. Thus, in a fed state, orexigenic NPY/AgRP neurones could act as GE neurones and monitor or signal moment by moment fluctuations and absolute glucose levels available. In a fasted state or state of negative energy balance, orexigenic NPY/AgRP neurones are active and switch to become GI neurones, whereby food intake and rapid

transient elevations in glucose levels indicate restoration of energy balance. Current thinking on glucose-sensing suggests that GI and GE neurones are considered independent components of function-specific circuits. However, data here could begin to challenge the conventional wisdom and raises the possibility of yet another level of plasticity associated with the glucose-sensing networks. Given the low n values with this aspect of the study, this remains merely speculation but worthy of further study.

The mechanisms by which GE and GI neurones sense changes in extracellular glucose was addressed in experiments shown in Chapter 5. GE neurones have been studied in great detail in many studies in the hypothalamus and brainstem. GE neurones described in Chapter 5 were characterised by mechanisms consistent with opening of ATP-sensitive potassium channels in response to reduced extracellular glucose and closing of these channels in response to increases in extracellular glucose. The data were therefore in broad agreement with numerous previous studies showing such a phenomena in the hypothalamus and brainstem neurones (e.g. Ashford *et al.*, 1990; Ibrahim *et al.*, 2003; Rowe *et al.*, 1996; Spanswick *et al.*, 1997; Lee *et al.*, 1999; Spanswick *et al.*, 2000; Song *et al.*, 2001; Wang *et al.*, 2004; Song & Routh, 2005; Miki *et al.*, 2001; Balfour *et al.*, 2006; van den Top *et al.*, 2007). ATP-sensitive potassium channels have been shown to be pivotal for glucose-sensing in the CNS by the use of knock-out studies and pharmacological approaches (Ashford *et al.*, 1990a; Rowe *et al.*, 1996; Spanswick *et al.*, 1997; Lee *et al.*, 1999; Spanswick *et al.*, 2000; Miki *et al.*, 2001) and in GE neurones are proposed to use functional K_{ATP} channels to sense glucose in much the same way as the pancreatic β-cell (Ashford *et al.*, 1990a; Yang *et al.*, 1999; van den Top *et al.*, 2007). GLUT transporters of hypothalamic neurones permit glucose influx at a rate dependent on extracellular glucose concentration (Kang *et al.*, 2004). Within the cell, glucose is phosphorylated by glucokinase (GK), a key rate-limiting step for glucose metabolism and considered the major mechanism for glucose sensing, and a key marker or characteristic of glucose-sensing neurones (Balfour *et al.*, 2006; Dunn-Meynell *et al.*, 2002). Glucose metabolism increases the intracellular ATP/ADP ratio causing the K_{ATP} channel to close and subsequent membrane depolarisation (Yang *et al.*, 1999; Levin *et al.*, 2001; Dunn-Meynell *et al.*, 2002; Kang *et al.*, 2004). The mechanism underlying glucose-mediated effects in the present study was further investigated here and interestingly, in addition to the

ATP-sensitive potassium channel-dependent mechanism described here and confirmed in studies on tissue from fasted rats, a second putative mechanism materialised. In a number of GE neurones in fed rats, a reduction in neuronal input resistance accompanied membrane hyperpolarisation induced by low extracellular glucose. Current voltage relations indicated a reversal potential of approximately -62 mV, close to the reversal potential for chloride ions under our recording conditions. Thus in addition to an action via ATP-sensitive potassium channels, a mechanism involving opening of chloride channels may be important for glucose sensing in GE neurones. Further work is required to clarify the ionic nature and properties of this putative glucose-sensing mechanism.

The mechanism by which GI neurones sense glucose is still not fully understood. GI neurones in ARC neurones from fed rats generally had higher input resistances, lower firing rates and more negative resting membrane potentials than their counterparts from fasted rats in 2.0 mM glucose, suggesting they sit at these resting membrane potentials due to a closure of one or more resting conductances. Reducing extracellular glucose, from 2.0 to 0.2 mM in neurones from fed and fasted animals induced an increase in firing rate and membrane depolarisation, associated with only minor changes in input resistance, the only clear reversal potential being established in the fasted ARC neurones, approximately -40 mV, suggesting possible activation of a non-selective cation conductance. However, in neurones from fasted animals, maintained in 0.2 mM glucose, and subject to increases in extracellular glucose, clear decreases in firing rate associated with significant membrane hyperpolarisation and progressive decrease in input resistance were observed. These data therefore suggest that GI neurones are more responsive and better activated in response to increases in extracellular glucose, as may be expected following food intake. This is further supported by the fact that an identified cluster 2 NPY/AgRP neurone was included in this group. The reversal potential associated with these responses was approximately -60 mV suggesting activation of one or more chloride conductances underlies this response. Thus, data described here support previous data suggesting activation of a chloride-dependent mechanism underlies glucose-induced inhibition of GI neurones (Song *et al.*, 2001; Routh, 2002; Fioramonti *et al.*, 2007).

The final subtype of glucose-sensing neurone described here were the GRA neurones which responded to a change in extracellular glucose with an initial inhibition or membrane hyperpolarisation, a response that was transient and that subsequently appeared to adapt. Only 2 GRA neurones were detected in this aspect of the study, both in cells from fed animals and both were classified according to a transient inhibition to a decrease in extracellular glucose from 2.0 to 0.2 mM, followed by an adaptation to this new level of glucose, with membrane depolarisation and establishment of a new steady-state firing rate. Subsequent increases in glucose concentration yielded concentration-dependent increases in firing rate and membrane depolarisation. The mechanism involved transient opening of chloride conductances, based on current voltage relations from one cell. However, these GRA neurones differ from those reported in Chapter 5 where both neurones were characterised by membrane hyperpolarisation that rapidly adapted leading to depolarisation and the establishment of a new steady-state firing rate, in response to increases in extracellular glucose from 0.0 to 2.0 mM. In both of these neurones, the initial, transient hyperpolarisation was associated with clear reductions in neuronal input resistance, consistent with activating a conductance, followed by depolarisation and an increase in conductance, the latter consistent with closure of the conductance. The low n-values prevented clear establishment of the mechanism in this rare subtype of ARC glucose-sensing neurone. These data therefore suggest two potential types of GRA neurone may be present in the ARC: those that transiently respond to decreases in extracellular glucose and those that transiently respond to increases in extracellular glucose. Given that these GRA neurones are rare in the ARC, further work is required to clarify their chemical phenotype, their function in glucose-sensing and whether they are true subtypes or the same subtype that modifies their glucose responsiveness depending on glucose and energy status. As already indicated, this is the first description of these neurones in the ARC. However, they do share distinct similarities to adapting sugar-sensing orexin-containing neurones of the LH (Williams *et al*., 2008). In the LH initial transient inhibition is thought to involve activation of a leak potassium conductance that subsequently adapts (Williams *et al*., 2008). These adapting neurones have been suggested to function in a combined transient and sustained glucosensing manner, along with GE and GI neurones, allowing glucose-sensing neurones to maintain sensitivity to small fluctuations in glucose levels while simultaneously encoding a

larger range of baseline glucose concentrations (Williams *et al*., 2008). The fact that glucose-sensing neurones in the ARC share features remarkably similar to "classic sensory neurones," that encode both static and dynamic responses to changes in the environment through tonic and rapidly adapting receptor-dependent mechanisms, is difficult to ignore. Thus glucose-sensing neurones in the ARC may operate through function-specific mechanisms to signal not only the overall change in glucose levels at the level of the plasma and CSF but also inform the brain of the rate of change of glucose levels. Further work is required to determine the mechanisms underlying these transient responses, determine their ability to sense changes in glucose, determine their chemical phenotype and determine where they project before the functional significance of these neurones can be realised.

Chapter 7

Analysis of response dynamics in glucose-sensing neurones in rat hypothalamic arcuate nucleus to changes in the concentration of extracellular glucose

7.1 Introduction

This chapter extends Chapter 6 with a further quantitative analysis of the activity of ARC glucose-sensing neurones recorded in both *ad libitum* fed and 24-hour fasted rats in response to stepwise changes in extracellular glucose concentration. In Chapter 6, the firing frequency (number of action potentials per unit time) was used as a main measure of neuronal activity to classify the responses of ARC glucose-sensing neurones. Here, we treat the firing rate as a variable P that varies continuously with time. We assume that, following a step change in external glucose concentration, P (written in a logistic function form) changes from an initial rate λ_1 to a final rate λ_2 with a time at half sigmoid T and with the transition between the two levels of activity itself requiring a time τ to be completed. We determine best-fitting values for these parameters, using the least-squares criterion, by fitting the time-integral of P to the cumulative activity of the neurone. Thus, if δ is the delta-Dirac function, t_i denotes the time at which the ith action potential was observed, with i running from 1 to n action potentials, our model is:

$$\int_0^t P(\omega)\,d\omega \;=\; \sum_{i=1}^{n} \int_0^t \delta(\omega - t_i)\,d\omega\,.$$

The following, wholly empirical, equation was used as a model for neuronal activity following a step change in external glucose concentration:

$$P(t)=\lambda_1 + (\lambda_2 - \lambda_1)\frac{e^{\frac{t-T}{\tau}}}{1+e^{\frac{t-T}{\tau}}} \qquad (7.1)$$

where λ_1 is the activity prior to a change in extracellular glucose concentration (action potentials/second, (Hz)); λ_2 is the activity at the end of each change in extracellular glucose concentration (action potentials/second, (Hz)); t is time (second); T is the period of time giving a half sigmoid (second); and τ is the duration of the transition (second), following a change in glucose levels. A representative example of a continuous whole-cell current-clamp recording of ARC neurone together with an activity plot with further explanation of these parameters is illustrated in Figures 7.1 Bi and Bii. The time-integral of *P(t)*, *Q(t)* was calculated as follows:

$$Q(t) = \int_0^t P(\omega)\,d\omega = \lambda_1 \int_0^t d\omega + (\lambda_2 - \lambda_1) \int_0^t \frac{e^{\frac{\omega - T}{\tau}}}{1 + e^{\frac{\omega - T}{\tau}}}\,d\omega$$

$$= \lambda_1 t + (\lambda_2 - \lambda_1)\,\tau \left[\ln\left\{1 + e^{\frac{\omega - T}{\tau}}\right\} \right]_0^t$$

$$= \lambda_1 t + (\lambda_2 - \lambda_1)\,\tau \left(\ln\left\{1 + e^{\frac{t - T}{\tau}}\right\} - \ln\left\{1 + e^{\frac{-T}{\tau}}\right\} \right)$$

$$Q(t) = \lambda_1 t + (\lambda_2 - \lambda_1)\,\tau \left[\ln \frac{1 + e^{\frac{t - T}{\tau}}}{1 + e^{\frac{-T}{\tau}}} \right] \qquad (7.2)$$

Some neurones displayed a biphasic response in response to a change in glucose level, such as the glucose-rapidly adapting (GRA) neurones that were described in Chapter 6. This response consists of two transitions, which is described by a straightforward extension of the above model:

$$\lambda_1 + (\lambda_2 - \lambda_1) \frac{e^{\frac{t - T_1}{\tau_1}}}{1 + e^{\frac{t - T_1}{\tau_1}}} + (\lambda_3 - \lambda_2) \frac{e^{\frac{t - T_2}{\tau_2}}}{1 + e^{\frac{t - T_2}{\tau_2}}}$$

where λ_1, λ_2, and λ_3 denote, respectively, the initial, intermediate and final activity of the neurone; T_1 and τ_1 characterise the timing of the first transition (from λ_1 to λ_2); and; T_2 and τ_2 characterise the timing of the second transition (from λ_2 to λ_3).

The integral for this extended model is as follows:

$$Q(t) = \lambda_1 t + (\lambda_2 - \lambda_1)\,\tau_1 \ln \frac{1 + e^{\frac{t - T_1}{\tau_1}}}{1 + e^{\frac{-T_1}{\tau_1}}} + (\lambda_3 - \lambda_2)\,\tau_2 \ln \frac{1 + e^{\frac{t - T_2}{\tau_2}}}{1 + e^{\frac{-T_2}{\tau_2}}} \quad .$$

To determine the quantity

$$\sum_{i=1}^{n} \int_0^t \delta(\omega - t_i)\,d\omega \,,$$

which represents the cumulative activity function, the procedure outlined in the following section was employed.

7.2 Methods

The cumulative action potentials of neurones were calculated from whole-cell patch-clamp recordings, using a MATLAB program. (MATLAB code is listed at the end of this chapter). Since the negative injected current, which was induced every five seconds to generate regular downward deflections in order to observe the opening and closure of ion channels, could trigger additional action potentials that were not strictly related to the extracellular glucose concentration, these additional action potentials were not counted. Figure 7.1A shows the trace of a recording indicating when action potentials were counted; the green bars represent intervals during which action potentials were counted and the red bar represents an interval when the action potentials were not counted.

To count action potentials, a time loop system was implemented in MATLAB. Each time loop lasts five seconds, which includes the negative current injection period and a small portion of the time slot before the next negative current injection. The current injections were applied every five seconds and each injection lasts one second, leaving a period of four seconds during which action potentials are counted. The program does not count any action potentials that may have been induced by the negative current injection (red bar, Figure 7.1A). Outside of this interval, action potentials are counted (green bar, Figure 7.1A). The period during which no counting is done is decided on a case-by-case basis for each individual neurone recording. Once the counting within the first five seconds is done, the time loop for counting restarts for the following negative current injection and is subsequently repeated every five seconds until the end of the recording. The time loop is triggered by the downward passage of the membrane potential through a lower threshold value. This value is called the "lower threshold" which is the certain negative membrane potential after the first few milliseconds, once negative current has been injected (Figure 7.1A). The lower threshold varies depending on the set-up of each recording. Furthermore, not all recordings have negative current injections at the beginning of the trace. In such cases, action potentials of recorded neurones are counted up until the point in time where the program first encounters the lower threshold. Once the program finds this lower threshold, the time

loop system for counting action potentials is triggered. The algorithm is shown here in the form of pseudocode:

Load file

Load whole-cell patch-clamp file (.abf) to MATLAB

Move this data to column 2

Insert "t" column in column 1 by multiplying sampling point with sampling interval obtained from the file (.abf)

End load (.abf) file

Settings

Set threshold for counting action potential

Set lower threshold for starting counting by time interval constraint

Set the time period for counting in each interval of negative injected current

Counting

Set global condition for a whole trace of data

if data does not reach the lower threshold
count action potentials as normal

else count action potentials as time interval with the period of time stated in setting section

end

Count action potentials as normal

```
if      data is larger than the setting threshold
            count as 1
                    add up counter
else    do not count
end
```

Count action potentials as time interval with the period of time stated in setting section

```
if      data is in the period of time during negative current and the time during
        action potentials induced by negative current
            do not count
else    count
            count action potentials as normal (above)
end
```

Once the cumulative numbers of action potentials were obtained from MATLAB, the data were transferred and saved in comma delimited (.csv) format in preparation for parameter estimation. Curve fitting of cumulative action potential was performed in *Mathematica* according to the following steps:

Import data from .csv file

Insert equation (7.2)

Fit raw data into equation (7.2) to find estimated parameter values by using the least-squares criterion

Insert equation (7.1)

Substitute the estimated parameter values into equation (7.1)

Plot graph of equation (7.1) with estimated parameters values

The estimated parameters from the curve fitting were then substituted into equation (7.1) to investigate the trend of neuronal activity with time.

Parameters values obtained from recorded ARC neurones exposed to changes in the concentration of extracellular glucose, in both *ad libitum* fed and 24-hour fasted rats, are presented below. In some neurones the activity at the end of each glucose exposure differs from the value recorded at the beginning of the following glucose exposure, as a result of drift during the two-minute interval between the traces, which was used to determine the current-voltage (I-V) relationships reported in Chapter 6. This I-V measurement requires negative current injection, which may affect the firing frequency.

7.3 Results

The dynamic behaviour of ARC neurones in response to changes in extracellular glucose was investigated by fitting cumulative activity data from whole-cell patch-clamp recordings to the integral of neuronal activity *P(t)* as described by equation (7.1). ARC neurones were recorded in rats that were fed *ad libitum* as well as in rats that had been fasted for a 24-hour period. The ATP concentration in the electrode solution was 5.0 mM for neurones obtained from *ad libitum* fed rats and 1.0 mM for neurones obtained from 24-hour fasted rats. As reported in Chapter 6, different groups of neurones could be distinguished on the basis of their responses to a step change in the extracellular glucose concentration from 2.0 to 0.2 mM. In order to characterise the differences between *ad libitum* fed and 24-hour fasted rats, parameters and neuronal responses induced by changes in glucose level are presented separately according to the following classification of response patterns:

(i) inhibition without reversal (glucose-excited ARC neurones);

(ii) inhibition with reversal (glucose-excited ARC neurones);

(iii) excitation (glucose-inhibited ARC neurones);

(iv) rapidly adapting;

(v) no response.

For each parameter, the differences among all response patterns of neurones were compared within each feeding regime. This was done only for the data obtained following a change in glucose level from 2.0 to 0.2 mM. Only good recordings of ARC

neurones from Chapter 6 were selected for study, i.e. 15 ARC neurones recorded in *ad libitum* fed rats and 17 ARC neurones recorded in 24-hour fasted rats. Recordings were deemed to be good if the trace of recording was not deteriorated either by any readily apparent artefacts or the seal to the attached cell being lost. Statistical tests comparing each parameter between *ad libitum* fed and 24-hour fasted rats were performed only on data sets that covered a sufficiently large number of recordings.

7.3.1 Inhibition without reversal: glucose-excited ARC neurones I

ARC neurones in this group exhibited hyperpolarisation following a decrease in extracellular glucose concentration from 2.0 to 0.2 mM, with an associated reduction in input resistance and firing frequency. Furthermore, following subsequent increases of the extracellular glucose level (0.5, 1.0, 2.0 and 5.0 mM), these neurones did not exhibit any reversal. For this reason this response pattern was named *inhibition without reversal* and the neurones were classified as *glucose-excited without reversal* (GE w/o R). Five ARC neurones of this type were recorded in *ad libitum* fed rats whereas only one such ARC neurone was recorded in the 24-hour fasted rats. No statistical tests were performed. An overview of the parameter estimates for these neurones at each glucose concentration is given in Table 7.1.

Figure 7.2A is a graphical representation of the final activity λ_2 of each recorded neurone at varying levels of extracellular glucose. Data for one neurone recorded in 24-hour fasted rats are presented only for a change in extracellular glucose concentration from 2.0 to 0.2 mM since the quality of the recording was subsequently compromised. Following a change in glucose level from 2.0 to 0.2 mM, the average activity decreased from 0.602 ± 0.158 Hz (λ_1, n = 5) to 0.114 ± 0.052 Hz (λ_2, n =5) in neurones recorded in *ad libitum* fed rats; correspondingly it also went down from 0.350 Hz (λ_1, n = 1) to 1.53×10^{-6} Hz (λ_2, n = 1) in the 24-hour fasted rat neurone, Figure 7.2B. At this glucose level, the average time neurones giving a half sigmoid (T) was 137 ± 50 seconds (n = 5) in *ad libitum* fed rats and 264 seconds (n = 1) in 24-hour fasted rats, Figure 7.3A. The average transition time (τ) was 101 ± 14.0 seconds (n = 5) and 67 seconds (n = 1) in *ad libitum* fed and 24-hour fasted rats, respectively (Figure 7.3B).

In *ad libitum* fed rats, an increase in glucose level from 0.2 to 0.5 mM induced a further reduction in neuronal activity from 0.038 ± 0.034 Hz (λ_1, n = 5) to 0.030 ± 0.021 Hz (λ_2, n = 5, Figure 7.2B) with a mean *T* of 121 ± 9.4 seconds (n = 2), Figure 7.3A. The transition time (τ) was 10 ± 9.9 seconds (n = 2), Figure 7.3B. Further reductions in the activity of neurones in this group were observed following an increase in extracellular glucose level from 0.5 to 1.0 mM. Activity decreased from 0.014 ± 0.010 Hz (λ_1, n = 5) to 0.010 ± 0.006 Hz (λ_2, n = 5, Figure 7.2B) with a mean time *T* of 176 ± 34.1 seconds (n = 2), Figure 7.3A. The transition time (τ) was 11 ± 5.6 seconds (n = 2), Figure 7.3B.

With a change in glucose level from 1.0 to 2.0 mM in *ad libitum* fed rats, the neuronal activity further decreased from 0.017 ± 0.017 Hz (λ_1, n = 5) to 0.002 ± 0.002 Hz (λ_2, n = 5; Figure 7.2B) with a time *T* of 161 seconds (n = 1), Figure 7.3A. The transition time τ of this group of neurone was 23 seconds (n = 1), Figure 7.3B. Finally, a change of extracellular glucose concentration from 2.0 to 5.0 mM resulted in a small reduction in neuronal activity from 0.009 ± 0.009 Hz (λ_1, n = 4) to 0.008 ± 0.008 Hz (λ_2, n = 5, Figure 7.2B) with an average time *T* of 150 seconds (n = 1) and a transition time of 10 seconds (n = 1), Figures 7.3A and B.

Time courses of activity/firing frequency following each change in extracellular glucose concentration are shown in Figures 7.4 A-E for *ad libitum* fed rats and Figure 7.5A for the 24-hour fasted rat.

7.3.2 Inhibition with reversal: glucose-excited ARC neurones II

Neurones in this group displayed hyperpolarisation following a decrease in glucose level from 2.0 to 0.2 mM with an associated reduction in input resistance and firing frequency. The initial response was similar to the response observed in the previous group. However, the hyperpolarisation of these neurones was reversed, resulting in a depolarisation, following further increases in extracellular glucose concentration (0.5, 1.0, 2.0 and 5.0 mM). Hence, this pattern was termed *inhibition with reversal* and the neurones were classified as *glucose-excited with reversal* (GE w/R). Within this group, four ARC neurones were recorded in *ad libitum* fed rats and eight

ARC neurones were recorded in 24-hour fasted rats. A sufficient number of recordings were available to warrant statistical tests to compare each parameter obtained between *ad libitum* fed and 24-hour fasted rats. An overview of the parameter estimates obtained for these neurones in each concentration of glucose is given in Table 7.2. The final level of activity in each single recorded neurone at each level of extracellular glucose is shown in Figures 7.6A and B. One-tailed Wilcoxon and Mann-Whitney test was used for statistical comparison of all parameters between neurones recorded from *ad libitum* fed and 24-hour fasted rats in all step changes of glucose level.

Following exposure to 0.2 mM (decreased from 2.0 mM) glucose, the average initial neuronal activity (in 2.0 mM) was 0.327 ± 0.278 Hz (λ_1, n = 4) in *ad libitum* fed rats and 0.328 ± 0.083 Hz (λ_1, n = 8) in 24-hour fasted rats, yielding no statistically detectable difference between these two different feeding regimes. In the presence of 0.2 mM glucose, the average neuronal activity decreased to 0.079 ± 0.052 Hz (λ_2, n = 4) and 0.087 ± 0.025 Hz (λ_2, n = 8) in *ad libitum* fed and 24-hour fasted rats, respectively, revealing no statistically detectable difference, Figure 7.6C. The half sigmoid time in *ad libitum* fed was 215 ± 215 seconds (n = 2), while the corresponding value in 24-hour fasted was 413 ± 106 seconds (n = 8), Figure 7.7A. Although neurones in 24-hour fasted rats took more time to change their activity than in *ad libitum* fed rats, there was no statistically detectable difference. The average transition time τ of these neurones was larger in *ad libitum* fed rats, 213 ± 201 seconds (n = 2), than in 24-hour fasted rats, 97 ± 36 seconds (n = 8), although no statistically significant difference was found, Figure 7.7B. Time courses of activity/firing frequency of these neurones with time with this application (2.0 to 0.2 mM glucose) in both *ad libitum* fed and 24-hour fasted rats are shown in Figures 7.8A and 7.9A, respectively.

The hyperpolarisation induced by 0.2 mM glucose in these neurones was reversed following an increase in extracellular glucose (0.5 mM). The activity of neurones increased from 0.051 ± 0.044 Hz (λ_1, n = 4) to 0.154 ± 0.093 Hz (λ_2, n = 4) in *ad libitum* fed rats, whereas it increased from 0.041 ± 0.021 Hz (λ_1, n = 7) to 0.268 ± 0.100 Hz (λ_2, n = 7) in 24-hour fasted rats, Figure 7.6C. No statistically detectable difference was observed for either λ_1 or λ_2. The average half sigmoid time

was much lower in *ad libitum* fed rats (78 ± 5 seconds, n = 2) than in 24-hour fasted rats (470 ± 53 seconds, n = 7), yielding a statistically detectable significance ($P < 0.05$; one-tailed Wilcoxon and Mann-Whitney test, Figure 7.7A). Similarly, the transition was lower in *ad libitum* fed rats, 14 ± 13 seconds (n = 2), than in 24-hour fasted rats (120 ± 65 seconds, n = 7), although this was not statistically significant (Figure 7.7B). Time courses of activity/firing frequency of these neurones with this application (0.2 to 0.5 mM glucose) in both *ad libitum* fed and 24-hour fasted rats are shown in Figures 7.8B and 7.9B, respectively.

Extracellular glucose concentration was further increased, from 0.5 mM to 1.0 mM. In *ad libitum* fed rats, the mean activity of neurones further increased from 0.114 ± 0.073 Hz (λ_1, n = 4) to 0.262 ± 0.077 Hz (λ_2, n = 4), while it increased from 0.168 ± 0.077 Hz (λ_1, n = 7) to 0.424 ± 0.224 Hz (λ_2, n = 7) in 24-hour fasted rats, Figure 7.6C. The half sigmoid time was 226 ± 75 seconds (n = 4) in *ad libitum* fed rats and 562 ± 175 seconds (n = 7) in 24-hour fasted rats, Figure 7.7A. The transition time was found to be 23 ± 42 (n = 4) in *ad libitum* fed rats and 42 ± 14 seconds (n = 7) in 24-hour fasted rats, respectively, as shown in Figure 7.7B. One-tailed Wilcoxon and Mann-Whitney test comparing each parameter between *ad libitum* fed and 24-hour fasted rats failed to reveal any statistically detectable differences. Time courses of activity/firing frequency of these neurones with at this exposure (0.5 to 1.0 mM glucose) in both *ad libitum* fed and 24-hour fasted rats are shown in Figures 7.8C and 7.9C, respectively.

An increase in glucose level from 1.0 to 2.0 mM induced further increases in activity of neurones from 0.167 ± 0.062 Hz (λ_1, n = 4) to 0.457 ± 0.136 Hz (λ_2, n = 5) in *ad libitum* fed rats and from 0.306 ± 0.146 Hz (λ_1, n = 4) to 0.375 ± 0.119 (λ_2, n = 5) in 24-hour fasted rats, Figure 7.6C. No statistically significant difference was found between the activities of neurones recorded in *ad libitum* fed and 24-hour fasted rats. The mean half sigmoid time before changing activity was 82 ± 27 seconds (n = 4) in *ad libitum* fed rats and 486 ± 155 seconds (n = 5) in 24-hour fasted rats, yielding a statistically detectable significance with $P < 0.01$ (one-tailed Wilcoxon and Mann-Whitney test), Figure 7.7A. The transition time τ was 14 ± 13 seconds in *ad libitum* fed rats (n = 4), much lower than the value of 75 ± 49 seconds found in 24-hour fasted rats

(n = 5), although not statistically significant, Figure 7.7B. Time courses of activity/firing frequency of these neurones in this exposure (1.0 to 2.0 mM glucose) in both *ad libitum* fed and 24-hour fasted rats are shown in Figures 7.8D and 7.9D, respectively.

Finally, an increase in glucose level from 2.0 to 5.0 mM was applied to neurones within this group. The mean activity of the neurones at the beginning of the application, λ_1, was 0.286 ± 0.002 Hz (n = 2) in *ad libitum* fed rats and 0.108 ± 0.053 Hz (n = 4) in 24-hour fasted rats, revealing no statistically detectable significance. The activity of neurones at the end of the application of 5.0 mM glucose, λ_2, was 0.258 ± 0.030 Hz (n = 2) and 0.176 ± 0.113 Hz (n = 4) in *ad libitum* fed and 24-hour fasted rats, respectively, Figure 7.6C. These values did not exhibit a statistically detectable difference. The average time, *T*, was 115 ± 11 seconds (n = 2) in *ad libitum* fed rats, whereas it was 843 ± 289 seconds (n = 4) in 24-hour fasted rats, revealing no statistically detectable difference, Figure 7.7A. Furthermore, the transition time (τ) was small in *ad libitum* fed rats, 7 ± 7 seconds (n = 2), compared to 116 ± 75 seconds (n = 4) in 24-hour fasted rats; however, this difference was not statistically significant, Figure 7.7B. Time courses of activity/firing frequency of these neurones with this treatment (2.0 to 5.0 mM glucose) in both *ad libitum* fed and 24-hour fasted rats are shown in Figures 7.8E and 7.9E, respectively.

7.3.3 Excitation: glucose-inhibited ARC neurones

The neurones in this group exhibited depolarisation in response to a decrease in extracellular glucose from 2.0 to 0.2 mM with an associated increase in firing frequency. Hence, the response pattern was called *excitation* and cells responding in this way were classified as *glucose-inhibited* (GI) neurones. With increased glucose levels (0.5, 1.0, 2.0 and 5.0 mM), the depolarisation of these neurones was reversed, resulting in a hyperpolarisation. However, some of these neurones displayed no reversal (exhibiting a firing frequency at least as high as when exposed to 0.2 mM extracellular glucose). These two response types are grouped together since there is only a small number of neurone of concern. Within this group, three ARC GI neurones recorded in *ad libitum* fed rats and four ARC GI neurones recorded in 24-hour fasted rats were investigated.

The numbers of recorded neurones within this group warranted the use of statistical tests to compare each parameter obtained between *ad libitum* fed and 24-hour fasted rats. An overview of all parameter estimates obtained for these neurones at each concentration of glucose is shown in Table 7.3. Graphical representations of the final activity λ_2 of each recorded neurone at varying levels of extracellular glucose are shown in Figure 7.10A and B. One-tailed Wilcoxon and Mann-Whitney test was used for statistical comparison of all parameters between neurones recorded from *ad libitum* fed and 24-hour fasted rats in all step changes of glucose level.

Upon exposure to 0.2 mM (decreased from 2.0 mM) glucose, depolarisation was observed in these neurones. The average activity increased from 0.077 ± 0.041 Hz (λ_1, n = 3) to 0.186 ± 0.073 Hz (λ_2, n = 3) in *ad libitum* fed rats, whereas it increased from 0.172 ± 0.061 Hz (λ_1, n = 4) to 0.271 ± 0.082 Hz (λ_2, n = 4) in 24-hour fasted rats, Figure 7.10C. The one-tailed Wilcoxon and Mann-Whitney test failed to reveal differences in activity between the two groups of rat. The time *T* was 459 ± 149 seconds (n = 3) in *ad libitum* fed rats and 529 ± 185 seconds (n = 4) in 24-hour fasted rats, respectively, giving no statistically detectable significance, Figure 7.11A. The transition time was 18 ± 9 seconds (n = 3) in *ad libitum* fed rats, and it was 16 ± 7 seconds (n = 4) in 24-hour fasted rats, which was not statistically different, Figure 7.11B. Time courses of firing frequency of these neurones following the step change from 2.0 to 0.2 mM glucose) in *ad libitum* fed and 24-hour fasted rats are shown in Figures 7.12A and 7.13A, respectively.

With an increased glucose level (0.2 to 0.5 mM), the activity of neurones in *ad libitum* fed rats increased from 0.184 ± 0.084 Hz (λ_1, n = 3) to 0.301 ± 0.217 Hz (λ_2, n = 3). However, neurones recorded in 24-hour fasted rats exhibited a small reduction in activity from 0.303 ± 0.105 Hz (λ_1, n = 4) to 0.269 ± 0.104 Hz (λ_2, n = 4), Figure 7.10C. The one-tailed Wilcoxon and Mann-Whitney test failed to reveal a difference between the two groups of rat for either λ_1 or λ_2. The mean time *T* in *ad libitum* fed rats was 263 ± 35 seconds (n = 3), which was much smaller than the time spent in 24-hour fasted rats group, 414 ± 63 seconds (n = 4), Figure 7.11A. However, this difference was not statistically different. The parameter τ in *ad libitum* fed rats was

39 ± 30 seconds (n = 3), whereas it was found to be 25 ± 15 seconds (n = 4) in 24-hour fasted rats, revealing no statistically detectable difference, Figure 7.11B. Time courses of firing frequency of these neurones in this treatment (0.2 to 0.5 mM glucose) in both *ad libitum* fed and 24-hour fasted rats are shown in Figures 7.12B and 7.13B, respectively.

A further increase in extracellular glucose, from 0.5 to 1.0 mM, resulted in similar responses. The activity of neurones in *ad libitum* fed rats increased from 0.162 ± 0.133 Hz (λ_1, n = 3) to 0.230 ± 0.174 Hz (λ_2, n = 3), whereas it was slightly reduced from 0.259 ± 0.096 Hz (λ_1, n = 4) to 0.250 ± 0.092 (λ_2, n = 4) in 24-hour fasted rats, Figure 7.10C. The average time, *T*, was 164 ± 43 seconds (n = 2) in *ad libitum* fed rats with a corresponding transition time of 14 ± 14 seconds (n = 2), while in 24-hour fasted rats the delay was more than twice as long, 369 ± 143 seconds (n = 3) whereas the transition time was comparable at 18 ± 9 seconds (n = 3), Figure 7.11. However, no difference was statistically detectable for any of these parameters. Time courses of the firing frequency of these neurones following a change from 0.5 to 1.0 mM glucose in *ad libitum* fed and 24-hour fasted rats are shown in Figures 7.12C and 7.13C, respectively.

Following a change in extracellular glucose level from 1.0 to 2.0 mM, the activity at the beginning (λ_1) of the recordings in *ad libitum* fed rats was 0.061 ± 0.033 Hz (n = 3), whereas the corresponding value in 24-hour fasted rats was comparable at 0.155 ± 0.155 Hz (n = 2). The activity at the end of the application (λ_2) was 0.048 ± 0.024 Hz (n = 3) in *ad libitum* fed rats and much higher in 24-hour fasted rats: 0.545 ± 0.140 Hz (n = 2; Figure 7.10C). No statistically detectable significance was observed in both λ_1 and λ_2. The delay time, *T*, in *ad libitum* fed rats (132 ± 37 seconds, n = 2) was larger than in 24-hour fasted rats (96 ± 35 seconds, n = 2), although not significantly, Figure 7.11A. The transition time, τ, in *ad libitum* fed rats (9 ± 3 seconds, n = 2) appeared to be much smaller than in 24-hour fasted rats (243 ± 231 seconds, n = 2, Figure 7.11B), although no statistically detectable significance was observed. Time courses of firing frequency of these neurones following

a change from 1.0 to 2.0 mM glucose in *ad libitum* fed and 24-hour fasted rats are shown in Figures 7.12D and 7.13D, respectively.

Finally, when 5.0 mM glucose was applied, a small change in activity of neurones recorded in both groups of rat was observed. The mean activity at the beginning (λ_1) in *ad libitum* fed rats was 0.015 ± 0.009 Hz (n = 3), whereas it was 0.600 ± 0.207 Hz (n = 2) in 24-hour fasted rats. The one-tailed Wilcoxon and Mann-Whitney test revealed no statistically significant difference. The final activity of neurones (λ_2) was 0.028 ± 0.015 Hz (n = 3) in *ad libitum* fed rats and 0.560 ± 0.228 Hz (n = 2) in 24-hour fasted rats, Figure 7.10C. Although there was a large difference in λ_2 between two groups of rat, no statistically significant difference was observed. The mean time *T* observed in *ad libitum* fed rats was 148 ± 45 seconds (n = 2), whilst it appeared to be much larger in 24-hour fasted rats: 327 ± 48 seconds (n = 2), although no difference could be statistically detected, Figure 7.11A. The transition time τ found for *ad libitum* fed rats was 6 ± 2 seconds (n = 2), whereas the change-over was very rapid in 24-hour fasted rats as their mean τ was 0.1 ± 0.06 seconds (n = 2), giving no statistically significant difference, Figure 7.11B. Time courses of the firing frequency of these neurones following a change from 2.0 to 5.0 mM glucose in *ad libitum* fed and 24-hour fasted rats are shown in Figures 7.12E and 7.13E, respectively.

7.3.4 Rapidly adapting ARC neurones

Neurones within this group exhibited a biphasic response in response to a change in the extracellular glucose concentration from 2.0 to 0.2 mM. Interestingly, not a single neurone exhibiting a biphasic response was found in 24-hour fasted rats. The following results are therefore all based on recordings obtained from *ad libitum* fed rats. Two neurones in *ad libitum* fed rats were found to have a biphasic response during decreased glucose level which was hyperpolarised then depolarised transiently in the presence of 0.2 mM glucose as reported in Chapter 6. These cells were therefore termed *glucose-rapidly adapting* (GRA) neurones. An overview of all parameter values obtained for these neurones in each concentration of glucose is shown in Table 7.4.

Graphical representation of λ_2 of both recorded neurones at varying levels of extracellular glucose including their λ_3 in 0.2 mM glucose is shown in Figure 7.14A.

Upon exposure to 0.2 mM (decreased from 2.0 mM) glucose, a biphasic response was observed as mentioned, i.e. hyperpolarisation followed by depolarisation, leading to three different activity values (λ_1, λ_2 and λ_3), two different times neurones spent to reach half sigmoid in each response (T_1 and T_2) and two different times neurones spent at the change-over point (τ_1 and τ_2). The average activity of these neurones decreased during the first response, viz. hyperpolarisation, from 0.335 ± 0.282 Hz (λ_1, n = 2) to 0.006 ± 0.000 Hz (λ_2, n = 2), Figure 7.14B, with a half sigmoid time of 348 ± 227 seconds (T_1, n = 2, Figure 7.15A) and τ_1 of 1.600 ± 0.6 seconds (n = 2, Figure 7.15B). By contrast, during the second response, the activity of neurones increased to 0.119 ± 0.030 Hz (λ_3, n = 2), Figure 7.14B, with a time T_2 of 768 ± 48 seconds (n = 2, Figure 7.15A) and a transition time τ_2 of 3 ± 2 seconds (n = 2, Figure 7.15 B). Time courses of activity/firing frequency of these neurones following a change from 2.0 to 0.2 mM glucose are shown in Figure 7.16A.

Following an increase in the extracellular glucose concentration from 0.2 to 0.5 mM, the mean activity of neurones increased from 0.042 ± 0.026 Hz (n = 2) to 0.156 ± 0.059 Hz (n = 2), Figure 7.14B. The time T was found to be 56 ± 34 seconds (n = 2, Figure 7.15 A) with a corresponding τ-value of 1.120 ± 1.031 seconds (n = 2, Figure 7.15B).

A further increase in glucose level from 0.5 to 1.0 mM induced an increase in the activity of neurones from 0.142 ± 0.059 Hz (n = 2) to 0.248 ± 0.030 Hz (n = 2), Figure 7.14B. The average time T was 137 ± 63 seconds (n = 2, Figure 7.15A) with a corresponding τ-value of 8 ± 7 seconds (n = 2, Figure 7.15B).

Similarly, a change from 1.0 to 2.0 mM glucose led to an increase in neuronal activity, from 0.041 ± 0.041 Hz (n = 2) to 0.310 ± 0.256 Hz (n = 2), Figure 7.14B, with an average time T of 146 ± 47 seconds (n = 2, Figure 7.15A) and a corresponding τ-value of 33 ± 32 (n = 2, Figure 7.15B).

Finally, in the presence of 5.0 mM glucose, neuronal activity increased yet further from 0.150 ± 0.145 Hz (n = 2) to 0.238 ± 0.218 Hz (n = 2), Figure 7.14B, with an

average delay T of 204 ± 23 seconds (n = 2, Figure 7.15A) and a small corresponding τ-value of 3 ± 1 seconds (n = 2, Figure 7.15B). Time courses are shown in Figure 7.16A-E.

7.3.5 Non-responsive ARC neurones

A final group of neurones consisted of cells which did not respond to any changes in extracellular glucose level, or failed to exhibit any marked change in firing frequency, and which were labelled *non-responsive* or *non glucose-sensing* neurones. A single non glucose-sensing neurone was encountered in the ARC of *ad libitum* fed rats whereas four such neurones were encountered in the ARC of 24-hour fasted rats. An overview of the parameter estimates obtained for these neurones at each concentration of glucose is given in Table 7.5. Figure 7.17A is a graphical representation of the final activity λ_2 of each recorded neurone at varying levels of extracellular glucose.

A change in extracellular glucose from 2.0 to 0.2 mM did not result in a sizable change in the activity of the neurone in the *ad libitum* fed rat which was from 0.077 Hz (n = 1) to 0.073 Hz (n = 1), whereas the activity of neurones recorded in 24-hour fasted rats decreased their activity from 0.347 ± 0.096 Hz (n = 4) to 0.276 ± 0.061 Hz (n = 4), Figure 7.17B. The average time T was 530 seconds (n = 1) in the *ad libitum* fed rat and 387 ± 154 seconds (n = 4) in 24-hour fasted rats, Figure 7.18A. The change-over time (τ), was found to be 9 seconds (n = 1) and 51 ± 25 seconds (n = 4) in the *ad libitum* fed and 24-hour fasted rats, respectively, Figure 7.18B.

An increased glucose level (from 0.2 to 0.5 mM) induced a small change in neuronal activity in 24-hour fasted rats from 0.211 ± 0.103 Hz (n = 4) to 0.243 ± 0.138 Hz (n = 4), whereas it slightly increased from 0.023 Hz (n = 1) to 0.154 Hz (n = 1) in the *ad libitum* fed rat, Figure 7.17B. The delay half sigmoid time was 30 seconds (n = 1) in the *ad libitum* fed rat and 325 ± 76 seconds (n = 4) in 24-hour fasted rats, Figure 7.18A. The parameter τ in these neurones was 0.4 seconds (n = 1) and 37 ± 15 seconds (n = 1) in the *ad libitum* fed and 24-hour fasted rats, respectively, Figure 7.18B.

In addition, a change in extracellular glucose level from 0.5 to 1.0 mM induced no change in the activity of neurones in the *ad libitum* fed rat which was 0.223 Hz (n = 1) at the beginning and was 0.213 Hz (n = 1) at the end of the treatment, Figure 7.17B. In 24-hour fasted rats, the neuronal activity also remained unchanged which was from 0.365 ± 0.117 Hz (n = 4) to 0.362 ± 0.112 Hz (n = 4), Figure 7.17B. Both the average time (*T*) and the average time neurones spent at the change-over (τ) of neurones in the *ad libitum* fed rat was less than the time in the 24-hour fasted rats, respectively. The parameter *T* of the *ad libitum* fed rat was 250 seconds (n = 1), whereas the mean value obtained in 24-hour fasted rats was 676 ± 124 seconds (n = 4), Figure 7.18A. The parameter τ of the *ad libitum* fed rat was 7 seconds (n = 1), whilst the corresponding value in 24-hour fasted rats was 54 ± 34 seconds (n = 4), Figure 7.18B.

With further application of 2.0 mM glucose, the average neuronal activity slightly decreased in the *ad libitum* fed rat from 0.156 Hz (n = 1) to 0.130 Hz (n = 1), and in the 24-hour fasted rats from 0.371 ± 0.151 Hz (n = 4) to 0.271 ± 0.052 Hz (n = 4), Figure 7.17B. Similar to the previous glucose step, both the parameters *T* and τ of the *ad libitum* fed rat were less than those times in 24-hour fasted rats. The time (*T*) was 100 seconds (n = 1, Figure 7.18 A) with a τ -value of 85 seconds (n = 1, Figure 7.18B) in the *ad libitum* fed rat, whereas the *T* of 24-hour fasted rats was 443 ± 147 seconds (n = 4, Figure 7.18 A) with a τ -value of 327 ± 322 seconds (n = 4, Figure 7.18B).

Finally, when 5.0 mM glucose was applied to these neurones, the activity of neurones at the beginning of the recording taken from the *ad libitum* fed rat was 0.034 Hz (n = 1), whereas it was 0.141 Hz (n = 1) at the end of the recording. In 24-hour fasted rats, the initial activity 0.384 ± 0.124 Hz (n = 4) and was 0.290 ± 0.136 Hz (n = 4) at the end of the recording, Figure 7.17B. The time *T* in the *ad libitum* fed rat was 22 seconds (n = 1), markedly shorter than the value of 274 ± 113 seconds (n = 4) found in 24-hour fasted rats, Figure 7.18A. In addition, the τ -value of the *ad libitum* fed rat was 0.7 seconds (n = 1), much quicker than the transition time of 63 ± 50 seconds (n = 4) in 24-hour fasted rats, Figure 7.18B.

Time courses of activity/firing frequency of these neurones following each change of extracellular glucose concentration in *ad libitum* fed and 24-hour fasted rats are shown in Figure 7.19 A-E and 7.20 A-E, respectively.

7.3.6 Parameter comparisons in different responses of neurones following a step change in glucose from 2.0 to 0.2 mM in *ad libitum* fed rats

Parameter values ($\Delta\lambda = \lambda_2 - \lambda_1$, T and τ) generated from different neurone responses to a change in extracellular glucose from 2.0 to 0.2 mM in *ad libitum* fed rats were compared. Only the application of glucose from 2.0 to 0.2 mM was investigated. The one-tailed Wilcoxon and Mann-Whitney test was performed in all comparisons.

In *ad libitum* fed rats, only three responses of neurones were studied: inhibition without reversal, inhibition with reversal and excitation. The rapidly adapting group was omitted from the comparison for clarity. The non responsive group was also excluded from as there was only one neurone in this group.

The change in activity between the start of experiment and the end of exposure to 0.2 mM glucose application, represented by $\Delta\lambda = \lambda_2 - \lambda_1$, was calculated in order to compare the differences of ARC neurones in different responses. A statistically detectable difference in $\Delta\lambda$ was observed between glucose-excited (without reversal) and glucose-inhibited ARC neurones ($P < 0.05$; one-tailed Wilcoxon and Mann-Whitney test) and between glucose-excited (with reversal) and glucose-inhibited ARC neurones ($P < 0.05$; one-tailed Wilcoxon and Mann-Whitney test), indicating a statistically detectable significance in neuronal activity changes following a change in glucose from 2.0 to 0.2 mM between glucose-excited and glucose-inhibited ARC neurones. However, no statistically detectable significance in $\Delta\lambda$ was observed between glucose-excited with and without reversal ARC neurones.

The half sigmoid time (T) was also compared statistically. A statistically detectable difference was observed only in one pair of response patterns of neurones between glucose-excited (without reversal) and glucose-inhibited ARC neurones ($P < 0.05$, one-tailed Wilcoxon and Mann-Whitney test). Hence, glucose-inhibited ARC neurones required a statistically significant longer time (459 ± 149 seconds) than

glucose-excited (without reversal) neurones (137 ± 50 seconds). However, no statistically detectable difference was observed between glucose-excited ARC neurones with and without reversal and between glucose-excited (with reversal) and glucose-inhibited ARC neurones.

The duration of the transition time (τ) was also compared in different groups of neurones. There was a statistically detectable difference in τ between glucose-excited (without reversal) and glucose-inhibited ARC neurones ($P < 0.05$, one-tailed Wilcoxon and Mann-Whitney test). Hence, glucose-inhibited neurones required significantly less change-over time (18 ± 9 seconds) than glucose-excited (without reversal) ARC neurones (101 ± 14 seconds). No differences could be detected at the 5% level between glucose-excited (with reversal) and glucose-inhibited ARC neurones or between glucose-excited ARC neurones with and without reversal.

7.3.7 Parameter comparisons in different responses of neurones during a change in glucose from 2.0 to 0.2 mM in 24-hour fasted rats

As with the *ad libitum* fed rats section above, three sets of parameters were compared for the response to change in extracellular glucose from 2.0 to 0.2 mM in 24-hour fasted rats. Only two groups of neurones, glucose-excited ARC neurones (with reversal) and glucose-inhibited ARC neurones could be statistically compared, due to small numbers of recordings in all other groups. The difference in activity between the start and the end of the exposure to 0.2 mM extracellular glucose, represented by $\Delta\lambda = \lambda_2 - \lambda_1$, was found to be statistically significant between glucose-excited ARC neurones (with reversal; 0.20 ± 0.07 Hz) and glucose-inhibited ARC neurones (0.10 ± 0.03 Hz), ($P < 0.01$, one-tailed Wilcoxon and Mann-Whitney test), whereas the parameters T and τ failed to show any statistically detectable difference between these two groups of neurones.

7.4 Discussion

Analysis of the responses observed in ARC glucose-sensing neurones reported in Chapter 6 was performed. The response of ARC neurones to changes in extracellular glucose concentration (2.0 - 0.2 - 0.5 - 1.0 - 2.0 - 5.0 mM) was investigated in both *ad libitum* fed and 24-hour fasted rats. An empirical sigmoid response function was assumed to describe the time course of the transition in neuronal activity and the integral of this function was fitted to cumulative action potential numbers to characterise the response dynamics. The quality of fit was generally very good, indicating that the empirical formula was adequate. Four parameters (λ_1, λ_2, T and τ) were estimated for each transition, employing the least-squares criterion. The estimates were compared for each response pattern of ARC neurones in both groups of feeding regimes, in order to characterise the behaviour of each neurone in more detail. The following response patterns were distinguished:

(i) inhibition without reversal (glucose-excited ARC neurones): GE w/o R;

(ii) inhibition with reversal (glucose-excited ARC neurones): GE w/R;

(iii) excitation (glucose-inhibited ARC neurones): GI;

(iv) rapidly adapting: GRA;

(v) non glucose-sensing: NGS.

In GE w/o R neurones, the average activity in *ad libitum* fed rats decreased throughout the experiment when exposed to increases in extracellular glucose concentration. Similarly, the single GE w/o R neurone observed in 24-hour fasted rats exhibited a reduction in activity from 2.0 to 0.2 mM, as was the case for *ad libitum* fed rats. The time delay (T) was between 120 and 176 seconds for all glucose concentrations in *ad libitum* fed rats, whereas the neurones from the 24-hour fasted rats responded more sluggishly, taking up to 264 seconds to respond to a change in glucose from 2.0 to 0.2 mM glucose. This supports the data obtained in Chapter 6 which indicated the average run-down time of GE neurones in a change in glucose from 2.0 to 0.2 mM was larger in 24-hour fasted rats than in *ad libitum* fed rats. Interestingly, the duration of the transition (τ) in *ad libitum* fed rats was large only following the transition from 2.0 to 0.2 mM extracellular glucose (101 seconds), whereas it was small (between 10 and 24 seconds) for the remainder of the glucose step changes.

The GE w/R neurones from rats exposed to either food regime all exhibited a decrease in mean activity as a result of a change in extracellular glucose from 2.0 to 0.2 mM glucose and subsequently reversed, exhibiting an increase in activity in the application of 0.5 mM glucose. These neurones continued increasing their activity for the rest of the experiment except in *ad libitum* fed rats where neurone activity decreased slightly when glucose was increased from 2.0 to 5.0 mM. The average delay time to reach half sigmoid (*T*) was more than 400 seconds in all applications of glucose in 24-hour fasted rats and less than 230 seconds in *ad libitum* fed rats following all step changes. This is entirely in line with the result (Chapter 6) that the average run-down time of GE neurones in a change in glucose from 2.0 to 0.2 mM in fasted rats was larger than in *ad libitum* fed rats. A statistically significant difference was also observed in these time differences between *ad libitum* fed and 24-hour fasted rats following a change in glucose from 0.2 to 0.5 mM ($P < 0.05$) and from 1.0 to 2.0 mM ($P < 0.01$). Similar to the inhibition without reversal group, the duration of the transition (τ) in *ad libitum* fed rats was the longest in the application from 2.0 to 0.2 mM glucose (~ 213 seconds) and was relatively small for the rest of experiments (between 7 and 24 seconds). The τ-value obtained for neurones in 24-hour fasted rats varied between 41 and 120 seconds throughout all applications.

In GI neurones, the average activity in both *ad libitum* fed and 24-hour fasted rats increased following a change in extracellular glucose from 2.0 to 0.2 mM, whereas it both increased and decreased in the rest of experiments for both feeding regimes. However, the λ_1-value for neurones from 24-hour fasted rats was larger than the λ_1-value for neurones from *ad libitum* fed rats at all levels of extracellular glucose. Correspondingly, λ_2 for neurones in 24-hour fasted rats was also larger than in *ad libitum* fed rats at all glucose levels, indicating that neurones in 24-hour fasted rats were more active than in neurones recorded in *ad libitum* fed rats, supporting the results presented in Chapter 6.

The time (*T*) was generally similar to that observed in GE neurones. GI neurones from 24-hour fasted rats had a longer delay time than GI neurones from *ad libitum* fed rats in all glucose changes except the transition from 1.0 to 2.0 mM extracellular glucose, where *T* for 24-hour fasted rats was less than *T* for *ad libitum* fed

rats. These results support the finding that the average run-up time of GI neurones in a change in glucose from 2.0 to 0.2 mM in fasted rats was larger than in *ad libitum* fed rats (see Chapter 6). Furthermore, the duration of the transition (τ) in neurones from rats exposed to either feeding regimes did not exhibit a consistent pattern.

Only two GRA neurones from *ad libitum* fed rats were investigated. A biphasic response of these neurones was obtained following a change in glucose level from 2.0 to 0.2 mM extracellular glucose; the primary response was inhibition and the secondary response was depolarisation, reversing the initial response. The neuronal activity then continued to increase with increased glucose level. The time (*T*) following the 2.0 to 0.2 mM glucose step was unusually long (768 ± 48 seconds) compared to the time (*T*) following other changes in glucose levels (0.5 – 1.0 – 2.0 and 5.0 mM). The transition time (τ) of these neurones was quite small in all changes in glucose levels, between 1 and 34 seconds.

In NGS neurones no major changes in activity were observed, although the activity of neurones at both the start and at the end of each exposure in the 24-hour fasted rats was greater than in *ad libitum* fed rats. This indicates that ARC neurones in 24-hour fasted rats were more active than those in *ad libitum* fed rats, supporting the data obtained in Chapter 6. Regarding the time (*T*) and the change-over period (τ), the results show that this group of neurones either took a comparatively small time or a very long time for a negligible change in activity for both *T* and τ for both feeding regimes.

For each parameter, the differences among all response patterns of neurones were also compared within each feeding regime. Since neurones were distinguished on the basis of their response to a step change in extracellular glucose concentrations from 2.0 to 0.2 mM, parameters obtained only from this change in glucose levels were compared. In *ad libitum* fed rats, the difference in activity of neurones at the start and at the end of glucose application, $\Delta\lambda$, the half sigmoid time (*T*) and the change-over period (τ) were compared among all response patterns. A statistically detectable significance in $\Delta\lambda$ was observed between glucose-excited (without reversal) and glucose-inhibited ARC neurones ($P < 0.05$) and between glucose-excited (with reversal) and glucose-inhibited ARC neurones ($P < 0.05$), whereas no statistically detectable significance was observed between glucose-excited with and without reversal ARC

neurones. Hence, the data indicates the difference in changing in neuronal activity following a change in glucose from 2.0 to 0.2 mM between glucose-excited and glucose-inhibited ARC neurones is detectable, supporting the difference in response patterns of these neurones. Furthermore, one-tailed Wilcoxon-Mann-Whitney test revealed a statistically significant difference in time T between glucose-excited (without reversal) and glucose-inhibited ARC neurones ($P < 0.05$) and in τ between glucose-excited (without reversal) and glucose-inhibited ARC neurones ($P < 0.05$), suggesting that glucose-excited neurones require a significantly shorter delay time (T) but longer change-over time (τ) than glucose-inhibited neurones.

In 24-hour fasted rats, the same investigation was applied although data from only two groups of neurones were compared statistically, i.e. GE w/R and GI. Due to an insufficient number of recordings in glucose-excited (without reversal) and glucose-rapidly adapting groups, no statistical test was performed on these two groups. Only the difference in activity of neurones at the start and at the end of glucose application, $\Delta\lambda$, was found to be significantly different between these two groups of neurones ($P < 0.01$), whereas the parameters T and τ did not exhibit statistically detectable differences. Similar to what was discussed in *ad libitum* fed rats, there was a statistically detectable difference in $\Delta\lambda$ between glucose-excited and glucose-inhibited ARC neurones when glucose was varied between 2.0 and 0.2 mM, supporting the difference in response patterns of these neurones.

In summary, (i) data on GE and NGS neurones supported the findings reported in Chapter 6 that neurones in 24-hour fasted rats were more active than in *ad libitum* fed rats; (ii) the half sigmoid time T was generally larger in neurones from 24-hour fasted rats than *ad libitum* fed rats, in particular in GE w/R from a change in glucose level from 0.2 to 0.5 mM and from 1.0 to 2.0 mM; (iii) there were statistically detectable differences with respect to all response parameters between GE w/o R and GI neurones in *ad libitum* fed rats; (iv) there were statistically detectable differences in $\Delta\lambda$ between GE w/R and GI neurones in *ad libitum* fed rats; and (v) there were statistically detectable differences as regards the activity change parameter $\Delta\lambda$ between GE w/R and GI neurones in 24-hour fasted rats.

It is important to note that with a very small sample size of data together with a use of a nonparametric statistical test in comparing two populations in this study, comparisons performed have less power and are less sensitive than the comparisons using a parametric test, such as the t-test. The lower power of the Wilcoxon Mann-Whitney test could cause a type II error in the statistics as the test can fail to detect a statistically difference when there is one. However, the Wilcoxon Mann-Whitney test is known as one of the most powerful tests in nonparametric tests, hence why it was applied in this study.

This chapter concludes with a tentative classification of response types. A firm confirmation of this classification awaits the collection of more recording from each of these types; this will allow more extensive statistical comparisons of response parameters. Furthermore, it is recommended that in future, whole-cell patch-clamp recordings are performed without any negative current injection, to avoid any bias in the observed numbers of action potentials.

The analysis performed in this chapter could be a good tool to study behaviours of POMC- and NPY-ARC glucose-sensing neurones provided that these two cell types, POMC and NPY, would be identified as the ARC glucose-sensing neurones.

MATLAB code for counting accumulative spikes of neurones

```
%load abf file to Matlab
sampling_interval = 0.0002;

d = abfload('G:\RPattaranit\Data from
   Axon\Ratchada\2007\October07\07o25023.abf','start',0,'stop','e');
d = single(d);
only_spikes = single([0,0]);
j = 1;
ans = size(d);
samples = ans(1,1);
for i = 1:samples
    d(i,2) = d(i,1);              %move original column 1 to column 2
    d(i,1) = i*sampling_interval; %insert 't' column
end
%end load abf file

%counting spikes
threshold = 20;
lower_threshold = -60;
count_spikes_by_time_flag = 0;
starting_point = 0;
current_injection_interval = 5;
ignore_counting_spikes_period = 2.00;

count_spikes_period = current_injection_interval -
ignore_counting_spikes_period;

enable_counting_spikes = 1;
spike_found_flag = 0;
spike_counter = 0;

for i = 1:samples
    if(d(i,2) <= lower_threshold)           % set global condition
        if(count_spikes_by_time_flag == 0)
            count_spikes_by_time_flag = 1;
            starting_point = i;
            enable_counting_spikes = 0;
        end
    end
    if(count_spikes_by_time_flag == 0)          % spike counting before
reaching the first lower threshold
        if(d(i,2) >= threshold)
            spike_found_flag = 1;
        else
            if(spike_found_flag == 1)
                spike_counter = spike_counter + 1;
                only_spikes(j,1) = d(i,1);
                only_spikes(j,2) = spike_counter;
                j = j + 1;
                spike_found_flag = 0;
            end
        end
```

```
    else                                        %% reaching the first
lower threshold
        if(i < (starting_point +
ignore_counting_spikes_period/sampling_interval))
            enable_counting_spikes = 0;
        else
            if(i >= (starting_point +
current_injection_interval/sampling_interval))
                enable_counting_spikes = 0;
                starting_point = i;
            else
                enable_counting_spikes = 1;
            end
        end

        if(enable_counting_spikes == 1)
            if(d(i,2) >= threshold)
                spike_found_flag = 1;
            else
                if(spike_found_flag == 1)
                    spike_counter = spike_counter + 1;
                    only_spikes(j,1) = d(i,1);
                    only_spikes(j,2) = spike_counter;
                    j = j + 1;
                    spike_found_flag = 0;
                end
            end
        end
    end
end
%end spike counting
```

Chapter 8

General discussion

One of the key aims of this study was to investigate the mechanisms by which ARC neurones detect, integrate and respond to changes in glucose levels, using an electrophysiological approach and to review mathematical models of energy homeostasis at a whole body level.

8.1 Mathematical models of energy homeostasis

Energy homeostasis requires the co-ordination of several metabolic fluxes at the systemic level among various organs in the periphery and the central nervous system. Among the hormonal factors regulating these fluxes, insulin occupies a central position due to its wide-ranging effects on plasma glucose levels, appetite, cell growth and internal energy stores (Brook, 2001). Hence, the insulin central loop could be considered as the fundamental "first-order" endocrine control with other factors, such as, glucagon and adipokines providing a "second-order" adjustment to the precise physiological circumstances (Schwartz *et al.*, 1987; Raju & Cryer, 2005).

The breakdown of the previously mentioned co-ordination of metabolic fluxes could ultimately lead to hyperglycaemia. Hence, clinical management of hyperglycaemia requires a thorough understanding of the interactions among the liver, pancreas, fat stores and plasma nutrient levels. An explicit representation of this complex dynamical system can aid the interpretation of diagnostic tests and help formulate therapeutic interventions. Numerous mathematical models relating to energy homeostasis are available. However, this makes it difficult for clinicians to choose the most suitable or appropriate model. Chapter 2 presents the most important models published to date, in a uniform format for ease of comparison. Plasma glucose and plasma insulin are at the heart of all these models and the models typically assume the form of a system of ordinary differential equations. Two main types of models discussed in this study are as follows; models which take place on a short time scale (minutes-to-hours) and models that describe a long time scale (days-to-years).

The survey starts with a short time scale with "glucocentric" models, which focus on plasma insulin and plasma glucose, and form the fundamental glycaemic homeostatic feedback loop. Only two state variables are needed for a model limited to this fundamental loop (Bolie, 1961). More advanced models can be viewed as variations of this simple two-state model.

Further models involved with time delay were studied. Because pancreatic β-cells and liver cells introduce such delays in their cellular responses to glucose and insulin, respectively, these delays can induce dynamical instability, i.e. oscillations in the plasma insulin and plasma glucose dynamics. The pancreatic β-cells introduce a time delay as the insulin secretion rate takes some time to adapt to the plasma glucose levels (Bennette, 2004; Li, 2007) and there is a delayed response in hepatic glucose production from glycogenolysis (Tolic *et al.*, 2000). Both of these delay models were extended using the delay-differential equations.

In addition, the simple two-state variable model mentioned above was then extended with additional state variables, which includes not only another important endocrine factor like glucagon, which is secreted in response to low glucose but also the remote compartments of insulin (Bergman *et al.*, 1981). The latter variable was added because the physiological response to insulin appears to lag behind the response expected on the basis of the insulin plasma level. Part of this lag could be explained from the distribution kinetics of insulin. This is a three-ordinary differential equation model which is known as the "standard minimal model" first proposed by Bergman *et al*. (1981).

Because the key aspect of energy homeostasis is the coordinated use of various metabolic fuels, the model was then extended to integrate with carbohydrate, fat and protein metabolism although the protein metabolism has received less attention. The glucose-fatty acid cycle is central to the interactions between carbohydrate and lipid metabolism (Randle *et al.*, 1963). Hence, a new variable which is non-esterified fatty acids (NEFAs) was added to extend the minimal model (Roy & Parker, 2006). A similar model to Roy & Parker's was proposed by Maas & Smith (2006) whose model explicitly represents internal reserves (glycogen and triacylglyceride (TAG) stores) as state variables (Maas, 2006; Mass, 2006).

Given that the processes underlying the development of obesity and diabetes take place on a longer time scale, various models were also studied that attempt to take this into account. The first model was extended from the basic glucocentric model in which the third variable, β-cell mass, was added (Topp *et al.*, 2000). Another model was also proposed by De Winter *et al*. (2006) in order to describe the deterioration of β-cell function corresponding to the remaining population of fully functional β-cell and insulin sensitivity (De Winter, 2006). De Winter *et al*.'s model is in the form of integro-differential equations. Maas & Smith (2006) further set the

adipocyte proliferation, an increase in the number of adipocytes in the body, to be another state variable. This model simulates the elevated lipidaemia and hyperinsulinaemia when the number of adipocytes in the body is low in comparison with the energy excess in the dietary intake. Furthermore, since co-ordination at the level of and between both periphery and CNS, is crucial for energy balance, Maas & Smith's model could be extended by adding plasma leptin as a state variable which is treated as the main adiposity signal driving the central response (Benoit *et al.*, 2004). The CNS was also added and it has a function to modulate food intake and energy expenditure.

These models mentioned above could be easily extended with more humoral factors in order to extend understanding of energy homeostasis at the body level. The model with 16 state variables was then proposed. This model was done by fitting together various models proposed in the literature. However, more humoral factors can also be added to extend this model. As it was previously mentioned that since the energy balance is controlled not only peripherally but also centrally, the model with the CNS involvement (e.g. Maas and Smith's model) would be appropriate for further extension. The hypothalamus plays a key role in controlling energy balance, particularly in the area called the ARC which contains neurones that are sensitive to the plasma levels of insulin, glucose (the focus of this thesis), ghrelin and leptin. These neurones modulate food intake as well as thyroid hormone axis (Spanswick *et al.*, 1997; Kim *et al.*, 2000; Barsh & Schwartz, 2002; Nowak *et al.*, 2002; Dobbins *et al.*, 2003; van den Top *et al.*, 2004). It is therefore appropriate to add the ARC into the energy homeostasis model in order to make it more physiologically realistic. The ARC glucose-sensing neurones study in Chapter 6 also suggests the importance of these neurones in energy homeostasis and that they are sensitive to a small variation of glucose levels. In addition, it has been reported that some glucose-sensing neurones contain NPY (Muroya *et al.*, 1999), whereas some glucose-sensing neurones are POMC neurones (Ibrahim *et al.*, 2003). This further confirms an involvement of these neurones in controlling energy balance. Hence, it is crucial to take these factors into consideration in the future modelling of energy homeostasis.

Overall, to describe dynamics on the life-history time scale, one starts with balance equations, augmented with a minimum of additional physiological state variables needed to describe the regulation of the flux terms in response to e.g.

dietary challenges. What is missing is a systematic way of deriving the dynamics of these additional state variables at the slow time scale from the underlying detailed dynamics at the fast physiological time scales.

Furthermore, because the integration between the CNS and the periphery networks via hormones and nutrients including glucose is required to maintain energy homeostasis and because glucose has shown to be the heart of all mathematical models of energy homeostasis, glucose-sensing in the CNS at the level of hypothalamic ARC was then focussed on in this project.

8.2 Effects of food withdrawal (fasting) on electrophysiological properties of rat ARC neurones

The main aim of this project is to investigate how the ARC neurones are able to detect and respond to changes in extracellular glucose levels and how such mechanisms may adapt depending on the energy status of the organism. In relation to this latter point, the effect of food withdrawal on glucose sensing was the key focus area. Fasting animals involves housing the organism on raised metal grids to prevent consumption of waste products. Thus two variables come into play: the effects of fasting and the effects of changes in housing and the stress or change in behaviour that this may lead to. To address these issues, an initial study was undertaken to investigate the electrophysiological properties of ARC neurones in normal fed rats and to compare these properties with fasted animals. A control group of fed animals housed in the same way as fasted animals was also included. Hence, the general membrane properties of ARC neurones, including subthreshold active conductances expressed by ARC neurones were examined in three different groups of rats: 1. rats fed *ad libitum*; 2. rats fed *ad libitum* housed in cages with a raised metal grid (control group) and 3. rats fasted for 24 hours housed in cages with a raised metal grid.

In this study ARC neurones were classified into 8 subgroups (clusters 1 to 8) based upon the differential expression of subthreshold conductances. This work builds on previous work aimed at building a framework of the functional organisation of the ARC (van den Top, 2002; Saker, 2009; Virdee, 2009).

The major findings of this study revealed statistically significant differences in some active and passive membrane properties including the expression of subthreshold active conductances between fasted and fed groups. The transient

outward rectifier in cluster 2 neurones was enhanced in 24-hour fasted rats compared to rats fed *ad libitum*. As the A-current in these neurones is thought to play a key role in setting the frequency of burst firing, the increased magnitude of the conductance in fasted rats suggests in a "hunger" state the dynamics of the burst firing may be subject to modulation (van den Top *et al*., 2004).

Cluster 5 neurones displayed the most significant differences in membrane properties of all clusters when fasted and fed groups were compared. These included a significant reduction in action potential duration in cluster 5 and 6 neurones recorded from fasted rats compared to rats fed *ad libitum*. The magnitude of I_h in cluster 5 neurones was subject to modulation, being enhanced in terms of both its contribution to reducing input resistance upon activation and the amplitude of the depolarising 'sag' that characterises this conductance, in neurones from fasted rats compared to fed. However, once again, this enhancement of I_h in these neurones was also to some extent mirrored in the control group for fasted rats, suggesting some changes induced reflected a response to the changes in housing conditions rather than entirely due to food withdrawal.

Cluster 7 neurones were characterised by a significantly greater membrane time-constant in rats fed *ad libitum* than both fasted and its corresponding fed control group. As the time-constant indicates the surface-area of the neurone, this decrease in time constant in fasted and its control group suggests a possible functional, anatomical reorganisation of these neurones. However, once again the change in housing appears to be the main factor influencing this level of plasticity in ARC neurones.

When the whole population of ARC neurones were compared between the three groups, independent of clusters, the resting membrane potentials in neurones were relatively similar. However, neurones recorded from rats fed *ad libitum* had a higher input resistance and spontaneous firing frequency than neurones recorded from fasted animals and their control group. In addition, the number of active neurones in both groups of rats housed on the metal grid was comparable and higher than the number of active neurones in normally housed rats fed *ad libitum*. This data indicated that the housing of animals on a raised metal grid, either with or without fasting was a significant factor contributing to the changes in activity in ARC neurones. Evidence for rat housing inducing stress and affecting the level of hormones, body weight and muscle performance has been previously

reported (Brown & Grunberg, 1995; Spangenberg *et al.*, 2005). Furthermore, rearing in individual housing of rodents causes changes in their behaviour, neurochemistry and anatomy compared to rearing and housing in groups (Globus *et al.*, 1973; Sahakian *et al.*, 1975; Thoa *et al.*, 1977; Weinstock *et al.*, 1978; Garzon *et al.*, 1979; Jorgensen & Bock, 1979; Gentsch *et al.*, 1981). Fasting alone causes stress and affects rat haematology and hormone release leading to changes in cholesterol, triglycerides, urea nitrogen and calcium levels in addition to decreases in body weight and insulin secretion (Grey *et al.*, 1970; Maejima & Nagase, 1991; Matsuzawa & Sakazume, 1994; Young & Landsberg, 1997). Future experiments need to be better designed and should take into account the "housing effect." Studies should include housing of animals in groups on raised metal grids for longer periods of time to allow them to acclimatise. Wherever possible, animals should be housed in groups to prevent "stress" associated with being housed in isolation.

In conclusion, the present study revealed changes in electrophysiological properties of ARC neurones between three different groups of rats: fed, fasted and a control group that were fed but housed in a manner similar to fasted rats. However, some of these changes in properties appear to reflect changes in housing conditions rather than as a result of purely negative energy state induced by fasting. Further work is required to address this issue.

8.3 Effects of intracellular ATP on rat ARC glucose-sensing neurones

To achieve the main aim of this project, investigating mechanisms of ARC glucose-sensing neurones in fed and fasted state, two important variables needed to be clarified. Firstly, what levels of extracellular glucose should be utilised in aCSF to mimic physiological levels in the brain. Secondly, although some neurones could sense glucose independently of glucose metabolism i.e. via the Na^+-coupled glucose transporters (SGLT), many glucose-sensing neurones rely on glycolytic activity and couple glucose metabolism directly to excitability through ATP-dependent mechanisms, what levels of ATP should be utilised for whole-cell recording (Dhar-Chowdhury *et al.*, 2007). The latter one is discussed here.

The role of ATP in regulating ion channel and pump activity, and thereby contributing to regulation of electrical activity is extremely well documented. However, exactly what the physiological levels are and if and how they change

depending on the status of the cell is less well understood. Previous work on hypothalamic neurones suggested GE neurones operate through closure of K_{ATP} channels but do so independent of cytosolic ATP concentration (Ainscow *et al.*, 2002). In addition, ATP concentrations in the rat brain have been shown to change both seasonally and during stress (Rozhanets *et al.*, 1974), and the effects of fasting, in itself a stressful phenomena, on the functional operation of these neurones, circuits and ATP levels are unknown. Hence, the role of intracellular ATP levels on the electrophysiological integrity of ARC glucose-sensing neurones and their ability to sense changes in extracellular glucose was investigated to determine the levels of ATP required to maintain resting membrane potential of glucose-sensing neurones in fed and fasted rats and to determine the effects of intracellular ATP on the ability of glucose-sensing neurones to detect changes in extracellular glucose concentrations. To do this, extracellular glucose levels were manipulated from 2.0 to 0.0 mM whilst intracellular ATP was manipulated by changing intracellular ATP levels in the pipette solution (0.0, 1.0, 2.0, 5.0 and 10.0 mM) using whole-cell patch-clamp recording techniques.

In fed rats, a concentration of intracellular ATP required to maintain cell membrane properties and functional capability for glucose-sensing lay between 4.0 to 5.0 mM. The corresponding concentration of intracellular ATP required to maintain cell membrane properties and functional capability for glucose sensing in 24-hour fasted rats lay between 1.0 to 2.0 mM. Taken together, two key findings are highlighted here. Firstly, cytosolic ATP levels are important for glucose-sensing in ARC neurones, thus our findings are at odds with those reported by Ainscow and colleagues (Ainscow *et al.*, 2002). The second important finding related to the differences in ATP levels required to maintain electrophysiological and glucose-sensing integrity with neurones recorded in fasted rats being characterised by either lower levels of intracellular ATP, changes in sensitivity to ATP or a combination of both compared to their fed, age-matched counterparts. Although the numbers of neurones included in this study were in some instances low, work from other colleagues in the lab (data not submitted as part of the thesis) have subsequently confirmed this to be the case and the levels of ATP needed to maintain glucose sensing cell function amount to around 1.0 mM for fasted rats and 4.0 mM for fed rats (Spanswick & van den Top, unpublished data).

The mechanism by which this apparent change in sensitivity to ATP is brought about in these neurones requires further investigation. Possible mechanisms and future experiments should address whether intracellular ATP levels are subject to a decrease in fasted rats, as has been suggested from models of stress where brain ATP levels decrease (Rozhanets *et al.*, 1974), a notion supported by data shown in Chapter 4 where stress may have been a factor involved in electrophysiological effects after fasting. Other factors may be changes in sensitivity of ion channels to ATP or changes in energy status may in themselves lead to changes in the sensitivity of the glucose-sensing machinery. Further work is required to clarify this issue.

Over the course of this aspect of the study, three types of glucose-sensing neurone were identified based upon their responsiveness to a reduction in extracellular glucose from 2.0 to 0.0 mM and 0.0 to 2.0 mM. They are GE, GI and GRA neurones. For GRA neurones, to author's knowledge, this is the first report of such a response.

GE neurones were the most common glucose-sensing neurones encountered in this study and it was found that changes in glucose levels in ARC GE neurones is mediated through the activity of ATP-sensitive potassium channels, which is in broad agreement with numerous previous studies showing such a phenomena in ARC, VMN and brainstem neurones (e.g. Ashford *et al.*, 1990; Rowe *et al.*, 1996; Spanswick *et al.*, 1997; Lee *et al.*, 1999; Spanswick *et al.*, 2000; Miki *et al.*, 2001; Balfour *et al*., 2006).

GI neurones were also observed in ARC neurones in this study and have been suggested to be orexigenic NPY/AgRP neurones (Muroya *et al.*, 1999), presumably functionally inhibited following a meal due to the transient increase in glucose reflecting food consumption.

Finally, the presence of GRA neurones was revealed for the first time in the ARC. These neurones share distinct similarities to adapting sugar-sensing neurones described in the orexigenic orexin-containing neurones of the lateral hypothalamus (LH; Williams *et al*., 2008). These adapting neurones, together with GE and GI, have been suggested to function in a combined transient and sustained glucosensing manner allowing the glucose-sensing neurones to maintain sensitivity to small fluctuations in glucose levels whilst simultaneously encoding a larger range of baseline glucose concentrations (Williams *et al*., 2008). Further work is required to determine the mechanism underlying these GRA neurones and their ability to sense

changes in glucose, to determine their chemical phenotype and where they project before the functional significance of these neurones can be realised.

In summary, data presented here suggests a key role for cytosolic ATP in glucose sensing in ARC neurones and that either the levels or sensitivity to ATP are key factors contributing to the maintenance of electrical activity in these neurones. Levels of or sensitivity to ATP is subject to modulation depending on the energy status of the organism which the data obtained in this study has driven the protocol described in Chapter 6 where 1.0 mM and 5.0 mM intracellular ATP were used to explore glucose-sensing mechanism in ARC neurones from fasted and fed rats, respectively. Finally, both GE and GI neurones were identified in the ARC and for the first time, neurones that detect and adapt to changes in extracellular glucose at the level of the ARC were reported.

8.4 ARC glucose-sensing neurones *in vitro* in fed and 24-hour fasted rats

This project aims to utilise appropriate intracellular ATP levels in the electrode solution of 5.0 and 1.0 in *ad libitum* fed and 24-hour fasted rats, respectively, determined earlier, to investigate the effects of physiological shifts in extracellular glucose over a range which varied from 2.0 to 0.2, 0.5, 1.0, 2.0 and 5.0 mM, the latter a hypothetical level that may be achieved following food intake. Additionally, because the plasma glucose levels in fasted rats is decreased compared to a normal feeding regime (Faggioni *et al.*, 2000; de Vries *et al.*, 2003), glucose-sensing neurones were investigated in 24-hour fasted rats by preparing and maintaining hypothalamic slices in 0.2 mM glucose.

The principal findings of this study were that three types of glucose-sensing neurone were identified: neurones inhibited by a reduction in extracellular glucose within a physiological range and excited by increases in glucose, thus termed glucose-excited (GE) neurones; neurones excited by a reduction and inhibited following elevation of extracellular glucose, thus termed glucose-inhibited (GI) neurones; finally neurones that showed an adaptive response to a change in extracellular glucose characterised by a transient change in membrane potential and firing frequency before adaptation to the new level of extracellular glucose concentration. These latter neurones were therefore termed glucose-rapidly adapting (GRA) neurones, which are reported here in the ARC for the first time.

From normal animals, fed *ad libitum*, recordings in hypothalamic slice preparations revealed around 56% of neurones were GE with a threshold concentration for detection of extracellular glucose around 1.0 mM. In rats that had been subject to a 24-hour fast, this sensitivity to extracellular glucose was increased with threshold concentrations for detection of glucose between 0.2 to 0.5 mM, suggesting increased sensitivity to extracellular glucose and decreased threshold for detection in GE neurones from fasted rats. This change in sensitivity appears to be directly related to the energy status of the organism and relatively independent of the intracellular ATP concentration. These data therefore have several important implications. Firstly, GE neurones in the ARC are "true" glucose-sensing neurones capable of detecting physiological changes in extracellular glucose. Thus this data is in agreement with previous studies showing GE neurones in the ARC (Song *et al.*, 2001; Wang *et al.*, 2004) that have been suggested to be anorexigenic POMC neurones (Ibrahim *et al.*, 2003). Furthermore, changing the energy status of the organism appeared to change the sensitivity of glucose-sensing neurones to extracellular glucose, fasting effectively leading to an enhanced sensitivity. Fasting rats for 24 hours reduces plasma glucose levels in rat (De Boer *et al.*, 1989; Faggioni *et al.*, 2000; de Vries *et al.*, 2003; Palou *et al.*, 2009), and plasma glucose levels ranging between 2-18 mM, correspond with brain (CSF) glucose levels between 0.2 and 4.5 mM (de Vries *et al.*, 2003), in VMH amounting to 1.5 mM in fed rats, reduced to 0.7 mM in overnight fasted rats (de Vries *et al.*, 2003; Mayer *et al.*, 2006). Thus, the range of glucose levels tested here in fed and fasted rats appears to be within the physiological range, given the available data. Taken together, these data strongly suggest a shift in the sensitivity of the glucose-sensing machinery in these GE neurones. The functional significance of this is unclear but may reflect a number of functional adaptations to energy status. For example, the relative insensitivity to further reductions in glucose in the fasted state could represent an adaptation to the lack of food and glucose availability, thus providing a potential "safety" mechanism. The increase in sensitivity to elevations in extracellular glucose may be multi-functional in terms of preparing the brain glucose-sensing machinery to orchestrate appropriate behaviours to maximise utilisation and/or storage of glucose when it becomes available, the increased sensitivity representing an adaptation to the energy status of the organism. Further work is required to address these issues.

Whilst this is the first report of such an adaptation in GE neurones, a similar change in sensitivity has recently been reported for orexigenic NPY GI neurones in the ARC where fasting was shown to enhance the response of ARC NPY-GI neurons to decreased extracellular glucose. The mechanism underlying this adaptation was suggested to be leptin and AMPkinase-dependent (Murphy *et al*., 2009). Whether such a leptin and AMPkinase-dependent mechanism operates in the GE neurones described here remains to be clarified.

GI neurones in this study were characterised by an increase in excitability upon a reduction in extracellular glucose and a decrease in excitability with an increase in glucose. GI neurones in fed rats were generally associated with lower spontaneous firing rates and more hyperpolarised resting membrane potentials compared to GI neurones from fasted rats suggesting these neurones were indicating a "hunger" state, if as previous reports suggest, subpopulations of orexigenic NPY neurones are also GI neurones. Data suggests GI neurones are sensitive to reduced extracellular glucose and have a threshold for response or detection to increased glucose of around 1.0 mM in fasted and fed states. A second population of ARC GI neurone in slices from fasted rats were also investigated where they were only subject to increases in extracellular glucose from a fasted state mimicked with a control glucose bathing medium concentration of 0.2 mM. In these neurones, increasing extracellular glucose from 0.2 to 0.5 mM glucose induced a clear decrease in firing rate and membrane hyperpolarisation suggesting a high degree of sensitivity to extracellular glucose. Subsequent increases in extracellular glucose were without further significant effect. These latter experiments were undertaken in higher intracellular ATP concentrations, thus a higher reliance of glucose-sensing GI neurones for intracellular ATP, than GE neurones, may explain these data. Alternatively the basal level of extracellular glucose itself may be the key driver dictating sensitivity of GI neurones to changes in extracellular glucose levels. Nevertheless, the sensitivity of GI neurones to changes in extracellular glucose appears to depend on separate mechanisms and intracellular and extracellular factors than their counterparts, the GE neurones. Functionally this may relate to different roles whereby GI neurones couple and relate more to different functions, for example feeding, than GE neurones. Further work is required, in particular on GI neurones, to address these issues.

The proportions of ARC GE versus GI neurones detected in fed versus fasted tissues varied considerably with around 56% of the population recorded in tissue from fed rats being identified as GE and only around 10% being GI. In the fasted scenario, this changed with around double the number of GI neurones detected (18%) compared to fed rats and the GE population reduced to around 37%. In the study of neurones maintained in 0.2 mM glucose and only subject to increases in extracellular glucose, this balance shifted further to 25% of neurones identified as GE and the same number, 25% of GI neurones. Whilst the numbers for all of these populations, particularly fasted, were not as high as would be ideally required, it is interesting to speculate that other levels of plasticity operate within the ARC glucose-sensing network. Thus it is tempting to speculate that glucose-sensing neurones can be modulated and in effect switched "on" or "off" depending on energy status. Thus, for example, in a fasted or hunger state, GI neurones are activated or recruited, reflecting low levels of extracellular glucose and negative energy balance, whereas GE neurones, required for co-ordinated behavioural responses to conserve and manage glucose fuel supplies, are "switched off" during this period of low glucose availability. Subsequently, upon food intake and increased glucose availability, GI neurones are switched off as the hunger and fasted state is alleviated and energy shortages restored. Conversely, upon food intake, GE neurones, required to co-ordinate behaviours to manage glucose stores and availability for the CNS, organs and tissues of the body, are recruited or "switched on." Further work is required to address these issues which at this point can only be speculation.

A second interesting observation made over the course of this study and worthy of note and speculation relates to NPY/AgRP neurones. As already pointed out above, ARC NPY neurones, at least a subpopulation of them, have been reported to be GI neurones (Muroya *et al*., 1999; Murphy *et al*., 2009; Fioramonti *et al.*, 2007). A subpopulation of ARC NPY/AgRP neurones in rat have also been previously described and characterised by their electrophysiological properties and responsiveness to orexigenic and anorexigenic signals (van den Top *et al*., 2004) and classified as cluster 2 neurones in the present and previous theses (van den Top, 2002; Lyons, 2004; Saker, 2009; Virdee, 2009). In the present work, the effects of physiological changes in extracellular glucose were investigated in cluster 2 neurones, two of which were recorded in slices prepared from fed rats and one from a fasted rat. Both cluster 2 NPY/AgRP neurones recorded in fed rats were classified

as GE neurones as lowering of extracellular glucose from 2.0 to 0.2 mM yielded membrane hyperpolarisation associated with a reduction in neuronal input resistance and an apparent inhibition or suppression of the A-like transient outward rectifier. Thus these characteristic neurones showed features consistent with being GE neurones capable of detecting physiological changes in glucose. However, the cluster 2 NPY/AgRP neurone recorded in tissue from a fasted rat showed characteristic features consistent with being a GI neurone. Taken together, these data raise an interesting possibility: specifically, glucose-sensing orexigenic NPY/AgRP neurones, or at least a subpopulation of them, can switch glucose-sensing function depending on energy status. Thus, in a fed state, orexigenic NPY/AgRP neurones could act as GE neurones, acting to monitor or signal moment by moment fluctuations and absolute glucose levels available. In a fasted state or state of negative energy balance, orexigenic NPY/AgRP neurones are active and switch to become GI neurones, whereby food intake and rapid transient elevations in glucose levels indicate restoration of energy balance. Current thinking on glucose-sensing is such that GI and GE neurones are considered independent components of function-specific circuits. However, data here could begin to challenge the conventional wisdom and raises the possibility of yet another level of plasticity associated with the glucose-sensing networks. Given the low n values with this aspect of the study, this remains merely speculation but worthy of further study.

GE neurones have been studied in great detail in many studies in the hypothalamus and brainstem. GE neurones were characterised by mechanisms consistent with opening of ATP-sensitive potassium channels in response to reduced extracellular glucose and closing of these channels in response to increases in extracellular glucose. The data were therefore in broad agreement with numerous previous studies showing such a phenomena in the hypothalamus and brainstem neurones (e.g. Ashford *et al.*, 1990; Ibrahim *et al.*, 2003; Rowe *et al.*, 1996; Spanswick *et al.*, 1997; Lee *et al.*, 1999; Spanswick *et al.*, 2000; Song *et al.*, 2001; Wang *et al.*, 2004; Song & Routh, 2005; Miki *et al.*, 2001; Balfour *et al.*, 2006; van den Top *et al.*, 2007). ATP-sensitive potassium channels have been shown to be pivotal for glucose-sensing in the CNS by the use of knock-out studies and pharmacological approaches (Ashford *et al.*, 1990; Rowe *et al.*, 1996; Spanswick *et al.*, 1997; Lee *et al.*, 1999; Spanswick *et al.*, 2000; Miki *et al.*, 2001) and in GE neurones are proposed to use functional K_{ATP} channels to sense glucose in much

the same way as the pancreatic β-cell (Ashford *et al.*, 1990; Yang *et al.*, 1999; van den Top *et al.*, 2007). The mechanism underlying glucose-mediated effects in the present study was further investigated here and interestingly, in addition to the ATP-sensitive potassium channel-dependent mechanism described here and confirmed in studies on tissue from fasted rats, a second putative mechanism materialised. Thus in addition to an action via ATP-sensitive potassium channels, a mechanism involving opening of chloride channels or a mechanism involving a combination between potassium channels and electrogenic ion pumps may be important for glucose sensing in GE neurones. Further work is required to clarify the ionic nature and properties of this putative glucose-sensing mechanism.

The mechanisms by which GI neurones sense glucose has been less clear for some time. GI neurones in ARC neurones from fed rats generally had higher input resistances, lower firing rates and more negative resting membrane potentials than their counterparts from fasted rats in 2.0 mM glucose, suggesting they sit at these resting membrane potentials due to a closure of one or more resting conductances. Reducing extracellular glucose, from 2.0 to 0.2 mM in these neurones from fed and fasted animals induced an increase in firing rate and membrane depolarisation, associated with only minor changes in input resistance. However, in neurones from fasted animals, maintained in 0.2 mM glucose and subject to increases in extracellular glucose, clear decreases in firing rate associated with significant membrane hyperpolarisation and progressive decrease in input resistance were observed. These data therefore suggest that GI neurones are more responsive and better activated in response to increases in extracellular glucose, as may be expected following food intake. This is further supported by the fact that an identified cluster 2 NPY/AgRP neurone was included in this group. The reversal potential associated with these responses was approximately -60 mV suggesting activation of one or more chloride conductances underlies this response. Thus, data described here support previous data suggesting activation of a chloride-dependent mechanism underlies glucose-induced inhibition of GI neurones (Song *et al.*, 2001; Routh, 2002; Fioramonti *et al.*, 2007).

The final subtype of glucose-sensing neurone described here were the GRA neurones which responded to a change in extracellular glucose with an initial inhibition or membrane hyperpolarisation, a response that was transient and that subsequently appeared to adapt. Only 4 GRA neurones were recorded and suggested

two types of GRA neurone may be present in the ARC, those that transiently respond to decreases in extracellular glucose and those that transiently respond to increases in extracellular glucose. Given that these GRA neurones are rare in the ARC, further work is required to clarify their chemical phenotype, their function in glucose-sensing and whether they are true subtypes or the same subtype that modifies their glucose responsiveness depending on glucose and energy status. As already indicated, this is the first description of these neurones in the ARC. However, they do share distinct similarities to adapting sugar-sensing orexin-containing neurones of the LH (Williams *et al*., 2008). In the LH initial transient inhibition is thought to involve activation of a leak potassium conductance that subsequently adapts (Williams *et al*., 2008). These adapting neurones have been suggested to function in a combined transient and sustained glucosensing manner, along with GE and GI neurones, allowing glucose-sensing neurones to maintain sensitivity to small fluctuations in glucose levels while simultaneously encoding a larger range of baseline glucose concentrations (Williams *et al*., 2008). The fact that glucose-sensing neurones in the ARC share features remarkably similar to "classic sensory neurones," that encode both static and dynamic responses to changes in the environment through tonic and rapidly adapting receptor-dependent mechanisms, is difficult to ignore. Thus glucose-sensing neurones in the ARC may operate through function-specific mechanisms to signal not only the overall change in glucose levels at the level of the plasma and CSF but also inform the brain of the rate of change of glucose levels. Further work is required to determine the mechanisms underlying these transient responses, to determine their ability to sense changes in glucose, to determine their chemical phenotype and where they project before the functional significance of these neurones can be realised.

Furthermore, throughout the present studies, both changes in spontaneous AMPA receptor-mediated excitatory postsynaptic potentials (EPSPs) and GABA-mediated inhibitory postsynaptic potentials (IPSPs) were also detected in some neurones following changes in extracellular glucose concentration (e.g. Figure 5.6). This data indicated indirect effects in response to changes in glucose levels through modulation of presynaptic neurones, suggesting a network effect. However, the details of this synaptic connectivity were beyond the scope of the present study which focussed on direct postsynaptic effects on glucose-sensing neurones. Further work is required to recognise the component parts of these

glucose-sensing neural networks which most likely involve aspects of the lateral hypothalamus, paraventricular nucleus, ventromedial nucleus as well as the ARC.

Further analysis of the responses of these glucose-sensing neurones was performed with a mathematical approach and is discussed below.

8.5 Analysis of response dynamics in ARC glucose-sensing neurones

Analysis of the responses observed in ARC neurones in response to changes in extracellular glucose concentration (2.0 - 0.2 - 0.5 - 1.0 - 2.0 - 5.0 mM) was further investigated in both fed and 24-hour fasted rats using a mathematical approach. An empirical sigmoid response function was assumed to describe the time course of the transition in neuronal activity and the integral of this function was fitted to cumulative action potential numbers to characterise the response dynamics. Four parameters (λ_1, λ_2, T and τ) were estimated for each transition, employing the least-squares criterion. The parameter λ_1 is the activity prior to a change in extracellular glucose concentration (action potentials/second, (Hz)); λ_2 is the activity at the end of each change in extracellular glucose concentration (action potentials/second, (Hz)); T is the period of time in which the neurone reaches the half sigmoid, following a change in glucose level (seconds); and τ is the duration of the transition (seconds). These parameters were statistically compared in both *ad libitum* fed and 24-hour fasted rats in order to characterise the behaviour of each ARC neurone in more detail.

The responses of ARC neurones to changes in extracellular glucose concentrations (2.0 - 0.2 – 0.5 – 1.0 – 2.0 – 5.0 mM) in the present study were distinguished into five different groups, based on the change in firing frequency of neurones between 2.0 and 0.2 mM glucose treatment. The five groups are as follows: inhibition without reversal (glucose-excited ARC neurones, GE w/o R), inhibition with reversal (glucose-excited ARC neurones, GE w/R), excitation (glucose-inhibited ARC neurones, GI), rapidly adapting (GRA) and non glucose-sensing neurones (neurones which did not respond to any changes in glucose level).

In the inhibition without reversal group (GE w/o R), the average activity (firing frequency) of neurones recorded in both *ad libitum* fed and 24-hour fasted rats decreased with changes in glucose levels. The time (T) from 2.0 to 0.2 mM glucose

in 24-hour fasted rats was longer than the time in fed rats, supporting the data discussed earlier showing the average run-down time of GE neurones to a change in glucose from 2.0 to 0.2 mM in fasted rats was larger than in fed rats. The duration of the transition (τ) in fed rats was large only following the transition from 2.0 to 0.2 mM extracellular glucose, whereas it was relatively small for the remainder of the glucose step changes.

In the group characterised by a reversible inhibition (GE w/R), the average activity of recorded neurones in both food regimes decreased as a result of a change in 2.0 to 0.2 mM glucose, subsequently reversed in 0.5 mM glucose and continued to increase activity for the rest of the experiment. The average half sigmoid time (*T*) for all applications of glucose in 24-hour fasted rats was much larger than *T* in fed rats following all step changes, in particular in a step change in glucose from 0.2 to 0.5 mM and from 1.0 to 2.0 mM where a statistically detectable difference in *T* was observed. This is entirely in line with the result shown experimentally that the average run-down time of GE neurones to a change in glucose from 2.0 to 0.2 mM in 24-hour fasted rats was larger than that observed in fed rats. Similar to the inhibition without reversal group, the duration of the transition (τ) in fed rats was the longest in the shift from 2.0 to 0.2 mM glucose and was relatively small for the rest of experiments. No other statistically detectable difference was observed in this group of neurones.

In GI neurones, the average activity increased in both groups of rats following a change in glucose from 2.0 to 0.2 mM, whereas it both increased and decreased in the rest of experiments for both feeding regimes. Interestingly, both λ_1 and λ_2, the activity prior to and at the end of a change in extracellular glucose of neurones recorded in 24-hour fasted rats were larger than the λ_1 and λ_2 in fed rats at all levels of extracellular glucose. This result supports experimental data showing that the neurones recorded in 24-hour fasted rats were more active than neurones recorded from fed rats. A change in glucose from 1.0 to 2.0 mM, revealed the average time delay (*T*) in 24-hour fasted rats to be longer than the delay time (*T*) in fed rats. These results support the experimental data showing that the average run-up time of GI neurones to a change in glucose from 2.0 to 0.2 mM in fasted rats was larger than in fed rats. Furthermore, the duration of the transition (τ) in neurones from rats exposed to either feeding regimes did not exhibit a consistent pattern.

No statistically detectable difference in parameters was observed in this group of neurones, suggesting no statistically significant difference in neuronal behaviour of glucose-inhibited neurones between two feeding regimes.

A biphasic response of neurones was observed in neurones recorded in fed rats. Exposure to 0.2 mM glucose induced hyperpolarisation followed by a reversal and depolarisation. The neuronal activity then continued to increase with increased glucose levels. The time (*T*) following a change in glucose from 2.0 to 0.2 mM was unusually long comparing to other experiments. The transition time (τ) of these neurones was quite small in all changes in glucose levels.

It should be noted that there was no particular pattern of the transition time (τ) in all recorded neurones in these groups, whereas the average time (*T*) of GE w/o R, GE w/R and GI neurones recorded in 24-hour fasted rats was larger than in fed rats with almost all step changes of glucose level. These results suggest that fasting is another key factor affecting the dynamic behaviour of ARC glucose-sensing neurones.

In the final group, non glucose-sensing neurones, no major change in neuronal activity was observed. However, both λ_1 and λ_2 of 24-hour fasted rats were greater than in fed rats in all glucose treatments, again supporting the experimental data showing that neurones recorded in 24-hour fasted rats were more active than those in fed rats. Regarding the time (*T*) and the transition time (τ), the results showed that this group of neurones either took a comparatively small time or a very long time for a negligible change in activity for both *T* and τ for both feeding regimes.

Each parameter at a step change from 2.0 to 0.2 mM glucose (a step change used to distinguish neurones on the basis of their response) within each feeding regime was compared in order to characterise the differences among all response patterns of neurones. In fed rats, a statistically detectable significance in $\lambda_2 - \lambda_1$ was observed between GE and GI neurones, confirming a difference in response patterns between these two groups. In addition, it was observed that GE neurones required statistically significantly shorter time (*T*) but longer transition time (τ) than GI neurones.

In 24 hours fasted rats, only $\lambda_2 - \lambda_1$ was observed to be significantly different between GE and GI neurones, confirming a difference in response patterns between these two groups of neurones.

A firm confirmation of this classification awaits the collection of more recordings from each of these types; this will allow more extensive statistical comparisons of response parameters to avoid any statistically error during testing. Furthermore, it is recommended that in future, whole-cell patch-clamp recordings are performed without any negative current injection, to avoid any bias in the observed numbers of action potentials.

Overall, the mathematical approach of this study has helped presenting the behaviour of neurones in response to changes in glucose levels with time including the time these neurones wait before changing its activity and the duration of the transition. This approach facilitates the prediction of neurones behaviour over a longer period of time. However, the results obtained showed that following a change in glucose level in each step, once the response reached the peak and stable state, the plot of neuronal behaviour exhibited a constant activity and did not change by time.

In conclusion, this project has extended our understanding of glucose-sensing neurones in the rat hypothalamic ARC using both a mathematical and a biological approach. The specific functional and chemical phenotype of each type of glucose-sensing neurones remains largely unknown. To date, there have been reports that ARC NPY neurones are GI neurones (Murayo *et al*., 1999), although the data described here suggest that this may depend on energy status. Whether ARC GE neurones are of the POMC phenotype is also controversial and requires further study (Ibrahim *et al.*, 2003; Routh *et al.*, 2004). Other neuronal populations and functional phenotypes exist in the ARC, in addition to NPY and POMC. Thus establishing the proportion of NPY and POMC glucose-sensing neurones, determining their physiological function and determining the as yet unidentified glucose-sensing neurones is a major goal for future work. Furthermore, it is unlikely that these glucose-sensing neurones are not also exposed to basal hormonal and nutrient signals of peripheral energy homeostasis (e.g. insulin, leptin and free fatty acids) *in vivo*. Hence, the study of the interaction of these hormonal and nutrient signals to glucose-sensing neurones is crucial. Recently, Cotero & Routh have shown the effects of insulin on both activity and the glucose sensitivity of GE neurones within the physiological range of extracellular glucose concentrations. They reported that

insulin blunts the response of VL-VMN GE neurones to decreased glucose, which is consistent with a role of insulin as a satiety factor (Cotero & Routh, 2009). The interaction between glucose and leptin in the CNS remains unclear. Finally, with some evidence showing that: (i) some GE neurones were found to sense glucose via a K_{ATP} channel-dependent mechanism (Ashcroft & Gribble, 1999; van den Top *et al.*, 2007); (ii) insulin and leptin inhibited GE neurones via activation of K_{ATP} channel (Spanswick *et al.*, 1997; Spanswick *et al.*, 2000) and (iii) K_{ATP} channels are expressed on functionally antagonistic neuronal populations in the ARC (i.e. orexigenic NPY/AgRP and anorexigenic POMC/CART; van den Top *et al.*, 2007), it is believed that the K_{ATP} channel could be a key link mediating interactions between leptin-, insulin- and glucose-sensing.

References

Aarsland A, Chinkes D & Wolfe RR. (1997). Hepatic and whole-body fat synthesis in humans during carbohydrate overfeeding. *Am J Clin Nutr* **65,** 1774-1782.

Abbott CR, Kennedy AR, Wren AM, Rossi M, Murphy KG, Seal LJ, Todd JF, Ghatei MA, Small CJ & Bloom SR. (2003). Identification of hypothalamic nuclei involved in the orexigenic effect of melanin-concentrating hormone. *Endocrinology* **144,** 3943-3949.

Adan RA, Cone RD, Burbach JP & Gispen WH. (1994). Differential effects of melanocortin peptides on neural melanocortin receptors. *Mol Pharmacol* **46,** 1182-1190.

Adan RA, Vanderschuren LJ & la Fleur SE. (2008). Anti-obesity drugs and neural circuits of feeding. *Trends Pharmacol Sci* **29,** 208-217.

Adrian TE, Allen JM, Bloom SR, Ghatei MA, Rossor MN, Roberts GW, Crow TJ, Tatemoto K & Polak JM. (1983). Neuropeptide Y distribution in human brain. *Nature* **306,** 584-586.

Adrian TE, Ferri GL, Bacarese-Hamilton AJ, Fuessl HS, Polak JM & Bloom SR. (1985). Human distribution and release of a putative new gut hormone, peptide YY. *Gastroenterology* **89,** 1070-1077.

Aguilar-Bryan L, Clement JPt, Gonzalez G, Kunjilwar K, Babenko A & Bryan J. (1998). Toward understanding the assembly and structure of KATP channels. *Physiol Rev* **78,** 227-245.

Ahima RS, Prabakaran D, Mantzoros C, Qu D, Lowell B, Maratos-Flier E & Flier JS. (1996). Role of leptin in the neuroendocrine response to fasting. *Nature* **382,** 250-252.

Ainscow EK, Mirshamsi S, Tang T, Ashford ML & Rutter GA. (2002). Dynamic imaging of free cytosolic ATP concentration during fuel sensing by rat hypothalamic neurones: evidence for ATP-independent control of ATP-sensitive K(+) channels. *J Physiol* **544,** 429-445.

Air EL, Strowski MZ, Benoit SC, Conarello SL, Salituro GM, Guan XM, Liu K, Woods SC & Zhang BB. (2002). Small molecule insulin mimetics reduce food intake and body weight and prevent development of obesity. *Nat Med* **8,** 179-183.

Akasu T, Shoji S & Hasuo H. (1993). Inward rectifier and low-threshold calcium currents contribute to the spontaneous firing mechanism in neurons of the rat suprachiasmatic nucleus. *Pflugers Arch* **425,** 109-116.

Albers HE & Ferris CF. (1984). Neuropeptide Y: role in light-dark cycle entrainment of hamster circadian rhythms. *Neurosci Lett* **50,** 163-168.

Allen YS, Bloom SR & Polak JM. (1986). The neuropeptide Y-immunoreactive neuronal system: discovery, anatomy and involvement in neurodegenerative disease. *Hum Neurobiol* **5,** 227-234.

Anand BK & Brobeck JR. (1951). Localization of a "feeding center" in the hypothalamus of the rat. *Proc Soc Exp Biol Med* **77,** 323-324.

Anand BK, Chhina GS, Sharma KN, Dua S & Singh B. (1964). Activity of Single Neurons in the Hypothalamic Feeding Centers: Effect of Glucose. *Am J Physiol* **207,** 1146-1154.

Andrew S & Ritter S. (2003). Localized glucoprivation of hindbrain but not hypothalamic sites stimulates CORT and glucagon secretion. *Appetite* **4,** 315.

Arase K, York DA, Shimizu H, Shargill N & Bray GA. (1988). Effects of corticotropin-releasing factor on food intake and brown adipose tissue thermogenesis in rats. *Am J Physiol* **255,** E255-259.

Arora S & Anubhuti. (2006). Role of neuropeptides in appetite regulation and obesity--a review. *Neuropeptides* **40,** 375-401.

Asakawa A, Inui A, Kaga T, Katsuura G, Fujimiya M, Fujino MA & Kasuga M. (2003). Antagonism of ghrelin receptor reduces food intake and body weight gain in mice. *Gut* **52,** 947-952.

Ashcroft FM & Gribble FM. (1999). ATP-sensitive K+ channels and insulin secretion: their role in health and disease. *Diabetologia* **42,** 903-919.

Ashford ML, Boden PR & Treherne JM. (1990). Glucose-induced excitation of hypothalamic neurones is mediated by ATP-sensitive K+ channels. *Pflugers Arch* **415,** 479-483.

Ashford ML, Boden PR & Treherne JM. (1990). Tolbutamide excites rat glucoreceptive ventromedial hypothalamic neurones by indirect inhibition of ATP-K+ channels. *Br J Pharmacol* **101,** 531-540.

Ashford ML, Sturgess NC, Trout NJ, Gardner NJ & Hales CN. (1988). Adenosine-5'-triphosphate-sensitive ion channels in neonatal rat cultured central neurones. *Pflugers Arch* **412,** 297-304.

Bagdade JD, Porte D, Jr. & Bierman EL. (1967). Diabetic lipemia. A form of acquired fat-induced lipemia. *N Engl J Med* **276,** 427-433.

Baker RA & Herkenham M. (1995). Arcuate nucleus neurons that project to the hypothalamic paraventricular nucleus: neuropeptidergic identity and consequences of adrenalectomy on mRNA levels in the rat. *J Comp Neurol* **358,** 518-530.

Balasubramaniam AA. (1997). Neuropeptide Y family of hormones: receptor subtypes and antagonists. *Peptides* **18,** 445-457.

Balfour RH, Hansen AM & Trapp S. (2006). Neuronal responses to transient hypoglycaemia in the dorsal vagal complex of the rat brainstem. *J Physiol* **570,** 469-484.

Bard JA, Walker MW, Branchek TA & Weinshank RL. (1995). Cloning and functional expression of a human Y4 subtype receptor for pancreatic polypeptide, neuropeptide Y, and peptide YY. *J Biol Chem* **270,** 26762-26765.

Barsh GS & Schwartz MW. (2002). Genetic approaches to studying energy balance: perception and integration. *Nat Rev Genet* **3,** 589-600.

Baskin DG, Wilcox BJ, Figlewicz DP & Dorsa DM. (1988). Insulin and insulin-like growth factors in the CNS. *Trends Neurosci* **11,** 107-111.

Bates SH & Myers MG. (2004). The role of leptin-->STAT3 signaling in neuroendocrine function: an integrative perspective. *J Mol Med* **82,** 12-20.

Batterham RL, Cowley MA, Small CJ, Herzog H, Cohen MA, Dakin CL, Wren AM, Brynes AE, Low MJ, Ghatei MA, Cone RD & Bloom SR. (2002). Gut hormone PYY(3-36) physiologically inhibits food intake. *Nature* **418,** 650-654.

Batterham RL, Heffron H, Kapoor S, Chivers JE, Chandarana K, Herzog H, Le Roux CW, Thomas EL, Bell JD & Withers DJ. (2006). Critical role for peptide YY in protein-mediated satiation and body-weight regulation. *Cell Metab* **4,** 223-233.

Beck B. (2006). Neuropeptide Y in normal eating and in genetic and dietary-induced obesity. *Philos Trans R Soc Lond B Biol Sci* **361,** 1159-1185.

Bell ME, Bhatnagar S, Akana SF, Choi S & Dallman MF. (2000). Disruption of arcuate/paraventricular nucleus connections changes body energy balance and response to acute stress. *J Neurosci* **20,** 6707-6713.

Bennette DLG, S.A. (2004). Global stability in a model of the glucose-insulin interaction with time delay. *Euro Jnl of Applied Mathematics* **15,** 203-221.

Benoit SC, Clegg DJ, Seeley RJ & Woods SC. (2004). Insulin and leptin as adiposity signals. *Recent Prog Horm Res* **59,** 267-285.

Bergman RN, Phillips LS & Cobelli C. (1981). Physiologic evaluation of factors controlling glucose tolerance in man: measurement of insulin sensitivity and beta-cell glucose sensitivity from the response to intravenous glucose. *J Clin Invest* **68,** 1456-1467.

Bernardis LL & Bellinger LL. (1996). The lateral hypothalamic area revisited: ingestive behavior. *Neurosci Biobehav Rev* **20,** 189-287.

Billington CJ, Briggs JE, Grace M & Levine AS. (1991). Effects of intracerebroventricular injection of neuropeptide Y on energy metabolism. *Am J Physiol* **260,** R321-327.

Bing C, Wang W, Pickavance L & Williams G. (1996). The central regulation of energy homeostasis: roles of neuropeptide Y and other brain peptides. *Biochem Soc Trans* **24,** 559-565.

Bittencourt JC, Presse F, Arias C, Peto C, Vaughan J, Nahon JL, Vale W & Sawchenko PE. (1992). The melanin-concentrating hormone system of the rat brain: an immuno- and hybridization histochemical characterization. *J Comp Neurol* **319,** 218-245.

Bjorbaek C, Uotani S, da Silva B & Flier JS. (1997). Divergent signaling capacities of the long and short isoforms of the leptin receptor. *J Biol Chem* **272,** 32686-32695.

Bloom FE, Rossier J, Battenberg EL, Bayon A, French E, Henriksen SJ, Siggins GR, Segal D, Browne R, Ling N & Guillemin R. (1978). beta-endorphin: cellular localization, electrophysiological and behavioral effects. *Adv Biochem Psychopharmacol* **18,** 89-109.

Boden G, Chen X, Kolaczynski JW & Polansky M. (1997). Effects of prolonged hyperinsulinemia on serum leptin in normal human subjects. *J Clin Invest* **100,** 1107-1113.

Bolie VW. (1961). Coefficients of normal blood glucose regulation. *J Appl Physiol* **16,** 783-788.

Bouskila Y & Dudek FE. (1995). A rapidly activating type of outward rectifier K+ current and A-current in rat suprachiasmatic nucleus neurones. *J Physiol* **488 (Pt 2),** 339-350.

Boutayeb A & Chetouani A. (2006). A critical review of mathematical models and data used in diabetology. *Biomed Eng Online* **5,** 43.

Brief DJ & Davis JD. (1984). Reduction of food intake and body weight by chronic intraventricular insulin infusion. *Brain Res Bull* **12,** 571-575.

Broadwell RD, Balin BJ, Salcman M & Kaplan RS. (1983). Brain-blood barrier? Yes and no. *Proc Natl Acad Sci U S A* **80,** 7352-7356.

Broberger C. (1999). Hypothalamic cocaine- and amphetamine-regulated transcript (CART) neurons: histochemical relationship to thyrotropin-releasing hormone, melanin-concentrating hormone, orexin/hypocretin and neuropeptide Y. *Brain Res* **848,** 101-113.

Broberger C, De Lecea L, Sutcliffe JG & Hokfelt T. (1998). Hypocretin/orexin- and melanin-concentrating hormone-expressing cells form distinct populations in the rodent lateral hypothalamus: relationship to the neuropeptide Y and agouti gene-related protein systems. *J Comp Neurol* **402,** 460-474.

Broberger C, Johansen J, Johansson C, Schalling M & Hokfelt T. (1998). The neuropeptide Y/agouti gene-related protein (AGRP) brain circuitry in normal, anorectic, and monosodium glutamate-treated mice. *Proc Natl Acad Sci U S A* **95,** 15043-15048.

Broberger C, Landry M, Wong H, Walsh JN & Hokfelt T. (1997). Subtypes Y1 and Y2 of the neuropeptide Y receptor are respectively expressed in pro-opiomelanocortin- and neuropeptide-Y-containing neurons of the rat hypothalamic arcuate nucleus. *Neuroendocrinology* **66,** 393-408.

Brook CGD & Marshall NJ. (2001). *Essential endocrinology*. Blackwell Science, Oxford, UK.

Brown KJ & Grunberg NE. (1995). Effects of housing on male and female rats: crowding stresses male but calm females. *Physiol Behav* **58,** 1085-1089.

Brownlee M. (2001). Biochemistry and molecular cell biology of diabetic complications. *Nature* **414,** 813-820.

Bruning JC, Gautam D, Burks DJ, Gillette J, Schubert M, Orban PC, Klein R, Krone W, Muller-Wieland D & Kahn CR. (2000). Role of brain insulin receptor in control of body weight and reproduction. *Science* **289,** 2122-2125.

Burdakov D & Gonzalez JA. (2009). Physiological functions of glucose-inhibited neurones. *Acta Physiol (Oxf)* **195,** 71-78.

Burdakov D, Jensen LT, Alexopoulos H, Williams RH, Fearon IM, O'Kelly I, Gerasimenko O, Fugger L & Verkhratsky A. (2006). Tandem-pore K+ channels mediate inhibition of orexin neurons by glucose. *Neuron* **50,** 711-722.

Cabrele C & Beck-Sickinger AG. (2000). Molecular characterization of the ligand-receptor interaction of the neuropeptide Y family. *J Pept Sci* **6,** 97-122.

Caldwell PC, Hodgkin AL, Keynes RD & Shaw TL. (1960). The effects of injecting 'energy-rich' phosphate compounds on the active transport of ions in the giant axons of Loligo. *J Physiol* **152,** 561-590.

Campbell JD & Paul RJ. (1992). The nature of fuel provision for the Na+,K(+)-ATPase in porcine vascular smooth muscle. *J Physiol* **447,** 67-82.

Campfield LA, Smith FJ, Guisez Y, Devos R & Burn P. (1995). Recombinant mouse OB protein: evidence for a peripheral signal linking adiposity and central neural networks. *Science* **269,** 546-549.

Carey PE, Halliday J, Snaar JE, Morris PG & Taylor R. (2003). Direct assessment of muscle glycogen storage after mixed meals in normal and type 2 diabetic subjects. *Am J Physiol Endocrinol Metab* **284,** E688-694.

Challis BG, Pinnock SB, Coll AP, Carter RN, Dickson SL & O'Rahilly S. (2003). Acute effects of PYY3-36 on food intake and hypothalamic neuropeptide expression in the mouse. *Biochem Biophys Res Commun* **311,** 915-919.

Chemelli RM, Willie JT, Sinton CM, Elmquist JK, Scammell T, Lee C, Richardson JA, Williams SC, Xiong Y, Kisanuki Y, Fitch TE, Nakazato M, Hammer RE, Saper CB & Yanagisawa M. (1999). Narcolepsy in orexin knockout mice: molecular genetics of sleep regulation. *Cell* **98,** 437-451.

Chen G, Koyama, K., Yuan, X., Lee, Y., Zhou, Y.-T., O'Doherty, R., Newgard, C.B., & Unger, R.H. (1993). Disappearance of body fat in normal rats induced by adenovirus-mediated leptin gene therapy. *Proc Natl Acad Sci USA* **93,** 14795-14799.

Cheung CC, Clifton DK & Steiner RA. (1997). Proopiomelanocortin neurons are direct targets for leptin in the hypothalamus. *Endocrinology* **138,** 4489-4492.

Chronwall BM. (1985). Anatomy and physiology of the neuroendocrine arcuate nucleus. *Peptides* **6 Suppl 2,** 1-11.

Cone RD. (1999). The Central Melanocortin System and Energy Homeostasis. *Trends Endocrinol Metab* **10,** 211-216.

Cone RD. (2005). Anatomy and regulation of the central melanocortin system. *Nat Neurosci* **8,** 571-578.

Cone RD, Cowley MA, Butler AA, Fan W, Marks DL & Low MJ. (2001). The arcuate nucleus as a conduit for diverse signals relevant to energy homeostasis. *Int J Obes Relat Metab Disord* **25 Suppl 5,** S63-67.

Connor JA & Stevens CF. (1971). Prediction of repetitive firing behaviour from voltage clamp data on an isolated neurone soma. *J Physiol* **213,** 31-53.

Connor JA & Stevens CF. (1971). Voltage clamp studies of a transient outward membrane current in gastropod neural somata. *J Physiol* **213,** 21-30.

Considine RV, Sinha MK, Heiman ML, Kriauciunas A, Stephens TW, Nyce MR, Ohannesian JP, Marco CC, McKee LJ, Bauer TL & et al. (1996). Serum immunoreactive-leptin concentrations in normal-weight and obese humans. *N Engl J Med* **334,** 292-295.

Constanti A & Galvan M. (1983). Fast inward-rectifying current accounts for anomalous rectification in olfactory cortex neurones. *J Physiol* **335,** 153-178.

Cota D, Proulx K, Smith KA, Kozma SC, Thomas G, Woods SC & Seeley RJ. (2006). Hypothalamic mTOR signaling regulates food intake. *Science* **312,** 927-930.

Cotero VE & Routh VH. (2009). Insulin blunts the response of glucose-excited neurons in the ventrolateral-ventromedial hypothalamic nucleus to decreased glucose. *Am J Physiol Endocrinol Metab* **296,** E1101-1109.

Cowley MA, Smart JL, Rubinstein M, Cerdan MG, Diano S, Horvath TL, Cone RD & Low MJ. (2001). Leptin activates anorexigenic POMC neurons through a neural network in the arcuate nucleus. *Nature* **411,** 480-484.

Cowley MA, Smith RG, Diano S, Tschop M, Pronchuk N, Grove KL, Strasburger CJ, Bidlingmaier M, Esterman M, Heiman ML, Garcia-Segura LM, Nillni EA, Mendez P, Low MJ, Sotonyi P, Friedman JM, Liu H, Pinto S, Colmers WF, Cone RD & Horvath TL. (2003). The distribution and mechanism of action of ghrelin in the CNS demonstrates a novel hypothalamic circuit regulating energy homeostasis. *Neuron* **37,** 649-661.

Dallaporta M, Perrin J & Orsini JC. (2000). Involvement of adenosine triphosphate-sensitive K+ channels in glucose-sensing in the rat solitary tract nucleus. *Neurosci Lett* **278,** 77-80.

Davidson MH, Hauptman J, DiGirolamo M, Foreyt JP, Halsted CH, Heber D, Heimburger DC, Lucas CP, Robbins DC, Chung J & Heymsfield SB. (1999). Weight control and risk factor reduction in obese subjects treated for 2 years with orlistat: a randomized controlled trial. *Jama* **281,** 235-242.

De Boer SF, Koopmans SJ, Slangen JL & Van der Gugten J. (1989). Effects of fasting on plasma catecholamine, corticosterone and glucose concentrations under basal and stress conditions in individual rats. *Physiol Behav* **45,** 989-994.

De Gaetano A & Arino O. (2000). Mathematical modelling of the intravenous glucose tolerance test. *J Math Biol* **40,** 136-168.

de Lecea L, Kilduff TS, Peyron C, Gao X, Foye PE, Danielson PE, Fukuhara C, Battenberg EL, Gautvik VT, Bartlett FS, 2nd, Frankel WN, van den Pol AN, Bloom FE, Gautvik KM & Sutcliffe JG. (1998). The hypocretins: hypothalamus-specific peptides with neuroexcitatory activity. *Proc Natl Acad Sci U S A* **95,** 322-327.

de Vries MG, Arseneau LM, Lawson ME & Beverly JL. (2003). Extracellular glucose in rat ventromedial hypothalamus during acute and recurrent hypoglycemia. *Diabetes* **52,** 2767-2773.

De Winter W, DeJongh, J., Post, T., Ploeger, B., Urquhart, R., Moules, I., Eckland, D. & Danhof, M. (2006). A mechanism-based disease progression model for comparison of long-term effects of prioglitazone, metformin and gliclazide on disease processes underlying type 2 diabetes mellitus. *J Pharmacokin Pharmacodyn* **33,** 313-343.

Degen L, Matzinger D, Drewe J & Beglinger C. (2001). The effect of cholecystokinin in controlling appetite and food intake in humans. *Peptides* **22,** 1265-1269.

DelParigi A, Tschop M, Heiman ML, Salbe AD, Vozarova B, Sell SM, Bunt JC & Tataranni PA. (2002). High circulating ghrelin: a potential cause for hyperphagia and obesity in prader-willi syndrome. *J Clin Endocrinol Metab* **87,** 5461-5464.

Dhar-Chowdhury P, Malester B, Rajacic P & Coetzee WA. (2007). The regulation of ion channels and transporters by glycolytically derived ATP. *Cell Mol Life Sci* **64,** 3069-3083.

Dobbins RL, Szczepaniak LS, Zhang W & McGarry JD. (2003). Chemical sympathectomy alters regulation of body weight during prolonged ICV leptin infusion. *Am J Physiol Endocrinol Metab* **284,** E778-787.

Douglass J, McKinzie AA & Couceyro P. (1995). PCR differential display identifies a rat brain mRNA that is transcriptionally regulated by cocaine and amphetamine. *J Neurosci* **15,** 2471-2481.

Dow J, Lindsay G & Morrison J. (1996). *Biochemistry: Molecules, Cells and the Body*. Prentice Hall.

Dryden S, Pickavance L, Frankish HM & Williams G. (1995). Increased neuropeptide Y secretion in the hypothalamic paraventricular nucleus of obese (fa/fa) Zucker rats. *Brain Res* **690,** 185-188.

Dube MG, Kalra SP & Kalra PS. (1999). Food intake elicited by central administration of orexins/hypocretins: identification of hypothalamic sites of action. *Brain Res* **842,** 473-477.

Dunn-Meynell AA, Routh VH, Kang L, Gaspers L & Levin BE. (2002). Glucokinase is the likely mediator of glucosensing in both glucose-excited and glucose-inhibited central neurons. *Diabetes* **51,** 2056-2065.

Elias CF, Lee C, Kelly J, Aschkenasi C, Ahima RS, Couceyro PR, Kuhar MJ, Saper CB & Elmquist JK. (1998). Leptin activates hypothalamic CART neurons projecting to the spinal cord. *Neuron* **21,** 1375-1385.

Elias CF, Saper CB, Maratos-Flier E, Tritos NA, Lee C, Kelly J, Tatro JB, Hoffman GE, Ollmann MM, Barsh GS, Sakurai T, Yanagisawa M & Elmquist JK. (1998). Chemically defined projections linking the mediobasal hypothalamus and the lateral hypothalamic area. *J Comp Neurol* **402,** 442-459.

Elmquist JK, Bjorbaek C, Ahima RS, Flier JS & Saper CB. (1998). Distributions of leptin receptor mRNA isoforms in the rat brain. *J Comp Neurol* **395,** 535-547.

Engelborghs K, Lemaire V, Belair J & Roose D. (2001). Numerical bifurcation analysis of delay differential equations arising from physiological modeling. *J Math Biol* **42,** 361-385.

English PJ, Ghatei MA, Malik IA, Bloom SR & Wilding JP. (2002). Food fails to suppress ghrelin levels in obese humans. *J Clin Endocrinol Metab* **87,** 2984.

Erecinska M & Dagani F. (1990). Relationships between the neuronal sodium/potassium pump and energy metabolism. Effects of K+, Na+, and adenosine triphosphate in isolated brain synaptosomes. *J Gen Physiol* **95,** 591-616.

Faggioni R, Moser A, Feingold KR & Grunfeld C. (2000). Reduced leptin levels in starvation increase susceptibility to endotoxic shock. *Am J Pathol* **156,** 1781-1787.

Fajans SS, Bell GI & Polonsky KS. (2001). Molecular mechanisms and clinical pathophysiology of maturity-onset diabetes of the young. *N Engl J Med* **345,** 971-980.

Fan W, Boston BA, Kesterson RA, Hruby VJ & Cone RD. (1997). Role of melanocortinergic neurons in feeding and the agouti obesity syndrome. *Nature* **385,** 165-168.

Faust IM, Johnson PR, Stern JS & Hirsch J. (1978). Diet-induced adipocyte number increase in adult rats: a new model of obesity. *Am J Physiol* **235,** E279-286.

Fereday A, Gibson NR, Cox M, Pacy PJ & Millward DJ. (1998). Variation in the apparent sensitivity of the insulin-mediated inhibition of proteolysis to amino acid supply determines the efficiency of protein utilization. *Clin Sci (Lond)* **95,** 725-733.

Ferreira M, Jr., Browning KN, Sahibzada N, Verbalis JG, Gillis RA & Travagli RA. (2001). Glucose effects on gastric motility and tone evoked from the rat dorsal vagal complex. *J Physiol* **536,** 141-152.

Fioramonti X, Contie S, Song Z, Routh VH, Lorsignol A & Penicaud L. (2007). Characterization of glucosensing neuron subpopulations in the arcuate nucleus: integration in neuropeptide Y and pro-opio melanocortin networks? *Diabetes* **56,** 1219-1227.

Fioramonti X, Lorsignol A, Taupignon A & Penicaud L. (2004). A new ATP-sensitive K+ channel-independent mechanism is involved in glucose-excited neurons of mouse arcuate nucleus. *Diabetes* **53,** 2767-2775.

Foster LA, Ames NK & Emery RS. (1991). Food intake and serum insulin responses to intraventricular infusions of insulin and IGF-I. *Physiol Behav* **50,** 745-749.

Fraley GS & Ritter S. (2003). Immunolesion of norepinephrine and epinephrine afferents to medial hypothalamus alters basal and 2-deoxy-D-glucose-induced neuropeptide Y and agouti gene-related protein messenger ribonucleic acid expression in the arcuate nucleus. *Endocrinology* **144,** 75-83.

Frayn KN. (2003). *Metabolic regulation: a human perspective*. W.B. Saunders, Philadelphia, PA.

Frayn KN, Coppack SW, Humphreys SM, Clark ML & Evans RD. (1993). Periprandial regulation of lipid metabolism in insulin-treated diabetes mellitus. *Metabolism* **42,** 504-510.

Friedman JM & Halaas JL. (1998). Leptin and the regulation of body weight in mammals. *Nature* **395,** 763-770.

Fry M, Hoyda TD & Ferguson AV. (2007). Making sense of it: roles of the sensory circumventricular organs in feeding and regulation of energy homeostasis. *Exp Biol Med (Maywood)* **232,** 14-26.

Furuse M, Matsumoto M, Mori R, Sugahara K, Kano K & Hasegawa S. (1997). Influence of fasting and neuropeptide Y on the suppressive food intake induced by intracerebroventricular injection of glucagon-like peptide-1 in the neonatal chick. *Brain Res* **764,** 289-292.

Ganong WF. (2000). Circumventricular organs: definition and role in the regulation of endocrine and autonomic function. *Clin Exp Pharmacol Physiol* **27,** 422-427.

Gao Q & Horvath TL. (2007). Neurobiology of feeding and energy expenditure. *Annu Rev Neurosci* **30,** 367-398.

Garber AJ, Karl IE & Kipnis DM. (1976). Alanine and glutamine synthesis and release from skeletal muscle. I. Glycolysis and amino acid release. *J Biol Chem* **251,** 826-835.

Garber AJ, Karl IE & Kipnis DM. (1976). Alanine and glutamine synthesis and release from skeletal muscle. II. The precursor role of amino acids in alanine and glutamine synthesis. *J Biol Chem* **251,** 836-843.

Garzon J, Fuentes JA & Del Rio J. (1979). Antidepressants selectively antagonize the hyperactivity induced in rats by long-term isolation. *Eur J Pharmacol* **59,** 293-296.

Gautvik KM, de Lecea L, Gautvik VT, Danielson PE, Tranque P, Dopazo A, Bloom FE & Sutcliffe JG. (1996). Overview of the most prevalent hypothalamus-specific mRNAs, as identified by directional tag PCR subtraction. *Proc Natl Acad Sci U S A* **93,** 8733-8738.

Gentsch C, Lichtsteiner M & Feer H. (1981). Individual housing of rats causes divergent changes in spontaneous and reactive activity *Cellular and Molecular Life Sciences (CMLS)* **37,** 61-62.

Gerald C, Walker MW, Criscione L, Gustafson EL, Batzl-Hartmann C, Smith KE, Vaysse P, Durkin MM, Laz TM, Linemeyer DL, Schaffhauser AO, Whitebread S, Hofbauer KG, Taber RI, Branchek TA & Weinshank RL. (1996). A receptor subtype involved in neuropeptide-Y-induced food intake. *Nature* **382,** 168-171.

Gerald C, Walker MW, Vaysse PJ, He C, Branchek TA & Weinshank RL. (1995). Expression cloning and pharmacological characterization of a human hippocampal neuropeptide Y/peptide YY Y2 receptor subtype. *J Biol Chem* **270,** 26758-26761.

Gibbs J, Young RC & Smith GP. (1973). Cholecystokinin decreases food intake in rats. *J Comp Physiol Psychol* **84,** 488-495.

Gibney MJ, Macdonald, I.A. & Roche, H.M. (2003). *Nutrition and metabolism* Blackwell Publishing, Oxford, UK.

Glaum SR, Hara M, Bindokas VP, Lee CC, Polonsky KS, Bell GI & Miller RJ. (1996). Leptin, the obese gene product, rapidly modulates synaptic transmission in the hypothalamus. *Mol Pharmacol* **50,** 230-235.

Glitsch HG & Tappe A. (1993). The Na+/K+ pump of cardiac Purkinje cells is preferentially fuelled by glycolytic ATP production. *Pflugers Arch* **422,** 380-385.

Globus A, Rosenzweig MR, Bennett EL & Diamond MC. (1973). Effects of differential experience on dendritic spine counts in rat cerebral cortex. *J Comp Physiol Psychol* **82,** 175-181.

Gottsch ML, Clifton DK & Steiner RA. (2004). Galanin-like peptide as a link in the integration of metabolism and reproduction. *Trends Endocrinol Metab* **15,** 215-221.

Grandt D, Schimiczek M, Beglinger C, Layer P, Goebell H, Eysselein VE & Reeve JR, Jr. (1994). Two molecular forms of peptide YY (PYY) are abundant in human blood: characterization of a radioimmunoassay recognizing PYY 1-36 and PYY 3-36. *Regul Pept* **51,** 151-159.

Greenstein B & Wood DF. (2006). *The endocrine system at a glance*. Blackwell Publishing, Oxford, UK.

Grey NJ, Goldring S & Kipnis DM. (1970). The effect of fasting, diet, and actinomycin D on insulin secretion in the rat. *J Clin Invest* **49,** 881-889.

Gropp E, Shanabrough M, Borok E, Xu AW, Janoschek R, Buch T, Plum L, Balthasar N, Hampel B, Waisman A, Barsh GS, Horvath TL & Bruning JC. (2005). Agouti-related peptide-expressing neurons are mandatory for feeding. *Nat Neurosci* **8,** 1289-1291.

Grundemar L, Krstenansky JL & Hakanson R. (1993). Activation of neuropeptide Y1 and neuropeptide Y2 receptors by substituted and truncated neuropeptide Y analogs: identification of signal epitopes. *Eur J Pharmacol* **232,** 271-278.

Grundemar L, Wahlestedt C & Reis DJ. (1991). Long-lasting inhibition of the cardiovascular responses to glutamate and the baroreceptor reflex elicited by neuropeptide Y injected into the nucleus tractus solitarius of the rat. *Neurosci Lett* **122,** 135-139.

Guan JL, Uehara K, Lu S, Wang QP, Funahashi H, Sakurai T, Yanagizawa M & Shioda S. (2002). Reciprocal synaptic relationships between orexin- and melanin-concentrating hormone-containing neurons in the rat lateral hypothalamus: a novel circuit implicated in feeding regulation. *Int J Obes Relat Metab Disord* **26,** 1523-1532.

Guan XM, Yu H, Trumbauer M, Frazier E, Van der Ploeg LH & Chen H. (1998). Induction of neuropeptide Y expression in dorsomedial hypothalamus of diet-induced obese mice. *Neuroreport* **9,** 3415-3419.

Gulledge AT, Kampa BM & Stuart GJ. (2005). Synaptic integration in dendritic trees. *J Neurobiol* **64,** 75-90.

Guo Y, Ma L, Enriori PJ, Koska J, Franks PW, Brookshire T, Cowley MA, Salbe AD, Delparigi A & Tataranni PA. (2006). Physiological evidence for the involvement of peptide YY in the regulation of energy homeostasis in humans. *Obesity (Silver Spring)* **14,** 1562-1570.

Guyon A, Tardy MP, Rovere C, Nahon JL, Barhanin J & Lesage F. (2009). Glucose inhibition persists in hypothalamic neurons lacking tandem-pore K+ channels. *J Neurosci* **29,** 2528-2533.

Hahn TM, Breininger JF, Baskin DG & Schwartz MW. (1998). Coexpression of Agrp and NPY in fasting-activated hypothalamic neurons. *Nat Neurosci* **1,** 271-272.

Hakansson ML, Brown H, Ghilardi N, Skoda RC & Meister B. (1998). Leptin receptor immunoreactivity in chemically defined target neurons of the hypothalamus. *J Neurosci* **18,** 559-572.

Halaas JL, Boozer C, Blair-West J, Fidahusein N, Denton DA & Friedman JM. (1997). Physiological response to long-term peripheral and central leptin infusion in lean and obese mice. *Proc Natl Acad Sci U S A* **94,** 8878-8883.

Halaas JL, Gajiwala KS, Maffei M, Cohen SL, Chait BT, Rabinowitz D, Lallone RL, Burley SK & Friedman JM. (1995). Weight-reducing effects of the plasma protein encoded by the obese gene. *Science* **269,** 543-546.

Halliwell JV & Adams PR. (1982). Voltage-clamp analysis of muscarinic excitation in hippocampal neurons. *Brain Res* **250,** 71-92.

Hanson ES & Dallman MF. (1995). Neuropeptide Y (NPY) may integrate responses of hypothalamic feeding systems and the hypothalamo-pituitary-adrenal axis. *J Neuroendocrinol* **7,** 273-279.

Haque MS, Minokoshi Y, Hamai M, Iwai M, Horiuchi M & Shimazu T. (1999). Role of the sympathetic nervous system and insulin in enhancing glucose uptake in peripheral tissues after intrahypothalamic injection of leptin in rats. *Diabetes* **48,** 1706-1712.

Hasin Y & Barry WH. (1984). Myocardial metabolic inhibition and membrane potential, contraction, and potassium uptake. *Am J Physiol* **247,** H322-329.

Haslam DW & James WP. (2005). Obesity. *Lancet* **366,** 1197-1209.

Hausman DB, DiGirolamo M, Bartness TJ, Hausman GJ & Martin RJ. (2001). The biology of white adipocyte proliferation. *Obes Rev* **2,** 239-254.

Hetherington A & Ranson SW. (1940). Hypothalamic lesions and adiposity in the rat. *The Anatomical Record* **78,** 149-172.

Heymsfield SB, Greenberg AS, Fujioka K, Dixon RM, Kushner R, Hunt T, Lubina JA, Patane J, Self B, Hunt P & McCamish M. (1999). Recombinant leptin for weight loss in obese and lean adults: a randomized, controlled, dose-escalation trial. *Jama* **282,** 1568-1575.

Hill JW, Williams KW, Ye C, Luo J, Balthasar N, Coppari R, Cowley MA, Cantley LC, Lowell BB & Elmquist JK. (2008). Acute effects of leptin require PI3K signaling in hypothalamic proopiomelanocortin neurons in mice. *J Clin Invest* **118,** 1796-1805.

Ho G & MacKenzie RG. (1999). Functional characterization of mutations in melanocortin-4 receptor associated with human obesity. *J Biol Chem* **274,** 35816-35822.

Horvath TL, Bechmann I, Naftolin F, Kalra SP & Leranth C. (1997). Heterogeneity in the neuropeptide Y-containing neurons of the rat arcuate nucleus: GABAergic and non-GABAergic subpopulations. *Brain Res* **756,** 283-286.

Howard AD, Wang R, Pong SS, Mellin TN, Strack A, Guan XM, Zeng Z, Williams DL, Jr., Feighner SD, Nunes CN, Murphy B, Stair JN, Yu H, Jiang Q, Clements MK, Tan CP, McKee KK, Hreniuk DL, McDonald TP, Lynch KR, Evans JF, Austin CP, Caskey CT, Van der Ploeg LH & Liu Q. (2000). Identification of receptors for neuromedin U and its role in feeding. *Nature* **406,** 70-74.

Hoyt EC, Lund PK, Winesett DE, Fuller CR, Ghatei MA, Bloom SR & Ulshen MH. (1996). Effects of fasting, refeeding, and intraluminal triglyceride on proglucagon expression in jejunum and ileum. *Diabetes* **45,** 434-439.

Hu K, Huang CS, Jan YN & Jan LY. (2003). ATP-sensitive potassium channel traffic regulation by adenosine and protein kinase C. *Neuron* **38,** 417-432.

Huang Q, Rivest R & Richard D. (1998). Effects of leptin on corticotropin-releasing factor (CRF) synthesis and CRF neuron activation in the paraventricular hypothalamic nucleus of obese (ob/ob) mice. *Endocrinology* **139,** 1524-1532.

Hugl SR, White MF & Rhodes CJ. (1998). Insulin-like growth factor I (IGF-I)-stimulated pancreatic beta-cell growth is glucose-dependent. Synergistic activation of insulin receptor substrate-mediated signal transduction pathways by glucose and IGF-I in INS-1 cells. *J Biol Chem* **273,** 17771-17779.

Huguenard JR. (1996). Low-threshold calcium currents in central nervous system neurons. *Annu Rev Physiol* **58,** 329-348.

Huguenard JR & Prince DA. (1994). Intrathalamic rhythmicity studied in vitro: nominal T-current modulation causes robust antioscillatory effects. *J Neurosci* **14,** 5485-5502.

Huszar D, Lynch CA, Fairchild-Huntress V, Dunmore JH, Fang Q, Berkemeier LR, Gu W, Kesterson RA, Boston BA, Cone RD, Smith FJ, Campfield LA, Burn P & Lee F. (1997). Targeted disruption of the melanocortin-4 receptor results in obesity in mice. *Cell* **88,** 131-141.

Ibrahim N, Bosch MA, Smart JL, Qiu J, Rubinstein M, Ronnekleiv OK, Low MJ & Kelly MJ. (2003). Hypothalamic proopiomelanocortin neurons are glucose responsive and express K(ATP) channels. *Endocrinology* **144,** 1331-1340.

Imagawa A, Hanafusa T, Miyagawa J & Matsuzawa Y. (2000). A novel subtype of type 1 diabetes mellitus characterized by a rapid onset and an absence of diabetes-related antibodies. Osaka IDDM Study Group. *N Engl J Med* **342,** 301-307.

Inagaki N & Seino S. (1998). ATP-sensitive potassium channels: structures, functions, and pathophysiology. *Jpn J Physiol* **48,** 397-412.

Irani BG, Le Foll C, Dunn-Meynell A & Levin BE. (2008). Effects of leptin on rat ventromedial hypothalamic neurons. *Endocrinology* **149,** 5146-5154.

Ivy AC & Oldberg E. (1928). A Hormone mechanism for gall bladder contraction an evacuation. *Am J Physiol* **86,** 599–613.

Izzekutz B, Bortz, W.M., Miller, H.I. & Paul, P. (1967). Turnover rate of plasma FFA in humans and in dogs. *Metabolism* **16,** 1001-1009.

Jacobowitz DM & O'Donohue TL. (1978). alpha-Melanocyte stimulating hormone: immunohistochemical identification and mapping in neurons of rat brain. *Proc Natl Acad Sci U S A* **75,** 6300-6304.

James WP, Astrup A, Finer N, Hilsted J, Kopelman P, Rossner S, Saris WH & Van Gaal LF. (2000). Effect of sibutramine on weight maintenance after weight loss: a randomised trial. STORM Study Group. Sibutramine Trial of Obesity Reduction and Maintenance. *Lancet* **356,** 2119-2125.

Jequier E. (2002). Leptin signaling, adiposity, and energy balance. *Ann N Y Acad Sci* **967,** 379-388.

Jones DP. (1986). Intracellular diffusion gradients of O2 and ATP. *Am J Physiol* **250,** C663-675.

Joost HG & Thorens B. (2001). The extended GLUT-family of sugar/polyol transport facilitators: nomenclature, sequence characteristics, and potential function of its novel members (review). *Mol Membr Biol* **18,** 247-256.

Jorgensen OS & Bock E. (1979). Brain-specific proteins in the occipital cortex of rats housed in enriched and impoverished environments. *Neurochem Res* **4,** 175-187.

Kadowaki T & Yamauchi T. (2005). Adiponectin and adiponectin receptors. *Endocr Rev* **26,** 439-451.

Kadowaki T, Yamauchi T & Kubota N. (2008). The physiological and pathophysiological role of adiponectin and adiponectin receptors in the peripheral tissues and CNS. *FEBS Lett* **582,** 74-80.

Kahn CR. (2003). Knockout mice challenge our concepts of glucose homeostasis and the pathogenesis of diabetes. *Exp Diabesity Res* **4,** 169-182.

Kaiyala KJ, Woods SC & Schwartz MW. (1995). New model for the regulation of energy balance and adiposity by the central nervous system. *Am J Clin Nutr* **62,** 1123S-1134S.

Kalra SP, Dube MG, Fournier A & Kalra PS. (1991). Structure-function analysis of stimulation of food intake by neuropeptide Y: effects of receptor agonists. *Physiol Behav* **50,** 5-9.

Kalra SP, Dube MG, Sahu A, Phelps CP & Kalra PS. (1991). Neuropeptide Y secretion increases in the paraventricular nucleus in association with increased appetite for food. *Proc Natl Acad Sci U S A* **88,** 10931-10935.

Kamegai J, Tamura H, Shimizu T, Ishii S, Sugihara H & Wakabayashi I. (2000). Central effect of ghrelin, an endogenous growth hormone secretagogue, on hypothalamic peptide gene expression. *Endocrinology* **141,** 4797-4800.

Kamegai J, Tamura H, Shimizu T, Ishii S, Sugihara H & Wakabayashi I. (2001). Chronic central infusion of ghrelin increases hypothalamic neuropeptide Y and Agouti-related protein mRNA levels and body weight in rats. *Diabetes* **50,** 2438-2443.

Kamohara S, Burcelin R, Halaas JL, Friedman JM & Charron MJ. (1997). Acute stimulation of glucose metabolism in mice by leptin treatment. *Nature* **389,** 374-377.

Kandel ER, Schwartz JH & Jessell TM. (2000). *Principles of Neural Science* McGraw-Hill Medical.

Kane GC, Liu XK, Yamada S, Olson TM & Terzic A. (2005). Cardiac KATP channels in health and disease. *J Mol Cell Cardiol* **38,** 937-943.

Kang L, Routh VH, Kuzhikandathil EV, Gaspers LD & Levin BE. (2004). Physiological and molecular characteristics of rat hypothalamic ventromedial nucleus glucosensing neurons. *Diabetes* **53,** 549-559.

Karl IE, Garber AJ & Kipnis DM. (1976). Alanine and glutamine synthesis and release from skeletal muscle. III. Dietary and hormonal regulation. *J Biol Chem* **251,** 844-850.

Karschin C, Ecke C, Ashcroft FM & Karschin A. (1997). Overlapping distribution of K(ATP) channel-forming Kir6.2 subunit and the sulfonylurea receptor SUR1 in rodent brain. *FEBS Lett* **401,** 59-64.

Keener J & Sneyd J. (1998). *Mathematical Physiology*. Springer, Berlin, Germany.

Keesey RE & Hirvonen MD. (1997). Body weight set-points: determination and adjustment. *J Nutr* **127,** 1875S-1883S.

Kennedy BG, Lunn G & Hoffman JF. (1986). Effects of altering the ATP/ADP ratio on pump-mediated Na/K and Na/Na exchanges in resealed human red blood cell ghosts. *J Gen Physiol* **87,** 47-72.

Kennedy GC. (1953). The role of depot fat in the hypothalamic control of food intake in the rat. *Proc R Soc Lond B Biol Sci* **140,** 578-596.

Kim MS, Small CJ, Stanley SA, Morgan DG, Seal LJ, Kong WM, Edwards CM, Abusnana S, Sunter D, Ghatei MA & Bloom SR. (2000). The central melanocortin system affects the hypothalamo-pituitary thyroid axis and may mediate the effect of leptin. *J Clin Invest* **105,** 1005-1011.

Knight BL & Iliffe J. (1973). The effect of glucose, insulin and noradrenaline on lipolysis, and on the concentrations of adenosine 3':5'-cyclic monophosphate and adenosine 5'-triphosphate in adipose tissue. *Biochem J* **132,** 77-82.

Kojima M, Hosoda H, Date Y, Nakazato M, Matsuo H & Kangawa K. (1999). Ghrelin is a growth-hormone-releasing acylated peptide from stomach. *Nature* **402,** 656-660.

Kooijman SALM. (2000). *Dynamics enery and mass budgets in biological systems*. Cambridge University Press, Cambridge, UK.

Korner J, Inabnet W, Conwell IM, Taveras C, Daud A, Olivero-Rivera L, Restuccia NL & Bessler M. (2006). Differential effects of gastric bypass and banding on circulating gut hormone and leptin levels. *Obesity (Silver Spring)* **14,** 1553-1561.

Kow LM & Pfaff DW. (1989). Responses of hypothalamic paraventricular neurons in vitro to norepinephrine and other feeding-relevant agents. *Physiol Behav* **46,** 265-271.

Koylu EO, Couceyro PR, Lambert PD, Ling NC, DeSouza EB & Kuhar MJ. (1997). Immunohistochemical localization of novel CART peptides in rat hypothalamus, pituitary and adrenal gland. *J Neuroendocrinol* **9,** 823-833.

Kubota N, Yano W, Kubota T, Yamauchi T, Itoh S, Kumagai H, Kozono H, Takamoto I, Okamoto S, Shiuchi T, Suzuki R, Satoh H, Tsuchida A, Moroi M, Sugi K, Noda T, Ebinuma H, Ueta Y, Kondo T, Araki E, Ezaki O, Nagai R, Tobe K, Terauchi Y, Ueki K, Minokoshi Y & Kadowaki T. (2007). Adiponectin stimulates AMP-activated protein kinase in the hypothalamus and increases food intake. *Cell Metab* **6,** 55-68.

Kulkarni RN, Winnay JN, Daniels M, Bruning JC, Flier SN, Hanahan D & Kahn CR. (1999). Altered function of insulin receptor substrate-1-deficient mouse islets and cultured beta-cell lines. *J Clin Invest* **104,** R69-75.

Lam NT, Lewis JT, Cheung AT, Luk CT, Tse J, Wang J, Bryer-Ash M, Kolls JK & Kieffer TJ. (2004). Leptin increases hepatic insulin sensitivity and protein tyrosine phosphatase 1B expression. *Mol Endocrinol* **18,** 1333-1345.

Larhammar D, Blomqvist AG, Yee F, Jazin E, Yoo H & Wahlested C. (1992). Cloning and functional expression of a human neuropeptide Y/peptide YY receptor of the Y1 type. *J Biol Chem* **267,** 10935-10938.

Larsen PJ, Tang-Christensen M & Jessop DS. (1997). Central administration of glucagon-like peptide-1 activates hypothalamic neuroendocrine neurons in the rat. *Endocrinology* **138,** 4445-4455.

Laurent D, Hundal RS, Dresner A, Price TB, Vogel SM, Petersen KF & Shulman GI. (2000). Mechanism of muscle glycogen autoregulation in humans. *Am J Physiol Endocrinol Metab* **278,** E663-668.

Lederer WJ & Nichols CG. (1989). Nucleotide modulation of the activity of rat heart ATP-sensitive K+ channels in isolated membrane patches. *J Physiol* **419,** 193-211.

Lee GH, Proenca R, Montez JM, Carroll KM, Darvishzadeh JG, Lee JI & Friedman JM. (1996). Abnormal splicing of the leptin receptor in diabetic mice. *Nature* **379,** 632-635.

Lee K, Dixon AK, Richardson PJ & Pinnock RD. (1999). Glucose-receptive neurones in the rat ventromedial hypothalamus express KATP channels composed of Kir6.1 and SUR1 subunits. *J Physiol* **515 (Pt 2),** 439-452.

Levin BE. (2006). Metabolic sensing neurons and the control of energy homeostasis. *Physiol Behav* **89,** 486-489.

Levin BE, Dunn-Meynell AA & Routh VH. (1999). Brain glucose sensing and body energy homeostasis: role in obesity and diabetes. *Am J Physiol* **276,** R1223-1231.

Levin BE & Routh VH. (1996). Role of the brain in energy balance and obesity. *Am J Physiol* **271,** R491-500.

Levin BE, Routh VH, Kang L, Sanders NM & Dunn-Meynell AA. (2004). Neuronal glucosensing: what do we know after 50 years? *Diabetes* **53,** 2521-2528.

Levin N, Nelson C, Gurney A, Vandlen R & de Sauvage F. (1996). Decreased food intake does not completely account for adiposity reduction after ob protein infusion. *Proc Natl Acad Sci U S A* **93,** 1726-1730.

Levy JR, Gyarmati J, Lesko JM, Adler RA & Stevens W. (2000). Dual regulation of leptin secretion: intracellular energy and calcium dependence of regulated pathway. *Am J Physiol Endocrinol Metab* **278,** E892-901.

Li AJ & Ritter S. (2004). Glucoprivation increases expression of neuropeptide Y mRNA in hindbrain neurons that innervate the hypothalamus. *Eur J Neurosci* **19,** 2147-2154.

Li J, Kuang, Y. (2001). Analysis of IVGTT glucose-insulin interaction models with time delay. *Disc Contin Dyn Syst-Ser* **B,** 103-124.

Li J, Kuang, Y. (2007). Analysis of a model of the glucoes-insulin regulatory system with two delays. *SIAM J Appl Math* **67,** 757-776.

Li J, Kuang Y & Mason CC. (2006). Modeling the glucose-insulin regulatory system and ultradian insulin secretory oscillations with two explicit time delays. *J Theor Biol* **242,** 722-735.

Lin HC & Chey WY. (2003). Cholecystokinin and peptide YY are released by fat in either proximal or distal small intestine in dogs. *Regul Pept* **114,** 131-135.

Lin L, Faraco J, Li R, Kadotani H, Rogers W, Lin X, Qiu X, de Jong PJ, Nishino S & Mignot E. (1999). The sleep disorder canine narcolepsy is caused by a mutation in the hypocretin (orexin) receptor 2 gene. *Cell* **98,** 365-376.

Llinas R & Yarom Y. (1981). Electrophysiology of mammalian inferior olivary neurones in vitro. Different types of voltage-dependent ionic conductances. *J Physiol* **315,** 549-567.

Loewy A. (1990). *Anatomy of autonomic nervous system: An overview. In central regulation of autonomic functions*. Oxford University press.

Ludwig DS, Mountjoy KG, Tatro JB, Gillette JA, Frederich RC, Flier JS & Maratos-Flier E. (1998). Melanin-concentrating hormone: a functional melanocortin antagonist in the hypothalamus. *Am J Physiol* **274,** E627-633.

Luque CA & Rey JA. (2002). The discovery and status of sibutramine as an anti-obesity drug. *Eur J Pharmacol* **440,** 119-128.

Lynch RM & Balaban RS. (1987). Coupling of aerobic glycolysis and Na+-K+-ATPase in renal cell line MDCK. *Am J Physiol* **253,** C269-276.

Lyons DJ. (2005). The metabolic and neuropeptidergic modulation of rat arcuate neurones *in vitro*. In *Department of Biological Sciences*. University of Warwick, Coventry.

Maas J & Smith J. (2006). Modelling adipose tissue production and the development of obesity. Multi-disciplinary Centre for Integrative Biology, University of Nottingham, Nottingham.

MacLeod KT. (1989). Effects of hypoxia and metabolic inhibition on the intracellular sodium activity of mammalian ventricular muscle. *J Physiol* **416,** 455-468.

Maejima K & Nagase S. (1991). Effect of starvation and refeeding on the circadian rhythms of hematological and clinico-biochemical values, and water intake of rats. *Jikken Dobutsu* **40,** 389-393.

Maffei M, Fei H, Lee GH, Dani C, Leroy P, Zhang Y, Proenca R, Negrel R, Ailhaud G & Friedman JM. (1995). Increased expression in adipocytes of ob RNA in mice with lesions of the hypothalamus and with mutations at the db locus. *Proc Natl Acad Sci U S A* **92,** 6957-6960.

Makroglou A, Li, J. & Kuang, Y. (2006). Mathematical models and software tools for the glucose-insulin regulatory system and diabetes: an overview. *Appl Numer Math* **56,** 559-573.

Marks JL, Porte D, Jr., Stahl WL & Baskin DG. (1990). Localization of insulin receptor mRNA in rat brain by in situ hybridization. *Endocrinology* **127,** 3234-3236.

Marty N, Dallaporta M & Thorens B. (2007). Brain glucose sensing, counterregulation, and energy homeostasis. *Physiology (Bethesda)* **22,** 241-251.

Masaki T, Yoshimichi G, Chiba S, Yasuda T, Noguchi H, Kakuma T, Sakata T & Yoshimatsu H. (2003). Corticotropin-releasing hormone-mediated pathway of leptin to regulate feeding, adiposity, and uncoupling protein expression in mice. *Endocrinology* **144,** 3547-3554.

Matsuzawa T & Sakazume M. (1994). Effects of fasting on haematology and clinical chemistry values in the rat and dog *Comparative Haematology International* **4,** 152-156.

Mayer CH, Fink H, Rex A & Voigt JP. (2006). Changes in extracellular hypothalamic glucose in relation to feeding. *Eur J Neurosci* **24,** 1695-1701.

Mayer J. (1953). Glucostatic mechanism of regulation of food intake. *N Engl J Med* **249,** 13-16.

Mayer J. (1955). Regulation of energy intake and the body weight: the glucostatic theory and the lipostatic hypothesis. *Ann N Y Acad Sci* **63,** 15-43.

McCormick DA & Pape HC. (1990). Properties of a hyperpolarization-activated cation current and its role in rhythmic oscillation in thalamic relay neurones. *J Physiol* **431,** 291-318.

McMinn JE, Baskin DG & Schwartz MW. (2000). Neuroendocrine mechanisms regulating food intake and body weight. *Obes Rev* **1,** 37-46.

McNay EC, Fries TM & Gold PE. (2000). Decreases in rat extracellular hippocampal glucose concentration associated with cognitive demand during a spatial task. *Proc Natl Acad Sci U S A* **97,** 2881-2885.

McNay EC & Gold PE. (1999). Extracellular glucose concentrations in the rat hippocampus measured by zero-net-flux: effects of microdialysis flow rate, strain, and age. *J Neurochem* **72,** 785-790.

McNay EC, McCarty RC & Gold PE. (2001). Fluctuations in brain glucose concentration during behavioral testing: dissociations between brain areas and between brain and blood. *Neurobiol Learn Mem* **75,** 325-337.

Mercer LP, Kelley DS, Humphries LL & Dunn JD. (1994). Manipulation of central nervous system histamine or histaminergic receptors (H1) affects food intake in rats. *J Nutr* **124,** 1029-1036.

Merchenthaler I, Lane M & Shughrue P. (1999). Distribution of pre-pro-glucagon and glucagon-like peptide-1 receptor messenger RNAs in the rat central nervous system. *J Comp Neurol* **403,** 261-280.

Meyer C, Dostou JM, Welle SL & Gerich JE. (2002). Role of human liver, kidney, and skeletal muscle in postprandial glucose homeostasis. *Am J Physiol Endocrinol Metab* **282,** E419-427.

Miki T, Liss B, Minami K, Shiuchi T, Saraya A, Kashima Y, Horiuchi M, Ashcroft F, Minokoshi Y, Roeper J & Seino S. (2001). ATP-sensitive K+ channels in the hypothalamus are essential for the maintenance of glucose homeostasis. *Nat Neurosci* **4,** 507-512.

Milhorn HT. (1966). *The application of control theory to physiological systems*. W.B. Saunders, Philadelphia, PA.

Minami K, Miki T, Kadowaki T & Seino S. (2004). Roles of ATP-sensitive K+ channels as metabolic sensors: studies of Kir6.x null mice. *Diabetes* **53 Suppl 3,** S176-180.

Minami T, Shimizu N, Duan S & Oomura Y. (1990). Hypothalamic neuronal activity responses to 3-hydroxybutyric acid, an endogenous organic acid. *Brain Res* **509,** 351-354.

Minokoshi Y, Alquier T, Furukawa N, Kim YB, Lee A, Xue B, Mu J, Foufelle F, Ferre P, Birnbaum MJ, Stuck BJ & Kahn BB. (2004). AMP-kinase regulates food intake by responding to hormonal and nutrient signals in the hypothalamus. *Nature* **428,** 569-574.

Mirshamsi S, Laidlaw HA, Ning K, Anderson E, Burgess LA, Gray A, Sutherland C & Ashford ML. (2004). Leptin and insulin stimulation of signalling pathways in arcuate nucleus neurones: PI3K dependent actin reorganization and KATP channel activation. *BMC Neurosci* **5,** 54.

Miyazaki T, Dun NJ, Kobayashi H & Tosaka T. (1996). Voltage-dependent potassium currents of sympathetic preganglionic neurons in neonatal rat spinal cord thin slices. *Brain Res* **743,** 1-10.

Mizuno TM, Kleopoulos SP, Bergen HT, Roberts JL, Priest CA & Mobbs CV. (1998). Hypothalamic pro-opiomelanocortin mRNA is reduced by fasting and [corrected] in ob/ob and db/db mice, but is stimulated by leptin. *Diabetes* **47,** 294-297.

Mizuno Y & Oomura Y. (1984). Glucose responding neurons in the nucleus tractus solitarius of the rat: in vitro study. *Brain Res* **307,** 109-116.

Mondal MS, Date Y, Yamaguchi H, Toshinai K, Tsuruta T, Kangawa K & Nakazato M. (2005). Identification of ghrelin and its receptor in neurons of the rat arcuate nucleus. *Regul Pept* **126,** 55-59.

Moran TH. (2006). Gut peptide signaling in the controls of food intake. *Obesity (Silver Spring)* **14 Suppl 5,** 250S-253S.

Moran TH, Robinson PH, Goldrich MS & McHugh PR. (1986). Two brain cholecystokinin receptors: implications for behavioral actions. *Brain Res* **362,** 175-179.

Moriguchi T, Sakurai T, Nambu T, Yanagisawa M & Goto K. (1999). Neurons containing orexin in the lateral hypothalamic area of the adult rat brain are activated by insulin-induced acute hypoglycemia. *Neurosci Lett* **264,** 101-104.

Mountjoy KG, Mortrud MT, Low MJ, Simerly RB & Cone RD. (1994). Localization of the melanocortin-4 receptor (MC4-R) in neuroendocrine and autonomic control circuits in the brain. *Mol Endocrinol* **8,** 1298-1308.

Mukhopadhyay A, De Gaetano, A. & Arino, A. . (2004). Modeling the intra-venous glucose tolerance test: a global study for a single-distributed-delay model. *SDIsc Contin Dyn Syst-Ser* **B** 407-417.

Muroya S, Yada T, Shioda S & Takigawa M. (1999). Glucose-sensitive neurons in the rat arcuate nucleus contain neuropeptide Y. *Neurosci Lett* **264,** 113-116.

Murphy BA, Fioramonti X, Jochnowitz N, Fakira K, Gagen K, Contie S, Lorsignol A, Penicaud L, Martin WJ & Routh VH. (2009). Fasting enhances the response of arcuate neuropeptide Y (NPY)-glucose-inhibited (GI) neurons to decreased extracellular glucose. *Am J Physiol Cell Physiol*.

Nakamura S, Kiyosue T & Arita M. (1989). Glucose reverses 2,4-dinitrophenol induced changes in action potentials and membrane currents of guinea pig ventricular cells via enhanced glycolysis. *Cardiovasc Res* **23,** 286-294.

Nakano Y, Oomura Y, Lenard L, Nishino H, Aou S, Yamamoto T & Aoyagi K. (1986). Feeding-related activity of glucose- and morphine-sensitive neurons in the monkey amygdala. *Brain Res* **399,** 167-172.

Nakazato M, Murakami N, Date Y, Kojima M, Matsuo H, Kangawa K & Matsukura S. (2001). A role for ghrelin in the central regulation of feeding. *Nature* **409,** 194-198.

Nargund RP, Strack AM & Fong TM. (2006). Melanocortin-4 receptor (MC4R) agonists for the treatment of obesity. *J Med Chem* **49,** 4035-4043.

Nauck MA, Niedereichholz U, Ettler R, Holst JJ, Orskov C, Ritzel R & Schmiegel WH. (1997). Glucagon-like peptide 1 inhibition of gastric emptying outweighs its insulinotropic effects in healthy humans. *Am J Physiol* **273,** E981-988.

Neary NM, Goldstone AP & Bloom SR. (2004). Appetite regulation: from the gut to the hypothalamus. *Clin Endocrinol (Oxf)* **60,** 153-160.

Nilsson LH & Hultman E. (1973). Liver glycogen in man--the effect of total starvation or a carbohydrate-poor diet followed by carbohydrate refeeding. *Scand J Clin Lab Invest* **32,** 325-330.

Niswender KD, Morton GJ, Stearns WH, Rhodes CJ, Myers MG, Jr. & Schwartz MW. (2001). Intracellular signalling. Key enzyme in leptin-induced anorexia. *Nature* **413,** 794-795.

Noma A. (1983). ATP-regulated K+ channels in cardiac muscle. *Nature* **305,** 147-148.

Nowak KW, Kaczmarek P, Mackowiak P, Ziolkowska A, Albertin G, Ginda WJ, Trejter M, Nussdorfer GG & Malendowicz LK. (2002). Rat thyroid gland expresses the long form of leptin receptors, and leptin stimulates the function of the gland in euthyroid non-fasted animals. *Int J Mol Med* **9,** 31-34.

Obici S, Feng Z, Morgan K, Stein D, Karkanias G & Rossetti L. (2002). Central administration of oleic acid inhibits glucose production and food intake. *Diabetes* **51,** 271-275.

Obici S, Zhang BB, Karkanias G & Rossetti L. (2002). Hypothalamic insulin signaling is required for inhibition of glucose production. *Nat Med* **8,** 1376-1382.

Okabayashi Y, Maddux BA, McDonald AR, Logsdon CD, Williams JA & Goldfine ID. (1989). Mechanisms of insulin-induced insulin-receptor downregulation. Decrease of receptor biosynthesis and mRNA levels. *Diabetes* **38,** 182-187.

Okada T, Liew CW, Hu J, Hinault C, Michael MD, Krtzfeldt J, Yin C, Holzenberger M, Stoffel M & Kulkarni RN. (2007). Insulin receptors in beta-cells are critical for islet compensatory growth response to insulin resistance. *Proc Natl Acad Sci U S A* **104,** 8977-8982.

Okamoto K, Wang W, Rounds J, Chambers EA & Jacobs DO. (2001). ATP from glycolysis is required for normal sodium homeostasis in resting fast-twitch rodent skeletal muscle. *Am J Physiol Endocrinol Metab* **281,** E479-488.

Ollmann MM, Wilson BD, Yang YK, Kerns JA, Chen Y, Gantz I & Barsh GS. (1997). Antagonism of central melanocortin receptors in vitro and in vivo by agouti-related protein. *Science* **278,** 135-138.

Oomura Y. (1983). Glucose as a regulator of neuronal activity. *Adv Metab Disord* **10,** 31-65.

Oomura Y, Kimura K, Ooyama H, Maeno T, Iki M & Kuniyoshi M. (1964). Reciprocal Activities of the Ventromedial and Lateral Hypothalamic Areas of Cats. *Science* **143,** 484-485.

Oomura Y, Nakamura T, Sugimori M & Yamada Y. (1975). Effect of free fatty acid on the rat lateral hypothalamic neurons. *Physiol Behav* **14,** 483-486.

Oomura Y, Ono T, Ooyama H & Wayner MJ. (1969). Glucose and osmosensitive neurones of the rat hypothalamus. *Nature* **222,** 282-284.

Oomura Y, Ooyama H, Sugimori M, Nakamura T & Yamada Y. (1974). Glucose inhibition of the glucose-sensitive neurone in the rat lateral hypothalamus. *Nature* **247,** 284-286.

Palou M, Sanchez J, Rodriguez AM, Priego T, Pico C & Palou A. (2009). Induction of NPY/AgRP orexigenic peptide expression in rat hypothalamus is an early event in fasting: relationship with circulating leptin, insulin and glucose. *Cell Physiol Biochem* **23,** 115-124.

Pape HC. (1996). Queer current and pacemaker: the hyperpolarization-activated cation current in neurons. *Annu Rev Physiol* **58,** 299-327.

Pardini AW, Nguyen HT, Figlewicz DP, Baskin DG, Williams DL, Kim F & Schwartz MW. (2006). Distribution of insulin receptor substrate-2 in brain areas involved in energy homeostasis. *Brain Res* **1112,** 169-178.

Pattaranit R & van den Berg HA. (2008). Mathematical models of energy homeostasis. *Journal of the Royal Society, Interface / the Royal Society* **5,** 1119-1135.

Pattaranit R, van den Berg HA & Spanswick D. (2008). The development of insulin resistance in Type 2 diabetes: insights from knockout studies. *Sci Prog* **91,** 285-316.

Pelleymounter MA, Cullen MJ, Baker MB, Hecht R, Winters D, Boone T & Collins F. (1995). Effects of the obese gene product on body weight regulation in ob/ob mice. *Science* **269,** 540-543.

Penicaud L, Leloup C, Fioramonti X, Lorsignol A & Benani A. (2006). Brain glucose sensing: a subtle mechanism. *Curr Opin Clin Nutr Metab Care* **9,** 458-462.

Penicaud L, Leloup C, Lorsignol A, Alquier T & Guillod E. (2002). Brain glucose sensing mechanism and glucose homeostasis. *Curr Opin Clin Nutr Metab Care* **5,** 539-543.

Pennartz CM, De Jeu MT, Geurtsen AM, Sluiter AA & Hermes ML. (1998). Electrophysiological and morphological heterogeneity of neurons in slices of rat suprachiasmatic nucleus. *J Physiol* **506 (Pt 3),** 775-793.

Perrin C, Knauf C & Burcelin R. (2004). Intracerebroventricular infusion of glucose, insulin, and the adenosine monophosphate-activated kinase activator, 5-aminoimidazole-4-carboxamide-1-beta-D-ribofuranoside, controls muscle glycogen synthesis. *Endocrinology* **145,** 4025-4033.

Peruzzo B, Pastor FE, Blazquez JL, Schobitz K, Pelaez B, Amat P & Rodriguez EM. (2000). A second look at the barriers of the medial basal hypothalamus. *Exp Brain Res* **132,** 10-26.

Philipson KD & Nishimoto AY. (1983). ATP-dependent Na+ transport in cardiac sarcolemmal vesicles. *Biochim Biophys Acta* **733,** 133-141.

Pickering AE, Spanswick D & Logan SD. (1991). Whole-cell recordings from sympathetic preganglionic neurons in rat spinal cord slices. *Neurosci Lett* **130,** 237-242.

Pocai A, Lam TK, Gutierrez-Juarez R, Obici S, Schwartz GJ, Bryan J, Aguilar-Bryan L & Rossetti L. (2005). Hypothalamic K(ATP) channels control hepatic glucose production. *Nature* **434,** 1026-1031.

Porte D, Jr. & Woods SC. (1981). Regulation of food intake and body weight in insulin. *Diabetologia* **20 Suppl,** 274-280.

Prigeon RL, Roder ME, Porte D, Jr. & Kahn SE. (1996). The effect of insulin dose on the measurement of insulin sensitivity by the minimal model technique. Evidence for saturable insulin transport in humans. *J Clin Invest* **97,** 501-507.

Qi Y, Takahashi N, Hileman SM, Patel HR, Berg AH, Pajvani UB, Scherer PE & Ahima RS. (2004). Adiponectin acts in the brain to decrease body weight. *Nat Med* **10,** 524-529.

Qu D, Ludwig DS, Gammeltoft S, Piper M, Pelleymounter MA, Cullen MJ, Mathes WF, Przypek R, Kanarek R & Maratos-Flier E. (1996). A role for melanin-concentrating hormone in the central regulation of feeding behaviour. *Nature* **380,** 243-247.

Raju B & Cryer PE. (2005). Maintenance of the postabsorptive plasma glucose concentration: insulin or insulin plus glucagon? *Am J Physiol Endocrinol Metab* **289,** E181-186.

Randle PJ, Garland PB, Hales CN & Newsholme EA. (1963). The glucose fatty-acid cycle. Its role in insulin sensitivity and the metabolic disturbances of diabetes mellitus. *Lancet* **1,** 785-789.

Reyes TM, Lewis K, Perrin MH, Kunitake KS, Vaughan J, Arias CA, Hogenesch JB, Gulyas J, Rivier J, Vale WW & Sawchenko PE. (2001). Urocortin II: a member of the corticotropin-releasing factor (CRF) neuropeptide family that is selectively bound by type 2 CRF receptors. *Proc Natl Acad Sci U S A* **98,** 2843-2848.

Rhim H, Kinney GA, Emmerson PJ & Miller RJ. (1997). Regulation of neurotransmission in the arcuate nucleus of the rat by different neuropeptide Y receptors. *J Neurosci* **17,** 2980-2989.

Ritter S, Dinh TT & Zhang Y. (2000). Localization of hindbrain glucoreceptive sites controlling food intake and blood glucose. *Brain Res* **856,** 37-47.

Ritter S, Llewellyn-Smith I & Dinh TT. (1998). Subgroups of hindbrain catecholamine neurons are selectively activated by 2-deoxy-D-glucose induced metabolic challenge. *Brain Res* **805,** 41-54.

Robinson BG, Emanuel RL, Frim DM & Majzoub JA. (1988). Glucocorticoid stimulates expression of corticotropin-releasing hormone gene in human placenta. *Proc Natl Acad Sci U S A* **85,** 5244-5248.

Roh C, Han J, Tzatsos A & Kandror KV. (2003). Nutrient-sensing mTOR-mediated pathway regulates leptin production in isolated rat adipocytes. *Am J Physiol Endocrinol Metab* **284,** E322-330.

Rosenbaum M, Goldsmith R, Bloomfield D, Magnano A, Weimer L, Heymsfield S, Gallagher D, Mayer L, Murphy E & Leibel RL. (2005). Low-dose leptin reverses skeletal muscle, autonomic, and neuroendocrine adaptations to maintenance of reduced weight. *J Clin Invest* **115,** 3579-3586.

Rosenbaum M, Nicolson M, Hirsch J, Murphy E, Chu F & Leibel RL. (1997). Effects of weight change on plasma leptin concentrations and energy expenditure. *J Clin Endocrinol Metab* **82,** 3647-3654.

Rother E, Konner AC & Bruning JC. (2008). Neurocircuits integrating hormone and nutrient signaling in control of glucose metabolism. *Am J Physiol Endocrinol Metab* **294,** E810-816.

Rothwell NJ. (1990). Central effects of CRF on metabolism and energy balance. *Neurosci Biobehav Rev* **14,** 263-271.

Routh VH. (2002). Glucose-sensing neurons: are they physiologically relevant? *Physiol Behav* **76,** 403-413.

Routh VH, McArdle JJ, Sanders NM, Song Z. & R. aW. (2007). *Glucose Sensing Neurons*. Springer US.

Routh VH, Song Z & Liu X. (2004). The role of glucosensing neurons in the detection of hypoglycemia. *Diabetes Technol Ther* **6,** 413-421.

Rowe IC, Boden PR & Ashford ML. (1996). Potassium channel dysfunction in hypothalamic glucose-receptive neurones of obese Zucker rats. *J Physiol* **497 (Pt 2),** 365-377.

Rowe IC, Treherne JM & Ashford ML. (1996). Activation by intracellular ATP of a potassium channel in neurones from rat basomedial hypothalamus. *J Physiol* **490 (Pt 1),** 97-113.

Roy A & Parker RS. (2006). Dynamic modeling of free fatty acid, glucose, and insulin: an extended "minimal model". *Diabetes Technol Ther* **8,** 617-626.

Rozhanets VV, Gavrishchuk EG, Rodionov IM, Volchek AG & Kulaev IS. (1974). ATP content in the rat brain during stress. *Bull Exp Biol Med* **77,** 622-624.

Rubio MA, Gargallo M, Isabel Millan A & Moreno B. (2007). Drugs in the treatment of obesity: sibutramine, orlistat and rimonabant. *Public Health Nutr* **10,** 1200-1205.

Saad MF, Anderson RL, Laws A, Watanabe RM, Kades WW, Chen YD, Sands RE, Pei D, Savage PJ & Bergman RN. (1994). A comparison between the minimal model and the glucose clamp in the assessment of insulin sensitivity across the spectrum of glucose tolerance. Insulin Resistance Atherosclerosis Study. *Diabetes* **43,** 1114-1121.

Sahakian BJ, Robbins TW, Morgan MJ & Iversen SD. (1975). The effects of psychomotor stimulants on stereotypy and locomotor activity in socially-deprived and control rats. *Brain Res* **84,** 195-205.

Sahu A. (1998). Evidence suggesting that galanin (GAL), melanin-concentrating hormone (MCH), neurotensin (NT), proopiomelanocortin (POMC) and neuropeptide Y (NPY) are targets of leptin signaling in the hypothalamus. *Endocrinology* **139,** 795-798.

Saker L. (2009). Metabolic and Serotonergic Modulation of Hypothalamic Arcuate Nucleus Neurones *in vitro*. In *Clinical Sciences Research Institute, Warwick Medical School*. University of Warwick, Coventry.

Sakurai T, Amemiya A, Ishii M, Matsuzaki I, Chemelli RM, Tanaka H, Williams SC, Richardson JA, Kozlowski GP, Wilson S, Arch JR, Buckingham RE, Haynes AC, Carr SA, Annan RS, McNulty DE, Liu WS, Terrett JA, Elshourbagy NA, Bergsma DJ & Yanagisawa M. (1998). Orexins and orexin receptors: a family of hypothalamic neuropeptides and G protein-coupled receptors that regulate feeding behavior. *Cell* **92,** 573-585.

Salway JG. (2004). *Metabolism at a glance*. Blackwell Science, Oxford, UK.

Sanacora G, Kershaw M, Finkelstein JA & White JD. (1990). Increased hypothalamic content of preproneuropeptide Y messenger ribonucleic acid in genetically obese Zucker rats and its regulation by food deprivation. *Endocrinology* **127,** 730-737.

Saper CB, Swanson LW & Cowan WM. (1979). An autoradiographic study of the efferent connections of the lateral hypothalamic area in the rat. *J Comp Neurol* **183,** 689-706.

Scarpace PJ, Matheny M, Pollock BH & Tumer N. (1997). Leptin increases uncoupling protein expression and energy expenditure. *Am J Physiol* **273,** E226-230.

Schioth HB, Muceniece R, Mutulis F, Bouifrouri AA, Mutule I & Wikberg JE. (1999). Further pharmacological characterization of the selective melanocortin 4 receptor antagonist HS014: comparison with SHU9119. *Neuropeptides* **33,** 191-196.

Schoeller DA, Cella LK, Sinha MK & Caro JF. (1997). Entrainment of the diurnal rhythm of plasma leptin to meal timing. *J Clin Invest* **100,** 1882-1887.

Schuit FC, Huypens P, Heimberg H & Pipeleers DG. (2001). Glucose sensing in pancreatic beta-cells: a model for the study of other glucose-regulated cells in gut, pancreas, and hypothalamus. *Diabetes* **50,** 1-11.

Schwartz MW, Baskin DG, Kaiyala KJ & Woods SC. (1999). Model for the regulation of energy balance and adiposity by the central nervous system. *Am J Clin Nutr* **69,** 584-596.

Schwartz MW, Bergman RN, Kahn SE, Taborsky GJ, Jr., Fisher LD, Sipols AJ, Woods SC, Steil GM & Porte D, Jr. (1991). Evidence for entry of plasma insulin into cerebrospinal fluid through an intermediate compartment in dogs. Quantitative aspects and implications for transport. *J Clin Invest* **88,** 1272-1281.

Schwartz MW, Seeley RJ, Woods SC, Weigle DS, Campfield LA, Burn P & Baskin DG. (1997). Leptin increases hypothalamic pro-opiomelanocortin mRNA expression in the rostral arcuate nucleus. *Diabetes* **46,** 2119-2123.

Schwartz MW, Sipols AJ, Grubin CE & Baskin DG. (1993). Differential effect of fasting on hypothalamic expression of genes encoding neuropeptide Y, galanin, and glutamic acid decarboxylase. *Brain Res Bull* **31,** 361-367.

Schwartz MW, Woods SC, Porte D, Jr., Seeley RJ & Baskin DG. (2000). Central nervous system control of food intake. *Nature* **404,** 661-671.

Schwartz NS, Clutter WE, Shah SD & Cryer PE. (1987). Glycemic thresholds for activation of glucose counterregulatory systems are higher than the threshold for symptoms. *J Clin Invest* **79,** 777-781.

Sedaghat AR, Sherman, A. & Quon, M.J. (1992). A mathematical model of metabolic insulin signalling pathways. *Am J Physiol Endocrinol Metab* **283,** E1084-E1101.

Seeley RJ, Yagaloff KA, Fisher SL, Burn P, Thiele TE, van Dijk G, Baskin DG & Schwartz MW. (1997). Melanocortin receptors in leptin effects. *Nature* **390,** 349.

Seoane LM, Lopez M, Tovar S, Casanueva FF, Senaris R & Dieguez C. (2003). Agouti-related peptide, neuropeptide Y, and somatostatin-producing neurons are targets for ghrelin actions in the rat hypothalamus. *Endocrinology* **144,** 544-551.

Shimada M, Tritos NA, Lowell BB, Flier JS & Maratos-Flier E. (1998). Mice lacking melanin-concentrating hormone are hypophagic and lean. *Nature* **396,** 670-674.

Shiraishi T. (1991). Noradrenergic neurons modulate lateral hypothalamic chemical and electrical stimulation-induced feeding by sated rats. *Brain Res Bull* **27,** 347-351.

Shiuchi T, Nakagami H, Iwai M, Takeda Y, Cui T, Chen R, Minokoshi Y & Horiuchi M. (2001). Involvement of bradykinin and nitric oxide in leptin-mediated glucose uptake in skeletal muscle. *Endocrinology* **142,** 608-612.

Silber HE, Jauslin PM, Frey N, Gieschke R, Simonsson US & Karlsson MO. (2007). An integrated model for glucose and insulin regulation in healthy volunteers and type 2 diabetic patients following intravenous glucose provocations. *J Clin Pharmacol* **47,** 1159-1171.

Silver IA & Erecinska M. (1994). Extracellular glucose concentration in mammalian brain: continuous monitoring of changes during increased neuronal activity and upon limitation in oxygen supply in normo-, hypo-, and hyperglycemic animals. *J Neurosci* **14,** 5068-5076.

Silver IA & Erecinska M. (1998). Glucose-induced intracellular ion changes in sugar-sensitive hypothalamic neurons. *J Neurophysiol* **79,** 1733-1745.

Silverman M. (1991). Structure and function of hexose transporters. *Annu Rev Biochem* **60,** 757-794.

Sim LJ & Joseph SA. (1991). Arcuate nucleus projections to brainstem regions which modulate nociception. *J Chem Neuroanat* **4,** 97-109.

Sloth B, Holst JJ, Flint A, Gregersen NT & Astrup A. (2007). Effects of PYY1-36 and PYY3-36 on appetite, energy intake, energy expenditure, glucose and fat metabolism in obese and lean subjects. *Am J Physiol Endocrinol Metab* **292,** E1062-1068.

Smith RG, Sun Y, Betancourt L & Asnicar M. (2004). Growth hormone secretagogues: prospects and potential pitfalls. *Best Pract Res Clin Endocrinol Metab* **18,** 333-347.

Song Z, Levin BE, McArdle JJ, Bakhos N & Routh VH. (2001). Convergence of pre- and postsynaptic influences on glucosensing neurons in the ventromedial hypothalamic nucleus. *Diabetes* **50,** 2673-2681.

Song Z & Routh VH. (2005). Differential effects of glucose and lactate on glucosensing neurons in the ventromedial hypothalamic nucleus. *Diabetes* **54,** 15-22.

Song Z & Routh VH. (2006). Recurrent hypoglycemia reduces the glucose sensitivity of glucose-inhibited neurons in the ventromedial hypothalamus nucleus. *Am J Physiol Regul Integr Comp Physiol* **291,** R1283-1287.

Sousa T, Domingos T & Kooijman SA. (2008). From empirical patterns to theory: a formal metabolic theory of life. *Philos Trans R Soc Lond B Biol Sci* **363,** 2453-2464.

Spangenberg EM, Augustsson H, Dahlborn K, Essen-Gustavsson B & Cvek K. (2005). Housing-related activity in rats: effects on body weight, urinary corticosterone levels, muscle properties and performance. *Lab Anim* **39,** 45-57.

Spanswick D, Smith MA, Groppi VE, Logan SD & Ashford ML. (1997). Leptin inhibits hypothalamic neurons by activation of ATP-sensitive potassium channels. *Nature* **390,** 521-525.

Spanswick D, Smith MA, Mirshamsi S, Routh VH & Ashford ML. (2000). Insulin activates ATP-sensitive K+ channels in hypothalamic neurons of lean, but not obese rats. *Nat Neurosci* **3,** 757-758.

Stanley BG, Kyrkouli SE, Lampert S & Leibowitz SF. (1986). Neuropeptide Y chronically injected into the hypothalamus: a powerful neurochemical inducer of hyperphagia and obesity. *Peptides* **7,** 1189-1192.

Stanley BG, Magdalin W, Seirafi A, Thomas WJ & Leibowitz SF. (1993). The perifornical area: the major focus of (a) patchily distributed hypothalamic neuropeptide Y-sensitive feeding system(s). *Brain Res* **604,** 304-317.

Steil GM, Volund A, Kahn SE & Bergman RN. (1993). Reduced sample number for calculation of insulin sensitivity and glucose effectiveness from the minimal model. Suitability for use in population studies. *Diabetes* **42,** 250-256.

Stephens TW, Basinski M, Bristow PK, Bue-Valleskey JM, Burgett SG, Craft L, Hale J, Hoffmann J, Hsiung HM, Kriauciunas A & et al. (1995). The role of neuropeptide Y in the antiobesity action of the obese gene product. *Nature* **377,** 530-532.

Steppan CM, Bailey ST, Bhat S, Brown EJ, Banerjee RR, Wright CM, Patel HR, Ahima RS & Lazar MA. (2001). The hormone resistin links obesity to diabetes. *Nature* **409,** 307-312.

Sturis J, Polonsky KS, Mosekilde E & Van Cauter E. (1991). Computer model for mechanisms underlying ultradian oscillations of insulin and glucose. *Am J Physiol* **260,** E801-809.

Sun Y, Wang P, Zheng H & Smith RG. (2004). Ghrelin stimulation of growth hormone release and appetite is mediated through the growth hormone secretagogue receptor. *Proc Natl Acad Sci U S A* **101,** 4679-4684.

Szewczyk JR & Laudeman C. (2003). CCK1R agonists: a promising target for the pharmacological treatment of obesity. *Curr Top Med Chem* **3,** 837-854.

Takai A & Tomita T. (1986). Glycolysis and oxidative phosphorylation during activation of the sodium pump in the taenia from guinea-pig caecum. *J Physiol* **381,** 65-75.

Tannenbaum GS, Gurd W & Lapointe M. (1998). Leptin is a potent stimulator of spontaneous pulsatile growth hormone (GH) secretion and the GH response to GH-releasing hormone. *Endocrinology* **139,** 3871-3875.

Tartaglia LA, Dembski M, Weng X, Deng N, Culpepper J, Devos R, Richards GJ, Campfield LA, Clark FT, Deeds J, Muir C, Sanker S, Moriarty A, Moore KJ, Smutko JS, Mays GG, Wool EA, Monroe CA & Tepper RI. (1995). Identification and expression cloning of a leptin receptor, OB-R. *Cell* **83,** 1263-1271.

Tasker JG & Dudek FE. (1991). Electrophysiological properties of neurones in the region of the paraventricular nucleus in slices of rat hypothalamus. *J Physiol* **434,** 271-293.

Tatemoto K, Carlquist M & Mutt V. (1982). Neuropeptide Y--a novel brain peptide with structural similarities to peptide YY and pancreatic polypeptide. *Nature* **296,** 659-660.

Taylor R, Magnusson I, Rothman DL, Cline GW, Caumo A, Cobelli C & Shulman GI. (1996). Direct assessment of liver glycogen storage by 13C nuclear magnetic resonance spectroscopy and regulation of glucose homeostasis after a mixed meal in normal subjects. *J Clin Invest* **97,** 126-132.

Taylor R, Price TB, Katz LD, Shulman RG & Shulman GI. (1993). Direct measurement of change in muscle glycogen concentration after a mixed meal in normal subjects. *Am J Physiol* **265,** E224-229.

Thoa NB, Tizabi Y & Jacobowitz DM. (1977). The effect of isolation on catecholamine concentration and turnover in discrete areas of the rat brain. *Brain Res* **131,** 259-269.

Tiikkainen M, Hakkinen AM, Korsheninnikova E, Nyman T, Makimattila S & Yki-Jarvinen H. (2004). Effects of rosiglitazone and metformin on liver fat content, hepatic insulin resistance, insulin clearance, and gene expression in adipose tissue in patients with type 2 diabetes. *Diabetes* **53,** 2169-2176.

Toffolo G, Bergman RN, Finegood DT, Bowden CR & Cobelli C. (1980). Quantitative estimation of beta cell sensitivity to glucose in the intact organism: a minimal model of insulin kinetics in the dog. *Diabetes* **29,** 979-990.

Tokita S, Takahashi K & Kotani H. (2006). Recent advances in molecular pharmacology of the histamine systems: physiology and pharmacology of histamine H3 receptor: roles in feeding regulation and therapeutic potential for metabolic disorders. *J Pharmacol Sci* **101,** 12-18.

Toledo-Rodriguez M, Blumenfeld B, Wu C, Luo J, Attali B, Goodman P & Markram H. (2004). Correlation maps allow neuronal electrical properties to be predicted from single-cell gene expression profiles in rat neocortex. *Cereb Cortex* **14,** 1310-1327.

Tolic IM, Mosekilde E & Sturis J. (2000). Modeling the insulin-glucose feedback system: the significance of pulsatile insulin secretion. *J Theor Biol* **207,** 361-375.

Tolle V, Kadem M, Bluet-Pajot MT, Frere D, Foulon C, Bossu C, Dardennes R, Mounier C, Zizzari P, Lang F, Epelbaum J & Estour B. (2003). Balance in ghrelin and leptin plasma levels in anorexia nervosa patients and constitutionally thin women. *J Clin Endocrinol Metab* **88,** 109-116.

Tong X, Porter LM, Liu G, Dhar-Chowdhury P, Srivastava S, Pountney DJ, Yoshida H, Artman M, Fishman GI, Yu C, Iyer R, Morley GE, Gutstein DE & Coetzee WA. (2006). Consequences of cardiac myocyte-specific ablation of KATP channels in transgenic mice expressing dominant negative Kir6 subunits. *Am J Physiol Heart Circ Physiol* **291,** H543-551.

Topp B, Promislow K, deVries G, Miura RM & Finegood DT. (2000). A model of beta-cell mass, insulin, and glucose kinetics: pathways to diabetes. *J Theor Biol* **206,** 605-619.

Trivedi P, Yu H, MacNeil DJ, Van der Ploeg LH & Guan XM. (1998). Distribution of orexin receptor mRNA in the rat brain. *FEBS Lett* **438,** 71-75.

Tschop M, Smiley DL & Heiman ML. (2000). Ghrelin induces adiposity in rodents. *Nature* **407,** 908-913.

Tuch B, Dunlop M & Proietto J. (2000). *Diabetes research A guide for postgraduates*. Harwood academic publishers.

Turton MD, O'Shea D, Gunn I, Beak SA, Edwards CM, Meeran K, Choi SJ, Taylor GM, Heath MM, Lambert PD, Wilding JP, Smith DM, Ghatei MA, Herbert J & Bloom SR. (1996). A role for glucagon-like peptide-1 in the central regulation of feeding. *Nature* **379,** 69-72.

van den Top M. (2002). Neuropeptide and hormonal signalling in mammalian central autonomic neurones. In *Department of Biological Sciences*. University of Warwick, Coventry.

van den Top M, Lee K, Whyment AD, Blanks AM & Spanswick D. (2004). Orexigen-sensitive NPY/AgRP pacemaker neurons in the hypothalamic arcuate nucleus. *Nat Neurosci* **7,** 493-494.

van den Top M, Lyons DJ, Lee K, Coderre E, Renaud LP & Spanswick D. (2007). Pharmacological and molecular characterization of ATP-sensitive K(+) conductances in CART and NPY/AgRP expressing neurons of the hypothalamic arcuate nucleus. *Neuroscience* **144,** 815-824.

Van der Heyden G, Vereecke J & Carmeliet E. (1985). The effect of cyanide on the K-current in guinea-pig ventricular myocytes. *Basic Res Cardiol* **80 Suppl 1,** 93-96.

van der Lely AJ, Tschop M, Heiman ML & Ghigo E. (2004). Biological, physiological, pathophysiological, and pharmacological aspects of ghrelin. *Endocr Rev* **25,** 426-457.

Van Gaal LF, Rissanen AM, Scheen AJ, Ziegler O & Rossner S. (2005). Effects of the cannabinoid-1 receptor blocker rimonabant on weight reduction and cardiovascular risk factors in overweight patients: 1-year experience from the RIO-Europe study. *Lancet* **365,** 1389-1397.

van Reil N. (2004). Minimal models for glucose and insulin kinetics - a MATLAB implementation, pp. 1-21. Eindhoven University of Technology, Department of Biomedical Engineering, Department of Electrical Engineering, BIOMIM & Control Systems.

Velkoska E, Morris MJ, Burns P & Weisinger RS. (2003). Leptin reduces food intake but does not alter weight regain following food deprivation in the rat. *Int J Obes Relat Metab Disord* **27,** 48-54.

Vettor R, Fabris R, Pagano C & Federspil G. (2002). Neuroendocrine regulation of eating behavior. *J Endocrinol Invest* **25,** 836-854.

Virdee JK. (2009). The electrophysiological and morphological characterisation of aminergic responsive neurones within the rat hypothalamic arcuate nucleus *in vitro*. In *Clinical Sciences Research Institute, Warwick Medical School*. University of Warwick, Coventry.

Vrang N, Larsen PJ, Clausen JT & Kristensen P. (1999). Neurochemical characterization of hypothalamic cocaine- amphetamine-regulated transcript neurons. *J Neurosci* **19,** RC5.

Wang J, Liu R, Hawkins M, Barzilai N & Rossetti L. (1998). A nutrient-sensing pathway regulates leptin gene expression in muscle and fat. *Nature* **393,** 684-688.

Wang R, Liu X, Hentges ST, Dunn-Meynell AA, Levin BE, Wang W & Routh VH. (2004). The regulation of glucose-excited neurons in the hypothalamic arcuate nucleus by glucose and feeding-relevant peptides. *Diabetes* **53,** 1959-1965.

Wang WH & Giebisch G. (1991). Dual modulation of renal ATP-sensitive K+ channel by protein kinases A and C. *Proc Natl Acad Sci U S A* **88,** 9722-9725.

Wank SA, Harkins R, Jensen RT, Shapira H, de Weerth A & Slattery T. (1992). Purification, molecular cloning, and functional expression of the cholecystokinin receptor from rat pancreas. *Proc Natl Acad Sci U S A* **89,** 3125-3129.

Watkins PJ. (2003). *ABC of diabetes*. BMJ Books, London, UK.

Watson SJ & Akil H. (1979). The presence of two alpha-MSH positive cell groups in rat hypothalamus. *Eur J Pharmacol* **58,** 101-103.

Weinstock M, Speiser Z & Ashkenazi R. (1978). Changes in brain catecholamine turnover and receptor sensitivity induced by social deprivation in rats. *Psychopharmacology (Berl)* **56,** 205-209.

White JD, Olchovsky D, Kershaw M & Berelowitz M. (1990). Increased hypothalamic content of preproneuropeptide-Y messenger ribonucleic acid in streptozotocin-diabetic rats. *Endocrinology* **126,** 765-772.

Wiegand SJ & Price JL. (1980). Cells of origin of the afferent fibers to the median eminence in the rat. *J Comp Neurol* **192,** 1-19.

Wild S, Roglic G, Green A, Sicree R & King H. (2004). Global prevalence of diabetes: estimates for the year 2000 and projections for 2030. *Diabetes Care* **27,** 1047-1053.

Wilding JP, Gilbey SG, Bailey CJ, Batt RA, Williams G, Ghatei MA & Bloom SR. (1993). Increased neuropeptide-Y messenger ribonucleic acid (mRNA) and decreased neurotensin mRNA in the hypothalamus of the obese (ob/ob) mouse. *Endocrinology* **132,** 1939-1944.

Willesen MG, Kristensen P & Romer J. (1999). Co-localization of growth hormone secretagogue receptor and NPY mRNA in the arcuate nucleus of the rat. *Neuroendocrinology* **70,** 306-316.

Williams G, Bing C, Cai XJ, Harrold JA, King PJ & Liu XH. (2001). The hypothalamus and the control of energy homeostasis: different circuits, different purposes. *Physiol Behav* **74,** 683-701.

Williams G, Harrold JA & Cutler DJ. (2000). The hypothalamus and the regulation of energy homeostasis: lifting the lid on a black box. *Proc Nutr Soc* **59,** 385-396.

Williams RH, Alexopoulos H, Jensen LT, Fugger L & Burdakov D. (2008). Adaptive sugar sensors in hypothalamic feeding circuits. *Proc Natl Acad Sci U S A* **105,** 11975-11980.

Williams RH & Burdakov D. (2009). Silencing of ventromedial hypothalamic neurons by glucose-stimulated K(+) currents. *Pflugers Arch*.

Wilson JM, Coderre E, Renaud LP & Spanswick D. (2002). Active and passive membrane properties of rat sympathetic preganglionic neurones innervating the adrenal medulla. *J Physiol* **545,** 945-960.

Wittam R & M. A. (1965). The connection between active cation transport and metabolism in erythrocytes. *Biochem J* **97,** 214-227.

Woerle HJ, Meyer C, Dostou JM, Gosmanov NR, Islam N, Popa E, Wittlin SD, Welle SL & Gerich JE. (2003). Pathways for glucose disposal after meal ingestion in humans. *Am J Physiol Endocrinol Metab* **284,** E716-725.

Wren AM, Small CJ, Abbott CR, Dhillo WS, Seal LJ, Cohen MA, Batterham RL, Taheri S, Stanley SA, Ghatei MA & Bloom SR. (2001). Ghrelin causes hyperphagia and obesity in rats. *Diabetes* **50,** 2540-2547.

Xu AW, Kaelin CB, Morton GJ, Ogimoto K, Stanhope K, Graham J, Baskin DG, Havel P, Schwartz MW & Barsh GS. (2005). Effects of hypothalamic neurodegeneration on energy balance. *PLoS Biol* **3,** e415.

Yang XJ, Kow LM, Funabashi T & Mobbs CV. (1999). Hypothalamic glucose sensor: similarities to and differences from pancreatic beta-cell mechanisms. *Diabetes* **48,** 1763-1772.

Yildiz BO, Suchard MA, Wong ML, McCann SM & Licinio J. (2004). Alterations in the dynamics of circulating ghrelin, adiponectin, and leptin in human obesity. *Proc Natl Acad Sci U S A* **101,** 10434-10439.

Young JB & Landsberg L. (1997). Suppression of sympathetic nervous system during fasting. *Obes Res* **5,** 646-649.

Zanella MT & Ribeiro Filho FF. (2009). Emerging drugs for obesity therapy. *Arq Bras Endocrinol Metabol* **53,** 271-280.

Zarjevski N, Cusin I, Vettor R, Rohner-Jeanrenaud F & Jeanrenaud B. (1993). Chronic intracerebroventricular neuropeptide-Y administration to normal rats mimics hormonal and metabolic changes of obesity. *Endocrinology* **133,** 1753-1758.

Zawar C & Neumcke B. (2000). Differential activation of ATP-sensitive potassium channels during energy depletion in CA1 pyramidal cells and interneurones of rat hippocampus. *Pflugers Arch* **439,** 256-262.

Zhang Y, Zhou J, Corll C, Porter JR, Martin RJ & Roane DS. (2004). Evidence for hypothalamic K+(ATP) channels in the modulation of glucose homeostasis. *Eur J Pharmacol* **492,** 71-79.

Zigman JM, Jones JE, Lee CE, Saper CB & Elmquist JK. (2006). Expression of ghrelin receptor mRNA in the rat and the mouse brain. *J Comp Neurol* **494,** 528-548.